Contributions to Model-Free Adaptive Control for Complex Mechanical Systems

Von der Fakultät für Ingenieurwissenschaften,
Abteilung Maschinenbau und Verfahrenstechnik
der
Universität Duisburg-Essen
zur Erlangung des akademischen Grades
eines
Doktors der Ingenieurwissenschaften
Dr.-Ing.
genehmigte Dissertation

von

Hoang Anh Pham
aus
Hai Phong, Vietnam

Gutachter: Univ.-Prof. Dr.-Ing. Dirk Söffker
Univ.-Prof. Dr.-Ing. Tamara Nestorović

Tag der mündlichen Prüfung: 22. Dezember 2020

Acknowledgement

First and foremost, I would like to give best thanks to my doctor supervisor Univ.-Prof. Dr.-Ing. Dirk Söffker for offering me the valuable opportunity to work in his group and for giving enthusiastic encouragements throughout my doctoral study. I am thankful for the chance he gave me to acquire the necessary knowledge for my academic carrier and to gain more insight into the fundamentals of scientific research. I greatly appreciate his enthusiasm, support, and guidance.

I am grateful to Univ.-Prof. Dr.-Ing. Tamara Nestorović from Ruhr-Universität Bochum for taking the place to be the second supervisor and for giving many helpful suggestions towards the completeness of my thesis.

Furthermore, I am using this opportunity to thank my previous and present colleagues of the Chair of Dynamics and Control at University of Duisburg-Essen. We have shared a lot of unforgettable moments during my doctoral study. Thanks to all vietnamese friends in Germany for sharing pleasant time during the past three years.

Special thanks to Vietnam International Education Development (VIED) and Vietnam Maritime University (VIMARU) for their financial support during my research period in Germany.

Finally and most importantly, I dedicate my heartful thanks to my parents, sister and her little family, and Ms Thi Duyen Nguyen for love, encouragements, belief, and support throughout many years.

Duisburg, Dezember 2020 Hoang Anh Pham

Kurzfassung

In der Regelungstechnik stützen sich traditionelle Methoden grundsätzlich auf das mathematische Modell eines Systems, um geeignete Kontrollschemata zu entwerfen. Zunächst muss das Modell erfolgreich entwickelt werden, dass das dynamische Verhalten des Systems unter bestimmten Betriebsbedingungen genau beschreibt. Theoretisch können auf der Grundlage des angenommenen Modells der Reglerentwurf und die Systemstabilitätsanalyse durchgeführt werden. In den letzten Jahrzehnten wurde eine alternative Regelungsstrategie entwickelt, die die verfügbaren Input-Output-Messungen des geschlossenen Regelkreises zur Analyse und zum Entwurf von Reglern verwendet. Durch diese neuartige datengetriebene bzw. modellfreie Regelungsmethode lässt sich der Aufwand für die Systemmodellierungsaufgaben deutlich reduzieren. Darüber hinaus werden durch die direkte Verwendung der aktualisierten Systemdaten die unbekannten zeitveränderlichen Parameter des gegebenen Systems bzw. Prozesses in jedem Betriebspunkt kontinuierlich ermittelt. Diese aktualisierten Parameter sind notwendig, um den erforderlichen Eingang für das zu regelnde System zu bestimmen.

In dieser Arbeit wird eine in letzter Zeit entwickelte, datengetriebene Regelungsmethode, die als modellfreie adaptive Regelung (MFAC) bezeichnet wird, intensiv untersucht, um weitere Verbesserungen der Regelungsleistung durch Anwendung der Methode auf dem Gebiet der Schwingungsreduktion zu erzielen. Das Hauptprinzip von MFAC ist der Ersatz der unbekannten komplizierten dynamischen Eigenschaften des ursprünglichen (nichtlinearen) Systems durch ein äquivalentes linearisiertes Modell, dass auf den online aktualisierten Input-Output-Daten des Systems basiert. Daher wird das angenommene Systemmodell zu jedem diskreten Zeitpunkt während des Systembetriebs aufgebaut. Um die Regelung zu entwerfen, sollten die identifizierten Parameter aus dem lokalen dynamischen Modell explizit verwendet werden. In dieser Arbeit werden verschiedene modifizierte/verbesserte MFAC-Strategien entwickelt, die effektiv auf eine Klasse komplexer mechanischer Systeme zur Schwingungsreduktion angewendet werden können.

Herkömmliche MFAC-Verfahren verwenden oft einen konventionellen Projektionsalgorithmus, um die unbekannten Systemparameter des linearisierten Datenmodells zu schätzen und zu aktualisieren. Um die Genauigkeit der Online-Ermittlung zu verbessern, wird in dieser Arbeit der rekursive Algorithmus der kleinsten Quadrate (RLSA) angewendet. Weiterhin kann die Nachlaufregelung des MFAC verbessert werden, indem nicht nur die aktuellen Ausgangsfehleramplituden, sondern auch die Fehlerschwankungen innerhalb eines Zeitintervalls fester Länge aus der Vergangenheit minimiert werden. Als Ergebnis wird eine modifizierte Regelung erzeugt.

Dabei wurde die dynamische Linearisierung in kompakter Form (CFDL) im MFAC-Design auch als eine vereinfachte Technik für die Systemlinearisierung in Betracht

gezogen. Das CFDL-Konzept wird in dieser Arbeit nicht nur auf das unbekannte (nichtlineare) System, sondern auch auf einen angenommenen nichtlinearen Regler angewendet werden. Anschließend wird eine linearisierte Reglerstruktur abgeleitet, in der eine Matrix von unbekannten Reglerparametern geschätzt wird. Durch den Vorschlag einer modifizierten Zielfunktion der Reglerparametermatrix wird ein verbesserter Schätzalgorithmus für die Online-Aktualisierung dieser Parameter eingeführt. Darüber hinaus werden auf den Grundlagen der MFAC und der verallgemeinerten Modellvorhersage-Regelung ein modifiziertes modellfreies adaptives prädiktives Regelungsprogramm erstellt, in dem RLSA und seine Modifikation zur Parameterermittlung anstelle des traditionellen Projektionsalgorithmus implementiert wird.

Eine weitere dynamische Linearisierungstechnik heißt Partial-Form Dynamic Linearization (PFDL), die im MFAC-Design für multivariable Systeme implementiert ist. In dieser Arbeit wird eine verbesserte PFDL-basierte datengetriebene Regelungsstrategie entwickelt. Es wird lokal ein Partialform-Datenmodell des Originalsystems konstruiert, das einen Satz unbekannter Parametermatrizen, also die Pseudo-Jacobi-Matrix, enthält. Diese Matrizen werden rekursiv unter Verwendung der gemessenen Eingangs-/Ausgangssignale des Systems aktualisiert. Zusätzlich zu den bekannten Ansätzen wird in dieser Studie die Verwendung der Online-Parameterschätzung auf der Grundlage der rekursiven Methode der kleinsten Quadrate auf das PFDL-Modell umgesetzt. Zur Realisierung der Regelung wird eine modifizierte PFDL-basierte Regelungseingangsgleichung vorgestellt, wobei die Minimierung der Schleppfehlerdifferenz berücksichtigt wird.

Um die Wirksamkeit der Kontrolle zu verifizieren, werden die vorgeschlagenen Regler verwendet, um die freien Schwingungen eines elastischen Schiffskrans zu reduzieren, die durch die von Null abweichende Anfangserregung der Nutzlast verursacht werden. Der Kran wird als ein typisches komplexes und flexibles System angesehen, bei dem die Schwingungen des elastischen Auslegers und der Nutzlast in der Ebene reduziert oder eliminiert werden müssen, um die Sicherheit des Kranbetriebs zu erhöhen. Simulationsergebnisse zeigen, dass die Winkelverschiebungen der Ausgangssignale sowie die Nutzlast durch den Einsatz der modifizierten modellfreien Regler innerhalb kurzer Zeit deutlich reduziert werden. Darüber hinaus arbeiten die vorgestellen MFAC-Programme effektiv, und es werden bessere Regelungsergebnisse erzielt, wenn mehrere Designreglerparameter im Vergleich zu konventionellen Methoden variiert werden.

Abstract

In control theory, traditional methods are basically relied on the mathematical model of a plant to design suitable control schemes. First, the model has to be successfully developed which reflects precisely the system dynamic behaviors within certain operating conditions. Theoretically, based on the true assumed plant model, the controller design and system stability analysis can be carried out. On the other hand, since the last few decades an alternative control strategy, which only utilizes the available input-output information from the closed-loop system to analyze and design controllers, has been proposed. This novel data-driven or model-free control method can reduce efforts spending on the system modeling tasks. In addition, by using directly the updated system data the unknown time-varying parameters of the given system/process and design controller are estimated and corrected continuously at each operating point. These updated parameters are necessary to determine the required control input energy.

In this thesis, a recently developed data-driven control method called model-free adaptive control (MFAC) will be intensively investigated to acquire further control performance improvements by applying the method to the field of vibration reduction. The main principle of MFAC is replacement of the unknown complicated dynamical characteristics of the initial (nonlinear) system by an equivalent linearized model based on the on-line updated system input-output data. Hence, the assumed system model is built up at each discrete-time instant during the system operation. To design control, the identified parameters from the local dynamic model should be utilized explicitly. This research will develop different modified/improved MFAC strategies which can be effectively applied to a class of complex mechanical systems for vibration reduction purpose.

Traditional MFAC often uses conventional projection algorithm to estimate and update the unknown system parameters of the linearized data model. To improve on-line estimation accuracy, in this thesis, recursive least-squares algorithm (RLSA) will be applied. Furthermore, the tracking control performance of MFAC can be improved by minimizing not only the current output error amplitudes, but also the error variations within a fixed-length of time window from the past. As a result, a modified control input law will be generated.

In addition, compact-form dynamic linearization (CFDL) has been considered in MFAC design as a simplified technique for system linearization. In this work, the CFDL concept will be applied not only to the unknown (nonlinear) plant but also to an assumed nonlinear controller. Subsequently, a linearized controller structure is derived, in which a matrix of unknown controller parameters needs to be estimated. By proposing a modified objective function of the controller parameter matrix, an improved estimation algorithm for updating these parameters on-line is introduced. Moreover, based on the fundamentals of MFAC and generalized model predictive

control, modified model-free adaptive predictive control programs are proposed, in which RLSA and its modification can be implemented for parameter estimation instead of using traditional projection algorithm.

Another dynamic linearization technique called partial-form dynamic linearization (PFDL) is implemented to the MFAC design for multivariable systems. In this contribution, an improved PFDL-based data-driven control strategy will be developed. A partial-form data model of the original system is constructed locally which contains a set of unknown parameter matrices namely pseudo-jacobian matrix. These matrices are recursively updated by using the measured system input-output signals. In addition to known approaches, in this study, on-line parameter estimation based on the recursive least-squares method is applied to the PFDL model. For control realization, a modified PFDL-based control input equation is proposed by considering minimization of the tracking error differences.

To verify control effectiveness, the proposed controllers will be executed to reduce the free-vibrations of an elastic ship-mounted crane due to the non-zero initial excitation of the payload. The crane is represented as a typical complex and flexible system, in which the in-plane oscillations of the elastic boom and the payload must be reduced or eliminated to increase the crane safety operation. Simulation results demonstrate that, the angular displacements of the output signals as well as the payload are reduced significantly within a short length of time by using the modified model-free controllers. Additionally, the proposed MFAC programs work effectively and better control results are obtained when varying several design controller parameters in comparison with conventional methods.

Contents

List of Figures

List of Tables

Nomenclature

Symbols

$\mathbf{A}$	System matrix
b, b_1	Small positive constants
$\mathbf{B}, \mathbf{B}_1, \mathbf{B}_2$	System input matrices
$\mathbf{B}_3, \mathbf{B}_4, \mathbf{B}_5$	Disturbance matrices
$\mathbf{C}$	Output matrix
$\mathbf{C}_1$	Measurement matrix
c, c_1, c_2	Design positive constants
d	Known integer
D	Set of previous system input-output data
$\mathbf{D}$	Input direct transmission matrix
$\mathbf{D}_1$	Unknown time-varying parameters
$\bar{e}$	Modeling error
E_{input}	Consumed input energy
$\mathbf{E}$	Disturbance matrix due to ship rolling
$\mathbf{e}$	Vector of output tracking errors
$\mathbf{e}_{N_y}$	Vector of predicted tracking errors
f	Unknown algebraic function
$\mathbf{F}$	Disturbance direct transmission matrix
G	Algorithm gain or gain matrix
G_v	Model coefficient
g	Unknown nonlinear vector-valued function
g^*	Unknown nonlinear function
$\mathbf{g}$	Vector of constant parameters
$\mathbf{G}$	Re-calculated system matrix
h	Smooth unknown nonlinear vector-valued function
$\mathbf{H}$	Re-calculated input matrix
J	Objective function
j	Weighting parameter
$\mathbf{J}$	Re-calculated disturbance matrix
k	Discrete-time variable
K	Unknown time-varying parameter (scalar)
$\mathbf{K}, \mathbf{K}_1, \mathbf{K}_2$	Unknown time-varying parameter matrices (vectors)
$\mathbf{K}_0$	Stiffness matrix
k_p, k_i	PI controller parameters
K^*	Set of varied controller gains (parameters)
L_1, L_2	Lengths of the upper cable
l	Length of the payload cable

L	Linearization length constant
m	Number of control inputs
m_y, m_u	Unknown system orders
m_1	Pulley mass
m_2	Payload mass
$\mathbf{M}_0$	Mass matrix
M	Positive constant
n	Number of unknown system parameters
n^*	Number of system inputs and outputs
$\mathbf{n}$	Nonlinear terms
N	Length of time window
$\mathbf{N}$	Disturbance matrix due to wind force
n_c, n_e	Assumed unknown controller orders
n_p	Fixed order model
N_y	Output prediction horizon
N_u	Control input prediction horizon
p	Discrete-time variable
P	Unknown time-varying parameter (scalar)
$\mathbf{P}, \mathbf{P}_1, \mathbf{P}_2$	Unknown time-varying parameter matrices (vectors)
p_2	Wind force
P_{K^*}	Trajectory of the relationship between tracking error and control input
$\mathbf{q}$	Generalized displacement vector
$\mathbf{Q}$	Re-calculated disturbance matrix
r	Number of system outputs
$\mathbf{S}$	Vector of identity matrices
T, T_1, T_2	Lengths of time window
t	Continuous-time variable
u	Control input signal (scalar)
$\mathbf{u}$	Control input signals (vector)
U	Vector of available input values
$\Delta\mathbf{U}$	Control input increment vector
$\Delta\mathbf{U}_{N_u}, \Delta\tilde{\mathbf{U}}_{N_u}$	Predicted control input increment vector within control input prediction horizon
$\Delta\mathbf{U}_{N_y}$	Predicted control input increment vector within output prediction horizon
$\mathbf{V}$	Constant coefficient matrix
$\mathbf{W}$	Constant coefficient matrix
$\mathbf{x}, \mathbf{x}_1, \mathbf{x}_2$	State vectors of the crane
Δx_2	Global position of the payload in x-direction
y	System output signal (scalar)
$\mathbf{y}$	System output signals (vector)

$\mathbf{y}^m$	Model system outputs (vector)
$\mathbf{y}^d$	Desired system outputs (vector)
$\mathbf{y}_m$	Measured system outputs (vector)
Y	Vector of available output values
Δy_2	Global position of the payload in y-direction
$\mathbf{Y}_{N_y}, \tilde{\mathbf{Y}}_{N_y}$	N_y-step-ahead output prediction vector
$\bar{\mathbf{Y}}, \tilde{\mathbf{Y}}$	Matrices of unknown time-varying parameters
$\mathbf{Y}^d_{N_y}$	Predicted desired output vector within output prediction horizon
α	Design positive constant
α_2	Angular displacement of the upper cable
β, β_0	Orientation of the boom axis
γ	Step-size constant
Δ	Increment unit
ε	Tracking error variations (vector)
η	Step-size constant
δ	Positive constant
θ	Known linear or nonlinear data function
θ_6	Angular displacement of the boom at node 6
$\lambda, \lambda_k, \lambda_{c1}, \lambda_{c2}, \lambda_p$	Constant weighting factors
μ	Step-size constant
$\Delta\delta$	Ship rolling
$\rho, \rho_k, \rho_1, \rho_p$	Step-size constants
$\Delta\rho$	Displacement of the luff angle
$\phi, \hat{\phi}$	System parameters (scalar)
$\Phi, \Phi_p, \hat{\Phi}$	Pseudo-Jacobian Matrix
$\Phi_{p,L}, \hat{\Phi}_{p,L}$	Sets of Pseudo-Jacobian Matrices
Φ_c	Pseudo-Gradient
ϕ_2	Angular displacement of the payload cable
$\phi_2^0, \dot{\phi}_2^0$	Initial payload position and velocity
Γ	Set of model coefficients
τ	Constant design parameter
$\hat{\Upsilon}$	Vector of previous parameter PJM (PFDL)
$\bar{\psi}$	Regression vector
ψ	Vector of parameters
$\Psi, \hat{\Psi}$	Pseudo-Partial Derivative
ω_6	Angular displacement of the boom at node 6
Ω	Vector of previous parameter PJM (CFDL)

Abbreviations

CFDL	Compact-Form Dynamic Linearization
CFDLc	Controller-based Compact-Form Dynamic Linearization
DDC	Data-Driven Control
FFDL	Full-Form Dynamic Linearization
FIR	Finite Impulse Response
FNN	Feedforward Neural Network
iPID	Intelligent Proportional-Integral-Derivative
IFT	Iterative Feedback Tuning
ILC	Iterative Learning Control
IIR	Infinite Impulse Response
I/O	Input/Output
iP	Intelligent Proportional
iPI	Intelligent Proportional-Integral
LLC	Lazy Learning Control
MBC	Model-based Control
MFAC	Model-free Adaptive Control
MFAPC	Model-free Adaptive Predictive Control
MFC	Model-free Control
MFSMC	Model-free Sliding Mode Control
MIMO	Multi-Input Multi-Output
MISO	Multi-Input Single-Output
MSE	Mean Square Error
MPC	Model Predictive Control
PA	Projection Algorithm
PFDL	Partial-Form Dynamic Linearization
PFDLc	Controller-based Partial-Form Dynamic Linearization
PG	Pseudo-Gradient
PI	Proportional Integral
PID	Proportional-Integral-Derivative
PJM	Pseudo-Jacobian Matrix
PPD	Pseudo-Partial Derivative
RLSA	Recursive Least-Squares Algorithm
RNN	Recurrent Neural Network
SISO	Single-Input Single-Output
SMC	Sliding Mode Control
SPSA	Simultaneous Perturbation Stochastic Approximation
UC	Unfalsified Control
VRFT	Virtual Reference Feedback Tuning

1 Introduction

1.1 Motivation and problem statement

In different fields of industry, automatic control techniques are necessary and have gained many achievements with well-developed theories as well as broad successful applications. The design of an appropriate controller satisfying some criteria like high performance, simple structure, and robustness in sense of external disturbance effects is extremely important with any modern industrial processes. Traditionally, to design a control scheme for any unknown plant, modeling of the system using first-principles, e.g., physical or chemical laws as well as dynamic identification has to be done firstly. When the mathematical model of the considered system is fully developed, many existing linear or nonlinear control methods including pole-zero assignment control, linear quadratic regulator, optimal control, Lyapulov-based control, etc. can be applied properly. However, in reality, most of practical systems or processes are nonlinear under the impact of unknown perturbations. In addition, many inevitable challenges still remain, so that control engineers have to encounter in system modeling procedure such as unmodeled dynamics, high-order model, or uncertainties. This leads to the emergence of robust/advanced or intelligent control methodologies.

As a branch of advanced control theory, adaptive control has become one of the most effective solutions to deal with dynamical changes or unknown internal/external disturbances acting on the system. According to [ÅW08], an adaptive control structure has the ability of adjusting the controller or system parameters to adapt with variations of the system operating conditions. Therefore, parameter adjustment mechanisms have to be present in the adaptive control topology which are able to estimate and update unknown controller parameters continuously (see Figure 1.1). Several well-known adaptive control schemes, in which the adjustment mechanism is explicitly implemented (model-reference adaptive control), or implicitly integrated (self-tuning regulators) in the controller structure have been introduced [ÅW08]. Nowadays, adaptive control together with robust control are the two advantageous tools to cope with parameter variations.

In recent years, due to the fact that the scale of actual industrial processes has been enlarged, control design of such complicated systems might be a challenging task. Additionally, with the enhancement of information technology, a very huge amount of the system input-output (I/O) information which is generated and stored in the system database during operation, is available. This brings to an innovative idea of using the valuable knowledge from the closed-loop system I/O data to analyze and, consequently, design a suitable control scheme. Therefore, a novel method so-called data-driven control (DDC) [HW13] has been introduced and received increasingly attention because by applying that, many efforts spending on modeling procedure

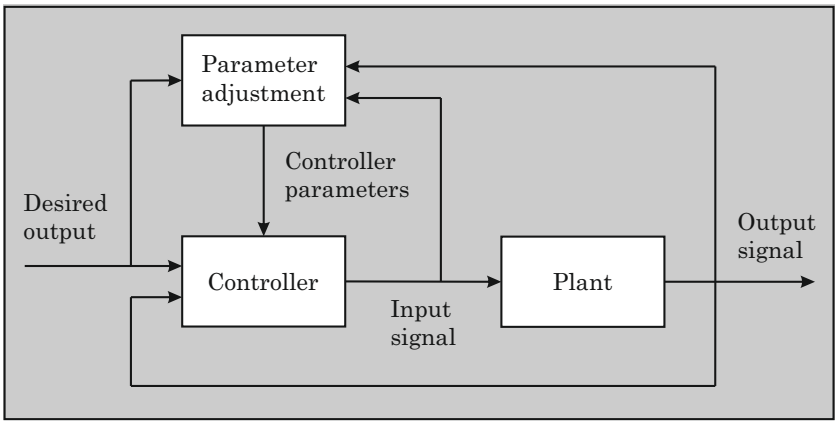

Figure 1.1: Block diagram of an adaptive control system (redrawn based on [ÅW08]).

can be avoided. To design a suitable controller for unknown (nonlinear) systems, only the measured (or calculated) system I/O signals are utilized. This means that every related model-based control difficulties, e.g., unmodeled dynamics, model uncertainties, nonlinearities, might be ignored in DDC. As discussed in [HJ13], the DDC strategies can be applied in case when the desired system dynamic model is extremely complicated with very high order, or involved nonlinearities. Furthermore, the control method is particularly useful when the plant model is not available (see Figure 1.2). Up to now, several data-driven control strategies have been proposed for both single-input single-output (SISO) and multiple-input multiple-output (MIMO) nonlinear systems such as model-free adaptive control [HH97], iterative learning control [BTA06], virtual reference feedback tuning control [GS00], etc. Further details related to the mentioned DDC methodologies are discussed in Chapter 2.

Vibrations often occur in mechanical flexible structures, and they are normally disadvantageous. To reduce or eliminate undesirable vibrations, especially for complex mechanical systems, modified or novel control strategies need to be investigated. In active vibration control, controller design methods are implemented to provide external control input signals acting on the vibrating systems via actuators [WN15]. On the other hand, another method to reduce unexpected vibrations in flexible systems is using additional damping or changing the stiffness of the system configurations. This method is known as passive vibration control [WN15].

As a typical flexible system, cranes are commonly used for lifting, lowering, or transferring cargo in many fields of industry like factories, ports, or construction. They can boost the performance of cargo transportation as well as reducing involved human activities. Cranes often operate under undesirable working conditions, e.g., heavy load, varied cable length, wind force. Structural oscillations are frequently observable, particularly in boom cranes which might lead to dangerous situations in

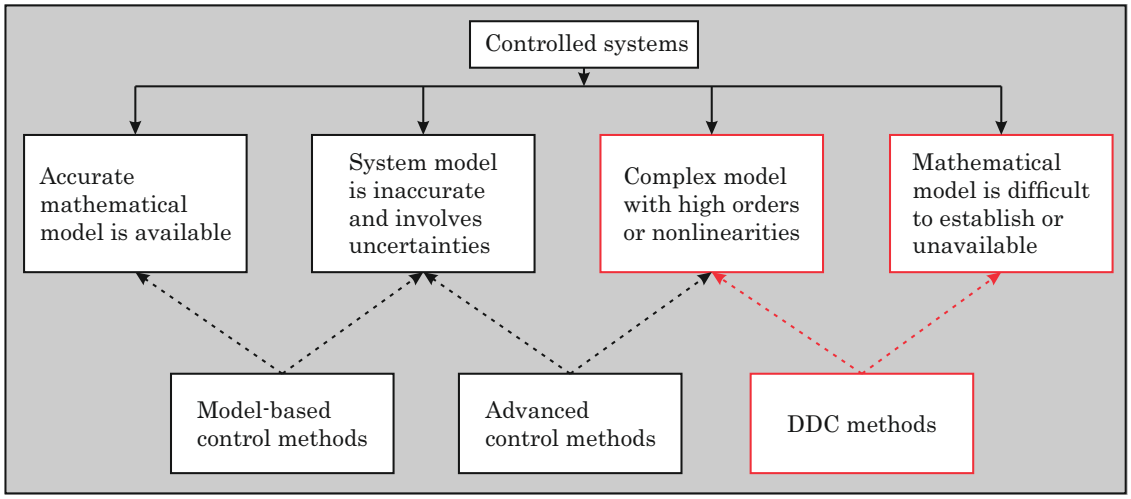

Figure 1.2: Objectives of data-driven control (redrawn based on [HJ13]).

the system operation. Therefore, research in vibration control with applications to elastic crane systems is highly motivated. Generally speaking, in most of the existing vibration control approaches for cranes, establishment of an accurate mathematical model which is assumed to reflect precisely the crane dynamic behaviors should be the initial step. Afterwards, a suitable control scheme can be designed depending on the true developed model. As discussed before, DDC or model-free control shows advantages which can be applied to crane control for reduction of the modeling task. Up to now, lack of model-free-oriented researches have been considered for vibration control problems of mechanical flexible systems, in particular for cranes.

Model-free adaptive control (MFAC) [HJ13] is represented as an effective DDC method. The key idea of this approach is linearization of the unknown system dynamics by an input-output related system model. This kind of local linearized model contains unknown time-varying parameters which can be adaptively adjusted. The system parameters are estimated and updated on-line by using only the available I/O data, and therefore, the assumed model is corrected consequently. Detail discussion regarding this kind of DDC control will be further illustrated in Chapter 2. From the author's point of view, potential aspects for modification of the MFAC design are related to on-line parameter estimation and control input calculation. Therefore, development of the modified/improved MFAC methods with application to vibration control of complex and flexible systems is crucial to guarantee the control expectations, e.g., satisfied efficiency, easy implementation, or low price.

1.2 Aims of this work

Motivated by several prospective aspects of DDC and MFAC as analyzed in the preceding section, this work aims to develop different data-driven control schemes based on the main theory of MFAC, and apply to vibration control of multivariable flexible systems. In general, MFAC often utilizes on-line parameter estimation algorithms to estimate and update unknown system parameters. Projection algorithm has been commonly applied to parameter estimation because of its simple structure. Beside that, other optimal on-line estimation algorithms such as recursive least-squares and its modifications can be further investigated to improve estimation accuracy of the model-free adaptive controllers. Moreover, to linearize the nonlinear system, the compact-form or partial-form dynamic linearization techniques can be implemented. The task of system identification is transferred into the adaptation of linearized model parameters to cope with the system dynamic changes based on the updated system I/O values. For control realization, traditional model-free control design uses the criteria of future output error minimization considering control input limitation. In this contribution, the output error variations within a predefined length of time window are considered in the control input objective function to improve overall tracking control performance. With respect to the intended elastic crane example as mentioned earlier, vibrations in cranes should be reduced or eliminated for safety reasons. To this end, the proposed control approaches will be applied to the elastic ship-mounted crane which is represented as a typical flexible system. The control target would be reduction of the in-plane vibrations of the elastic boom and the payload due to the non-zero initial excitation of the payload.

1.3 Thesis organization

This thesis consists of six chapters. Some main parts of the thesis have been published in the following conference proceedings [PS19a], [PS19b], [PS20a], [PS20c], [PS20d], or preparing as journal contributions [PS20b], [PS20e].

In the current chapter, introduction to traditional model-based control as well as data-driven control have been presented. The main control target of the work is vibration reduction of complex mechanical systems, specifically a ship-mounted crane using the modified MFAC methods. Therefore, several existing challenges in the field of vibration control related to cranes were illustrated.

In the next chapter, fundamental theories and literature review of different model-free control methods are discussed in detail. Four categories of the data-driven control principle are considered which cover most of the existing model-free control approaches. In addition, a variety of vibration control techniques focusing on cranes as well as some detail discussions with respects to data-driven and vibration control are given.

Chapter three dedicates to design of improved MFAC schemes for MIMO nonlinear systems using recursive least-squares estimation algorithm and the modification of control input calculation.

Chapter four concentrates on design of modified CFDL- and PFDL-based model-free adaptive controllers. A linearized controller structure is established, in which the unknown time-varying controller parameters can be recursively estimated via a modified algorithm which is proposed to improve on-line estimation accuracy. Furthermore, based on the principles of MFAC and model predictive control, modified/improved model-free adaptive predictive control programs will be discussed by utilizing explicitly the CFDL and PFDL concepts.

In the fifth chapter, an improved MFAC structure which applies the PFDL technique to the unknown nonlinear system will be introduced. The recursive least-squares approach can improve the estimation performance of a set of unknown system parameter matrices. As an illustrative example, the proposed control strategies in this thesis are implemented to a ship-mounted crane for vibration reduction purpose.

Finally, some main control ideas and conclusions from the discussed results together with suggested future works are outlined in the last chapter.

2 Fundamental theories and literature review

This chapter[1]provides the theoretical background and literature review of model-free or data-driven control. Four categories of data-driven control are known including on-line, off-line, or hybrid data usage together with model-based in combination with model-free control. Several vibration control approaches of flexible structures with the focus on crane control will be briefly discussed. A literature research in various control design techniques for different types of crane will be conducted. Furthermore, discussion about the selected model-free and vibration control methodologies are presented. Finally, the main ideas illustrated in this chapter are summarized in the last section.

The content, figures, and tables in this chapter are mainly based on the prepared journal papers [PS20b, PS20e] as well as the peer-reviewed conference papers [PS19b, PS20a, PS20c, PS20d]. Some of them in the conference papers have been partly modified in this chapter after previous publications.

2.1 Introduction to model-free/data-driven control

Design of automatic control systems has been extremely important in any field of science and technology since many decades. Nowadays, most of common control theories applied in control engineering can be divided into three classes namely classical control, modern control, and robust or advanced control [Oga10]. In modern control theory, modeling or identification of a linear/nonlinear object and its (time-varying) parameters can be conducted by using the first principles or the available system I/O data [Kir04]. Based on physical or chemical principles, a mathematical model of the considered system can be successfully achieved through the establishment of system dynamic equations. On the other hand, most of existing system identification tools rely entirely on the observed system data information to develop an I/O related plant model. Many well-known techniques for system identification can be found in the following textbooks [GS14, Lju99, VV07]. In general, the aforementioned control method is known as model-based control (MBC), in which a relatively accurate global dynamic model of the plant needs to be established firstly. Then, a suitable controller can be analyzed and designed depending on the assumed true dynamic model of the original system. With the development of science and engineering, the scale of industrial systems/processes is significantly enlarged, and becoming more complicated. In addition, due to the fact that most of systems in reality are highly nonlinear in the presence of unmodeled dynamics, uncertainties, or unknown external disturbances. Consequently, control of such systems is really a challenging

[1]Mathematical symbols are exclusively implemented to illustrate the content of the current chapter and will not be commonly applied to further chapters.

task. This leads to the next generation of control technology called robust/advanced control [SL91, Kha02]. From the 1950s up to now, many useful robust or advanced control methods have been proposed and applied successfully to both academia as well as industry such as adaptive control [ÅW08, IS12], model predictive control [CBA04, GP11], sliding mode control [Utk77, You78], etc. By applying the above model-based advanced control theories, the design closed-loop system can guarantee the two following properties: robust stability and robust performance [Oga10].

Since the last few years, because of the enhancement of information technology as well as industrial processes, e.g., chemical industry, machinery, mechatronics, transportation, a very huge amount of off-line or on-line I/O data which reflect precisely dynamical behaviors of the controlled process during operation can be generated and stored. This arises the idea of using directly these valuable data collected from the system to design suitable controllers. Therefore, an alternative solution to deal with control design, especially for unknown nonlinear systems has been explored recently called data-driven control (DDC) or model-free control (MFC). The fundamentals of MFC/DDC[2]is that, the desired controller can be completely investigated and implemented by using only on-line or off-line I/O signals from the closed-loop system without any explicit information related to model structure or modeling process. Hence, the unexpected model-based characteristics such as unmodeled dynamics, uncertainties, or nonlinearities that have to be addressed in MBC, are completely disappeared in MFC or DDC.

Regarding to the state-of-the-art MFC, to give an overview in terms of definition, classification, and discussion about some of the existing MFC approaches as well as related applications, a brief survey from MBC to MFC has been comprehensively reviewed in [HW13]. In addition, two effective DDC strategies namely model-free adaptive control and iterative learning control were discussed in [HCG17] including different dynamic linearization techniques. Moreover, many other data-driven control methods have been proposed since years to illustrate their potential feasibility. For example, in [YTY09, FJ13] novel intelligent proportional-integral-derivative (iPID) controllers were designed which shown improved control effectiveness in comparison with traditional PID control because the design controller parameters are changeable. Another branch of DDC which uses the stochastic approximation algorithm to estimate unknown system parameters based on the system measurements was introduced in [SC93, SC98]. Some further innovations in modification and design of DDC algorithms were presented. For instance, in [BWHQ18] the problem of control design for non-affine nonlinear systems with output saturation has been analyzed and solved. To cope with the linear quadratic tracking problem with delays, a data-driven adaptive dynamic programming algorithm was proposed in [LZYQ18] which explicitly uses the system input, output, and the reference trajectory to realize controllers. Regarding to tracking control problem of linear discrete-time systems,

[2]Model-free control and data-driven control are with the same meaning from now.

the idea of data-driven predictive control has been intensively discussed in [IFH01]. By using numerical iteration method, optimal controllers were designed in [ZXW15]. In the field of control design for marine systems, a MFC approach called unfalsified control [HPO18] has been applied to deal with the problems of dynamic positioning of marine vessels affected by unknown external disturbances. Regarding to vibration control of flexible structures, several novel data-driven control strategies have been proposed in [XSBS18, XWSS18]. Beside applications to control design, data-driven methods can be implemented to process monitoring and fault diagnosis for large-scaled industrial processes [YDXL14].

From the above literature observation, one conclusion can be drawn that, DDC/MFC might be applied in cases when the mathematical model of a system is with very high order, and contains unknown nonlinearities or uncertainties. Other situations, in which using DDC/MFC would be beneficial, are when establishment of a global dynamic model of the plant is very challenging or even not possible.

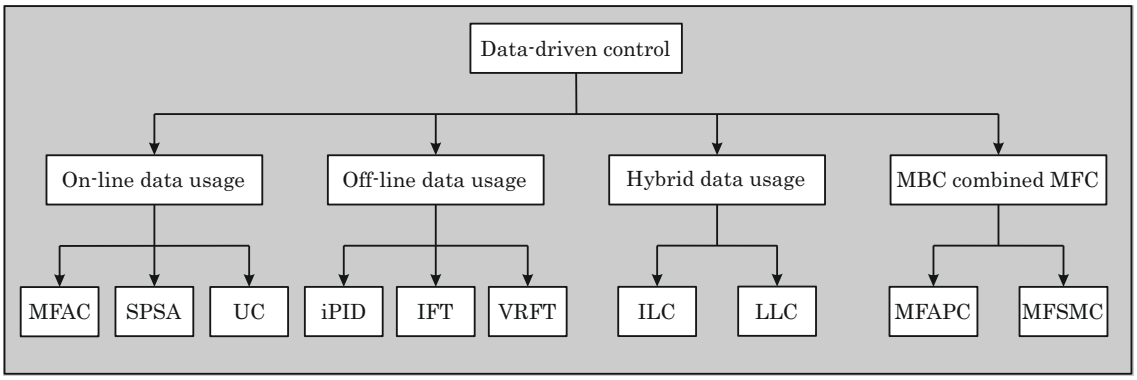

Figure 2.1: Classification of the discussed model-free control methods

MFAC:	Model-free Adaptive Control
SPSA:	Simultaneous Perturbation Stochastic Approximation
UC:	Unfalsified Control
iPID:	Intelligent Proportional-Integral-Derivative
IFT:	Iterative Feedback Tuning
VRFT:	Virtual Reference Feedback Tuning
ILC:	Iterative Learning Control
LLC:	Lazy Learning Control
MFAPC:	Model-free Adaptive Predictive Control
MFSMC:	Model-free Sliding Mode Control

Up to now, different ways to classify MFC/DDC exist, such as according to which kind of data usage [HJ13], the analyzed control algorithms, or the structure of the model-free controller used [HW13]. Within the main contexts of this thesis which

are primarily related to the modified/improved MFAC strategies, and a combination of model-based predictive control and model-free adaptive control as well as to provide a comprehensive overview of MFC based on off-line or on-line data from the system, the selected MFC methods are categorized into four classes as illustrated in Figure 2.1. Regarding to on-line MFC, three outstanding methods will be addressed including model-free adaptive control [HH97], simultaneous perturbation stochastic approximation data-driven control [Spa92], and unfalsified control [ST97], in which the main theory of model-free adaptive control and related applications will be mainly focused. In off-line DDC, the representative methods include PID/iPID [ÅH95], iterative feedback tuning control [Hja02], and virtual reference feedback tuning control [GS00]. The other MFC strategies which require both on-line and off-line system data (so-called hybrid data usage) compose of iterative learning control [ACM07], and lazy learning control [SA94]. Finally, based on the author's observation from recent publications in the model-free control field, the last group would be the combination of MBC and MFC which is represented by model-free adaptive predictive control [Ste99], and model-free sliding mode control [LY18]. In the next sections, discussion about the main principle, characteristics, and well-known applications of the mentioned MFC/DDC approaches will be illustrated. Based on that, a research gap between the current developed researches and the remaining open points in MFC/DDC can be recognized. As a result, proposed ideas for control improvements are mentioned. Detail discussion about the literature analysis is described in Section 2.7 of this chapter.

2.2 On-line data-driven control

The on-line DDC methods require the updated system I/O values which are determined up to the current time instant to estimate the unknown parameters of the linearized system model or the design controller. As illustrated in [GS14], the on-line data-driven algorithms often deal with sequential data. Therefore, these unknown (time-varying) parameters are recursively estimated within a sampling period of time. Some of the effective control approaches belonged to this group, including model-free adaptive control, SPSA-based model-free control, and unfalsified control will be briefly reviewed in this section.

2.2.1 Model-free adaptive control

One of the most outstanding MFC approaches namely model-free adaptive control (MFAC), which is based merely on the usage of on-line measurable data from the controlled process to realize control action, has been widely investigated in recent years. The main principle of MFAC is replacement of the complicated dynamical characteristics of the unknown nonlinear system by an equivalent linearized model

based on the closed-loop system I/O data [HH97]. In more detail, at every sampling instant during the system operation (in discrete-time) a virtual local dynamic model of the system is assumed to be established which contains unknown parameters. Up to now, different dynamic linearization techniques such as compact-form, partial-form, or full-form dynamic linearization [HJ13] have been developed to dynamically improve the quality of the assumed data model. The model parameters are time-varying, and can be estimated or updated recursively at each time instant by using the previous system input and output values. For control implementation, an objective function with respect to minimization of the future output tracking errors should be considered. Subsequently, based on the corrected system parameters and the current control errors, the control input signals are computed analytically. As mentioned before, several dynamic linearization techniques for system approximation in MFAC design have been introduced. In the compact-form dynamic linearization (CFDL) data model, all nonlinear properties and model estimation errors are fused into a scalar parameter (pseudo-partial derivative) for SISO systems, or a parameter matrix (pseudo-jacobian matrix) for MIMO systems. On the other hand, by applying the partial-form dynamic linearization (PFDL), or full-form dynamic linearization (FFDL) techniques, a set or different sets of unknown system parameter matrices (see Chapter 5 for the PFDL concept) have to be identified. Therefore, compared to the CFDL model, the system dynamic behaviors in the last two cases may not be extremely complicated. As discussed in [HJ13], MFAC possesses several attractive properties compared to MBC. First, only the available closed-loop system I/O data are used to analyze and design controllers. There is no information about structural model or involved model uncertainties. Second, MFAC does not require any external testing signals as well as training processes. Furthermore, MFAC may have simple structures leading to low computational load. Finally, the I/O stability, output error convergence, and robustness of the MFAC algorithms can be guaranteed under some reasonable pre-required assumptions.

In this thesis, different modified model-free adaptive control algorithms will be designed to control a class of discrete-time MIMO nonlinear systems. A general I/O description of the unknown system is written as

$$\mathbf{y}(k+1) = g\left(\mathbf{y}(k), \mathbf{y}(k-1), \ldots, \mathbf{y}(k-m_y), \mathbf{u}(k), \mathbf{u}(k-1), \ldots, \mathbf{u}(k-m_u)\right), \quad (2.1)$$

where $\mathbf{y}(k) \in R^r, \mathbf{u}(k) \in R^m$ are the current system output and control input vectors, respectively. Here, m_y and m_u denote the unknown system orders. The number of system inputs and outputs are indicated as m and r, correspondingly; whilst $g(\ldots)$ is an unknown nonlinear vector-valued function. The nonlinear system (2.1) which satisfies some preliminary assumptions as mentioned in [HJ13], with $\|\Delta\mathbf{u}(k)\| \neq 0, \Delta\mathbf{u}(k) = \mathbf{u}(k) - \mathbf{u}(k-1)$ or $\|\Delta\mathbf{U}(k)\| = \|\mathbf{U}(k) - \mathbf{U}(k-1)\| \neq 0$, where $\Delta\mathbf{U}(k) = [\Delta\mathbf{u}(k), \Delta\mathbf{u}(k-1), \ldots, \Delta\mathbf{u}(k-L+1)]^T$ and a control input linearization length constant $L \geq 1$, can be linearized locally at each time-step during the system operation as the CFDL and PFDL models [HJ11a], or the FFDL

model [YHZ18]. Based on the CFDL concept, the obtained linearized data model is described as

$$\Delta \mathbf{y}(k+1) = \Phi(k)\Delta \mathbf{u}(k), \tag{2.2}$$

which contains the unknown time-varying parameter matrix $\Phi(k)$ called pseudo-jacobian matrix (PJM), with $\Delta \mathbf{y}(k+1) = \mathbf{y}(k+1) - \mathbf{y}(k)$. The structure of the PJM in MIMO case is written as

$$\Phi(k) = \begin{bmatrix} \phi_{11}(k) & \phi_{12}(k) & \phi_{13}(k) & \dots & \phi_{1m}(k) \\ \phi_{21}(k) & \phi_{22}(k) & \phi_{23}(k) & \dots & \phi_{2m}(k) \\ \vdots & \vdots & \vdots & \ddots & \vdots \\ \phi_{r1}(k) & \phi_{r2}(k) & \phi_{r3}(k) & \dots & \phi_{rm}(k) \end{bmatrix}_{r \times m}, \tag{2.3}$$

assuming $\|\Phi(k)\| \leq b$ according to assumption 2 (see Chapter 3), with $b > 0$; that means the PJM $\Phi(k)$ is upper bounded at any time instant k.

According to [HJ13, HJ11a], to design a MFAC program for MIMO nonlinear systems the following steps have to be implemented:

- *Step 1:* Select one of the three existing dynamic linearized data models or three aforementioned dynamic linearization techniques including CFDL, PFDL, and FFDL
- *Step 2:* Estimate and update the unknown system parameters of the linearized data model (2.2) by using only the available system I/O data
- *Step 3:* Design MFAC algorithms based on the estimated model parameters and the current control errors
- *Step 4:* Calculate the time-varying system parameters repeatedly from step 2 by utilizing the updated system I/O information

A general MFAC scheme for unknown MIMO systems is shown in Figure 2.2 [PS19b]. In literature, a variety of MFAC strategies have been proposed together with many successful applications in control of both SISO and MIMO (nonlinear) systems. The state-of-the-art MFAC including different dynamic linearization techniques were presented in [HX19]. The authors focused on design of a FFDL-MFAC scheme with the closed-loop system stability analysis for a class of SISO nonlinear systems. In [HB11], the problem of data dropout which possibly occurs when implementing MFAC experiments was investigated. In addition, design of a receding horizon near-optimal tracking control program considering full unknown system dynamics in both of the state feedback and input channels was introduced in [ZLL18]. Furthermore, several novel MFAC approaches have been published in recent years such as [LHT+19, BHZ18, ZH14, XJL16, JLT17, LY17, LDJ19, TBT18]. In [CPSC10,

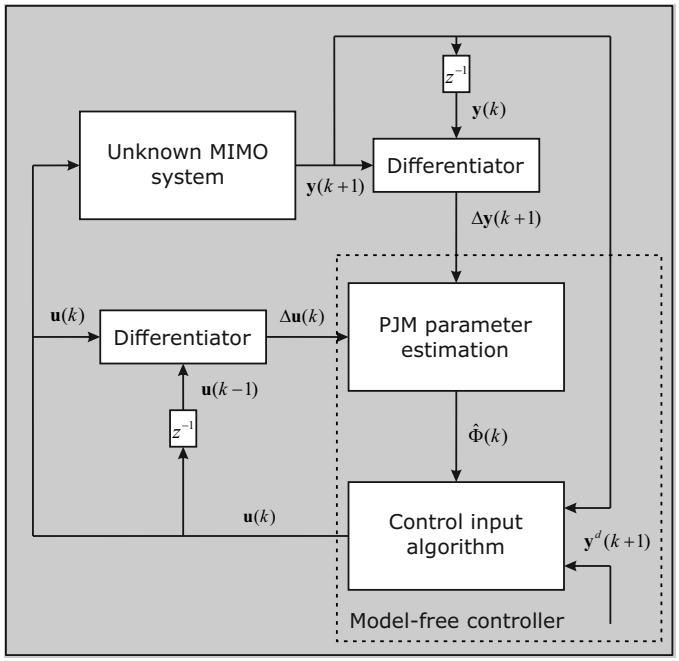

Figure 2.2: General model-free adaptive control scheme [PS19b]

CC09], model-free learning adaptive controllers based on pseudo-gradient concepts and optimization were designed for SISO nonlinear systems. By using the PFDL technique, many improved MFAC schemes have been proposed with experimental verification as given in [HJ11b, HJ08]. In term of MFAC design for MIMO systems, by using multi-observer models to linearize the unknown nonlinear system, a novel MFAC program has been discussed in [XJS14] with Lyapunov-based stability analysis. Additionally, by applying the CFDL and PFDL concepts not only to the nonlinear process but also to an assumed ideal controller, novel MFAC algorithms denoted as CFDLc or PFDLc-MFAC have been proposed in [ZH12, ZH15, HZ13] for SISO nonlinear systems in the presence of unknown disturbances.

2.2.2 Simultaneous perturbation stochastic approximation-based (SPSA) model-free control

To deal with the problem of finding optimal roots in the minimization procedure of a loss (cost) function, J. C. Spall et al. [Spa92, SC98] have proposed a novel method called simultaneous perturbation gradient approximation in the presence of noisy measurements. For adaptive control design of a class of unknown nonlinear systems, only the available system I/O data are utilized to approximate the nonlinear system dynamics via neural network or polynomial as well as to estimate the time-varying controller parameters [HJ13]. Since the optimal controller parameters

derived from minimization of a control performance criteria, an adaptive control law can be defined from the knowledge of the system I/O information.

To give an overview of the SPSA-based control method, as discussed in [SSSN08] a MIMO nonlinear system description is considered in discrete-time as

$$\mathbf{y}(k) = f(k-1) + \mathbf{u}(k-1) + \mathbf{d}(k), \tag{2.4}$$

where $\mathbf{y}(k), \mathbf{u}(k) \in R^m$ are the system output and control input vectors, respectively, and m is indicated as the dimension of the system I/O variables. Here $f(k-1) = f\left(\mathbf{y}(k-1), \mathbf{y}(k-2), \ldots, \mathbf{y}(k-p), \mathbf{u}(k-2), \mathbf{u}(k-3), \ldots, \mathbf{u}(k-q), \theta^*\right)$ is a dynamical nonlinear function of the previous system I/O signals, with p, q are the numbers of time-delayed plant outputs and inputs, correspondingly. The vector of ideal weighting parameters is denoted as θ^*. The overall bounded noise vector of the system is indicated as $\mathbf{d}(k)$. According to [SSSN08], the control input vector is defined as

$$\mathbf{u}(k-1) = -\hat{f}(k-1) + \mathbf{y}^d(k) + \varsigma \mathbf{s}(k-1), \tag{2.5}$$

where $\hat{f}(k-1) = \hat{f}(k-1, \hat{\theta}(k-1))$ is an approximation of the unknown nonlinear function $f(k-1)$ by using the estimated parameter vector $\hat{\theta}(k-1)$. The reference output vector is denoted as $\mathbf{y}^d(k)$, while $\mathbf{s}(k-1)$ is the output tracking error vector, with $\mathbf{s}(k-1) = \mathbf{y}(k-1) - \mathbf{y}^d(k-1)$. The design control parameter is denoted as ς. The estimation error vector of the SPSA-based model is defined as follows

$$\mathbf{e}(k) = \mathbf{s}(k) - \varsigma \mathbf{s}(k-1), \tag{2.6}$$

$$\mathbf{e}(k) = f(k-1) - \hat{f}(k-1) + \mathbf{d}(k). \tag{2.7}$$

The target is to find the closest root $\hat{\theta}(k-1)$ that is an approximation of the ideal weighting vector of the following gradient equation

$$\min g(\hat{\theta}(k-1)) = \min \frac{\partial L(\hat{\theta}(k-1))}{\partial \hat{\theta}(k-1)}, \tag{2.8}$$

where

$$L(\hat{\theta}(k-1)) = \frac{1}{2} \left\| f(k-1) - \hat{f}(k-1) \right\|^2, \tag{2.9}$$

is the cost function of the SPSA.

The SPSA algorithm for updating $\hat{\theta}(k)$ is written in a recursive formula according to [SSSN08] as

$$\hat{\theta}(k) = \hat{\theta}(k-1) - \alpha(k) \hat{g}(\hat{\theta}(k-1)), \tag{2.10}$$

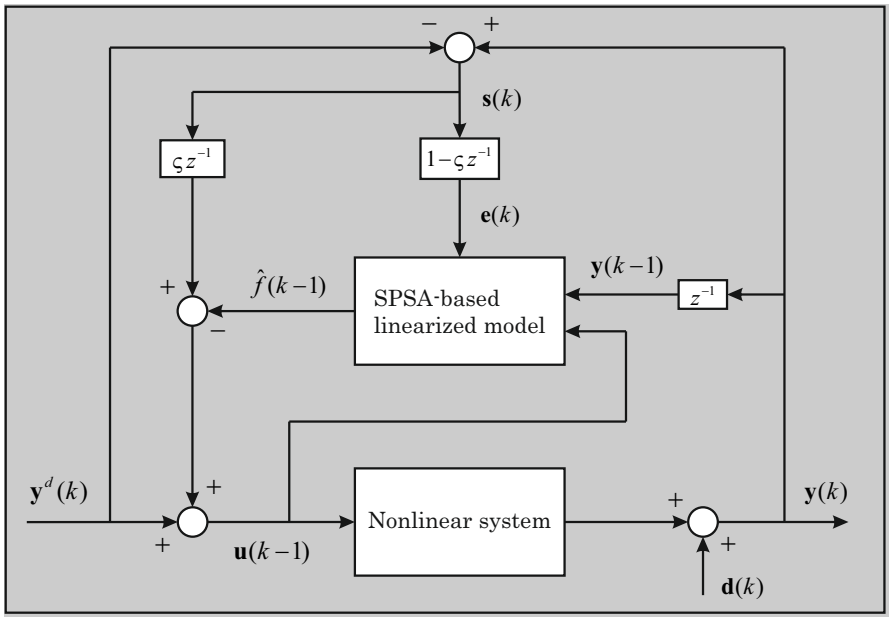

Figure 2.3: Block diagram of the SPSA-based model-free control (redrawn based on [SSSN08])

where $\alpha(k)$ is denoted as an adaptive learning rate, and $\hat{g}(\hat{\theta}(k-1))$ is a gradient approximation of the cost function $L(\hat{\theta}(k-1))$ in (2.9). The given control method is called simutaneous perturbation stochastic approximation-based model-free control. A block diagram of MFC using the SPSA approach is shown in Figure 2.3 [SSSN08].

Some of successful applications using the SPSA-based control method can be mentioned such as [SS98], in which the authors proposed a SPSA-based optimal distribution to deal with the problem of the optimal choice of random perturbations. In [MC08], J. L. Maryak et al. considered the theoretical and numerical global optimal convergence of the SPSA algorithm. Two novel theorems have been introduced which can lead the SPSA to a global optimizer. Furthermore, O. Granichin et al. [GA15] discussed the challenging problems of non-stationary optimization under observations with unknown but bounded noise. The obtained results reveal a finite bound of the differences between estimates and unknown time-varying parameters.

2.2.3 Unfalsified control

An adaptive robust control method called unfalsified control, in which only the plant I/O data are needed to determine an appropriate control law for unknown dynamic systems, will be briefly reviewed. This novel control approach was firstly developed by M. G. Safonov et al. in [ST97, ST95].

For a set of system measurement information $\mathbf{M}$, with $\mathbf{M} \subset \mathbf{U} \times \mathbf{Y}$, that contains a measured point of the system I/O data $(u_0, y_0) \in \mathbf{M}$, a control law $\mathbf{K}^* \in \mathbf{K}_{OK}$ is said to be an unfalsified control law with the knowledge of $(u_0, y_0) \in \mathbf{M}$ if and only if, for any system data point $(u_1, y_1) \in \mathbf{M}$

$$(\mathbf{K}^* \cap \{(r, y, u) \in \mathbf{R} \times \mathbf{Y} \times \mathbf{U} | r \in \mathbf{R}, y = y_1, u = u_1\}) \subset \tilde{T}_{spec}, \tag{2.11}$$

where r, y, u are indicated as the reference, output, and demanded control input which belong to the corresponding $\mathbf{R}, \mathbf{Y}, \mathbf{U}$-planes. A performance specification set is denoted as $\tilde{T}_{spec} \subset \mathbf{R} \times \mathbf{Y} \times \mathbf{U}$. Here, $\mathbf{K}_{OK} \subset \mathbf{K}_0$ is a subset of those control laws $\mathbf{K}^*$ whose ability to meet the specification $\tilde{T}_{spec}$ is unfalsified by the given measurement data $\mathbf{M}$ according to [ST95]. A general feedback control scheme is depicted in Figure 2.4. The control goal here is to determine the control law $\mathbf{K}^*$ for the unknown plant $\mathbf{P}$, so that the closed-loop system response satisfies the special performance requirement $\tilde{T}_{spec}$. The theoretical idea behind of unfalsified control is that, sets of controller parameters and/or control laws are falsified recursively by using only the system I/O data without any information related to the plant model. At each time instant k, the updated system I/O values will be utilized to evaluate the controller set before it can be inserted into the closed-loop system. Further detail information related to the control theorem and its proof can be found in [ST97].

Based on the fundamentals of unfalsified control above, several improvements of the method in terms of adaptive and robust control problems have been discussed in literature. For example, a data-driven robust control design was proposed in [Saf03] by applying the basis of the unfalsified control principle. In [CS04], an ellipsoid algorithm has been applied to approximate an unfalsified set. As a result, a set of unfalsified controller candidates could be found because of decreasing the volume ellipsoid. Furthermore, in [PS03] a general model reference adaptive control problem was illustrated using the unfalsification approach. A switch controller model-based system was generated for selection of candidate controller set. Regarding to input-output stability of a closed-loop system, an unfalsified adaptive switching control law under some environmental noises has been introduced in [BMST10]. In addition, an unfalsified control-based application to nonlinear robot manipulator was presented in [TS99]. Here, a novel control law has been designed to adaptively adjust different unknown time-varying parameters of the robot arm, especially in case of sudden changes in mass or load values of the system. A robust switching missile autopilot was investigated in [BFS98] by using the concept of unfalsified control. Hence, a novel algorithm to compute the fictitious reference signal has been proposed that leaded to the reduction of some mathematical calculations.

2.3 Off-line data-driven control

In the group of off-line data-driven control, the controller parameter estimation algorithms utilize explicitly the calculated or measured I/O data which have been stored

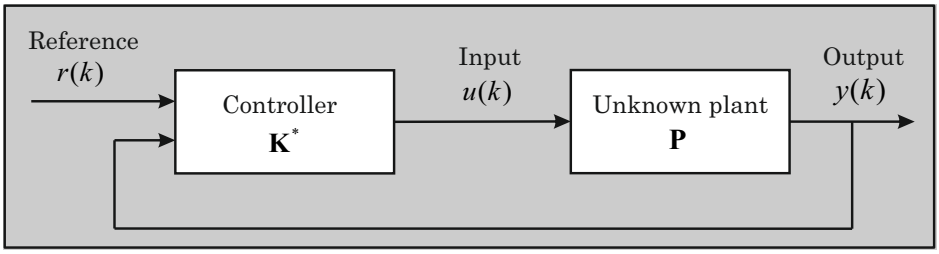

Figure 2.4: General feedback control scheme (redrawn based on [ST95])

in the system database. Therefore, a complete block of data information which is available for analysis, and no strict time limit on the process of analysis [GS14], are defined. In this section, three well-known off-line data-driven control methods including: i) traditional/intelligent PID, ii) iterative feedback tuning control, and iii) virtual reference feedback tuning control, are discussed.

2.3.1 Traditional/intelligent PID control

Nowadays, in most of actual controlled systems more than 95% of control loops are related to PID types. As introduced in [ÅH95], the PID controller possesses several advantageous properties. First, it provides feedback, and has the ability to eliminate steady-state offsets because of its integral part. Second, the control method can anticipate the future through derivative action. In addition, the controller structure is quite simple, and easy to be applied in most of practical applications. Finally, the PID controller can be implemented by using only the system I/O information. In PID control design, the optimization of parameter tuning process is highly motivated. Up to now, there is a plenty of analytical and practical methodologies for automatic tuning PID controller parameters as well as for adaptive adjustment corresponding with the variations of the system operation conditions. Regarding to the state-of-the-art PID control, the authors in [ÅH01] have discussed some main issues with respect to PID control problems such as specifications, stability, design, and applications as well as proposing several alternatives for PID control in the future. In [ACL05], K. H. Ang et al. presented an overview of the three-term functionalities for design and tuning PID control in patents, software packages, and commercial hardware modules. It provided a standardizing and modularizing PID control scheme for practical implementations. Furthermore, a survey of different adaptive techniques for tuning single-loop PID controller parameters such as gain scheduling, automatic tuning, or continuous adaptation has been introduced in [ÅHHH93]. Moreover, a survey of current tuning methods focusing on some novel auto-tuning procedures of PID controllers was presented by R. Gorez [Gor97]. In addition, in [LD01] three strategies for optimal-tuning of PID controller parameters were proposed. The controlled system was considered in cases of appearing

time-varying dynamics, or changing the system operating points. As an example of parameter-adaptive digital controller applications, a novel adaptive self-tuning PID control program [RI87] has been introduced which is based on a microprocessor controller. In [SDPB05], a robust PID control program was developed and applied to a programmable logic controller. The results of the paper demonstrated that the proposed method could be used as an effective solution for control design of nonlinear systems with perturbed parameters.

A standard PID control algorithm is illustrated in the following formula

$$u(t) = K\left[e(t) + \frac{1}{T_i}\int_0^t e(\tau)d\tau + T_d\frac{de(t)}{dt}\right], \tag{2.12}$$

where $u(t)$ is the control variable, and $e(t)$ is the control error, with $e(t) = y^d(t) - y(t)$. The reference and system output are denoted as $y^d(t)$ and $y(t)$, respectively. The standard PID controller can be divided into three parts: the P-part (proportional to the error), the I-part (proportional to the integral of the error), and the D-part (proportional to the derivative of the error). The functionalities of these terms have been summarized in [ACL05]. The controller parameters in (2.12) include the proportional gain K, integral time T_i, and derivative time T_d.

Recently, intelligent PID (iPID) control which is relied on the main theory of model-free control has been introduced [FJ08]. The fundamental idea of iPID control is replacement of unknown (nonlinear) system dynamics by an equivalent local model which is only valid during a very short time interval. By applying the DDC theory, in [YTY09] a novel data-driven PID controller was proposed for on-line automatic tuning control parameters by using the available system I/O data. Compared to other data-driven PID control approaches, the given method could reduce computation burdens effectively because of removed redundant data. As introduced in [FJ09], a linearized local dynamic model of a SISO nonlinear system is described as

$$y^{(\upsilon)} = F + \alpha u, \tag{2.13}$$

where α is a constant design parameter. The function $F = y^{(\upsilon)} - \alpha u$ is determined by using the updated system input u and output derivative $y^{(\upsilon)}$. Therefore, the dynamical behavior of F can be complicated because the unknown system nonlinearities or complex time-varying phenomena might be included. The derivation order υ is often equal to 1 or 2 [FJ09]. In case of $\upsilon = 2$, the following iPID control law is obtained as

$$u = -\frac{F}{\alpha} + \frac{\ddot{y}^d}{\alpha} + K_p e + K_i\int e + K_d\dot{e}, \tag{2.14}$$

where y^d is the desired system output, and the tracking control error is defined as $e = y^d - y$. The usual tuning parameters of the PID controller are given as K_p, K_i, and K_d.

2.3.2 Iterative feedback tuning control

One of the most effective tuning strategies among adaptive and iterative control algorithms namely iterative feedback tuning (IFT) control has been introduced in [Hja02]. The key idea of the IFT approach is that, the unknown (time-varying) controller parameters can be updated recursively by using only I/O information from closed-loop system experiments. At each iteration, the gradient-based objective function of the controller parameters should be estimated. According to [Hja02], a SISO closed-loop system in discrete-time domain is considered as

$$y(k) = P(q)u(k) + v_y(k), \tag{2.15}$$
$$u(k) = C(q,\rho)\left[r(k) - y(k)\right] + v_u(k), \tag{2.16}$$

where $P(q)$ is an unknown SISO operator with the shift operator q. The system input and output signals are denoted as $u(k)$ and $y(k)$, respectively. The transfer function of an appropriate controller is indicated as $C(q,\rho)$ with respect to the unknown parameters ρ. The reference signal of the closed-loop system is $r(k)$; while $v(k) = [v_y(k)\ v_u(k)]$ is a vector of unknown process disturbances.

The following steps will explain how the above mentioned gradient-based cost function can be approximated:

- *Step 1:* N measurements of the system output $y^1(\rho)$ are collected by carrying out normal experiments. Hence, the ouput is calculated as

$$y^1(\rho) = T_0(\rho)r + PS_0(\rho)v_u + S_0(\rho)v_y, \tag{2.17}$$

  where $T_0(\rho)$ and $S_0(\rho)$ are the achieved closed-loop response and sensitivity function with the controller $C(\rho)$.

- *Step 2:* New experiment is conducted by injecting the error signal $r - y^1(\rho)$ as an input to the process P. This new experiment is called gradient experiment as illustrated in Figure 2.5 with the presence of disturbances denoted as v_y^2 and v_u^2.

- *Step 3:* The gradient approximation

$$\frac{\partial \hat{y}}{\partial \rho}(\rho) = \frac{\partial C}{\partial \rho}(\rho)y^2(\rho) = \frac{\partial y}{\partial \rho}(\rho) + w(\rho), \tag{2.18}$$
$$w(\rho) = \frac{\partial C}{\partial \rho}(\rho)S(\rho)\left(v_y^2 + Pv_u^2\right), \tag{2.19}$$

  is taken, where $w(\rho)$ is introduced as the perturbation. Hence, the estimated gradient of the cost function $J(\rho)$ is defined as

$$\frac{d\hat{J}(\rho)}{d\rho} = \frac{1}{N}\sum_{k=1}^{N} \tilde{y}(k,\rho)\frac{\partial \hat{y}}{\partial \rho}(k,\rho), \tag{2.20}$$

where the error between the achieved $y(\rho)$ and desired response y^d is computed as $\tilde{y}(\rho) = y(\rho) - y^d$.

- *Step 4:* The adaptive controller parameter ρ in the next iteration is updated as

$$\rho(i+1) = \rho(i) - \gamma_i R^{-1}(i) \frac{d\hat{J}(\rho(i))}{d\rho}, \tag{2.21}$$

where the gradient approximation is determined in (2.20); whereas $\gamma_i > 0$ is a step-size constant, and $R(i)$ denotes as a positive definite matrix.

In literature, different IFT-based control methods are developed in the last decades. In [HPJ09], the convergence properties of the IFT control algorithm were improved by achieving informative data. Furthermore, the total number of necessary system experiments has been reduced significantly even in case of disturbed appearance. Moreover, in [HGG94] the authors proposed a local optimization approach which only needed the measured closed-loop system data to obtain the local minimum point of a cost function at each iteration. An objective function of the design adaptive controller parameters was considered which consists of two terms. The first term is related to minimization of the error between the achieved system response and the reference signal. Meanwhile, in the second term, the quadratic norm of the input signal should be optimized. The simulation results showed that, under the bounded signal assumption in the loop, a local minimum point of the cost function could be obtained. The optimal tuning algorithm (IFT-based algorithm) is also particularly useful for simple control loops such as PID control loop as mentioned in [HGGL98]. However, this method still requires more data and experiments. In addition, the problem of optimal tuning controller parameters applied to strongly nonlinear systems has been addressed in [Hja98]. It can be concluded that, the IFT-based tuning control method could be applicable for some kinds of system with non-smooth nonlinearities. In [RPP+11], a new approach for design of a convergent IFT-based control algorithm for second-order state feedback systems has been discussed, while the robustness constraint ability of the IFT controller was considered in [HVO16].

2.3.3 Virtual reference feedback tuning control

A direct data-driven control approach called virtual reference feedback tuning (VRFT) was firstly presented by G. O. Guardabassi et al. [GS00], in which the unknown controller parameters could be estimated directly by using off-line system I/O data with the introduction of a virtual reference signal. The data-driven control strategy was discussed for a class of linear time-invariant systems without any information about system model or system identification. As described in [GS00], three steps to conduct the VRFT control program are known:

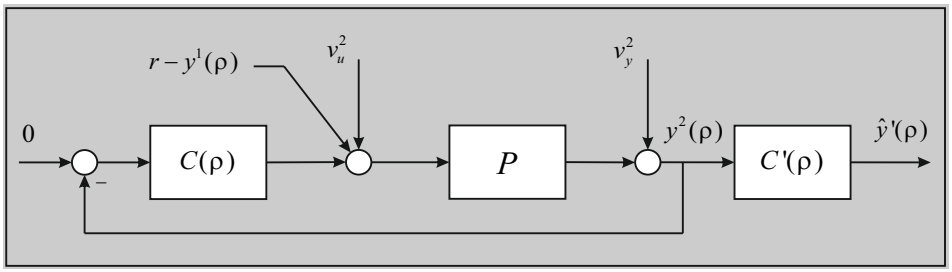

Figure 2.5: Gradient experiment (redrawn based on [Hja02])

- *Step 1:* A SISO plant G that needs to be controlled with a set of I/O open-loop measurements is considered in discrete-time as $\{\tilde{u}(k), \tilde{y}(k)\}_{k=1,2,\ldots,N}$. The reference model F^0 which consists of a single-input $y^0(k)$ and a single-output $y_M(k)$ is given. The measured system output $\tilde{y}(.)$ is assumed to be matched with the reference model output y_M for the same virtual reference input $\tilde{y}^0(.)$.

- *Step 2:* Based on the reference model F^0, the virtual reference input $\tilde{y}^0(.)$ as the counterimage of $\tilde{y}(.)$ could be found [GS00].

- *Step 3:* A feedback controller R could be designed, in which its output value indicated as $\hat{\tilde{u}}(.)$ gets as close as possible to $\tilde{u}(.)$ driven by the signals $\tilde{y}^0(.)$ and $\tilde{y}(.)$.

A control scheme of a deterministic system G is considered in Figure 2.6 without the effect of external disturbances. The reference model F^0 is written as

$$y_M(k) = F^0(z^{-1})y^0(k), \tag{2.22}$$

where z is the z-transform variable. The controller R of the system G is designed as

$$u(k) = R\left(z^{-1}, \theta\right) e(k), \tag{2.23}$$
$$e(k) = y^0(k) - y(k), \tag{2.24}$$

where $R\left(z^{-1}, \theta\right)$ is the controller transfer function depending on the vector of controller parameters θ. Based on the VRFT control method, with a given single I/O pair $\{\tilde{u}(k), \tilde{y}(k)\}_{k=1,2,\ldots,N}$ the estimated controller parameters $\hat{\theta}$ can be determined by minimizing the following objective function

$$J(\theta) = \frac{1}{N} \sum_{k=1}^{N} \left(\tilde{u}(k) - \hat{\tilde{u}}(k, \theta)\right)^2, \tag{2.25}$$

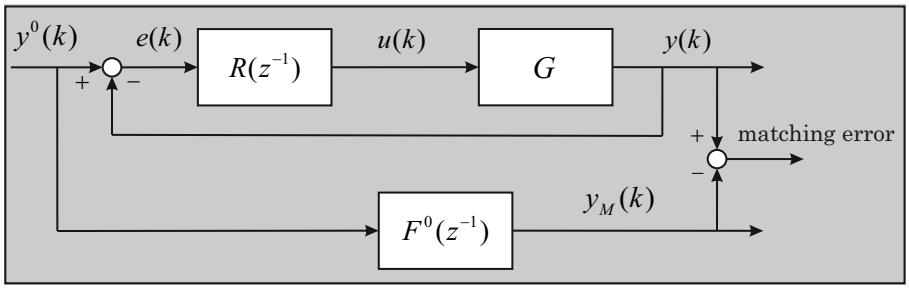

Figure 2.6: VRFT-based control structure for a deterministic system (redrawn based on [GS00])

where

$$\hat{\tilde{u}}(k,\theta) = K\left(z^{-1},\theta\right)\tilde{y}(k), \tag{2.26}$$

$$K\left(z^{-1},\theta\right) = R\left(z^{-1},\theta\right)\left[F^0(z^{-1})^{-1} - 1\right]. \tag{2.27}$$

In literature, the idea of VRFT has been used to control design of SISO and MIMO (nonlinear) systems. In [CS06], the given control method was applied to SISO nonlinear systems. The authors stated that, a global model reference optimization procedure has been implemented. As a result, there was no need to conduct many process experiments as well as to estimate the control cost gradient. In addition, the VRFT method has been extended to a two degree-of-freedom controller configuration [LCS02]. Particularly, in [PSSH04] both of the linear and nonlinear VFRT-based controllers were designed, and the improved control results could be observed in tracking assigned knee angle trajectories. In [RRPP17], a novel combination of MFC and VRFT methods, that leads to three different types of intelligent PID control algorithms namely VRFT-iP, VRFT-iPI, and VRFT-iPID, was introduced. The proposed controllers were implemented experimentally to the angular speed control of servo systems. Regarding to control design of MIMO nonlinear systems, several data-driven control schemes including MFAC, MFC, and VRFT have been designed, and applied successfully to the twin rotor aerodynamic system [RRP16].

2.4 Hybrid data-driven control

Several MFC methods use both on-line system I/O signals calculated at each time step during the system operation as well as the available previous I/O data stored in the database to realize control actions. This group of DDC is called hybrid data-driven control. In this section, two well-developed approaches known as iterative learning control and lazy learning control will be briefly discussed.

2.4.1 Iterative learning control

Iterative learning control (ILC) is an intelligent control approach which can be applied to a class of unknown/uncertain systems. The control objects of ILC are the dynamic systems that operate repetitively over a specified time interval. The fundamentals of ILC is that, based on the tracking control errors and the control input values from previous iterations, the required input in the next iteration-step can be determined. By using only the knowledge from the system data, the learning error convergence can be guaranteed when the total iteration numbers are big enough. The ILC methods utilize both on-line and off-line I/O data to calculate the optimal control input values. The structure of an ILC scheme is relatively simple which includes an integrator in the iteration domain [HJ13].

Regarding design of the basic ILC algorithm, a class of linear continuous-time systems can be represented as

$$\dot{x}_i(t) = Ax_i(t) + Bu_i(t), \tag{2.28}$$
$$y_i(t) = Cx_i(t), \tag{2.29}$$

where A, B, and C are the system, control input, and output matrices, respectively; whilst t is the time-domain variable and i is the iteration-domain variable. Under several prerequisite assumptions as given in [ACM07], the first-order ILC algorithm is defined as

$$u_{i+1}(t) = u_i(t) + \Gamma\dot{e}_i(t), \tag{2.30}$$

where the tracking control error at the iteration i is computed as $e_i(t) = y^d(t) - y_i(t)$. The reference output is denoted as $y^d(t)$, and Γ is a diagonal learning gain matrix. This matrix satisfies the following condition [ACM07]

$$\|I - CB\Gamma\|_j < 1, \tag{2.31}$$

where $j \in \{1, 2, \ldots, \infty\}$, and $\|.\|_j$ is an operator norm.

A PID-like structure of the ILC algorithm can be written as

$$u_{i+1}(t) = u_i(t) + \Phi e_i(t) + \Gamma\dot{e}_i(t) + \Psi \int e_i(t)dt, \tag{2.32}$$

where Φ, Γ, and Ψ are the design learning gain matrices. A basic ILC scheme is illustrated in Figure 2.7.

Many researches related to design of improved ILC strategies for different types of linear or nonlinear systems, have been introduced during the past decades. In [BTA06], a comprehensive review of ILC including the control algorithms, stability, performance, learning transient behavior, and the robustness was provided with

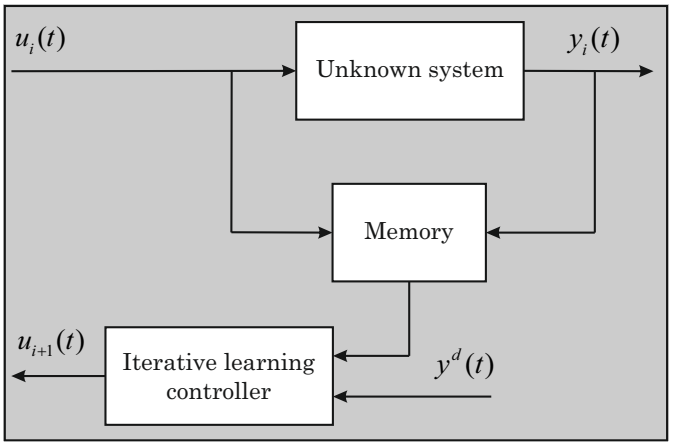

Figure 2.7: Basic ILC scheme (redrawn based on [ACM07])

respect to four ILC design techniques. In addition, three learning-type control approaches namely iterative learning control, repetitive control, and run-to-run control have been discussed by Y. Wang et al. [WGD09]. Learning-type control methods can be classified into two categories: direct-form and indirect-form. Discussions about main theories and how to design controllers were mentioned. Another illustrative example of ILC combined with a conventional feedback controller to improve motion control performance of direct-drive robotic manipulators was presented in [BKdS05]. The authors have considered the flexible dynamics of a robot in the design of ILC algorithm. Additionally, various novel ILC-based programs were proposed on the basis of the standard ILC principle. For example, the main contribution in [Saa05] was related to optimal forgetting matrix and learning gain matrix estimations of a P-type ILC algorithm in the presence of random disturbances and measurement noises. Furthermore, in [XXL05] an unknown system with input deadzone which could be nonlinear and state-dependent was considered. A novel ILC scheme has been designed which can achieve uniform learning convergence. In [JPS13], a norm-optimal iterative learning controller has been investigated for linear time-invariant systems, in which by using the system I/O data from previous iterations, the system impulse response can be estimated and integrated into the controller design. For sampled-data systems, ILC can be applied in the time and frequency domains [AX11]. In [HYY18], a novel ILC approach was proposed by applying the iterative dynamic linearization technique to an unknown ideal nonlinear controller. Hence, an adaptive learning controller with a learning gain, which can be tuned automatically at each system iteration, was conducted. For applications of ILC to nonlinear systems, in [Xu11] the ILC method has been discussed for two categories of nonlinear systems called global and local Lipschitz continuous functions. It can be noted that several open control problems such as observer-based ouput tracking control, ILC applied to infinite-dimensional systems, or partial differential equations are still highly mo-

tivated. When the control systems are nonlinear with unknown parameters which might vary at each iteration, a high-order internal model-based ILC program was presented in [YXH10]. Compared to other existing ILC approaches, the proposed method showed significant improved results. Recently, a high-order optimal iterative learning controller was designed for a class of nonlinear discrete-time systems [CHJH18]. To improve control performance, both of on-line and historical I/O data were used effectively.

2.4.2 Lazy learning control

In 1994, S. Schaal et al. [SA94] designed an intelligent learning control method which is based on system data set (system I/O information) to implement robot learning for challenging dynamic tasks. This control approach utilizes explicitly the system trained data set to build a local dynamic model which contains unknown parameters. In more detail, at every operating point (or query) of the system operation, a subset of data points are used to design a local linearized model. Therfore, different local models are created, and they have to memorize all data. Each local model will be implemented to design of a local controller at every time instant. The mentioned control method is often called memory-based learning control or lazy learning control. One type of the lazy learning techniques namely locally weighted learning, which is based on a locally weighted linear regression, was presented in [Aha97, AMS97]. This local model only requires a subset of training data in a restricted region around the location of the system operating point or a query. It can be noted that, several types of local models for lazy learning control design such as nearest neighbor, weighted average, or locally weighted regression were proposed. Different lazy learning control techniques were also reviewed in [BB04] to deal with the control problems of nonlinear systems. In the group of learning approaches, the lazy learning method requires the I/O data from the controlled system to estimate an approximate system model for control design. Recently, in [HLT17] a novel model-free adaptive predictive controller has been designed by using the lazy learning concept. The unknown time-varying controller parameters can be adjusted adaptively based on on-line and off-line data measurements in the system database.

2.5 Combination of model-based and model-free control

Model-free control can be combined with the well-developed MBC methods to design advanced/robust controllers. In this section, MFAC in combination with the two optimal and robust model-based control strategies namely model predictive control and sliding mode control will be briefly discussed.

2.5.1 Model-free adaptive predictive control

In control engineering theory, to design an appropriate controller for linear or nonlinear systems, the first step should be modeling or identification of the global dynamics of the plant. Then, based on the obtained system mathematical model, many existing control design techniques ranging from classical control to advanced/robust control theories can be applied to generate different control algorithms. This is the fundamentals of MBC theory. On the other hand, MFC or DDC can be an alternative solution to deal with control design of complex and highly nonlinear systems when the system I/O data can be easily measured or calculated. Up to now, many effective MFC approaches for control design of both linear or nonlinear systems have been proposed as reviewed in the preceding sections. Therefore, from the author's point of view, it could be helpful to combine several appealing MBC approaches with MFC to develop advanced and robust model-free control algorithms as well as to improve the model-free control performance. One possibility would be a combination of model predictive control (MPC) and model-free adaptive control (MFAC). In the following texts, several successful examples for a novel kind of MFC called model-free adaptive predictive control (MFAPC) will be briefly reviewed. In [GHLJ19], Y. Guo et al. proposed a novel MFAPC program based on the CFDL concept for a class of MIMO nonlinear systems in discrete-time. By using the MPC theory, the predicted system ouput and control input signals within a finite prediction time horizon were realized. Finally, the required control input values which were implemented to the system have been computed by using only the available system I/O data. Furthermore, based on the main theory of generalized predictive control, an adaptive PI control algorithm was proposed in [THLL99] for SISO nonlinear systems. The unknown controller parameters were estimated by applying a standard recursive least squares identification algorithm. In addition, the author in [Ste99] proposed the concept of model-free predictive control to cope with the existing nonlinear model-based predictive control challenges. The key idea of the proposal is that, instead of identifying a global dynamic model of the controlled plant, the system dynamics could be linearized locally based on the available process data from the database. In [WZWC18], an extended CFDL-based MFAPC has been designed and applied successfully to a MIMO nonlinear system. The experimental results demonstrated that better control performance of the proposed method was derived in comparison with traditional MPC and CFDL-MFAC.

2.5.2 Model-free sliding mode control

In actual control problems, unmodeled dynamics and model uncertainties often lead to a mismatch between the real controlled process and the developed mathematical model [ES98]. To deal with these difficulties, in modern control design many robust/advanced control techniques have been proposed since decades. One of the

most attractive robust control approaches is called sliding mode control (SMC). As introduced in [ES98], variable structure control systems need to be designed properly in SMC via a switching function. Then, a suitable control law is generated to ensure that the system states are attracted by this sliding function. Furthermore, with the development of MFC theories in recent years, it is possible to develop other novel control methods by combination of SMC and MFC. For example, a novel model-free adaptive sliding mode controller was designed in [XSJ18] concerning control input constraints for autonomous car parking systems. In the proposed control program, an on-line model identification strategy based only on the system I/O data, integral SMC algorithm, and dynamic antiwindup compensation algorithm were included to solve integral and actuator saturation problems in the controlled system. Moreover, different adaptive integral sliding mode control schemes subjected to tracking error constraints have been investigated for nonlinear systems [LY19b, LY19a, LY18]. By proposing a new transform error strategy, smaller steady-state errors can be achieved. Furthermore, the overall maximum overshoot was not smaller than a predefined value, and the convergence rate was less than a pre-selected constant. In [WLW$^+$16], SMC and MFAC were combined to constitute a data-driven model-free sliding mode control program for the robotic exoskeleton. To design controller, only the measured input torque and output velocity were implemented to obtain a sliding mode reaching law. Recently, MPC and SMC in combination with the CFDL-based MFAC approach have been proposed for control design of nonlinear discrete-time processes in the presence of unknown disturbances [WH19]. A perturbation estimation technique was applied to estimate the unknown disturbances. It is obvious that, no information about the system dynamic model need to be addressed in the control design of the aforementioned approaches.

2.6 Vibration control of flexible structures

Undesirable vibrations often occur in mechanical flexible structures such as elastic cranes, wind turbines, etc. due to the effects of both internal or external disturbances. These unwanted oscillations may reduce the system performance or even damage the structures if the amplitude and frequency of the disturbance signals are big enough. Therefore, research in different control strategies to suppress or eliminate vibrations in vibrating systems is highly motivated. This section will review several vibration control methods which have been widely applied by control engineers. In particular, a vital vibration control approach namely active vibration control is reviewed. Furthermore, the main context in this section is dedicated to discussion about different control approaches applied to cranes which are represented as a typical mechanical flexible system.

2.6.1 General vibration control methodologies

Generally, three approaches are well-known for vibration mitigation in mechanical flexible systems including: passive, semi-active, and active vibration control. Passive vibration control is normally related to the concepts of isolation and absorption [WN15]. By doing vibration control in passive ways, the process properties, e.g., geometrical parameters (thickness, length, etc.), or material properties (Young modulus, density, etc.), are often modified [Luu15]. Moreover, additional supplement devices called vibration absorbers could be appropriately attached into vibrating systems to reduce their oscillations. In semi-active vibration control, no control actuators are utilized. However, a semi-active element, i.e., a damper is typically applied. It can be interesting to note that, no external energy has to be added to the controlled systems by using the semi-active methods [WN15]. Active vibration control is the method of using design controllers (feedback or feed-forward) to mitigate unwanted vibrations actively; that means, external energy will be provided to the system via actuator devices. As discussed in [Luu15], an active vibration control topology generally includes three separate elements: sensors (to measure the system responses), actuators (to supply necessary external energy to the system), and controllers (to calculate the required input signals to control the system based on the received information from the sensors). Once the controllability and observability of the system are guaranteed, a suitable control algorithm can be designed by using various traditional and modern control approaches. The most important requirements for a vibration controlled system are stability, robustness, and high performance [WN15].

Regarding the state-of-the-art vibration control in flexible systems, some review contributions can be taken into account. To get an overview of vibration mitigation techniques and their applications to a variety of marine offshore structures, a comprehensive review paper has been published recently by R. Kandasamy et al. [KCT+16]. The authors concluded that, semi-active and hybrid vibration control (combining the robustness of the passive and active control methods) were preferable because of their potential implementation. Furthermore, different control approaches for vibration suppression of wind turbines have been discussed in literature. For instance, according to [ROC+15, XA20] vibration control strategies for wind turbine systems can be divided into three categories as mentioned earlier. Moreover, different types of damper devices and system controllers were illustrated in [ROC+15]. In [ZBH20], a review of vibration control methods which are being widely used in engineering structures with a dedication to anti-swing control of wind turbines has been intensively discussed.

2.6.2 Review of active vibration control for cranes

Cranes are machines which have been commonly used to transfer cargo (lifting and moving) from one place to another in ports, factories, building construction, etc.

They also can be equipped in large vessels (normally called ship-mounted cranes) for supporting cargo transportation to smaller ships in open sea. Cranes can be considered as typical flexible systems, in which vibrations are frequently generated due to structure themselves or external disturbance impacts. Crane vibrations are undesirable because they might lead to the system operation suspension. Therefore, development of effective vibration control strategies for cranes is essential. In [RMA+17], a variety of crane types and their configurations together with different control methods which have been widely applied to vibration control and (payload) tracking control within the last two decades were comprehensively reviewed. Establishment of a global crane model is necessary for control design, and this task should be done before a suitable control solution can be proposed. Normally, crane modeling is divided into two groups: single-pendulum and double-pendulum. In term of controller design, many effective strategies were developed and applied successfully to various types of crane systems, e.g., boom cranes, tower cranes, or bridge/gantry cranes [RMA+17]. The developed control approaches can be generally separated into three categories including open-loop, closed-loop, and hybrid-loop (a combination of open-loop and closed-loop), in which model-free or data-driven control should be integrated as a branch of closed-loop control. According to [RMA+17], several well-known control methods for a crane system are illustrated in Figure 2.8. Open-loop control strategies are relatively easy to implement. In contrast, the crane control performance of an open-loop system may be significantly reduced because of external disturbance effects, e.g., wind force or wave motion. Typical open-loop control techniques are selected as input shaping, filtering, and command smoothing. On the other side, nowadays most of common control methods applied to cranes are related to closed-loop control. There is a plenty of linear control techniques such as PID, linear quadratic regulation, state feedback control, etc. as well as nonlinear and/or advanced approaches, e.g., sliding mode control, adaptive control, intelligent control, which achieve high control efficiency, and are able to cope with uncertainties or unknown system perturbation. In recent years, MFC or DDC has been introduced to reduce the efforts of system modeling assignment. Therefore, novel MFC methods can be further investigated and/or combined with other effective MBC approaches to deal with the existing challenges in crane control such as strongly nonlinearities, system uncertainties, disturbance rejection, or computational complexity.

In literature, up to now many existing MBC strategies were utilized to deal with the problems of tracking and anti-sway control for different types of cranes. To control of overhead cranes, in [LFS19] an enhanced-coupling adaptive control program was discussed, in which payload hoisting/lowering as well as uncertain system parameters were integrated in the control algorithm. In [LYZW05, YY07], the adaptive sliding mode fuzzy and nonlinear adaptive controllers were designed, in which the linearized system model was transformed into two submodels for position and vibration control purposes [LYZW05]. In addition, the authors in [SWFC18] proposed a novel adaptive anti-swing control strategy for cranes with double-pendulum swing effects

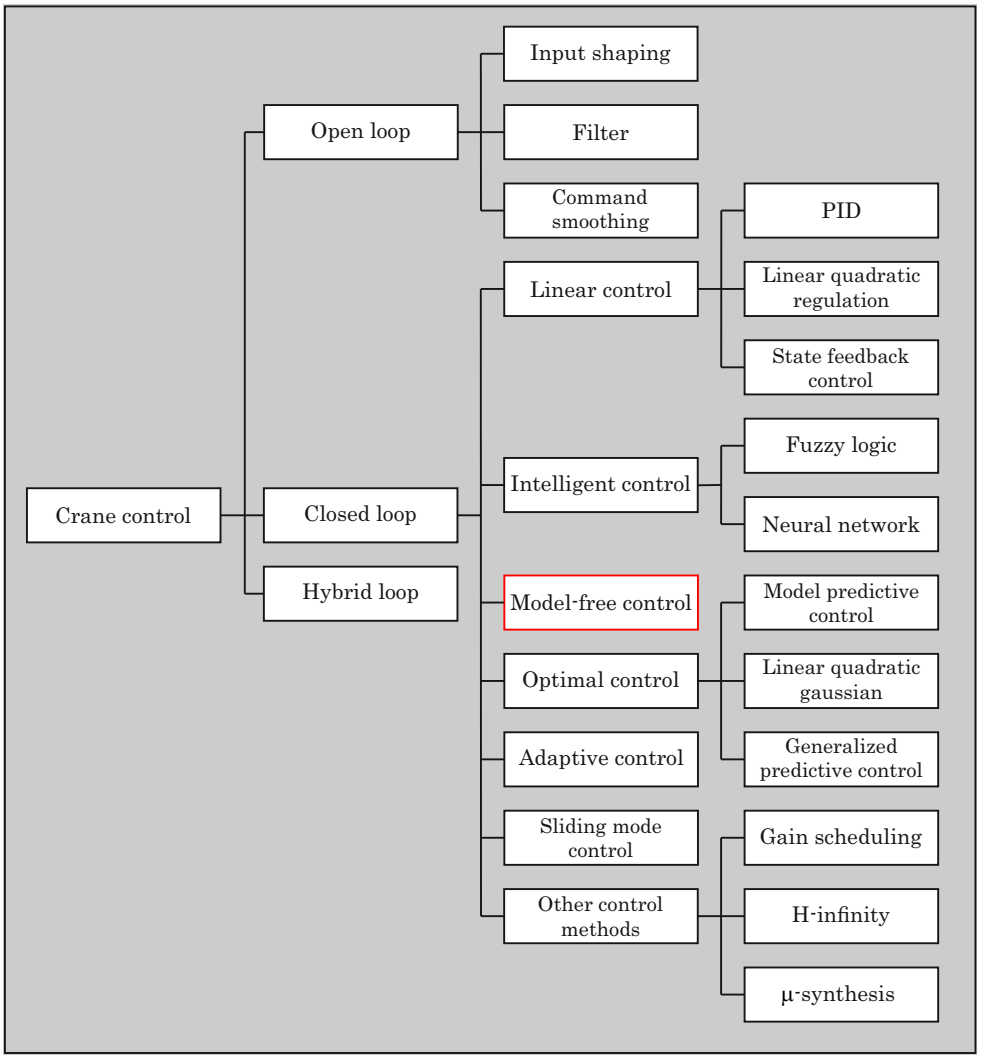

Figure 2.8: Control methods for a crane system (redrawn based on [RMA+17])

and system uncertain/unknown parameters. To design controller, the full nonlinear dynamic equations of the crane system have to be established. However, it was not required to simplify the system dynamics by doing linearization. Moreover, a study on robust model-based control to eliminate structural vibrations of an elastic gantry crane was presented in [GP19]. For control implementation, the crane mathematical model with additional uncertainty models need to be constructed firstly. Then, a robust controller was designed by using the H_∞-loop shaping procedure. In [CFS19], an efficient adaptive control method was introduced, in which a shaped energy-like function has been designed to ensure the closed-loop system stability and robustness in cases of parameter uncertainties and external noise. To study the actual dynamic behavior of a container crane, Z. N. Masoud et al. [MN03] developed

a mathematical model of the crane. Subsequently, a simplified version was used to design a delay feedback controller for the full nonlinear system model. As a robust control technique - sliding mode control (SMC) has been applied to crane control since years. In 2013, Le et al. [LL13] designed two robust controllers to carry out the assignments of payload tracking and anti-swing control of double-pendulum overhead cranes based on the conventional and modified SMC approaches. In addition, a second-order SMC scheme has been proposed by G. Bartolini et al. [BPU02] to deal with the problems of model uncertainties and unmodeled dynamic actuators of container cranes. Furthermore, a novel SMC strategy was discussed in [NH12] for an offshore container crane. The control objective is to suppress oscillations in the crane during its operation. A full dynamic model of the crane system needs to be firstly analyzed. A sliding mode anti-sway control scheme is then developed using the discussed model. Ship-mounted container cranes are represented as a highly under-actuated nonlinear machine. To design robust control for such a system, a novel adaptive control approach which includes a combination of second-order SMC and radial basis function network has been proposed in [LHP+18]. Additionally, the input-shaping control method can also be utilized in crane control, such as for tower crane control [VKS10], or overhead crane control [MA14]. Offshore boom cranes are often mounted on large ships to transfer cargo. Design of controllers for this type of crane normally encounters with some challenges such as unknown system parameters (length cable changes) or external disturbances (wind or sea wave). In [QFL19], an offshore ship-mounted crane was considered for both adaptive and robust tracking control purposes. An accurate mathematical model which concerns wave disturbance effects has been developed successfully. The controlled system was asymptotically stable based on Lyapunov analysis. Vibration control of offshore boom cranes was investigated in [LFSW18, FWSZ14], in which a system model has to be implemented, e.g., by conducting state transformation [LFSW18], or by applying Lagrange's method [FWSZ14]. A novel fuzzy robust control method for offshore ship cranes was introduced in [GC20]. The authors designed a fuzzy composite observer considering actuator fault and lumped disturbance. Based on estimated values, an adaptive control law was generated by applying the SMC technique. As discussed before, MFC/DDC is an intelligent control method which can be applied to crane control. However, from the author's point of view, not so many researches based on this kind of control were conducted in literature. One example is [RPP+19], in which a data-driven MFAC based on the CFDL concept has been proposed. The novel idea in the design control algorithm is that, a proportional-derivative component has been added into the standard MFAC law to improve overall tracking control performance. Another control approach called adaptive repetitive learning control was introduced for an offshore boom crane in [QFL17] which consists of an adaptive law and a learning mechanism. The control results in this contribution demonstrated that, the controlled system stability was guaranteed despite of unknown system parameters as well as external disturbances.

2.7 Discussion from literature review

For the above theoretical background and literature review, several discussions related to different MFC/DDC and vibration control approaches for cranes will be presented in this section.

2.7.1 Discussion about different model-free control methods

In the preceding sections, general information about MBC, MFC/DDC as well as a brief review of different MFC strategies have been discussed. It can be concluded that, the fundamental principle of the data-driven control can be regarded as design of a suitable control scheme for unknown (linear or nonlinear) plants without using any information related to the modeling process, but requiring available system I/O data. That means, in the design controller structure, no information about the system dynamic behaviors is required. However, as mentioned in [HJ13], controller structure is assumed to be known in advance in some methods, e.g., iPID, UC, SPSA, IFT, and VRFT. In these MFC approaches, the controller parameters are typically unknown and time-varying. They should be estimated by using the off-line or on-line I/O data from the controlled system. Therefore, the main difficulties in design of such controllers are parameter identification problem and optimization. They can be solved by a combination of control principles and mathematics. On the other side, in several MFC strategies establishment of a proper controller structure for a given unknown (nonlinear) system is particularly challenged because no system model is involved. However, thank to dynamic linearization techniques including CFDL, PFDL, and FFDL, local linearized data models of the process can be constructed under some pre-required assumptions. MFAC and LLC are two outstanding methods, in which their controller structures are relied on linearized dynamic models as well as certain optimization criterions [HJ13]. In addition, the unknown parameters in the assumed local models should be estimated and updated recursively based on the on-line system data (MFAC) or the off-line system data (LLC).

In Table 2.1, a summary of the introduced MFC/DDC approaches with respects to main characteristics, pre-required assumptions, and applications is illustrated. It can be noted that, for the on-line data-driven control methods such as MFAC, SPSA, UC, and LLC, the controller parameters can be updated adaptively. Conversely, for the other MFC strategies, e.g., iPID, IFT, VRFT, and ILC, no adaptive mechanism in the control structure is given. Furthermore, MFC strategies comparison is presented in Table 2.2 in terms of several major properties. Not many model-free control methods, in which stability analysis has been fully investigated such as MFAC, UC, or ILC. There is lack of closed-loop system stability analysis in most of the off-line data-based DDC approaches until now. Additionally, gradient approximation is explicitly required in MFAC, SPSA, UC, IFT, and LLC. Otherwise, in

Table 2.1: Summary of several MFC approaches with applications

Control method	**Reference**	**Application**	**Pre-required assumptions**	**Main properties**
MFAC	[HCG17, HX19]	Industrial processes; Motor control; Power control	Smooth system nonlinear function; Generalized Lipschitz condition	Applied dynamic linearization techniques; Local system model established; Gradient estimation; Adaptation of system/controller parameters
SPSA	[Spa92, GA15]	Traffic signal control; Wastewater treatment	Fixed controller structure; Global Lipschitz condition	Gradient approximation of control parameters required; Recursively update control parameters; Heavy computation; Slow convergence
UC	[ST97, ST95]	Robot manipulator; Industrial processes	Measurement information; Performance specification; A set of admissible controllers	Controller switching implementation; Controller structure is fixed; Adaptive and robust control strategy
iPID	[ACL05, FJ09]	95% industrial processes	Unknown	Unknown system dynamics replaced by local linearized model; Nonadaption and low computation; Fixed controller structure
IFT	[Hja02, HPJ09]	DC-servo with backlash; Flexible arm; Ball-on-beam; Inverted pendulum; Helicopter model	Fixed controller structure; Closed-loop system is assumed stable	Gradient-based approximation using trial signal; Recursive estimate control parameters; Nonadaption and heavy computation
VRFT	[GS00, CS06]	Robot manipulator; Motion control	Fixed linear controller structure; Reference model is inverse	Global minimization of standard model-reference performance; Controller parameter identification with prescribed structure; No iterations required
ILC	[ACM07, BTA06]	Industrial robots; Induction motors; Autonomous vehicles	Systems operate repetitively; Identical initial conditions; Global Lipschitz condition	Using previous actual system data to improve transient response performance; At each iteration, error information incorporated into control algorithm; Low computation
LLC	[SA94, Aha97]	Robot control; Three-tank liquid level control	Unknown	Local system linearized model established at each operating point; Local controller also designed; Estimated controller parameters adaptively

Table 2.2: Property comparison of different MFC/DDC methods

Properties	**MFAC**	**SPSA**	**UC**	**iPID**	**IFT**	**VRFT**	**ILC**	**LLC**
Data used	On-line	On-line	On-line	Off-line	Off-line	Off-line	On/Off-line	On/Off-line
Trial signal required	No	Yes	No	No	Yes	No	No	No
Time domain	Discrete	Discrete	Continuous	Discrete	Discrete	Discrete	Discrete	Discrete
Gradient estimation required	Yes	Yes	Yes	No	Yes	No	No	Yes
Stability analysis	Yes	No	Yes	No	No	No	Yes	No
Application to	MIMO	SISO	SISO	SISO	MIMO	MIMO	MIMO	SISO
Adaptive property	Yes	Yes	Yes	No	No	No	No	Yes
System type	Nonlinear	Nonlinear	Nonlinear	Linear	Linear	Linear	Nonlinear	Nonlinear
Known controller structure	No	Yes	Yes	Yes	Yes	Yes	Yes	No
Combination with MBC	Yes	Unknown	Unknown	Yes	Unknown	Unknown	Yes	Unknown

other approaches like iPID, VRFT, and ILC, the control input signals or controller parameters can be determined directly based on the available system information.

From the observed literature study, MFAC witnesses as one of the most effective data-driven control methods which can be designed properly to adapt with MIMO and nonlinear plants. A systematic framework of MFAC has been developed for both controller design and performance analysis [HJ13]. Moreover, the MFAC method can be combined with other useful MBC strategies, e.g., model predictive control or sliding mode control, that have been discussed in Section 2.5 with successful applications. However, some open points for research in the field of MFC/DDC, particularly in MFAC are still remaining. For example, on-line parameter estimation algorithms could be further investigated to improve estimation accuracy. To improve the MFAC tracking control performance, modifications are possibly implemented such as considering minimization of the control error variations in the control objective function. MFAC and MPC can also be considered together for development of modified model-free adaptive predictive control strategies by using different dynamic linearization techniques. Finally, as discussed in Section 2.2 MFAC has not been widely applied to MIMO (nonlinear) systems/processes, in particular to mechanical flexible structures for vibration reduction purpose. From the aforementioned reasons, a research gap between the current developed MFAC and a high performance oriented-MFAC to deal with vibration mitigation of MIMO flexible systems is defined. This thesis will concentrate on development of different improved MFAC schemes which can be effectively applied to vibration control of complex and flexible systems such as cranes. The recursive least-squares method which has not been widely considered

in literature will be intensively discussed in MFAC. In addition, design of modified MFAPC based on the CFDL and PFDL concepts for a class of MIMO nonlinear systems is motivated. Furthermore, modified control input calculation can be done by minimizing not only the upcoming output errors, but also the error variations within a fixed length of time interval in the past. Therefore, research in MFAC and its modifications could be an interesting topic.

2.7.2 Discussion about vibration control methods for cranes

As mentioned before, crane is represented as a typical flexible structure, in which vibrations of the elastic boom (for boom cranes) and/or the payload normally occur during its operation. These oscillations are unwanted because they might lead to suspension of the system. In Section 2.6, general information about (active) vibration control, especially a review of different control design methods applied to various types of crane have been addressed. For active vibration control of cranes, many approaches have been proposed since decades ranging from open-loop control to closed-loop control. Additionally, both of the traditional control approaches such as PID, linear quadratic regulation, etc. as well as the robust/advanced control strategies, e.g., adaptive control, sliding mode control, model predictive control, are briefly discussed. A comparison of the given vibration control methods for cranes is summarized in Table 2.3. Generally speaking, the open-loop control schemes such as input shaping, filtering, and command smoothing are with relatively simple structures, and easy to be implemented in practice. In addition, because of no feedback signals required for control design, they are also cheaper than others. However, to deal with several challenges in reality of the crane operation, e.g., model uncertainties, parameter changing, or unknown external perturbations, an adaptive mechanism could be integrated in the design robust open-loop controller [RMA$^+$17]. For the closed-loop vibration control of cranes, it can be seen that most of the discussed approaches require a global mathematical model of the system dynamics. For instance, in the linear quadratic regulator method, a linearized crane model (i.e., a state-space model) has to be derived. Afterwards, a suitable control law will be designed properly. Other advanced control methods namely adaptive control, model predictive control, or sliding mode control can deal with the problems of system parameter variations as well as unknown disturbance effects. However, in all of them a fully investigated (nonlinear) system model is necessary. For future research, the mentioned well-developed advanced control methodologies can be combined with other control theories, possibly in MBC or MFC, to improve vibration control and tracking control performance. Recently, intelligent control methods are quickly developed. Some of them are summarized in Table 2.3 including neural network and fuzzy logic control. It can be noted that, an accurate model of the controlled crane is assumed to be unknown when using intelligent control. Thus, a fuzzy model or a neural network model should be created instead. Therefore, they can be used for

control design of nonlinear systems. Additionally, the intelligent control approaches can be incorporated with other robust control strategies such as sliding mode control to obtain high efficiency and robustness. From the author's point of view, the discussed MFC/DDC methods in this chapter have not been widely applied to crane control, particularly in vibration reduction/suppression of cranes. In this thesis, MFAC with several feasible architectures shall be further explored, and applied to vibration reduction of elastic cranes. This is also the main objective of the thesis.

2.8 Summary

In this chapter, the fundamentals of several MFC/DDC approaches with classification have been reviewed. Four separate categories related to MFC including the on-line, off-line, hybrid data usage, and MBC combined with MFC groups, with the total of ten control strategies are briefly surveyed. In each of the selected MFC method, main (original) control ideas behind, control design strategies together with several outstanding applications or related works have been illustrated. In addition, vibration control of mechanical flexible systems dedicated to active vibration control methodologies for cranes are discussed carefully. Finally, discussion based on the literature review has been made. The model-free adaptive control approach with its dominated advantages have been selected for further research. Several improved model-free adaptive controllers can be designed and applied to reduce the undesirable vibrations of an elastic ship-mounted crane represented as a typical boom crane topology [PS19a].

[3]Finite Impulse Response
[4]Infinite Impulse Response
[5]Recurrent Neural Network
[6]Feedforward Neural Network

Table 2.3: Comparison of existing control approaches for cranes

Control method	**Reference**	**Application**	**Control type**	**Disadvantages**	**Main features/advantages**
Input shaping	[Sin09]	Gantry crane; Overhead crane; Tower crane; Container crane	Open-loop	Sensitive to external disturbances; Affected by system parameter variations	Convolving command input signal with impulses; Measure sensors not required; Fast to suppress vibration
Filtering	[GA07]	Rotary crane; Gantry crane; Boom crane; Overhead crane	Open-loop	IIR filters are difficult to control; Sensitive to external disturbances	Filters used for preconditioning input command signals; Including FIR[3] and IIR[4] filters; Real-time applications are possible
Command smoothing	[XHL13]	Bridge crane; Tower crane; Overhead crane	Open-loop	Cannot reject external disturbances; Only operating by human operator	Reduce vibrations by smoothing original command; Design a smoother based on system natural frequency and damping ratio
Linear quadratic regulator	[SOYU11]	Overhead crane; Boom crane	Closed-loop	Required linearized crane mathematical model; Nonlinear factors, e.g. wind, load mass not included	Simple control algorithms; Robustness of controller can be guaranteed
Model predictive control	[WXZ15]	Overhead crane; Boom crane; Tower crane	Closed-loop	Accurate system model required; System uncertainties are challenged	Optimal control input derived in case of constraints; Closed-loop stability assurance; Robustness against parametric uncertainties
Adaptive control	[ZMR+16]	Overhead crane; Tower crane	Closed-loop	System dynamic model has to be fully described; Complexity of control algorithms	Ability to estimate unknown parameters; System is asymptotically stable even with external disturbances
Neural network	[DUKY12]	Overhead crane; Tower crane; Shipboard crane	Closed-loop	Hard to develop convenient learning algorithm by using RNN[5]; FNN[6] is static network and lack of dynamic memory	Good nonlinear processing ability and robustness; Suitable to utilize global optimization
Fuzzy logic control	[Smo14]	Gantry crane; Overhead crane; Tower crane	Closed-loop	Lack of implementations in large-scale cranes	Accurate system model is not required; A fuzzy model is established; Ability to deal with unstable and nonlinear systems
Sliding mode control	[LL13]	Overhead crane; Container crane; Offshore crane	Closed-loop	Chattering might occur; Accurate mathematical model is required	Effective under uncertain conditions; Accurate and robust method; Could be combined with other methods for more precision and robustness

3 On-line parameter estimation-based model-free adaptive control

The MFAC approach has been selected for further research in this thesis. In this chapter, the main theory of MFAC which was initially developed by Z. Hou et al. [HJ13] for a class of SISO and MIMO nonlinear systems is discussed. Additionally, in this work, several MFAC modifications with respects to on-line parameter estimation and control input calculation are proposed. Furthermore, to demonstrate control effectiveness, application of the design MFAC strategies to a crane for vibration control purpose will be presented.

In Section 3.1, MFAC based on the projection algorithm will be briefly discussed for a general SISO nonlinear system. Then, the obtained algorithm is extended to the linearized data model of a class of MIMO nonlinear systems. To improve the performance of the parameter estimation process, the recursive least-squares algorithm is applied to both SISO and MIMO systems in Section 3.2. Moreover, an improved model-free controller is designed by proposing a modified objective function of the control input. Subsequently, in Section 3.3, vibration control results and discussion of an elastic ship-mounted crane subjected to the non-zero initial excitation of the payload are presented in case of using the proposed control programs. Finally, the main ideas of the chapter will be summarized in the last section.

The content, figures, and tables in this chapter are mainly based on the peer-reviewed conference papers [PS19a], [PS19b], and [PS20a]. Some of them have been partly modified in this chapter after previous publications.

3.1 Model-free adaptive control using projection algorithm

This section reviews the standard MFAC which is based on the projection algorithm [GS14]. First, the given on-line parameter estimation method is discussed for general unknown SISO systems. Then, the approach will be applied to a local linearized model of a class of MIMO nonlinear systems. Finally, the recursive least-squares algorithms of the system parameters as well as control input calculations are also presented.

3.1.1 On-line parameter estimation algorithms

As discussed in Chapter 2, accurate parameters of an unknown (nonlinear) dynamic system are normally difficult to be determined by using the first-principle methods (the laws of physics, chemistry, etc.) due to unknown disturbances, unmodeled dynamics, or nonlinearities. Another strategy to identify system dynamics is called

parameter estimation [GS14], in which a variety of on-line or off-line estimation algorithms can be implemented depending on the available system I/O data. In off-line parameter estimation, all of the system data should be collected and stored for the system dynamic analysis. There is no strict time limit on the process of analysis. Conversely, in on-line case, the unknown system parameters will be updated recursively by applying the newly calculated or measured system I/O information to the estimation algorithms. In model-free (adaptive) control, on-line parameter estimation methods are necessary, in which the unknown system parameters of a linearized dynamic model should be estimated and updated repeatedly within a specified sampling interval (or step-size). The sequential system input-output values will be used with the parameter estimation algorithms.

According to [GS14], a general structure of on-line parameter estimation for SISO nonlinear systems can be described in a recursive formula as

$$\hat{\phi}(k) = f\left(\hat{\phi}(k-1), D(k), k\right), \tag{3.1}$$

where $f(\ldots)$ is an algebraic function. Different structures of $f(\ldots)$ lead to different parameter estimation algorithms; while $\hat{\phi}(k), \hat{\phi}(k-1)$ indicate the estimated system parameters at discrete-time step k and $k-1$, respectively. The previous system I/O data are denoted as $D(k)$ which consists of the available inputs $U(k)$ and outputs $Y(k)$ from initial step ($k = 1$) up to current step (k)

$$D(k) = \{y(k), y(k-1), \ldots, u(k), u(k-1), \ldots\}. \tag{3.2}$$

A typical form of (3.1) that is generally used in practice is

$$\hat{\phi}(k) = \hat{\phi}(k-1) + G(k-1)\bar{\psi}(k-d)\bar{e}(k), \tag{3.3}$$

where $G(k-1)$ indicates an algorithm gain (or a gain matrix); whereas $\bar{\psi}(k-d)$ represents a regression vector composed of the input and output information from $D(k-d)$ in (3.2), with an integer d. Meanwhile, $\bar{e}(k)$ denotes a modeling error or the difference between the actual system output and the model output resulted by using the previous estimated parameter $\hat{\phi}(k-1)$. Based on the simplified equation 3.3, several on-line parameter estimation algorithms will be investigated in the upcoming sections.

In literature, an input-output description for a class of SISO linear or nonlinear dynamic systems can be written as

$$y(k) = \theta^T(k-1)\phi_0, \tag{3.4}$$

where $y(k)$ denotes the current system output (scalar); while $\theta(k-1)$ denotes the known linear or nonlinear data function of the previous input and output values

$$\begin{aligned} Y(k-1) &= \{y(k-1), y(k-2), \ldots\}, \\ U(k-1) &= \{u(k-1), u(k-2), \ldots\}, \end{aligned} \tag{3.5}$$

and ϕ_0 is a vector of unknown model parameters. To establish a parameter estimation algorithm for the linearized model (3.4), the following objective function [GS14] needs to be considered as

$$J = \frac{1}{2}\left\|\hat{\phi}(k) - \hat{\phi}(k-1)\right\|^2 + \lambda\left[y(k) - \theta^T(k-1)\hat{\phi}(k)\right], \tag{3.6}$$

where the term of $\left[y(k) - \theta^T(k-1)\hat{\phi}(k)\right]$ denotes the modeling error, and λ is a design weighting parameter. To minimize function J, the necessary conditions [GS14] are fulfilled as

$$\frac{\partial J}{\partial \hat{\phi}(k)} = 0, \tag{3.7}$$

$$\frac{\partial J}{\partial \lambda} = 0. \tag{3.8}$$

Therefore, by taking the partial derivatives of J, the above equations become

$$\hat{\phi}(k) - \hat{\phi}(k-1) - \lambda\theta(k-1) = 0, \tag{3.9}$$

$$y(k) - \theta^T(k-1)\hat{\phi}(k) = 0. \tag{3.10}$$

By substituting (3.9) into (3.10), the following equations are obtained as

$$y(k) - \theta^T(k-1)\left[\hat{\phi}(k-1) + \lambda\theta(k-1)\right] = 0, \tag{3.11}$$

$$\lambda = \frac{y(k) - \theta^T(k-1)\hat{\phi}(k-1)}{\theta^T(k-1)\theta(k-1)}. \tag{3.12}$$

From equations (3.12) and (3.9), a recursive parameter estimation equation called projection algorithm for unknown SISO systems is derived as

$$\hat{\phi}(k) = \hat{\phi}(k-1) + \frac{\theta(k-1)\left[y(k) - \theta^T(k-1)\hat{\phi}(k-1)\right]}{\theta^T(k-1)\theta(k-1)}. \tag{3.13}$$

In practice, to avoid the denominator of (3.13) equals to zero, an alternative algorithm is normally used as

$$\hat{\phi}(k) = \hat{\phi}(k-1) + \frac{\eta\theta(k-1)\left[y(k) - \theta^T(k-1)\hat{\phi}(k-1)\right]}{\mu + \theta^T(k-1)\theta(k-1)}, \tag{3.14}$$

where $0 < \eta < 1$ and $\mu > 0$ are step-size constants. The known initial system parameter is denoted as $\hat{\phi}(0)$. The estimation equation (3.14) has the same structure as (3.3). In the next subsection, the projection algorithm will be discussed for a class of unknown MIMO nonlinear systems by introducing another dynamic linearization technique.

3.1.2 Compact-form dynamic linearization technique

The main idea of the model-free adaptive control method is that, instead of modeling or identifying a precise mathematical model of the unknown system dynamic behaviors, different dynamic linearization techniques including CFDL, PFDL, or FFDL (as interpreted in Chapter 2) can be applied to establish equivalent linearized plant models. In this subsection, the existing MFAC approach based on the CFDL concept [HJ13] is reviewed for MIMO (nonlinear) systems. The core idea is that, at every sampling interval k of the system operation, a linearized data model of the original nonlinear system will be established which contains a matrix of unknown time-varying parameters. These parameters can be corrected and updated continuously by using only the closed-loop system I/O data. Subsequently, the discussed results will be utilized to design a modified MFAC scheme for a class of MIMO nonlinear systems in the upcoming section.

Considering a class of unknown MIMO nonlinear systems, a general I/O representation can be described in discrete-time as

$$\mathbf{y}(k+1) = g\left(\mathbf{y}(k), \mathbf{y}(k-1), \ldots, \mathbf{y}(k-m_y), \mathbf{u}(k), \mathbf{u}(k-1), \ldots, \mathbf{u}(k-m_u)\right), \quad (3.15)$$

where $\mathbf{y}(k) \in R^r, \mathbf{u}(k) \in R^m$ denote the actual system outputs and control inputs at current step k, respectively. Here, the unknown system orders are symbolized as the two positive integers m_y and m_u. Meanwhile, the number of system inputs and outputs are the two known integers denoted as m and r, correspondingly. The unknown nonlinear vector-valued function $g(\ldots)$ consists of the previous system inputs and outputs.

Following [HJ11a], two reasonable assumptions have to be considered for the system (3.15) to generate an equivalent dynamical form of the original nonlinear system.

Assumption 3.1: The partial derivatives of $g(\ldots)$ with respect to the control input vector $\mathbf{u}(k)$ exist and are considered as smooth.

Assumption 3.2: The generalized Lipschitz condition

$$\|\mathbf{y}(k+1) - \mathbf{y}(k)\| \leq b \|\mathbf{u}(k) - \mathbf{u}(k-1)\|, \quad (3.16)$$

is satisfied for the system (3.15) at each sampling time k with $\|\Delta\mathbf{u}(k)\| \neq 0$, where $\Delta\mathbf{y}(k+1) = \mathbf{y}(k+1) - \mathbf{y}(k)$, $\Delta\mathbf{u}(k) = \mathbf{u}(k) - \mathbf{u}(k-1)$, and b as a positive constant. Assumption 3.2 defines an upper limitation on the change rate of the system outputs driven by the change rate of the control inputs.

Theorem 3.1 *Based on the aforementioned assumptions, the unknown system* (3.15) *can be linearized locally at every step of the system operation. The simplified model called compact-form dynamic linearization (CFDL) data model is described as*

$$\Delta \boldsymbol{y}(k+1) = \Phi(k) \Delta \boldsymbol{u}(k), \quad (3.17)$$

where the matrix of unknown time-varying system parameters $\Phi(k)$ *or pseudo-jacobian matrix (PJM) can be estimated and updated repeatedly.*

The structure of the PJM in MIMO case is given as

$$\Phi(k) = \begin{bmatrix} \phi_{11}(k) & \phi_{12}(k) & \phi_{13}(k) & \dots & \phi_{1m}(k) \\ \phi_{21}(k) & \phi_{22}(k) & \phi_{23}(k) & \dots & \phi_{2m}(k) \\ \vdots & \vdots & \vdots & \ddots & \vdots \\ \phi_{r1}(k) & \phi_{r2}(k) & \phi_{r3}(k) & \dots & \phi_{rm}(k) \end{bmatrix}_{r\times m}, \tag{3.18}$$

assuming $\|\Phi(k)\| \leq b$ according to assumption 3.2; that means the PJM $\Phi(k)$ is upper bounded at any time-step k. It can be seen that each element value $\phi_{ij}(k)$ in (3.18), with $i \in [1, r]\,; j \in [1, m]$ is the pseudo-partial derivative (PPD) as discussed in [Mad19] for SISO nonlinear systems. In case of the sampling interval and control input increment vector $\Delta\mathbf{u}(k)$ are not too large, the PJM $\Phi(k)$ can be considered as slowly time-varying.

Proof 3.1 As already discussed for SISO case (see [Mad19]), based on the definition of $\Delta\mathbf{y}(k+1)$ and the system (3.15), the system output increment vector is expressed as

$$\begin{aligned} \Delta\mathbf{y}(k+1) &= g(\mathbf{y}(k), \dots, \mathbf{y}(k-m_y), \mathbf{u}(k), \mathbf{u}(k-1), \dots, \mathbf{u}(k-m_u)) \\ &- g(\mathbf{y}(k), \dots, \mathbf{y}(k-m_y), \mathbf{u}(k-1), \mathbf{u}(k-1), \dots, \mathbf{u}(k-m_u)) \\ &+ g(\mathbf{y}(k), \dots, \mathbf{y}(k-m_y), \mathbf{u}(k-1), \mathbf{u}(k-1), \dots, \mathbf{u}(k-m_u)) \\ &- g(\mathbf{y}(k-1), \dots, \mathbf{y}(k-m_y-1), \mathbf{u}(k-1), \mathbf{u}(k-2), \dots, \mathbf{u}(k-m_u-1)). \end{aligned} \tag{3.19}$$

By denoting

$$\begin{aligned} \Upsilon(k) &= g(\mathbf{y}(k), \dots, \mathbf{y}(k-m_y), \mathbf{u}(k-1), \mathbf{u}(k-1), \dots, \mathbf{u}(k-m_u)) \\ &- g(\mathbf{y}(k-1), \dots, \mathbf{y}(k-m_y-1), \mathbf{u}(k-1), \mathbf{u}(k-2), \dots, \mathbf{u}(k-m_u-1)), \end{aligned} \tag{3.20}$$

(3.19) is rewritten as

$$\Delta\mathbf{y}(k+1) = \frac{\partial g}{\partial \mathbf{u}(k)}\Delta\mathbf{u}(k) + \Upsilon(k), \tag{3.21}$$

according to assumption 3.1 and the differential mean value theorem [HJ11a]. The partial derivative values of $g(\dots)$ with respect to the control input $\mathbf{u}(k)$ are described as

$$\partial g/\partial \mathbf{u}(k) = \begin{bmatrix} \frac{\partial g_1}{\partial \mathbf{u}_1(k)} & \frac{\partial g_1}{\partial \mathbf{u}_2(k)} & \frac{\partial g_1}{\partial \mathbf{u}_3(k)} & \cdots & \frac{\partial g_1}{\partial \mathbf{u}_m(k)} \\ \frac{\partial g_2}{\partial \mathbf{u}_1(k)} & \frac{\partial g_2}{\partial \mathbf{u}_2(k)} & \frac{\partial g_2}{\partial \mathbf{u}_3(k)} & \cdots & \frac{\partial g_2}{\partial \mathbf{u}_m(k)} \\ \vdots & \vdots & \vdots & \ddots & \vdots \\ \frac{\partial g_r}{\partial \mathbf{u}_1(k)} & \frac{\partial g_r}{\partial \mathbf{u}_2(k)} & \frac{\partial g_r}{\partial \mathbf{u}_3(k)} & \cdots & \frac{\partial g_r}{\partial \mathbf{u}_m(k)} \end{bmatrix}. \tag{3.22}$$

For every fixed step k, the following equation should be considered by using a numerical matrix $\mathbf{M}(k)$ with r rows and m columns

$$\Upsilon(k) = \mathbf{M}(k)\Delta\mathbf{u}(k). \tag{3.23}$$

Considering the condition $\|\Delta\mathbf{u}(k)\| \neq 0$, (3.23) must have at least one solution $\mathbf{M}^*(k)$. Therefore, the obtained equation (3.21) can be rewritten as

$$\Delta\mathbf{y}(k+1) = (\underbrace{\frac{\partial g}{\partial\Delta\mathbf{u}(k)} + \mathbf{M}^*(k)}_{\Phi(k)})\Delta\mathbf{u}(k), \tag{3.24}$$

where $\|\Phi(k)\| \leq b$ as the result of assumption 3.2. Hence, the theorem 3.1 has been proven.

When the original system is multi-input single-output (MISO) with $\mathbf{u}(k) \in R^m, y(k) \in R$, the I/O system description can be expressed as

$$y(k+1) = g^*(y(k), \ldots, y(k-m_y), \mathbf{u}(k), \mathbf{u}(k-1), \ldots, \mathbf{u}(k-m_u)), \tag{3.25}$$

where $g^*(\ldots)$ is an unknown nonlinear function.

The system (3.25) satisfying two additional assumptions as introduced in [HJ13], with $\|\Delta\mathbf{u}(k)\| \neq 0$ could be expressed in the following CFDL data-driven structure as

$$\Delta y(k+1) = \Phi_c(k)\Delta\mathbf{u}(k), \tag{3.26}$$

where the time-varying parameter vector $\Phi_c(k) \in R^m$ called pseudo-gradient (PG). It is interesting to note that the PG $\Phi_c(k)$ in MISO case is a special case of the PJM $\Phi(k)$ in the MIMO linearization data model (3.17).

As discussed in [HJ13], the dynamics of the PJM matrix $\Phi(k)$ in (3.17) could not be interpreted mathematically because of a variety of possible complicated characteristics such as nonlinearities, unmodeled dynamics, or time-varying structure. On the other hand, the PJM behavior is easy to be determined numerically. Therefore, it can be estimated by using different existing parameter estimation algorithms. In Figure 3.1, an explanation of the PJM is illustrated graphically for the simple MIMO nonlinear system $\mathbf{y}(k+1) = g(\mathbf{u}(k))$ [HJ13]. It can be seen that the derivative values of the nonlinear function $g(\ldots)$ are assumed to be represented by the PJM $\Phi(k)$ at a certain time-step between $\mathbf{u}(k)$ and $\mathbf{u}(k-1)$. The unknown dynamic behavior of the original system is approximated by the blue-dashed line at every sampling period during the system operation (see Figure 3.1). The necessary condition is that, the derivative values of the nonlinear function $g(\ldots)$ do not change quickly; that means the PJM values are bounded.

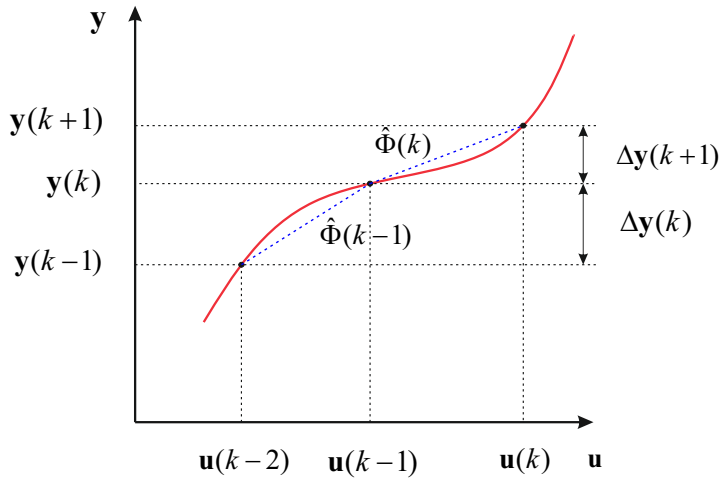

Figure 3.1: Geometric interpretation of the system parameters PJM (redrawn based on [HJ13])

3.1.3 Projection algorithm-based MFAC design

To design MFAC for a class of unknown MIMO nonlinear systems, the CFDL technique as discussed in the previous subsection can be applied to linearize the system dynamics. In addition, the unknown time-varying parameter matrix $\Phi(k)$ in the CFDL data model (3.17) needs to be updated continuously. In this subsection, the discussed projection algorithm in (3.13) or (3.14) will be extended to the MIMO nonlinear system (3.15). Based on the estimated PJM $\hat{\Phi}(k)$, a standard projection algorithm-based MFAC scheme can be designed. The stability and convergence of the closed-loop system are guaranteed under several reasonable assumptions [HJ13].

In case the number of control inputs and system outputs are identical ($m = r = n^*$), the PJM $\Phi(k)$ in (3.17) becomes a squared matrix. For system stability analysis, another assumption [HJ11a] has to be satisfied as

Assumption 3.3: The matrix PJM $\Phi(k)$ satisfies the diagonally dominant condition with the following boundaries $|\phi_{ij}(k)| \leq c_1; c_2 \leq |\phi_{ii}(k)| \leq \alpha c_2$, with $i, j = 1, 2, \ldots, n^*$; $i \neq j$; $\alpha \geq 1$, and the sign of all elements in $\Phi(k)$ is fixed. The two positive constants c_1, c_2 satisfy $c_2 > c_1 (2\alpha + 1) (n^* - 1)$. As interpreted in [HJ13], assumption 3 illustrates the relationship between the input and output data of the closed-loop system in case of the input coupling is not too large. When the I/O data of the controlled system are rich and accurate enough, the coupling among the system variables can be described via the diagonal dominant matrix $\Phi(k)$.

CFDL-based projection algorithm

The on-line parameter estimation algorithm of the PJM $\Phi(k)$ can be derived by minimizing the modeling errors between the actual (calculated or measured) system outputs $\mathbf{y}(k)$ and the model outputs $\mathbf{y}^m(k)$. To restrict a large variation of $\Phi(k)$, a constant weighting factor $\mu > 0$ is added. The objective function of the PJM is written as

$$J\left(\Phi(k)\right) = \|\mathbf{y}(k) - \mathbf{y}^m(k)\|^2 + \mu\|\Phi(k) - \Phi(k-1)\|^2, \tag{3.27}$$

where the model output vector $\mathbf{y}^m(k)$ can be replaced by the linearized CFDL data model

$$\mathbf{y}^m(k) = \mathbf{y}(k-1) + \Phi(k)\Delta\mathbf{u}(k-1). \tag{3.28}$$

The control input increment vector in (3.28) is defined as $\Delta\mathbf{u}(k-1) = \mathbf{u}(k-1) - \mathbf{u}(k-2)$. Substituting (3.28) in (3.27) leads to the cost function

$$J\left(\Phi(k)\right) = \|\mathbf{y}(k) - \mathbf{y}(k-1) - \Phi(k)\Delta\mathbf{u}(k-1)\|^2 + \mu\|\Phi(k) - \Phi(k-1)\|^2. \tag{3.29}$$

By minimizing (3.29) with respect to $\Phi(k)$, the following equations

$$\begin{aligned}
&\frac{\partial J}{\partial(\Phi(k))} = \left[\mathbf{y}(k) - \mathbf{y}(k-1) - \Phi(k)\Delta\mathbf{u}(k-1)\right]\left(-\Delta\mathbf{u}^T(k-1)\right) \qquad (3.30)\\
&+ \mu\left[\Phi(k) - \Phi(k-1)\right] = 0,\\
&\hat{\Phi}(k) = \hat{\Phi}(k-1) \qquad (3.31)\\
&+ \left[\Delta\mathbf{y}(k) - \hat{\Phi}(k-1)\Delta\mathbf{u}(k-1)\right]\Delta\mathbf{u}^T(k-1)\left[\mu\mathbf{I} + \Delta\mathbf{u}(k-1)\Delta\mathbf{u}^T(k-1)\right]^{-1},
\end{aligned}$$

are derived, where the output increment vector is $\Delta\mathbf{y}(k) = \mathbf{y}(k) - \mathbf{y}(k-1)$, and $\mathbf{I}$ is an identity matrix.

Equation (3.31) can be simplified by the following equation

$$\hat{\Phi}(k) = \hat{\Phi}(k-1) + \frac{\eta\left[\Delta\mathbf{y}(k) - \hat{\Phi}(k-1)\Delta\mathbf{u}(k-1)\right]\Delta\mathbf{u}^T(k-1)}{\mu + \|\Delta\mathbf{u}(k-1)\|^2}, \tag{3.32}$$

where $\eta \in (0, 1]$ denotes a step-size constant, and $\hat{\Phi}(k)$ as described in (3.18) is the estimated PJM of $\Phi(k)$. Equation (3.32) is called CFDL-based projection algorithm (CFDL-PA) [HJ13] which can be used to recursively update the system parameters $\Phi(k)$ at every sampling instant k. It should be noted that the algorithm (3.32) has the same structure with (3.3), in which the modeling error is denoted as $\bar{e}(k) = \Delta\mathbf{y}(k) - \hat{\Phi}(k-1)\Delta\mathbf{u}(k-1)$, and a regression vector of the previous system I/O data is $\bar{\psi}(k-d) = \Delta\mathbf{u}(k-1)$.

Design of CFDL-PA-based MFAC

For control realization, the goal here is to minimize the upcoming tracking errors between the desired output values (or references) $\mathbf{y}^d(k+1)$ and the actual system outputs $\mathbf{y}(k+1)$ considering input energy limitation by introducing a weighting factor λ. Therefore, the objective function of the control input $\mathbf{u}(k)$ is considered as

$$J(\mathbf{u}(k)) = \left\|\mathbf{y}^d(k+1) - \mathbf{y}(k+1)\right\|^2 + \lambda\|\mathbf{u}(k) - \mathbf{u}(k-1)\|^2. \tag{3.33}$$

A constant parameter $\lambda > 0$ needs to be added to limit the change rate of the required control inputs. To calculate $\mathbf{u}(k)$, the upcoming system output vector $\mathbf{y}(k+1)$ in (3.33) should be replaced by the linearized CFDL data model (3.17)

$$\mathbf{y}(k+1) = \mathbf{y}(k) + \Phi(k)\Delta\mathbf{u}(k). \tag{3.34}$$

Hence, the above cost function can be rewritten as

$$J(\mathbf{u}(k)) = \left\|\mathbf{y}^d(k+1) - \mathbf{y}(k) - \Phi(k)\Delta\mathbf{u}(k)\right\|^2 + \lambda\|\Delta\mathbf{u}(k)\|^2. \tag{3.35}$$

By minimizing (3.35) with respect to $\Delta\mathbf{u}(k)$, the following equations

$$\frac{\partial J}{\partial \Delta\mathbf{u}(k)} = \left[\mathbf{y}^d(k+1) - \mathbf{y}(k) - \Phi(k)\Delta\mathbf{u}(k)\right]\left(-\Phi^T(k)\right) + \lambda\Delta\mathbf{u}(k) = 0, \tag{3.36}$$

$$\mathbf{u}(k) = \mathbf{u}(k-1) + \left[\hat{\Phi}^T(k)\hat{\Phi}(k) + \lambda\mathbf{I}\right]^{-1}\hat{\Phi}^T(k)\left[\mathbf{y}^d(k+1) - \mathbf{y}(k)\right], \tag{3.37}$$

are obtained. In practical applications, to avoid matrix inversion calculation in (3.37) which could be challenging when the system input and output dimensions are big enough, a simplified control input law [HJ13] is considered as

$$\mathbf{u}(k) = \mathbf{u}(k-1) + \frac{\rho\hat{\Phi}^T(k)\left[\mathbf{y}^d(k+1) - \mathbf{y}(k)\right]}{\lambda + \left\|\hat{\Phi}(k)\right\|^2}, \tag{3.38}$$

where $\rho \in (0, 1]$ is a step-size constant. The unknown system parameter matrix $\Phi(k)$ can be estimated continuously by using the discussed CFDL-PA (3.32). As mentioned in [HJ11a], suitable choice of parameters λ and ρ in (3.38) can improve the model-free control performance and guarantee the closed-loop system stability as well.

3.2 Recursive least-squares-based model-free adaptive control

In this section, first another well-known on-line parameter estimation method namely recursive least-squares algorithm [GS14, ÅW08] is discussed for both unknown SISO and MIMO systems. Then, the idea of a modified model-free adaptive controller for a class of MIMO nonlinear systems is proposed. Finally, steps for the MFAC design are given.

3.2.1 Recursive least-squares estimation algorithm

Parameter estimation plays an important role in system identification. A variety of parameter estimation methods have been widely investigated since the last decades. To design adaptive controllers, unknown system and controller parameters should be estimated and updated automatically by using mathematical algorithms. As a fundamental technique, least-squares method can be applied effectively in case of the system model is linear in parameters [ÅW08]. According to the least-squares principle of Gauss [ÅW08], the unknown system parameters of a determined mathematical model should be chosen to minimize the sum of the squares of the differences between the real system outputs and the modeling outputs (or calculated outputs) which are generated by the system model. Based on this principle, in this subsection, an on-line parameter estimation algorithm for a general model of a class of SISO systems is discussed. Next, the derived algorithm will be applied to estimate the unknown system parameters for a class of MIMO nonlinear systems.

As discussed in [ÅW08], a general model of SISO systems can be represented as

$$y(k) = \theta_1(k)\phi_0^1 + \theta_2(k)\phi_0^2 + \ldots + \theta_n(k)\phi_0^n = \theta^T(k)\phi_0, \tag{3.39}$$

where $y(k)$ is the system output at time-step k. The known I/O data functions generated from the system model are denoted as $\theta^T(k) = [\theta_1(k)\ \theta_2(k)\ \ldots\ \theta_n(k)]$, with n is the number of unknown parameters. The model parameter vector is denoted as $\phi_0 = [\phi_0^1\ \phi_0^2\ \ldots\ \phi_0^n]^T$. The model (3.39) is normally called regression model with the regression variables θ.

Under the sense of the least-squares theory, the optimal parameters ϕ should be defined to minimize the difference between the model output (estimated) and the actual output (measured). To this end, the following least-squares objective function is considered at each step k as

$$J(\phi, k) = \frac{1}{2}\sum_{i=1}^{k}\big(y(i) - \theta^T(i)\phi\big)^2, \tag{3.40}$$

where $i = 1, 2, \ldots, k$ is the discrete-time variable of the model (3.39). By differentiating function (3.40) with respect to ϕ and letting it zeros, the following equations are obtained

$$\frac{\partial J}{\partial \phi} = \big[y(i) - \theta^T(i)\phi\big]\,(-\theta(i)) = 0, \tag{3.41}$$

$$\hat{\phi} = \big[\theta^T(i)\theta(i)\big]^{-1}\theta^T(i)y(i), \tag{3.42}$$

where $\hat{\phi}$ is denoted as the estimated value of ϕ.

With the notations

$$Y(k) = [y(1)\ y(2)\ \ldots\ y(k)]^T, \tag{3.43}$$

$$\psi(k) = [\theta(1)\ \theta(2)\ \ldots\ \theta(k)]^T, \tag{3.44}$$

$$P(k) = \left[\psi^T(k)\psi(k)\right]^{-1} = \left[\sum_{i=1}^{k} \theta^T(i)\theta(i)\right]^{-1}, \tag{3.45}$$

(3.42) can be rewritten as

$$\hat{\phi} = \left[\psi^T(k)\psi(k)\right]^{-1}\psi^T(k)Y(k). \tag{3.46}$$

From (3.46), the derived system parameter $\hat{\phi}$ at step k is calculated as

$$\hat{\phi}(k) = \left[\sum_{i=1}^{k} \theta^T(i)\theta(i)\right]^{-1} \left[\sum_{i=1}^{k} \theta(i)y(i)\right]. \tag{3.47}$$

Substituting (3.45) into (3.47) gives

$$\hat{\phi}(k) = P(k) \left[\sum_{i=1}^{k} \theta(i)y(i)\right]. \tag{3.48}$$

In addition, (3.48) can be rewritten as

$$\hat{\phi}(k) = P(k) \left[\sum_{i=1}^{k-1} \theta(i)y(i) + \theta(k)y(k)\right]. \tag{3.49}$$

Therefore, the estimated parameter $\hat{\phi}(k-1)$ at previous step $k-1$ is computed according to (3.48) as

$$\hat{\phi}(k-1) = P(k-1)\sum_{i=1}^{k-1} \theta(i)y(i), \tag{3.50}$$

$$\sum_{i=1}^{k-1} \theta(i)y(i) = P^{-1}(k-1)\hat{\phi}(k-1). \tag{3.51}$$

Moreover, parameter $P^{-1}(k)$ is calculated from (3.45) as follows

$$P^{-1}(k) = \sum_{i=1}^{k} \theta^T(i)\theta(i) = \sum_{i=1}^{k-1} \theta^T(i)\theta(i) + \theta^T(k)\theta(k), \tag{3.52}$$

$$P^{-1}(k) = P^{-1}(k-1) + \theta^T(k)\theta(k). \tag{3.53}$$

Based on the equations (3.49), (3.51), and (3.53) the following algorithm is established for the SISO system described in (3.39) as

$$\hat{\phi}(k) = P(k)\left[P^{-1}(k-1)\hat{\phi}(k-1) + \theta(k)y(k)\right], \tag{3.54}$$

$$\hat{\phi}(k) = P(k)\left[P^{-1}(k)\hat{\phi}(k-1) - \theta^T(k)\theta(k)\hat{\phi}(k-1) + \theta(k)y(k)\right], \tag{3.55}$$

$$\hat{\phi}(k) = \hat{\phi}(k-1) + K(k)\left[y(k) - \theta^T(k)\hat{\phi}(k-1)\right], \tag{3.56}$$

where $K(k) = P(k)\theta(k)$ is a vector of unknown parameters. To calculate $P(k)$ and $K(k)$, by using the matrix inversion lemma [ÅW08] the following equations are achieved

$$P(k) = \left[P^{-1}(k-1) + \theta^T(k)\theta(k)\right]^{-1}, \tag{3.57}$$

$$P(k) = P(k-1) - P(k-1)\theta(k)\left[I + \theta^T(k)P(k-1)\theta(k)\right]^{-1}\theta^T(k)P(k-1), \tag{3.58}$$

$$K(k) = P(k)\theta(k) = P(k-1)\theta(k)\left[I + \theta^T(k)P(k-1)\theta(k)\right]^{-1}. \tag{3.59}$$

The discussed equations (3.56), (3.58), and (3.59) with an assumption that the matrix $\psi(k)$ in (3.44) has full rank have been called recursive least-squares algorithm (RLSA), in which the initial parameters are denoted as $\hat{\phi}(1)$ and $P(0)$.

Now the above RLSA will be applied to a class of unknown MIMO systems. As discussed in the preceding subsections, the unknown system (3.15) can be linearized locally and reformulated as a CFDL data model as

$$\Delta\mathbf{y}(i) = \Phi(i)\theta^T(i), \tag{3.60}$$

where $i = 1, 2, \ldots, k$ is denoted as the system discrete-time variable. The unknown system parameter matrix is $\Phi(i)$. The known I/O data function indicated as $\theta^T(i)$ is equivalent with the known data functions $\theta^T(k)$ in (3.39) for the SISO case.

To establish the estimation algorithm of the matrix Φ, considering the following objective function

$$J(\Phi, k) = \frac{1}{2}\sum_{i=1}^{k}\left(\Delta\mathbf{y}(i) - \Phi(i)\theta^T(i)\right)^2 + \frac{1}{2}\gamma\sum_{i=1}^{k}\Delta\Phi^2(i), \tag{3.61}$$

where $\gamma \geq 0$ is a step-size constant, and the variation of the parameters PJM Φ is represented as $\Delta\Phi(i) = \Phi(i) - \Phi(i-1)$. Minimization of (3.61) can be executed by taking $\frac{\partial J}{\partial \Phi} = 0$ as

$$\frac{\partial J}{\partial \Phi} = \left[\Delta\mathbf{y}(i) - \Phi(i)\theta^T(i)\right](-\theta(i)) + \gamma\left(\Phi(i) - \Phi(i-1)\right) = 0. \tag{3.62}$$

As a result, the estimated parameter matrix $\hat{\Phi}(k)$ at current step k is calculated as

$$\hat{\Phi}(k) = \hat{\Phi}(k-1) + \left[\sum_{i=1}^{k} \Delta\mathbf{y}(i)\theta(i) - \hat{\Phi}(k-1)\sum_{i=1}^{k}\theta^T(i)\theta(i)\right]\left[\gamma\mathbf{I} + \sum_{i=1}^{k}\theta^T(i)\theta(i)\right]^{-1}. \tag{3.63}$$

Moreover, the following results achieved from the SISO case in (3.52), (3.53) can be easily applied to MIMO systems

$$\mathbf{P}^{-1}(k) = \sum_{i=1}^{k}\theta^T(i)\theta(i), \tag{3.64}$$

$$\mathbf{P}^{-1}(k-1) = \mathbf{P}^{-1}(k) - \theta^T(k)\theta(k). \tag{3.65}$$

Substituting (3.64) into (3.63), gives

$$\hat{\Phi}(k) = \hat{\Phi}(k-1) + \left[\sum_{i=1}^{k-1}\Delta\mathbf{y}(i)\theta(i) + \Delta\mathbf{y}(k)\theta(k) - \hat{\Phi}(k-1)\mathbf{P}^{-1}(k)\right]\left[\gamma\mathbf{I} + \mathbf{P}^{-1}(k)\right]^{-1}. \tag{3.66}$$

In addition, the PJM values $\hat{\Phi}(k-1)$ at previous step $k-1$ are computed as

$$\hat{\Phi}(k-1) = \hat{\Phi}(k-2) + \left[\sum_{i=1}^{k-1}\Delta\mathbf{y}(i)\theta(i) - \hat{\Phi}(k-2)\mathbf{P}^{-1}(k-1)\right]\left[\gamma\mathbf{I} + \mathbf{P}^{-1}(k-1)\right]^{-1}, \tag{3.67}$$

$$\sum_{i=1}^{k-1}\Delta\mathbf{y}(i)\theta(i) = \Delta\hat{\Phi}(k-1)\left[\gamma\mathbf{I} + \mathbf{P}^{-1}(k-1)\right] + \hat{\Phi}(k-2)\mathbf{P}^{-1}(k-1), \tag{3.68}$$

with $\Delta\hat{\Phi}(k-1) = \hat{\Phi}(k-1) - \hat{\Phi}(k-2)$.
Substituting (3.68) into (3.66), yields

$$\Delta\hat{\Phi}(k) = \left[\Delta\hat{\Phi}(k-1)\gamma + \hat{\Phi}(k-1)\mathbf{P}^{-1}(k-1) + \Delta\mathbf{y}(k)\theta(k) - \hat{\Phi}(k-1)\mathbf{P}^{-1}(k)\right]\left[\gamma\mathbf{I} + \mathbf{P}^{-1}(k)\right]^{-1}, \tag{3.69}$$

with $\Delta\hat{\Phi}(k) = \hat{\Phi}(k) - \hat{\Phi}(k-1)$. The parameter matrix $\mathbf{P}^{-1}(k-1)$ in (3.69) can be replaced by (3.65). Finally, the following equations are derived

$$\Delta\hat{\Phi}(k) = \left[\Delta\mathbf{y}(k) - \hat{\Phi}(k-1)\theta^T(k)\right]\theta(k)\left[\gamma\mathbf{I} + \mathbf{P}^{-1}(k)\right]^{-1} + \gamma\Delta\hat{\Phi}(k-1)\left[\gamma\mathbf{I} + \mathbf{P}^{-1}(k)\right]^{-1}. \tag{3.70}$$

In this case, computational burden can be reduced by considering the constant parameter $\gamma = 0$, that means (3.70) becomes

$$\hat{\Phi}(k) = \hat{\Phi}(k-1) + \Big[\Delta \mathbf{y}(k) - \hat{\Phi}(k-1)\theta^T(k)\Big]\mathbf{K}(k), \tag{3.71}$$

where $\mathbf{K}(k) = \theta(k)\mathbf{P}(k)$ is a matrix of unknown parameters.

Based on the matrix inversion lemma [ÅW08], the unknown parameter matrices $\mathbf{P}(k)$ and $\mathbf{K}(k)$ are determined as

$$\mathbf{P}(k) = \mathbf{P}(k-1) - \mathbf{P}(k-1)\theta(k)\big[\mathbf{I} + \theta^T(k)\mathbf{P}(k-1)\theta(k)\big]^{-1}\theta^T(k)\mathbf{P}(k-1), \tag{3.72}$$

$$\mathbf{K}(k) = \theta(k)\mathbf{P}(k) = \theta(k)\mathbf{P}(k-1)\big[\mathbf{I} + \theta^T(k)\mathbf{P}(k-1)\theta(k)\big]^{-1}. \tag{3.73}$$

It is interesting to note that, the known I/O data function $\theta^T(k)$ in (3.71) of the CFDL model is defined as

$$\theta^T(k) = \Delta \mathbf{u}(k-1). \tag{3.74}$$

Therefore, the obtained parameter estimation algorithm called CFDL-based recursive least-squares algorithm (CFDL-RLSA) for a class of unknown MIMO nonlinear systems is written as

$$\hat{\Phi}(k) = \hat{\Phi}(k-1) + \Big[\Delta \mathbf{y}(k) - \hat{\Phi}(k-1)\Delta \mathbf{u}(k-1)\Big]\mathbf{K}(k), \tag{3.75}$$

$$\begin{aligned}\mathbf{K}(k) &= \Delta \mathbf{u}^T(k-1)\mathbf{P}(k) \\ &= \Delta \mathbf{u}^T(k-1)\mathbf{P}(k-1)\big[\mathbf{I} + \Delta \mathbf{u}(k-1)\mathbf{P}(k-1)\Delta \mathbf{u}^T(k-1)\big]^{-1},\end{aligned} \tag{3.76}$$

$$\begin{aligned}\mathbf{P}(k) = \mathbf{P}(k-1) &- \mathbf{P}(k-1)\Delta \mathbf{u}^T(k-1) \\ &\big[\mathbf{I} + \Delta \mathbf{u}(k-1)\mathbf{P}(k-1)\Delta \mathbf{u}^T(k-1)\big]^{-1}\Delta \mathbf{u}(k-1)\mathbf{P}(k-1).\end{aligned} \tag{3.77}$$

3.2.2 Modified MFAC for MIMO nonlinear systems

As discussed in the previous subsections, for a class of unknown MIMO nonlinear systems (3.15) by utilizing the CFDL technique, an equivalent linearized data model (3.17) can be assumed to be established virtually. The unknown time-varying parameter matrix $\Phi(k)$ in (3.17) should be estimated and updated recursively by using the discussed CFDL-PA (3.32) or the CFDL-RLSA (3.75), (3.76), and (3.77). In this part, the estimated parameters PJM are used to design a modified MFAC for multivariable systems. The key new idea is that, to improve tracking control performance not only the output tracking errors, but also the tracking error variations within a specified length of time window should be minimized. Therefore, the control goal is to minimize the upcoming tracking errors between

the desired output values $\mathbf{y}^d(k+1)$ and the actual system outputs $\mathbf{y}(k+1)$, denoted as $\mathbf{e}(k+1) = \mathbf{y}^d(k+1) - \mathbf{y}(k+1)$ as well as the control error differences $\Delta\mathbf{e}(k) = \mathbf{e}(k) - \mathbf{e}(k-1) = \Delta\mathbf{y}^d(k+1) - \Delta\mathbf{y}(k)$. To restrict the control input variation, a weighting factor λ is used. The control input law can be established by proposing a modified objective function of $\mathbf{u}(k)$ as

$$J(\mathbf{u}(k)) = \left\|\mathbf{y}^d(k+1) - \mathbf{y}(k+1)\right\|^2 + j\left\|\Delta\mathbf{y}^d(k+1) - \Delta\mathbf{y}(k+1) - \Delta\mathbf{y}(k)\right\|^2 + \lambda\|\mathbf{u}(k) - \mathbf{u}(k-1)\|^2, \tag{3.78}$$

where $\lambda > 0, j > 0$ are the design weighting parameters. Compared to (3.33), here the term of $\left\|\Delta\mathbf{y}^d(k+1) - \Delta\mathbf{y}(k+1) - \Delta\mathbf{y}(k)\right\|$ is added representing the variations of the output tracking errors.

The actual system outputs $\mathbf{y}(k+1)$ in (3.78) can be approximated by applying the CFDL model outputs (3.17)

$$\Delta\mathbf{y}(k+1) = \Phi(k)\Delta\mathbf{u}(k), \tag{3.79}$$

$$\mathbf{y}(k+1) = \mathbf{y}(k) + \Phi(k)\Delta\mathbf{u}(k). \tag{3.80}$$

Substituting (3.79) and (3.80) into (3.78), yields the following cost function

$$J(\mathbf{u}(k)) = \left\|\mathbf{y}^d(k+1) - \mathbf{y}(k) - \Phi(k)\Delta\mathbf{u}(k)\right\|^2 + j\left\|\Delta\mathbf{y}^d(k+1) - \Phi(k)\Delta\mathbf{u}(k) - \Delta\mathbf{y}(k)\right\|^2 + \lambda\|\Delta\mathbf{u}(k)\|^2. \tag{3.81}$$

By differentiating (3.81) regarding to $\Delta\mathbf{u}(k)$, the following equations are derived

$$\frac{\partial J}{\partial\Delta\mathbf{u}(k)} = \left(-\Phi^T(k)\right)\left[\mathbf{y}^d(k+1) - \mathbf{y}(k) - \Phi(k)\Delta\mathbf{u}(k)\right] + j\left(-\Phi^T(k)\right)\left[\Delta\mathbf{y}^d(k+1) - \Phi(k)\Delta\mathbf{u}(k) - \Delta\mathbf{y}(k)\right] + \lambda\Delta\mathbf{u}(k) = 0, \tag{3.82}$$

$$\Delta\mathbf{u}(k) = \left[\hat{\Phi}^T(k)\hat{\Phi}(k)\,(1+j) + \lambda\mathbf{I}\right]^{-1}\hat{\Phi}^T(k)\left[\mathbf{y}^d(k+1) - \mathbf{y}(k)\right] + \left[\hat{\Phi}^T(k)\hat{\Phi}(k)\,(1+j) + \lambda\mathbf{I}\right]^{-1} j\hat{\Phi}^T(k) \left[\mathbf{y}^d(k+1) - \mathbf{y}^d(k) - (\mathbf{y}(k) - \mathbf{y}(k-1))\right]. \tag{3.83}$$

Equation (3.83) requires the calculation of matrix inversion which might be complicated if the system input and output dimensions are large. Therefore, a simplified control input equation is rewritten as

$$\mathbf{u}(k) = \mathbf{u}(k-1) + \frac{\rho\hat{\Phi}^T(k)\left[\mathbf{y}^d(k+1) - \mathbf{y}(k)\right]}{\lambda + (1+j)\left\|\hat{\Phi}(k)\right\|^2} + \frac{j\hat{\Phi}^T(k)\left[\mathbf{y}^d(k+1) - \mathbf{y}^d(k) - (\mathbf{y}(k) - \mathbf{y}(k-1))\right]}{\lambda + (1+j)\left\|\hat{\Phi}(k)\right\|^2}, \tag{3.84}$$

where $\rho \in (0, 1]$ is a step-size constant.

The control input equation (3.84) is slightly different compared with (3.38). As discussed in [PS19b], the term of $\left[\mathbf{y}^d(k+1) - \mathbf{y}^d(k) - (\mathbf{y}(k) - \mathbf{y}(k-1))\right]$ in (3.84) only considers the minimization of the tracking error variations within one step from previous steps with very small amplitudes. Therefore, to improve control performance the extended error differences within a predefined length of time window $N > 0$ are taken into account. Finally, the following modified control input law is achieved [PS20a] by taking the same procedure as the establishment of (3.84)

$$\mathbf{u}(k) = \mathbf{u}(k-1) + \frac{\rho\hat{\Phi}^T(k)\left[\mathbf{y}^d(k+1) - \mathbf{y}(k)\right]}{\lambda + (1+j)\left\|\hat{\Phi}(k)\right\|^2} + \frac{j\hat{\Phi}^T(k)\left[\varepsilon(k) - \varepsilon(k-N)\right]}{\lambda + (1+j)\left\|\hat{\Phi}(k)\right\|^2}, \tag{3.85}$$

where $\varepsilon(k) = \mathbf{y}^d(k+1) - \mathbf{y}(k); \varepsilon(k-N) = \mathbf{y}^d(k-N+1) - \mathbf{y}(k-N)$ are denoted as the error variations at sampling intervals k and $k-N$, respectively. Meanwhile, $\hat{\Phi}(k)$ is the estimated PJM by using the discussed CFDL-PA (3.32) or the CFDL-RLSA (3.75), (3.76), and (3.77). In MIMO case, an improved model-free controller which applies the CFDL-RLSA and modified control law (3.85) has been discussed in [PS20a]. The control law (3.85) contains several design parameters such as λ, ρ, and j. Suitable choices of them can improve the model-free control performance.

3.2.3 Steps for model-free controller design using the CFDL technique

The MFAC design can be applied to control a class of unknown MIMO nonlinear systems, in which the system I/O data have to be directly measured or calculated. In Figure 3.2 [PS20a], a modified MFAC scheme using the CFDL-RLSA for on-line parameter estimation is shown. To realize MFAC program, the following steps have to be implemented:

- *Step 1:* Based on the CFDL technique as well as the available I/O information from the controlled system, the unknown time-varying parameter matrix PJM $\hat{\Phi}(k)$ is estimated and updated recursively. Different on-line estimation algorithms such as CFDL-PA or CFDL-RLSA as discussed previously can be utilized. According to [HJ13] and assumption 3.3, to improve the ability in on-line tracking time-varying parameters, a reset condition needs to be considered as follows

$$\begin{aligned} \hat{\phi}_{ii}(k) = \hat{\phi}_{ii}(1) \;\; if \;\; & \left|\hat{\phi}_{ii}(k)\right| < c_2 \;\; or \;\; \left|\hat{\phi}_{ii}(k)\right| > \alpha c_2 \\ or \;\; & \operatorname{sgn}\left(\hat{\phi}_{ii}(k)\right) \neq \operatorname{sgn}\left(\hat{\phi}_{ii}(1)\right), \end{aligned} \tag{3.86}$$

$$\begin{aligned} \hat{\phi}_{ij}(k) = \hat{\phi}_{ij}(1) \;\; if \;\; & \left|\hat{\phi}_{ij}(k)\right| > c_1 \\ or \;\; & \operatorname{sgn}\left(\hat{\phi}_{ij}(k)\right) \neq \operatorname{sgn}\left(\hat{\phi}_{ij}(1)\right), \end{aligned} \tag{3.87}$$

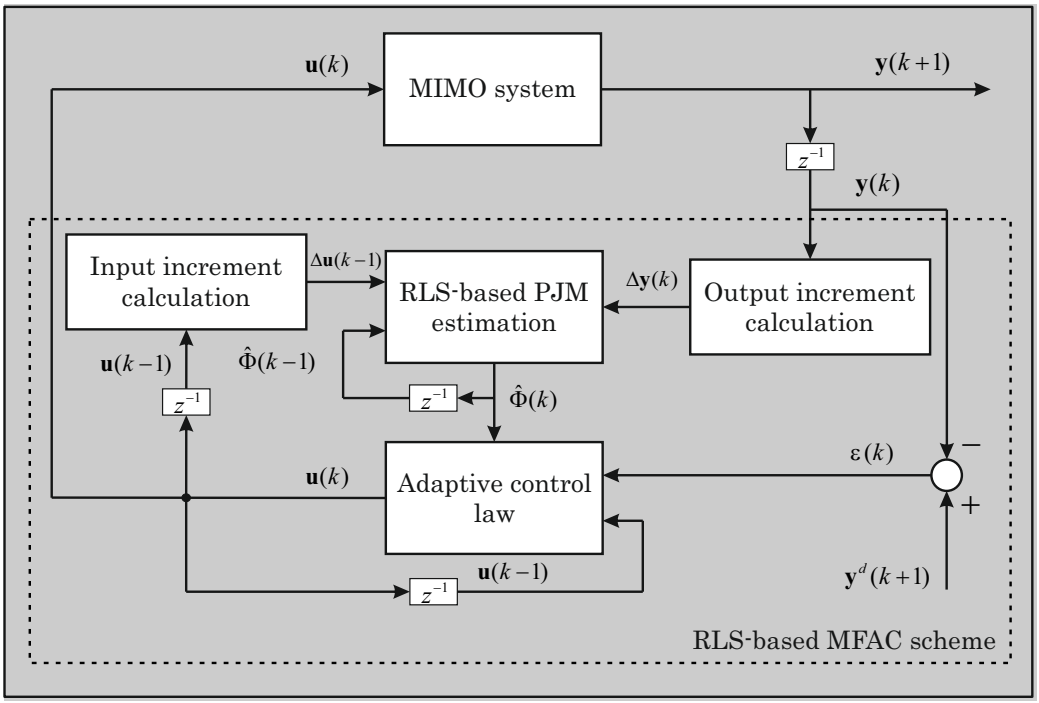

Figure 3.2: Modified MFAC scheme using CFDL-based RLS estimation algorithm [PS20a]

where $\hat{\phi}_{ii}(1), \hat{\phi}_{ij}(1)$ are the given initial values of the PJM, with $i, j = 1, 2, \ldots, n^*$ and $i \neq j$ according to assumption 3.3 (see Section 3.1).

- *Step 2:* Based on the estimated PJM $\hat{\Phi}(k)$ and the current output tracking errors $\varepsilon(k)$ (see Figure 3.2), the required control input values $\mathbf{u}(k)$ are computed via (3.38). In addition, by considering minimization of the control errors within a suitable length of time window $N > 0$, the improved control input signals are determined by using (3.85) for the overall model-free control performance improvement.

- *Step 3:* Next, the calculated control inputs $\mathbf{u}(k)$ are implemented to the system to fulfill the initial control requirements. Finally, the upcoming outputs $\mathbf{y}(k+1)$ are measured or calculated directly, and the given procedure will be carried out repeatedly.

3.3 A case study: vibration control of an elastic crane

In this section, an application of the proposed CFDL-based model-free adaptive controllers to vibration control of an elastic ship-mounted crane represented as a

typical flexible system is discussed. The crane with an elastic part of the boom was initially developed in Y. M. Al-Sweiti et al. [AS07] for cargo transportation purpose. First, the crane configuration and its related mathematical model are briefly introduced. Subsequently, simulation results of the crane in cases of without- and with controllers will be illustrated. Additionally, control performance is evaluated in both transient and stationary phases by varying the design controller parameters.

3.3.1 Crane configuration and related mathematical model

As an example of mechanical flexible systems, this subsection discusses the configuration and related model of the elastic ship-mounted crane. The crane with an elastic light-weight boom is normally equipped in large ships to transfer cargo from one ship to another in an open sea. During the crane operation particularly in the cargo transfer process, due to the effects of undesirable environmental conditions such as wave-induced motions or strong wind force represented as unknown external disturbances, large vibrations can be produced in the crane system. In addition, because of the non-zero initial excitation of the payload, in-plane vibrations of the elastic boom as well as the payload and upper cables may appear that might lead to suspension of the crane operation. Therefore, it is necessary to implement the design controllers to guarantee the crane safety.

The crane configuration is depicted in Figure 3.3, whereas its boom has been divided into two parts: rigid part (BC) including a movable suspension point B' of the upper cable and elastic part (AB). The rotational moment M_A is assumed to be applied to the lower point A (at node 1) of the boom which is mounted with the ship. The crane is represented as a double pendulum system. The upper pendulum includes a frictionless pulley m_1 riding on the upper cable suspended from two different points of the boom: a fixed point C and a movable point B' along the rigid part BC. Meanwhile, the lower pendulum consists of the payload m_2 suspended by the payload cable l from the pulley m_1. The control target is to suppress the vibrations of the elastic part (AB) represented by the angle θ_6 (at node 6) of the boom with respect to the x-axis (see Figure 3.3), the angular displacements of the payload cable ϕ_2 and the upper cable α_2. The system output vector is written as

$$\mathbf{y}_m(k) = [\Delta\theta_6(k)\ \Delta\alpha_2(k)\ \Delta\phi_2(k)]^T, \tag{3.88}$$

where k is the discrete-time variable, and Δ indicates the increment unit.

In this contribution, in-plane oscillations of the crane are mainly considered which could be more dangerous in practical applications rather than heave and pitch motion-induced vibrations. To ensure the controllability of the elastic boom and the payload, as discussed in [Al-06], three control input variables are defined including the displacements of the luff angle $\Delta\rho$, the total length of the upper cable ΔL

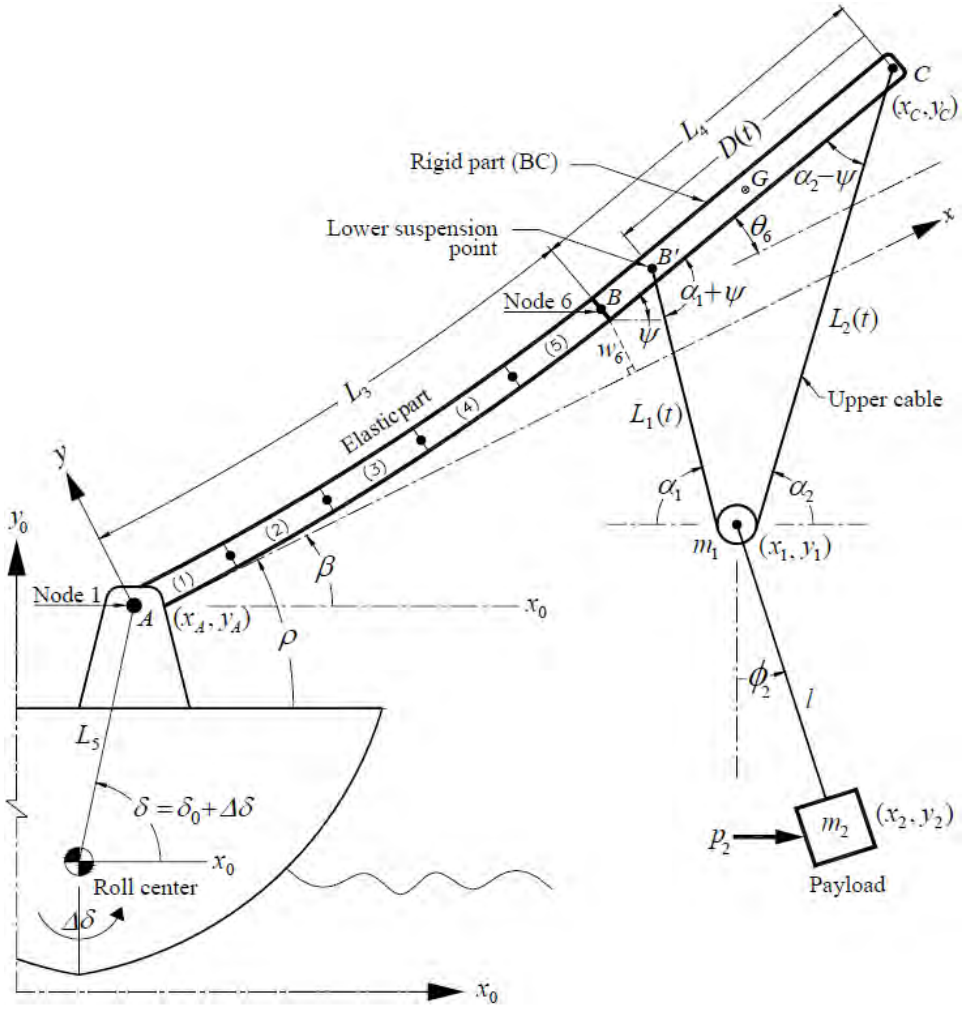

Figure 3.3: Configuration of the elastic ship-mounted crane with the "Maryland Rigging" [Al-06]

with $L = L_1 + L_2$, and the lower suspension point position ΔD of the upper cable (see Figure 3.3). Hence, the control input vector is described as

$$\mathbf{u}(k) = [\Delta\rho(k)\ \Delta L(k)\ \Delta D(k)]^T. \tag{3.89}$$

In model-free adaptive control, to estimate and update the unknown system parameters PJM at current step, the available system I/O data from previous steps must be used. For this purpose, the mathematical dynamic model of the crane has to be investigated, and therefore needs to be transformed in discrete-time domain. As illustrated in [Al-06], by applying the finite element method to analysis of the kinematics and kinetics of the elastic boom, the pulley, and the payload, the nonlinear

equation of motion of the crane is obtained as

$$\mathbf{M}_0\ddot{\mathbf{q}} + \mathbf{K}_0\mathbf{q} = \mathbf{B}_1\mathbf{u} + \mathbf{B}_2\ddot{\mathbf{u}} + \mathbf{B}_3\Delta\delta + \mathbf{B}_4\Delta\ddot{\delta} + \mathbf{B}_5 p_2 + \mathbf{n}. \tag{3.90}$$

The generalized displacement vector is denoted as

$$\mathbf{q} = [\Delta\omega_2\ \Delta\theta_2\ \ldots\ \Delta\omega_6\ \Delta\theta_6\ \Delta\alpha_2\ \Delta\phi_2]^T, \tag{3.91}$$

where ω_i and θ_i denote the nodal transitional and rotational displacements at node i of the boom with respect to the x-axis (see Figure 3.3). The control input vector in (3.90) is represented by

$$\mathbf{u} = [\Delta\rho\ \Delta L\ \Delta D]^T. \tag{3.92}$$

The total mass and stiffness matrices are indicated as $\mathbf{M}_0$ and $\mathbf{K}_0$, respectively. The system input matrices are $\mathbf{B}_1$ and $\mathbf{B}_2$; whereas $\mathbf{B}_3, \mathbf{B}_4$, and $\mathbf{B}_5$ are the disturbance matrices. All of the nonlinear terms of the system dynamics are integrated in the vector $\mathbf{n}$. As mentioned earlier, the external disturbance signals acting on the crane include the ship rolling $\Delta\delta$ and the unknown wind force p_2. Further detail about the structures of $\mathbf{M}_0, \mathbf{K}_0, \mathbf{B}_1, \mathbf{B}_2, \mathbf{B}_3, \mathbf{B}_4$, and $\mathbf{B}_5$ can be found in [Al-06].

The measurement output vector $\mathbf{y}_m$ and the interested outputs $\mathbf{y}$ are described as

$$\mathbf{y}_m = [\Delta\theta_6\ \Delta\alpha_2\ \Delta\phi_2]^T = \mathbf{C}_1\mathbf{q}, \tag{3.93}$$

$$\mathbf{y} = [\Delta x_2\ \Delta y_2]^T, \tag{3.94}$$

where $\Delta x_2, \Delta y_2$ are the differences of the global position of the payload with respect to the x_0y_0-coordinate system. The measurement matrix, which describes the positions of the sensors on the crane, is symbolized as $\mathbf{C}_1$.
By checking the influence of different nonlinear terms $\mathbf{n}$ in (3.90) on the dynamic behaviors of the crane under various initial conditions and excitations [Al-06], it can be concluded that the nonlinear terms $\mathbf{n}$ have no significant effects on the crane responses. Therefore, the system model (3.90) can be illustrated in a linearized form by setting $\mathbf{n} = \mathbf{0}$.

By denoting

$$\mathbf{x}_1 = \mathbf{M}_0\mathbf{q} - \mathbf{B}_2\mathbf{u} - \mathbf{B}_4\Delta\delta, \tag{3.95}$$

$$\mathbf{x}_2 = \mathbf{M}_0\dot{\mathbf{q}} - \mathbf{B}_2\dot{\mathbf{u}} - \mathbf{B}_4\Delta\dot{\delta}, \tag{3.96}$$

the state-space representation of the crane at the current equilibrium point is written as

$$\dot{\mathbf{x}} = \mathbf{A}\mathbf{x} + \mathbf{B}\mathbf{u} + \mathbf{E}\Delta\delta + \mathbf{N}p_2, \tag{3.97}$$

where $\mathbf{x} = [\mathbf{x}_1\ \mathbf{x}_2]^T$ is the state vector; whilst the system and input matrices are described as

$$\mathbf{A} = \begin{bmatrix} \mathbf{0} & \mathbf{I} \\ -\mathbf{K}_0\mathbf{M}_0^{-1} & \mathbf{0} \end{bmatrix}, \qquad \mathbf{B} = \begin{bmatrix} \mathbf{0} \\ \mathbf{B}_1 - \mathbf{K}_0\mathbf{M}_0^{-1}\mathbf{B}_2 \end{bmatrix}, \tag{3.98}$$

respectively. Furthermore,

$$\mathbf{E} = \begin{bmatrix} \mathbf{0} \\ \mathbf{B}_3 - \mathbf{K}_0\mathbf{M}_0^{-1}\mathbf{B}_4 \end{bmatrix}, \qquad \mathbf{N} = \begin{bmatrix} \mathbf{0} \\ \mathbf{B}_5 \end{bmatrix}, \tag{3.99}$$

are the disturbance matrices due to the ship rolling ($\Delta\delta$) and the wind force (p_2), correspondingly.

The measurement output equation is expressed as

$$\mathbf{y}_m = \mathbf{C}\mathbf{x} + \mathbf{D}\mathbf{u} + \mathbf{F}\Delta\delta, \tag{3.100}$$

where

$$\mathbf{C} = \begin{bmatrix} \mathbf{C}_1\mathbf{M}_0^{-1} & \mathbf{0} \end{bmatrix}, \tag{3.101}$$

is the system output matrix, and

$$\mathbf{D} = \mathbf{C}_1\mathbf{M}_0^{-1}\mathbf{B}_2, \qquad \mathbf{F} = \mathbf{C}_1\mathbf{M}_0^{-1}\mathbf{B}_4, \tag{3.102}$$

are denoted as the input and disturbance direct transmission matrices, respectively.

To design MFAC, the above state-space equations (3.97), (3.100) have to be represented in discrete-time domain as

$$\begin{aligned} \mathbf{x}(k+1) &= \mathbf{G}\mathbf{x}(k) + \mathbf{H}\mathbf{u}(k) + \mathbf{J}\Delta\delta(k) + \mathbf{Q}p_2(k), \\ \mathbf{y}_m(k) &= \mathbf{C}\mathbf{x}(k) + \mathbf{D}\mathbf{u}(k) + \mathbf{F}\Delta\delta(k), \end{aligned} \tag{3.103}$$

where the recalculated system and input matrices are denoted as $\mathbf{G}$ and $\mathbf{H}$, while $\mathbf{J}$ and $\mathbf{Q}$ are represented as the disturbance matrices.

3.3.2 Simulation results

Uncontrolled case

In this work, no external disturbances are considered, that means $\Delta\delta(k) = p_2(k) = 0$ in (3.103). However, because of the non-zero initial position of the payload m_2 denoted by ϕ_2^0, significant undesirable oscillations can be observed in the crane if no controller is used. In Figure 3.4, the simulated system outputs are shown from the beginning up to $t = 20$ [s] of the simulation due to the non-zero initial angular

Table 3.1: Initial parameters of the lab-scaled elastic crane [PS20a]

Parameter	**Description**	**Value [Unit]**
β_0	Orientation of the boom axis	$\pi/4$ [rad]
D_0	Low-point suspension cable	0.55 [m]
L_0	Length of the upper cable	1.6 [m]
l	Length of the payload cable	0.5 [m]
m_1	Mass of the pulley	0.5 [kg]
m_2	Mass of the payload	5.0 [kg]
$\dot{\phi}_2^0$	Initial payload angular velocity	5.0 [rad/s]
ϕ_2^0	Initial payload angular displacement	1.0 [rad]

velocity of the payload $\dot{\phi}_2^0 = 5.0$ [rad/s]. In addition, the displacements of the payload with respect to the x_0- and y_0-axis in uncontrolled case are described in Figure 3.5. It can be seen that, in case no controller is used, large oscillations arise which could be dangerous and might suspend the cargo transportation of the crane. Furthermore, to simulate different dynamic behaviors of the crane under a variety of initial excitation conditions, the system output signals as well as the payload vibration results with respect to the non-zero initial angle of the payload $\phi_2^0 = 1.0$ [rad] are given in Figure 3.6 and Figure 3.7, respectively, within $t = 20$ [s]. In this thesis, the lab-scaled boom crane system which was established in [Al-06] is considered for numerical simulations. Several initial parameters of the crane are given in Table 3.1.

Simulation results by using the modified PA-MFAC

In Section 3.2, a modified MFAC has been proposed to control of a class of unknown MIMO nonlinear systems. By considering minimization of the upcoming output tracking errors as well as the error variations, a modified control input law has been established in (3.85). To realize control action, the system unknown time-varying parameters (PJM) should be estimated at every sampling interval during the system operation. Two on-line parameter estimation strategies have been discussed including the CFDL projection algorithm (3.32) in Section 3.1, and the CFDL recursive least-squares algorithm (3.75), (3.76), and (3.77) in Section 3.2. Here, the discussed modified MFAC which utilizes the standard CFDL-PA will be applied to reduce the vibrations of the ship-mounted crane. Different control input equations are implemented to fulfill control requirements including the standard CFDL-PA-based

Table 3.2: Parameters of the design model-free and PI controllers [PS19b]

Parameter	**Meaning**	**Value**
η	Step-size constant	0.55
μ	Constant weighting factor	15
ρ	Step-size constant	0.005
λ_1	Weighting factor of the modified MFAC	0.5
λ_2	Weighting factor of the normal MFAC	1.25
j	Design weighting parameter	0.035
k_p	PI control parameter	0.002
k_i	PI control parameter	0.1

MFAC in (3.38) and the modified one in (3.85). First, tracking control evaluation regarding to the system outputs as well as the payload displacement is illustrated. Then, to evaluate the control performance of the design method subjected to varying controller parameters, control input energy-based evaluation will be discussed. The proposed approach is compared with the normal CFDL-MFAC (3.38) [PS19a], and industrial PI control.

The vibration control results of the two angular displacements $\Delta\alpha_2$ and $\Delta\phi_2$ of the upper cable and payload cable, respectively, are shown in Figure 3.8 in case no external disturbance effects are considered. In uncontrolled case (red dash line), the crane shows vibrations only because of the non-zero initial angular velocity of the payload $\dot{\phi}_2^0 = 5.0$ [rad/s]. In case of using controllers, it can be seen that the vibrations of the upper and payload cables are reduced by using the modified CFDL-PA controller (orange line). Better results of the modified MFAC are observed in comparison with the normal CFDL-MFAC (green dot line) as well as the PI controller (blue dash line). Vibration control results of the payload position are illustrated in Figure 3.9. The controllers are turned on from $t = 30$ [s], and in uncontrolled case, the simulation stops at $t = 100$ [s]. Better control performance can be observed according to smaller control errors when using the modified model-free controller compared to the other conventional approaches. In Table 3.2 [PS19b], several design parameters of the model-free and PI controllers are given.

To evaluate control performance of the discussed methods when varying controller parameters, the relationship between the control input energy $\int_{t_1}^{t_2} \mathbf{u}^2(t)dt$ and the output tracking error or the payload transition $\int_{t_1}^{t_2} \mathbf{e}^2(t)dt$ is considered within a

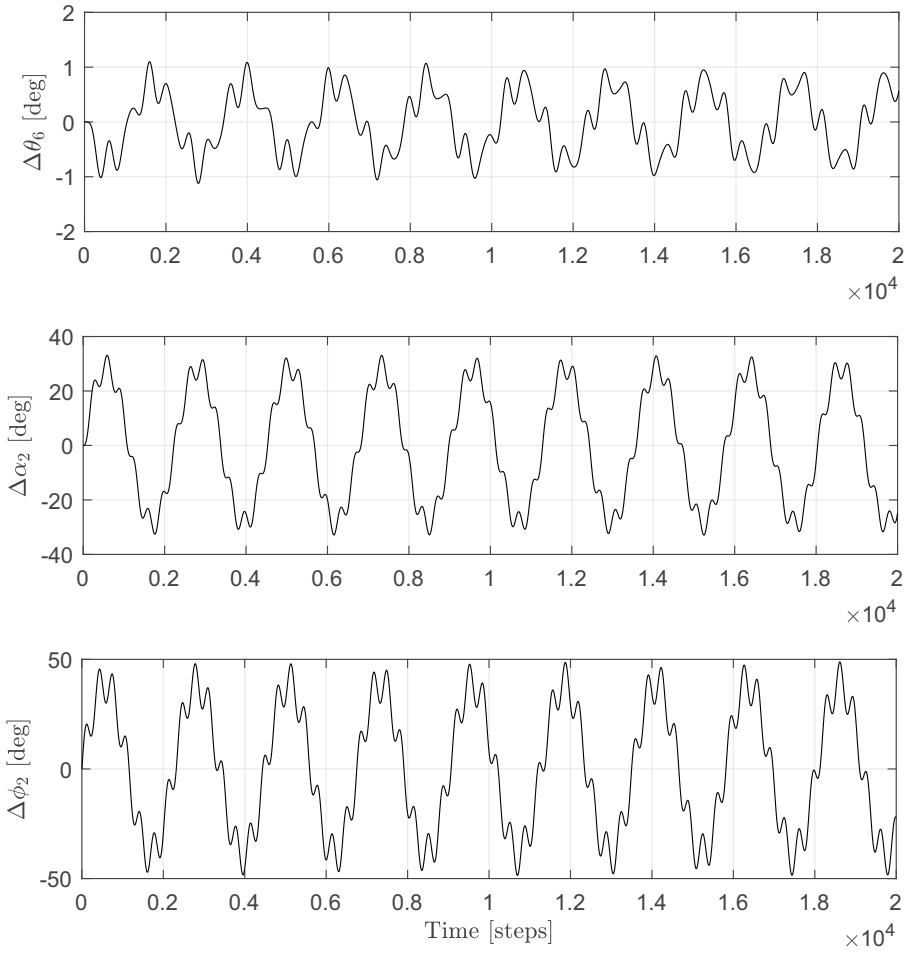

Figure 3.4: Vibration results of the output vector $\mathbf{y}_m$ with respect to the initial condition $\dot{\phi}_2^0 = 5.0$ [rad/s]

specified length of time window $T = [t_1, t_2]$ [s] as

$$P_{K^*} = \left[\int_{t_1}^{t_2} \mathbf{u}^2(t)dt, \int_{t_1}^{t_2} \mathbf{e}^2(t)dt \right]_{K^*}, \tag{3.104}$$

where $K^* = \{\lambda_1, \lambda_2, k_p, k_i\}$ is a set of parameters of the modified CFDL-MFAC (λ_1), normal CFDL-MFAC (λ_2), and PI control, respectively. To obtain the best illustration of different trajectories P_{K^*}, via trial simulations the control parameter intervals can be designed. Here, the important parameters which can improve the model-free control performance are considered as $\lambda_1 \in [0.1, 7.5]$ and $\lambda_2 \in [0.5, 25.0]$; whereas the varied PI controller parameters are $k_p \in [0.0005, 0.06]$ and $k_i \in [0.0001, 0.20]$. The trajectory of the control input energy $\mathbf{u} = [\Delta L \ \Delta D]$

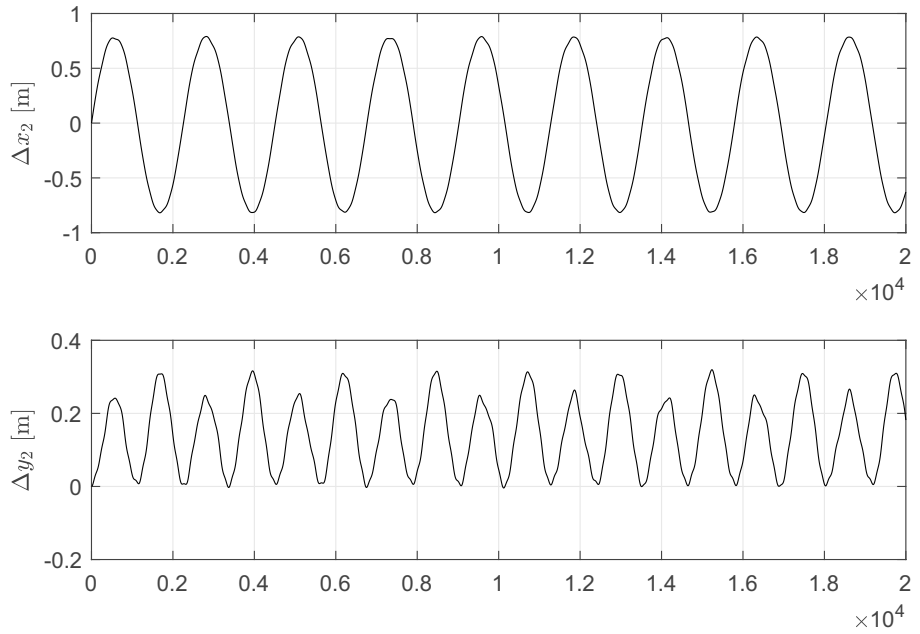

Figure 3.5: Vibration results of the payload m_2 with respect to the initial condition $\dot{\phi}_2^0 = 5.0$ [rad/s]

and the control errors $\mathbf{e} = [\Delta x_2\ \Delta y_2]$ is denoted as P_{K^*}. In Figure 3.10, control performance evaluation with respect to the criteria (3.104) within the simulation interval $T_1 = [30, 180]$ [s] (transient phase) is shown. The trajectory P_{K^*} of the modified model-free controller (violet dot) is closer to the origin $(0, 0)$ than that of the normal MFAC (blue dot) and PI control (red dot). In addition, the control quality in stationary phase $T_2 = [140, 180]$ [s] is graphically presented in Figure 3.11. In general, the improved MFAC (violet dot) shows better results regarding obtained smaller control errors than the others. In Table 3.3, control performance comparison is illustrated numerically in transient phase. The mean squared error (MSE) as well as the consumed input energy (E_{input}) of different control approaches are calculated within the total length of simulation time T [steps] as follows

$$MSE = \frac{1}{T}\sum_{k=1}^{T} \mathbf{e}^2(k), \tag{3.105}$$

$$E_{input} = \frac{1}{T}\sum_{k=1}^{T} \mathbf{u}^2(k). \tag{3.106}$$

It can be seen from the Table 3.3 that, in transient phase T_1, the modified MFAC obtains smallest control errors with $\int \mathbf{e}^2(t)dt$ (45.3190) and MSE (0.0251). The standard MFAC requires less input energy according to $\int \mathbf{u}^2(t)dt$ (0.0493) and E_{input} ($2.7444e^{-5}$). In stationary phase T_2, the control comparison results are

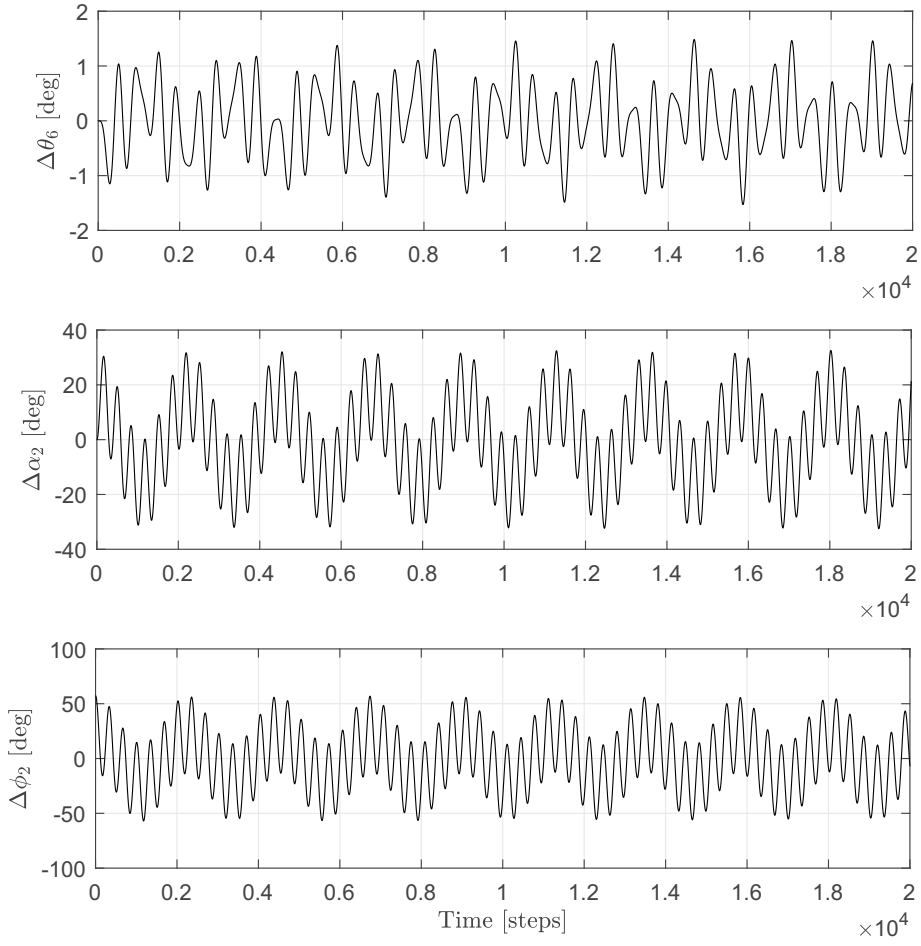

Figure 3.6: Vibration results of the output vector $\mathbf{y}_m$ with respect to the initial condition $\phi_2^0 = 1.0$ [rad]

given in Table 3.4. Generally, the modified CFDL-MFAC achieves smaller control errors; whereas the normal CFDL-MFAC possesses less input energy consumption among the discussed controllers.

Simulation results by using the modified RLSA-MFAC

In this part, the improved MFAC which utilizes the CFDL recursive least-squares algorithm (3.75), (3.76), and (3.77) is applied to vibration control of the elastic crane. Vibration control results are derived in case no external disturbance is considered. However, large unexpected in-plane oscillations might occur in the system due to the non-zero initial excitation of the payload ($\dot{\phi}_2^0 = 5.0$ [rad/s] in Table 3.1). To evaluate control efficiency, the standard PA-MFAC in (3.38) (see [PS19a]) and traditional PI

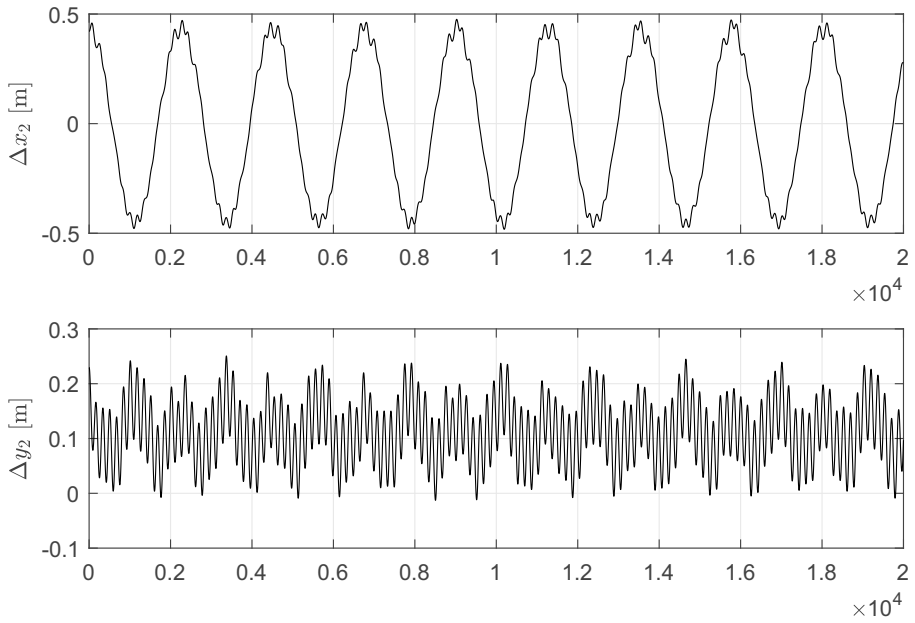

Figure 3.7: Vibration results of the payload m_2 with respect to the initial condition $\phi_2^0 = 1.0$ [rad]

Table 3.3: Parameter-based control performance comparison in transient phase

Control method	$\int \mathbf{e}^2(t)dt$	$\int \mathbf{u}^2(t)dt$	MSE	E_{input}
PI control	98.5515	0.2768	0.0547	$1.5381e^{-4}$
Normal CFDL-MFAC	61.4639	0.0493	0.0341	$2.7444e^{-5}$
Modified CFDL-MFAC	45.3190	0.0989	0.0251	$5.4962e^{-5}$

control are used for comparison. In Figure 3.12, the results of vibration suppression with respect to the payload position are shown in x_0- and y_0-direction. Compared to the standard PA-MFAC (yellow line) and PI control (blue dash line), the proposed RLSA-MFAC (green line) has significant improvement in the results of payload vibration reduction. The control part of the simulation starts from $t = 30$ [s], and it can be seen from Figure 3.12 that it takes only $\Delta t = 10$ [s] to suppress the payload swings in case of using the modified model-free controller. In Table 3.5 [PS20a], several design parameters of the modified RLSA-MFAC and PI controller are illustrated. The uncontrolled case (red dash line) is also simulated within $t = 50$ [s] to observe the system dynamic behavior. Furthermore, Figure 3.13 presents comparison of vibration control regarding the system outputs $\Delta\alpha_2$ and $\Delta\phi_2$. It is clear that the proposed control method (green line) performs better results compared to the other conventional approaches.

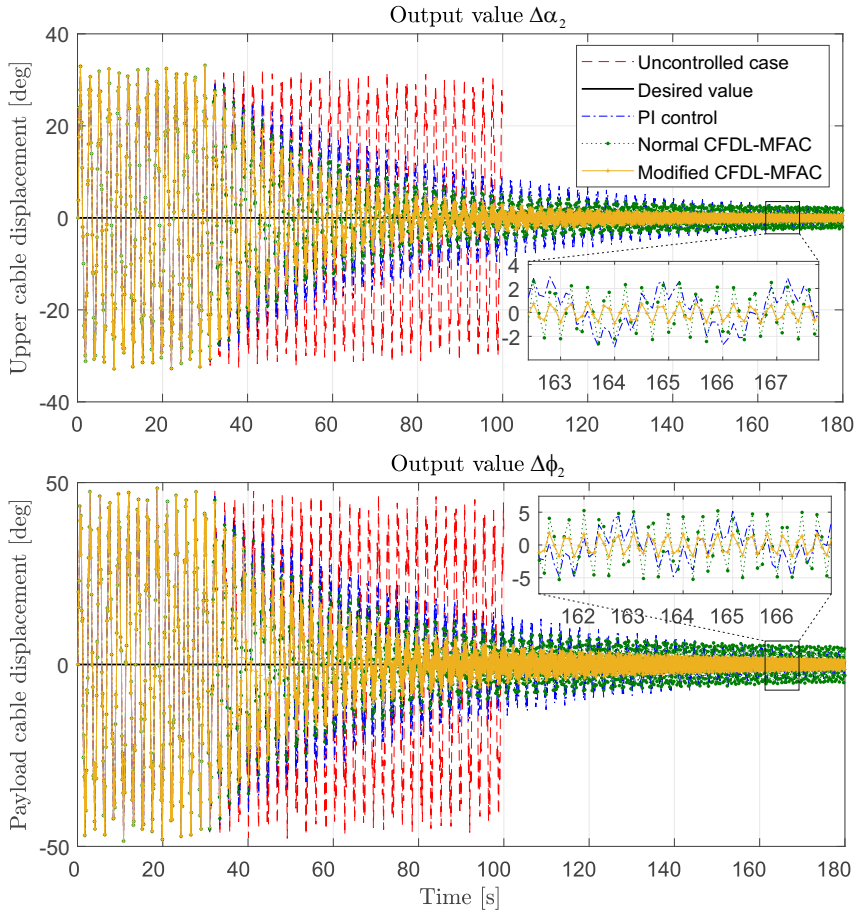

Figure 3.8: Vibration control results with respect to the outputs $\Delta\alpha_2$ and $\Delta\phi_2$ [PS19b]

Next, the control input energy-based evaluation which uses the criteria (3.104) is carried out. A set of controller gains K^* is defined as $K^* = \{\lambda_1, \lambda_2, k_p, k_i\}$, in which the constant weighting factors of the modified RLSA-MFAC and the normal PA-MFAC are λ_1 and λ_2 as mentioned in Table 3.5, respectively, with $\lambda_1, \lambda_2 \in [1.0, 45.0]$; whereas the design PI controller parameters are $k_p \in [0.0005, 0.08]$ and $k_i \in [0.0001, 0.25]$. It can be observed from Figure 3.14 that, in case of considering the interval length of time for simulation $T_1 = [t_1, t_2] = [30, 140]$ [s] (transient phase) by varying the controller gains K^*, the proposed RLSA-MFAC (green dot) has the trajectory P_{K^*} closer to the origin $(0, 0)$ in comparison with the normal PA-MFAC (blue dot) and PI control (red dot). In stationary phase $T_2 = [110, 140]$ [s], the trajectories P_{K^*} of the design controllers are depicted in Figure 3.15. Generally speaking, by changing parameters K^* the modified RLSA-MFAC results (green dot) seem to be closer to the origin with respect to smaller control errors. On the

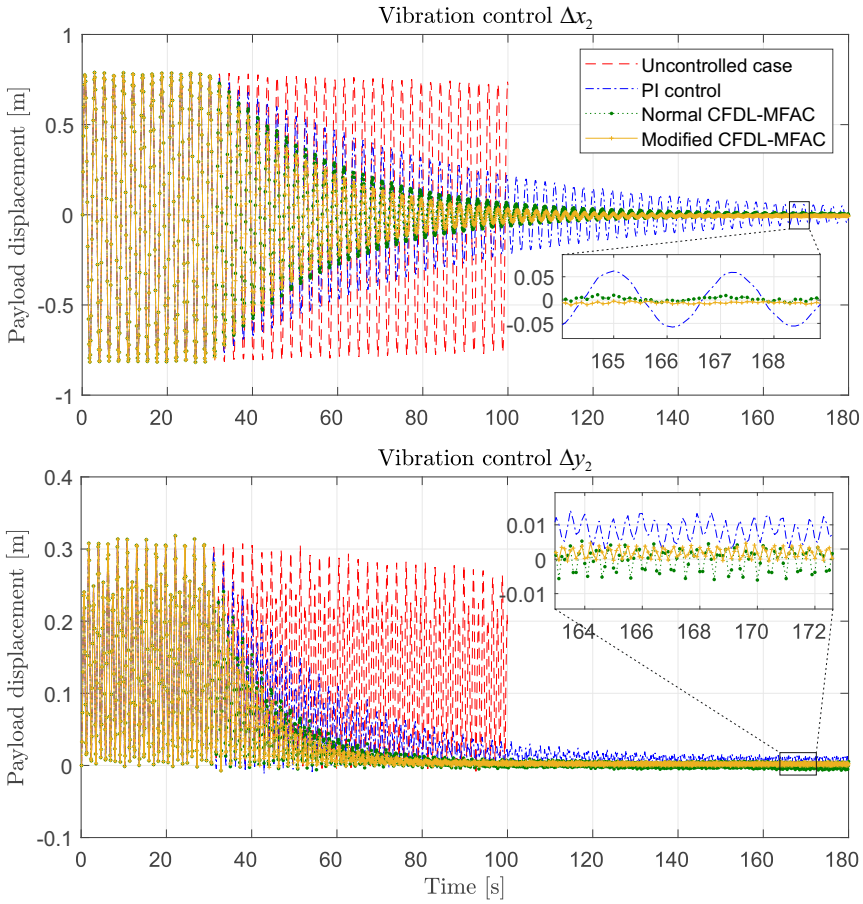

Figure 3.9: Vibration control results with respect to the payload position Δx_2 and Δy_2 [PS19b]

other hand, the modified model-free controller consumes more input energy than the other approaches.

In addition, the control effectiveness of the three discussed methods are compared numerically in Table 3.6 and Table 3.7 for both transient and stationary phase, correspondingly. In general, the RLSA-MFAC achieves the smallest numbers of the total control errors $\int \mathbf{e}^2(t)dt$ in transient phase (6.3008) as well as in stationary phase (0.0265). Furthermore, it is interesting to note that in stationary period, the improved model-free controller requires less control input energy $\int \mathbf{u}^2(t)dt$ ($9.9073e^{-4}$) than the other two controllers. However, in transient phase the smallest numbers of $\int \mathbf{u}^2(t)dt$ (0.0473), and E_{input} ($3.3792e^{-5}$) belongs to the normal PA-MFAC (see Table 3.6).

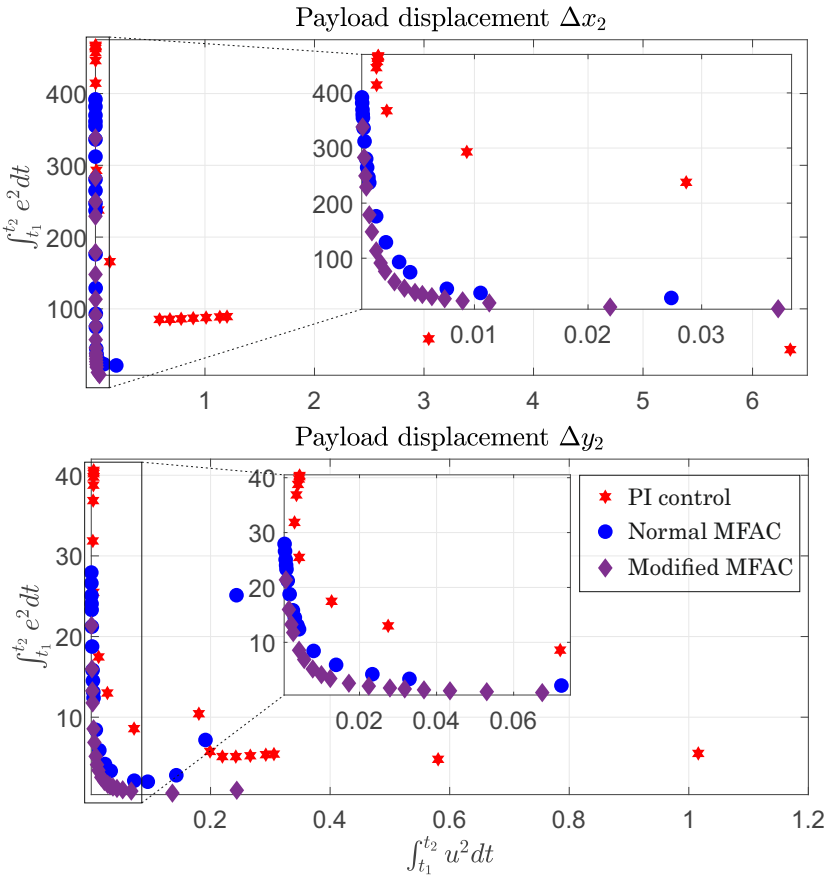

Figure 3.10: Control performance evaluation in transient phase regarding the criteria (3.104)

Table 3.4: Parameter-based control performance comparison in stationary phase

Control method	$\int \mathbf{e}^2(t)dt$	$\int \mathbf{u}^2(t)dt$	MSE	E_{input}
PI control	1.4330	0.0605	$7.9616e^{-4}$	$3.3646e^{-5}$
Normal CFDL-MFAC	2.0882	0.0020	0.0011	$1.1637e^{-6}$
Modified CFDL-MFAC	0.3294	0.0145	$1.8303e^{-4}$	$8.1105e^{-6}$

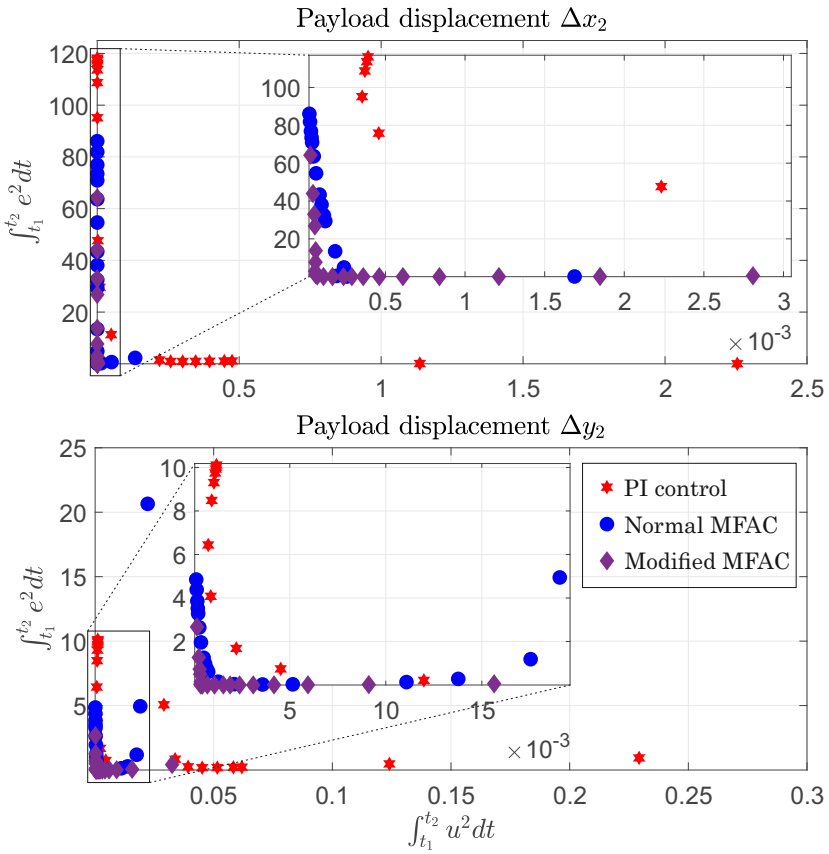

Figure 3.11: Control performance evaluation in stationary phase regarding the criteria (3.104)

Table 3.5: Design parameters of the model-free and PI controllers [PS20a]

Parameter	**Meaning**	**Value**
ρ	Step-size constant	0.6
λ_1	Weighting factor of the modified RLSA-MFAC	2.4
λ_2	Weighting factor of the normal PA-MFAC	1.25
j	Design weighting parameter	0.06
k_p	PI control parameter	0.002
k_i	PI control parameter	0.1

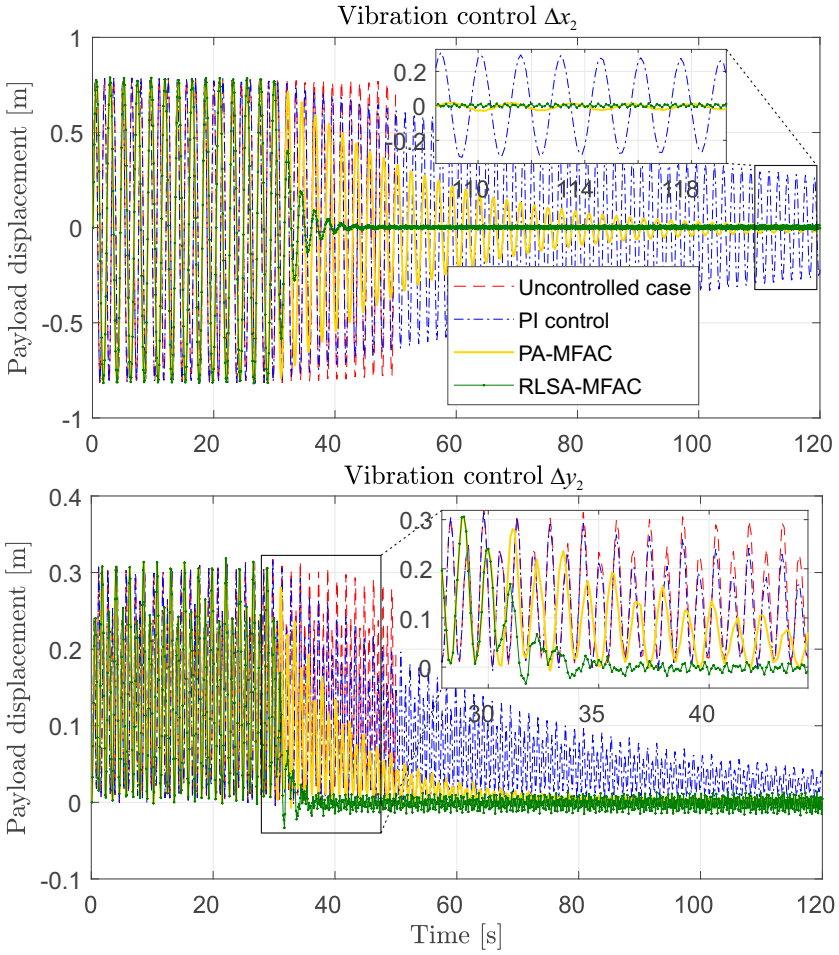

Figure 3.12: Comparison of vibration suppression with respect to the payload position Δx_2 and Δy_2 [PS20a]

Table 3.6: Comparison of control input energy-based evaluation in transient phase

Control method	$\int \mathbf{e}^2(t)dt$	$\int \mathbf{u}^2(t)dt$	MSE	E_{input}
PI control	97.1267	0.2163	0.0693	$1.5457e^{-4}$
Normal PA-MFAC	59.3759	0.0473	0.0424	$3.3792e^{-5}$
Modified RLSA-MFAC	6.3008	0.7179	0.0045	$5.1281e^{-4}$

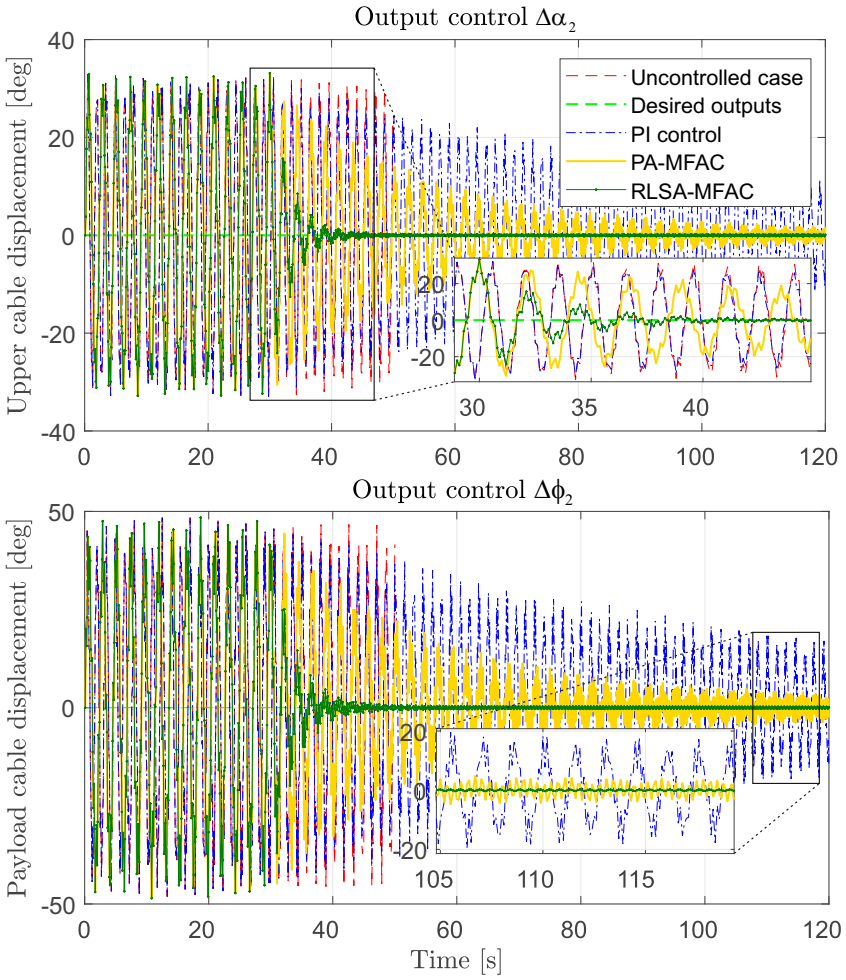

Figure 3.13: Comparison of vibration control with respect to the outputs $\Delta\alpha_2$ and $\Delta\phi_2$ [PS20a]

Table 3.7: Comparison of control input energy-based evaluation in stationary phase

Control method	$\int \mathbf{e}^2(t)dt$	$\int \mathbf{u}^2(t)dt$	MSE	E_{input}
PI control	3.4127	0.0414	0.0024	$2.9631e^{-5}$
Normal PA-MFAC	2.2092	0.0016	0.0015	$1.2084e^{-6}$
Modified RLSA-MFAC	0.0265	$9.9073e^{-4}$	$1.8979e^{-5}$	$7.0766e^{-7}$

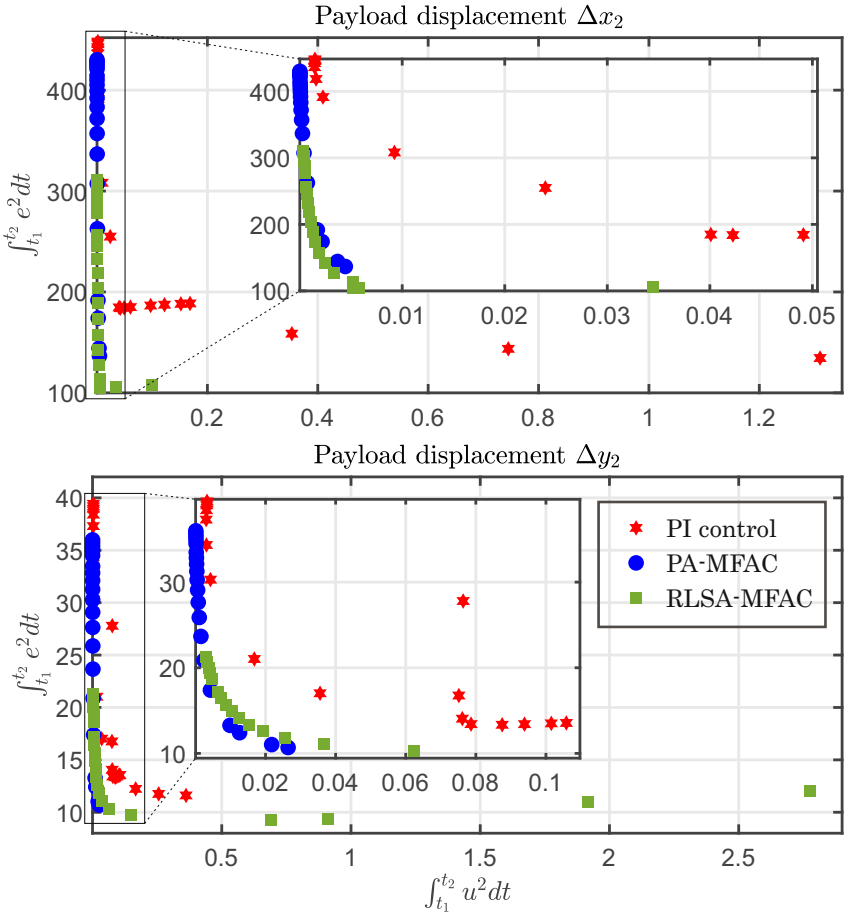

Figure 3.14: Control performance evaluation in transient phase regarding the criteria (3.104)

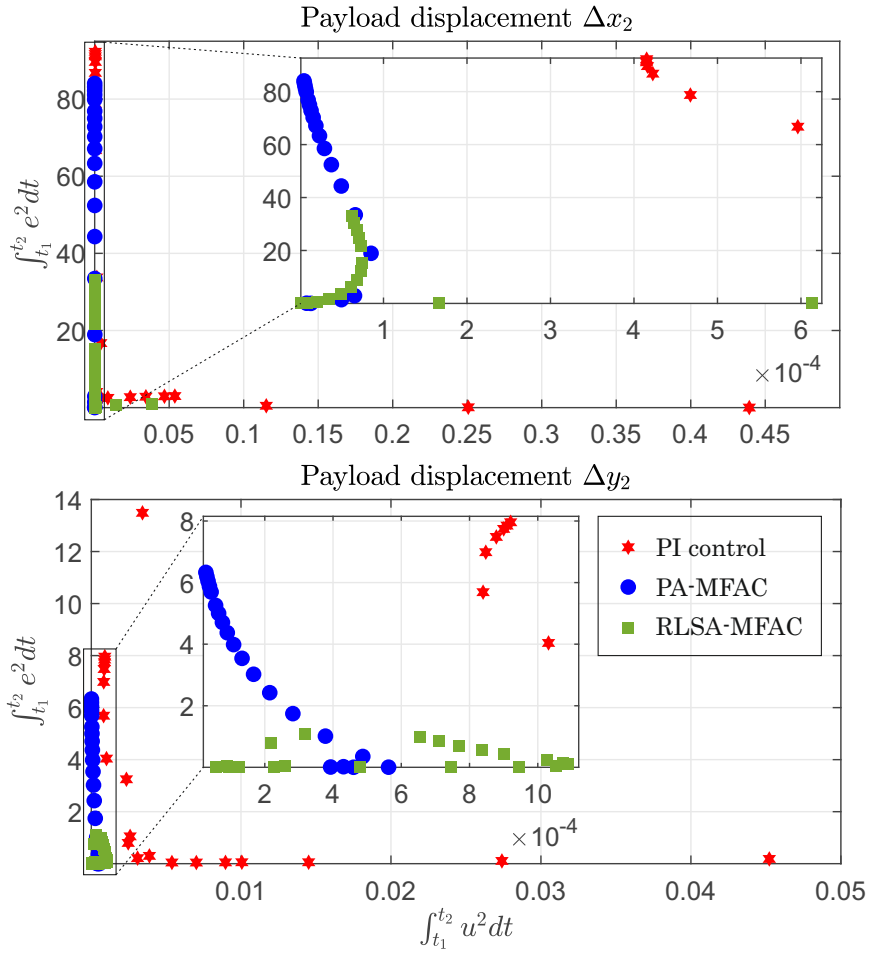

Figure 3.15: Control performance evaluation in stationary phase regarding the criteria (3.104)

3.4 Summary

In this chapter, two innovative ideas for MFAC modification have been proposed and intensively discussed for a class of discrete-time MIMO nonlinear systems.

First, based on the fundamental theory of the conventional MFAC method, an improved control input algorithm was developed. The control target is not only minimizing the output tracking errors but also the error variations within a specified length of time window. The modified model-free controller was designed using the concept of compact-form dynamic linearization.

Second, different from traditional MFAC which utilizes projection algorithm for unknown parameter estimation, this study proposed the method of using recursive least-squares algorithm to improve parameter estimation accuracy. Based on the corrected system parameters and the current tracking errors, the updated control input signals can be calculated by applying the modified control input law.

To verify control performance, the proposed control programs have been implemented to vibration reduction of an elastic ship-mounted crane via simulations. The discussed crane is represented as a typical flexible system with known orders. Vibration control results of the elastic boom and the payload position were clearly shown and compared with the standard MFAC as well as an industrial PI controller. The results indicated that significant improvement in oscillation elimination of the crane was obtained with respects to smaller vibrating amplitudes and faster control responses in comparison with the traditional methods. Moreover, the performance evaluation of the considered model-free control strategies have been analyzed in case of varying a set of the design controller parameters. Both of transient and stationary phases are considered. The relationship between the control input energy and the total derived tracking errors was judged. The simulation results demonstrated that the modified controllers show better tracking control efficiency regarding small control errors. However, the improved data-driven controllers still require more control input energy, particularly in transient phase compared to the other approaches.

4 Design of modified model-free adaptive control based on CFDL and PFDL techniques

Different modified MFAC strategies are proposed in this chapter. By using the CFDL concept, a linearized controller structure is assumed to be constructed, in which the unknown time-varying parameters of the local controller can be updated continuously. A modified objective function of the controller parameter matrix is proposed to improve estimation accuracy. Furthermore, improved model-free adaptive predictive control schemes are presented for a class of MIMO nonlinear systems. Based on the fundamentals of model predictive control, the generalized compact-form and partial-form predictive equations of the system outputs as well as appropriate control input algorithms will be designed. The recursive least-squares algorithm and its modification are used for system parameter estimation and prediction. Vibration control of an elastic ship-mounted crane is addressed by utilizing the proposed control schemes.

This chapter is organized as follows. In Section 4.1 and Section 4.2, a modified MFAC program is designed by using the CFDL concept not only for system linearization but also for the structural establishment of a linear controller. Section 4.3 and Section 4.4 discuss different model-free adaptive predictive control algorithms which can be implemented to reduce the vibrations of an elastic crane. Vibration control results and discussion are given in Section 4.5. Finally, some main ideas of the chapter are summarized in the last section.

The content, figures, and tables in this chapter have been accepted for publication in the following conference papers [PS20c, PS20d] or prepared as a journal article [PS20b]. Some of them are partly modified in this chapter after previous reviews and before final submission.

4.1 Model-free adaptive control using CFDL technique

In this section, MFAC design based on the CFDL concept is discussed. First, the mentioned dynamic linearization technique which can be applied to MIMO nonlinear systems is briefly reviewed. To estimate the unknown system parameters (PJM), the CFDL-PA or CFDL-RLSA (see Chapter 3) can be used properly. In addition, a compact-form linearized controller structure, which is assumed to be established at each sampling instant during the system operation, will be designed. Then, a standard controller parameter estimation equation is reviewed in case of multivariable systems.

4.1.1 CFDL-based parameter estimation algorithms

First, the CFDL technique [HJ13], which has been applied to establish a local linearized data model of unknown MIMO nonlinear systems and the on-line parameter estimation algorithms as discussed in the previous chapter will be briefly reviewed in this subsection. Then, by using the same idea of implementing the CFDL concept to the original system, this technique can be applied to an assumed unknown (nonlinear) controller based on some reasonable pre-required assumptions. Consequently, a linearized controller structure is established locally at every sampling interval together with the linearized system model. In addition, the unknown time-varying parameters of the design controller are estimated repeatedly by using the updated parameters from the local system model.

For a class of unknown MIMO nonlinear systems, a general I/O description can be written in discrete-time as

$$\mathbf{y}(k+1) = g\left(\mathbf{y}(k), \mathbf{y}(k-1), \ldots, \mathbf{y}(k-m_y), \mathbf{u}(k), \mathbf{u}(k-1), \ldots, \mathbf{u}(k-m_u)\right), \quad (4.1)$$

where m_y and m_u are two undefined positive integers indicating the unknown system orders. The unknown nonlinear function $g(\ldots)$ consists of the previous available control inputs and system outputs.

With the two reasonable assumptions as mentioned in Section 3.1, a linearized data-driven model or a CFDL model of the system (4.1) is given as

$$\Delta\mathbf{y}(k+1) = \Phi(k)\Delta\mathbf{u}(k), \quad (4.2)$$

in which the pseudo-jacobian matrix or PJM $\Phi(k)$ is unknown and time-varying. The system model (4.2) is virtually built by applying the CFDL concept. The matrix PJM appears as

$$\Phi(k) = \begin{bmatrix} \phi_{11}(k) & \phi_{12}(k) & \phi_{13}(k) & \ldots & \phi_{1m}(k) \\ \phi_{21}(k) & \phi_{22}(k) & \phi_{23}(k) & \ldots & \phi_{2m}(k) \\ \vdots & \vdots & \vdots & \ddots & \vdots \\ \phi_{r1}(k) & \phi_{r2}(k) & \phi_{r3}(k) & \ldots & \phi_{rm}(k) \end{bmatrix}_{r\times m}, \quad (4.3)$$

where the size of the PJM depends on the number of system inputs (m) and outputs (r). To design suitable controllers for the original system (4.1), the parameter matrix $\Phi(k)$ in (4.2) needs to be estimated and updated repeatedly via the discussed CFDL-PA as

$$\hat{\Phi}(k) = \hat{\Phi}(k-1) + \frac{\eta\left[\Delta\mathbf{y}(k) - \hat{\Phi}(k-1)\Delta\mathbf{u}(k-1)\right]\Delta\mathbf{u}^T(k-1)}{\mu + \|\Delta\mathbf{u}(k-1)\|^2}, \quad (4.4)$$

or the CFDL-RLSA as

$$\hat{\Phi}(k) = \hat{\Phi}(k-1) + \left[\Delta\mathbf{y}(k) - \hat{\Phi}(k-1)\Delta\mathbf{u}(k-1)\right]\mathbf{K}(k), \tag{4.5}$$

$$\begin{aligned}\mathbf{K}(k) &= \Delta\mathbf{u}^T(k-1)\mathbf{P}(k) \\ &= \Delta\mathbf{u}^T(k-1)\mathbf{P}(k-1)\left[\mathbf{I} + \Delta\mathbf{u}(k-1)\mathbf{P}(k-1)\Delta\mathbf{u}^T(k-1)\right]^{-1},\end{aligned} \tag{4.6}$$

$$\begin{aligned}\mathbf{P}(k) = \mathbf{P}(k-1) &- \mathbf{P}(k-1)\Delta\mathbf{u}^T(k-1) \\ &\left[\mathbf{I} + \Delta\mathbf{u}(k-1)\mathbf{P}(k-1)\Delta\mathbf{u}^T(k-1)\right]^{-1}\Delta\mathbf{u}(k-1)\mathbf{P}(k-1).\end{aligned} \tag{4.7}$$

From the above algorithms, to estimate the PJM at current step k, the closed-loop I/O data of the controlled system from the previous steps $k-1$ and $k-2$ have to be directly utilized. In the next subsection, the CFDL concept is used to linearize an assumed unknown nonlinear controller.

4.1.2 CFDL concept applied to an assumed nonlinear controller

As introduced in [HZ13], it is assumed that an unknown data-driven controller which can stabilize the original nonlinear system (4.1) can be represented in discrete-time as

$$\mathbf{u}(k) = h\left(\mathbf{u}(k-1), \mathbf{u}(k-2), \ldots, \mathbf{u}(k-n_c), \mathbf{e}(k+1), \mathbf{e}(k), \ldots, \mathbf{e}(k-n_e)\right), \tag{4.8}$$

where $h(\ldots)$ is a smooth unknown nonlinear vector-valued function, and $\mathbf{e}(k) = \mathbf{y}^d(k) - \mathbf{y}(k)$ is denoted as a vector of current tracking errors with the desired outputs (references) $\mathbf{y}^d(k)$ and the actual outputs $\mathbf{y}(k)$. Here n_c and n_e are two positive integers indicated as the unknown orders of the assumed controller (4.8). It can be noted that since the nonlinear function $h(\ldots)$ and the upcoming output control errors $\mathbf{e}(k+1)$ are not available up to current step k, the desired controller is only theoretically described in (4.8).

As mentioned earlier, the CFDL concept can be used to obtain a compact-form linearized controller structure. To this end, the two following assumptions [HZ13] need to be considered as

Assumption 4.1: The controller (4.8) is a smooth nonlinear function, and its partial derivatives $\partial h/\partial \mathbf{e}$ are continuous.

Assumption 4.2: The generalized Lipschitz condition

$$\|\mathbf{u}(k) - \mathbf{u}(k-1)\| \leq c\,\|\mathbf{e}(k+1) - \mathbf{e}(k)\|, \tag{4.9}$$

has to be fulfilled for the controller (4.8), with $c > 0$ and $\|\mathbf{e}(k+1) - \mathbf{e}(k)\| \neq 0$. This assumption imposes an upper limitation on the change rate of the controller outputs $\mathbf{u}(k)$ driven by the change rate of the tracking errors $\mathbf{e}(k)$.

Theorem 4.1 *Based on the aforementioned assumptions, the unknown nonlinear controller* (4.8) *can be linearized locally as a CFDL-based data model (CFDLc)*

$$\Delta \boldsymbol{u}(k) = \Psi(k)\Delta \boldsymbol{e}(k+1), \tag{4.10}$$

where $\Psi(k)$ *is an unknown time-varying parameter matrix of the design controller called pseudo-partial derivative (PPD) which should be estimated and updated continuously, and* $\|\Psi(k)\| \leq c$ *for any step* k *according to assumption 4.2. In addition, the control input and tracking error increment vectors are defined as* $\Delta \boldsymbol{u}(k) = \boldsymbol{u}(k) - \boldsymbol{u}(k-1), \Delta \boldsymbol{e}(k+1) = \boldsymbol{e}(k+1) - \boldsymbol{e}(k)$ *with* $\|\Delta \boldsymbol{e}(k+1)\| \neq 0$.

Proof 4.1 Based on the definition of $\Delta \mathbf{u}(k)$ and the controller structure (4.8), the control input increment vector is illustrated as

$$\begin{aligned}
&\Delta \mathbf{u}(k) = \mathbf{u}(k) - \mathbf{u}(k-1) \\
&= h\left(\mathbf{u}(k-1), \mathbf{u}(k-2), \ldots, \mathbf{u}(k-n_c), \mathbf{e}(k+1), \mathbf{e}(k), \ldots, \mathbf{e}(k-n_e)\right) \\
&- h\left(\mathbf{u}(k-1), \mathbf{u}(k-2), \ldots, \mathbf{u}(k-n_c), \mathbf{e}(k), \mathbf{e}(k), \ldots, \mathbf{e}(k-n_e)\right) \\
&+ h\left(\mathbf{u}(k-1), \mathbf{u}(k-2), \ldots, \mathbf{u}(k-n_c), \mathbf{e}(k), \mathbf{e}(k), \ldots, \mathbf{e}(k-n_e)\right) \\
&- h\left(\mathbf{u}(k-2), \mathbf{u}(k-3), \ldots, \mathbf{u}(k-n_c-1), \mathbf{e}(k), \mathbf{e}(k-1), \ldots, \mathbf{e}(k-n_e-1)\right).
\end{aligned} \tag{4.11}$$

The first two items in (4.11) can be represented based on Cauchy's mean value theorem as

$$\begin{aligned}
&= h\left(\mathbf{u}(k-1), \mathbf{u}(k-2), \ldots, \mathbf{u}(k-n_c), \mathbf{e}(k+1), \mathbf{e}(k), \ldots, \mathbf{e}(k-n_e)\right) \\
&- h\left(\mathbf{u}(k-1), \mathbf{u}(k-2), \ldots, \mathbf{u}(k-n_c), \mathbf{e}(k), \mathbf{e}(k), \ldots, \mathbf{e}(k-n_e)\right) \\
&= \frac{\partial h}{\partial \mathbf{e}(k+1)}\left[\mathbf{e}(k+1) - \mathbf{e}(k)\right] \\
&= \frac{\partial h}{\partial \mathbf{e}(k+1)}\Delta \mathbf{e}(k+1).
\end{aligned} \tag{4.12}$$

By denoting

$$\begin{aligned}
&\Lambda(k) = h\left(\mathbf{u}(k-1), \mathbf{u}(k-2), \ldots, \mathbf{u}(k-n_c), \mathbf{e}(k), \mathbf{e}(k), \ldots, \mathbf{e}(k-n_e)\right) \\
&- h\left(\mathbf{u}(k-2), \mathbf{u}(k-3), \ldots, \mathbf{u}(k-n_c-1), \mathbf{e}(k), \mathbf{e}(k-1), \ldots, \mathbf{e}(k-n_e-1)\right),
\end{aligned} \tag{4.13}$$

(4.11) can be rewritten as

$$\Delta \mathbf{u}(k) = \frac{\partial h}{\partial \mathbf{e}(k+1)}\Delta \mathbf{e}(k+1) + \Lambda(k), \tag{4.14}$$

where $\frac{\partial h}{\partial \mathbf{e}(k+1)}$ are the partial derivative values of $h(\ldots)$ with respect to tracking errors at a certain mean point within the interval $[\mathbf{e}(k)\ \mathbf{e}(k+1)]$.

For every fixed step k, the following equation can be given by using a numerical matrix $\mathbf{H}(k)$ as

$$\Lambda(k) = \mathbf{H}(k)\Delta \mathbf{e}(k+1). \tag{4.15}$$

Considering the condition $\|\Delta\mathbf{e}(k+1)\| \neq 0$, (4.15) must have at least one solution $\mathbf{H}^*(k)$ at each sampling interval k. Hence, the obtained equation (4.14) is equivalent to

$$\Delta\mathbf{u}(k) = (\underbrace{\frac{\partial h}{\partial \mathbf{e}(k+1)} + \mathbf{H}^*(k)}_{\Psi(k)})\Delta\mathbf{e}(k+1), \tag{4.16}$$

where $\|\Psi(k)\| \leq c$ holds due to the result of assumption 4.2. Hence, theorem 4.1 has been proven. In case of SISO systems, the corresponding proof has been discussed in [ZH12].

Theoretically, it can be assumed that the unknown controller (4.8) can generate perfect control input signals to derive perfect control performance [ZH12]; that means the upcoming output tracking errors $\mathbf{e}(k+1) = [0]$. From practical point of view, however, the tracking errors $\mathbf{e}(k+1)$ will not vanish completely at sampling instant $k+1$ because of system uncertainties or parameter estimation errors. Therefore, in practical applications, the re-defined actual control error vectors should be considered as

$$\varepsilon(k+1) = \mathbf{y}^d(k+1) - \mathbf{y}(k+1), \tag{4.17}$$
$$\varepsilon(k) = \mathbf{y}^d(k) - \mathbf{y}(k). \tag{4.18}$$

Hence, the practical control law based on the CFDL controller model (4.10) is derived as

$$\Delta\mathbf{u}(k) = -\Psi(k)\varepsilon(k), \tag{4.19}$$
$$\mathbf{u}(k) = \mathbf{u}(k-1) - \Psi(k)\varepsilon(k). \tag{4.20}$$

From the equivalent dynamic data model of the controlled system in (4.2), assuming $\mathbf{y}^d(k+1) = \mathbf{y}^d(k) = const$ (regulator problem), the following error dynamic equations are illustrated as

$$\mathbf{y}^d(k+1) - \mathbf{y}(k+1) = \mathbf{y}^d(k) - \mathbf{y}(k) - \Phi(k)\Delta\mathbf{u}(k), \tag{4.21}$$
$$\varepsilon(k+1) = \varepsilon(k) - \Phi(k)\Delta\mathbf{u}(k). \tag{4.22}$$

Substituting (4.19) into (4.22), results in

$$\varepsilon(k+1) = \varepsilon(k) + \Phi(k)\Psi(k)\varepsilon(k), \tag{4.23}$$
$$\varepsilon(k+1) = [\mathbf{I} + \Phi(k)\Psi(k)]\,\varepsilon(k), \tag{4.24}$$

where $\Phi(k)$ and $\Psi(k)$ are the unknown PJM and PPD parameter matrices of the original system (4.1) and the assumed nonlinear controller (4.8), respectively.

The unknown controller parameter matrix $\Psi(k)$ should be estimated to calculate the required control input $\mathbf{u}(k)$ in (4.20). Therefore, the following objective function with respect to the PPD matrix needs to be minimized

$$J\left(\Psi(k)\right) = \left\|\mathbf{y}^d(k+1) - \mathbf{y}(k+1)\right\|^2 + \lambda_k \|\Psi(k) - \Psi(k-1)\|^2, \tag{4.25}$$

where $\lambda_k > 0$ is a weighting factor which has been added to limit the change rate of $\Psi(k)$. Based on the CFDL data model of the plant as

$$\mathbf{y}(k+1) = \mathbf{y}(k) + \Phi(k)\Delta\mathbf{u}(k), \tag{4.26}$$

$$\mathbf{y}(k+1) = \mathbf{y}(k) - \Phi(k)\Psi(k)\varepsilon(k), \tag{4.27}$$

(4.25) becomes

$$J\left(\Psi(k)\right) = \left\|\mathbf{y}^d(k+1) - \mathbf{y}(k) + \Phi(k)\Psi(k)\varepsilon(k)\right\|^2 + \lambda_k \|\Psi(k) - \Psi(k-1)\|^2. \tag{4.28}$$

By minimizing (4.28) in term of $\Psi(k)$, the following equations are obtained

$$\frac{\partial J}{\partial \Psi(k)} = \left[\mathbf{y}^d(k+1) - \mathbf{y}(k) + \Phi(k)\Psi(k)\varepsilon(k)\right]\left[\Phi^T(k)\varepsilon^T(k)\right] \tag{4.29}$$
$$+ \lambda_k \left[\Psi(k) - \Psi(k-1)\right] = 0,$$

$$\hat{\Psi}(k) = \hat{\Psi}(k-1) - \frac{\rho_k \left[\mathbf{y}^d(k+1) - \mathbf{y}(k) + \hat{\Psi}(k-1)\hat{\Phi}(k)\varepsilon(k)\right]\hat{\Phi}^T(k)\varepsilon^T(k)}{\lambda_k + \left\|\hat{\Phi}(k)\varepsilon(k)\right\|^2}, \tag{4.30}$$

where $\rho_k > 0$ denoted as a step-size constant. The system parameter matrix $\hat{\Phi}(k)$ in (4.30) could be estimated via the CFDL-PA (4.4) or the CFDL-RLSA (4.5), (4.6), and (4.7). Finally, the updated control input vector $\mathbf{u}(k)$ is calculated recursively via (4.20) by using the actual control errors $\varepsilon(k)$ in (4.18) and the estimated PPD parameters $\hat{\Psi}(k)$ in (4.30).

4.2 Modified CFDLc-based model-free adaptive control

In this section, a modified estimation algorithm of the controller parameter matrix or PPD $\Psi(k)$ in the control law (4.20) is proposed. The key idea of modification is that, the actual tracking errors $\varepsilon(k+1)$ as well as the error variations $\Delta\varepsilon(k-N)$ within a specified length of sampling interval $N > 0$ are minimized to improve control performance. The modified control approach has been implemented successfully to an inverted elastic cantilever beam as an example of SISO nonlinear systems [MS18]. A modified objective function of the PPD matrix is firstly introduced in this study. As a result, by minimizing this cost function, a novel parameter estimation algorithm

of the design controller is generated which allows to update the parameters $\Psi(k)$ recursively. Based on the updated controller parameters and the current output tracking errors, the required control input signals $\mathbf{u}(k)$ is computed. Explanation of how to apply the proposed method to control a class of unknown MIMO nonlinear systems as well as several necessary steps to execute the design control scheme will be addressed at the end of the section.

4.2.1 Modified controller parameter estimation algorithm

Based on the existing objective function of $\Psi(k)$ as given in (4.25), here a modified one is proposed as

$$J\left(\Psi(k)\right) = \left\|\mathbf{y}^d(k+1) - \mathbf{y}(k+1)\right\|^2 + \tau\left\|\Delta\mathbf{y}^d(k+1) - \Delta\mathbf{y}(k+1) - \Delta\mathbf{y}(k)\right\|^2 + \lambda_k\|\Psi(k) - \Psi(k-1)\|^2, \tag{4.31}$$

where $\tau > 0$ denotes a constant design parameter. To minimize the tracking error variations, the term of $\left\|\Delta\mathbf{y}^d(k+1) - \Delta\mathbf{y}(k+1) - \Delta\mathbf{y}(k)\right\|$ is added into (4.31). The actual system output vector $\mathbf{y}(k+1)$ and output increment vector $\Delta\mathbf{y}(k+1)$ in (4.31) can be replaced by the system CFDL data model as follows

$$\mathbf{y}(k+1) = \mathbf{y}(k) - \Phi(k)\Psi(k)\varepsilon(k), \tag{4.32}$$

$$\Delta\mathbf{y}(k+1) = -\Phi(k)\Psi(k)\varepsilon(k), \tag{4.33}$$

where the system parameter matrix is denoted as $\Phi(k)$ or PJM.

Substituting (4.32) and (4.33) into (4.31), yields the following cost function

$$J\left(\Psi(k)\right) = \left\|\mathbf{y}^d(k+1) - \mathbf{y}(k) + \Phi(k)\Psi(k)\varepsilon(k)\right\|^2 + \tau\left\|\Delta\mathbf{y}^d(k+1) + \Phi(k)\Psi(k)\varepsilon(k) - \Delta\mathbf{y}(k)\right\|^2 + \lambda_k\|\Psi(k) - \Psi(k-1)\|^2. \tag{4.34}$$

Differentiating (4.34) with respect to $\Psi(k)$ and letting it zero, the following equations

$$\begin{aligned}\frac{\partial J}{\partial \Psi(k)} &= \left[\mathbf{y}^d(k+1) - \mathbf{y}(k) + \Phi(k)\Psi(k)\varepsilon(k)\right]\left[\Phi^T(k)\varepsilon^T(k)\right] \\ &+ \tau\left[\Delta\mathbf{y}^d(k+1) + \Phi(k)\Psi(k)\varepsilon(k) - \Delta\mathbf{y}(k)\right]\left[\Phi^T(k)\varepsilon^T(k)\right] \\ &+ \lambda_k\left[\Psi(k) - \Psi(k-1)\right] = 0,\end{aligned} \tag{4.35}$$

$$\begin{aligned}\hat{\Psi}(k) &= \hat{\Psi}(k-1) \\ &- \frac{\rho_k\left[\mathbf{y}^d(k+1) - \mathbf{y}(k) + (1+\tau)\,\hat{\Psi}(k-1)\hat{\Phi}(k)\varepsilon(k)\right]\hat{\Phi}^T(k)\varepsilon^T(k)}{\lambda_k + (1+\tau)\left\|\hat{\Phi}(k)\varepsilon(k)\right\|^2} \\ &- \frac{\tau\left[\mathbf{y}^d(k+1) - \mathbf{y}(k) - \left(\mathbf{y}^d(k) - \mathbf{y}(k-1)\right)\right]\hat{\Phi}^T(k)\varepsilon^T(k)}{\lambda_k + (1+\tau)\left\|\hat{\Phi}(k)\varepsilon(k)\right\|^2},\end{aligned} \tag{4.36}$$

are derived. The estimation algorithm (4.36) is slightly different with the standard algorithm (4.30). As discussed in [PS19b, MS18], the output error differences determined as $\left[\mathbf{y}^d(k+1)-\mathbf{y}^d(k)-(\mathbf{y}(k)-\mathbf{y}(k-1))\right]$ in (4.36) only consider minimizing one step of the tracking errors from previous steps with relatively small amplitudes. Therefore, to improve tracking control performance the extended error variations within a length of $N>0$ sampling instants are considered as $\left[\mathbf{y}^d(k+1)-\mathbf{y}(k)-\left(\mathbf{y}^d(k-N+1)-\mathbf{y}(k-N)\right)\right]$, resulting in the modified recursive estimation equation

$$\begin{aligned}\hat{\Psi}(k) &= \hat{\Psi}(k-1) \\ &- \frac{\rho_k\left[\mathbf{y}^d(k+1)-\mathbf{y}(k)+(1+\tau)\,\hat{\Psi}(k-1)\hat{\Phi}(k)\varepsilon(k)\right]\hat{\Phi}^T(k)\varepsilon^T(k)}{\lambda_k+(1+\tau)\left\|\hat{\Phi}(k)\varepsilon(k)\right\|^2} \\ &- \frac{\tau\left[\varepsilon(k)-\varepsilon(k-N)\right]\hat{\Phi}^T(k)\varepsilon^T(k)}{\lambda_k+(1+\tau)\left\|\hat{\Phi}(k)\varepsilon(k)\right\|^2},\end{aligned} \tag{4.37}$$

where $\varepsilon(k)=\mathbf{y}^d(k+1)-\mathbf{y}(k); \varepsilon(k-N)=\mathbf{y}^d(k-N+1)-\mathbf{y}(k-N)$ are indicated as the actual output tracking errors at step k and $k-N$, respectively. Here $\rho_k>0$ is a step-size constant. The system parameter matrix $\hat{\Phi}(k)$ in (4.37) should be estimated by using the CFDL-PA (4.4) or the CFDL-RLSA (4.5), (4.6), and (4.7).

4.2.2 Control scheme for application to unknown MIMO systems

The proposed method can be applied to control a class of unknown MIMO (nonlinear) systems. The modified control scheme is illustrated in Figure 4.1. To design the CFDLc-based model-free controller, the following steps have to be considered:

- *Step 1:* Based on the CFDL data model and the available I/O data from the system, the unknown PJM parameters $\hat{\Phi}(k)$ are estimated and updated continuously by using different on-line parameter estimation algorithms. According to [HJ13] and assumption 3.3 in Section 3.1, to improve the ability in tracking time-varying parameters a reset condition is defined as

$$\begin{aligned}\hat{\phi}_{ii}(k)=\hat{\phi}_{ii}(1)\ \ if\ \ &\left|\hat{\phi}_{ii}(k)\right|<c_2\ \ or\ \ \left|\hat{\phi}_{ii}(k)\right|>\alpha c_2 \\ or\ \ &\operatorname{sgn}\left(\hat{\phi}_{ii}(k)\right)\neq\operatorname{sgn}\left(\hat{\phi}_{ii}(1)\right),\end{aligned} \tag{4.38}$$

$$\begin{aligned}\hat{\phi}_{ij}(k)=\hat{\phi}_{ij}(1)\ \ if\ \ &\left|\hat{\phi}_{ij}(k)\right|>c_1 \\ or\ \ &\operatorname{sgn}\left(\hat{\phi}_{ij}(k)\right)\neq\operatorname{sgn}\left(\hat{\phi}_{ij}(1)\right),\end{aligned} \tag{4.39}$$

where $\hat{\phi}_{ii}(1), \hat{\phi}_{ij}(1)$ are the initial values of the PJM, with $i, j = 1, 2, \ldots, n^*$ and $i \neq j$ (according to assumption 3.3). The two positive constants are c_1, c_2 with $c_2 > c_1 (2\alpha + 1) (n^* - 1) ; \alpha \geq 1$.

- *Step 2:* By using the updated PJM $\hat{\Phi}(k)$ and the actual tracking errors $\varepsilon(k)$, the time-varying controller parameters $\hat{\Psi}(k)$ can be estimated via (4.37). To increase the on-line tracking ability of the matrix PPD, another reset condition [HZ13] should be considered as

$$\left\|\hat{\Psi}(k)\right\| = -b_1 \ \ if \ \ \left\|\hat{\Psi}(k)\right\| > b_1 \ \ or \ \ \left\|\hat{\Psi}(k)\right\| < -b_1, \tag{4.40}$$

where $b_1 > 0$ is a small constant. It can be noted that the sign of all elements of the matrix $\hat{\Psi}(k)$ is always negative, whereas that of the matrix $\hat{\Phi}(k)$ is positive (according to the reset conditions (4.38), (4.39), and (4.40)), that means the future tracking errors $\varepsilon(k+1)$ converge to zero according to the error dynamic equation (4.24).

- *Step 3:* Based on the corrected PPD $\hat{\Psi}(k)$ and actual output tracking errors $\varepsilon(k)$, the current control input vector $\mathbf{u}(k)$ is updated via (4.20). Then, the system output values $\mathbf{y}(k+1)$ in the next sampling instant $k+1$ will be measured or computed, and the given process is carried out repeatedly.

4.3 Compact-form dynamic linearization-based model-free predictive control

Model predictive control (MPC) has become more attractive in control engineering for the last decades because of its efficiency and robustness. In this study, an effective control strategy is proposed for vibration reduction of mechanical flexible systems, in which establishment of a global dynamic model of the controlled system is not necessary. A modified model-free adaptive predictive controller will be designed by combination of the MPC and MFC theories. The control idea is that, based on the CFDL technique [HJ13], the future system outputs within a finite prediction horizon can be predicted in sequence. The data-driven predictive model of the system only requires the closed-loop I/O information, and therefore the future control input increments as well as the unknown time-varying system parameters namely pseudo-jacobian matrix (PJM) can be estimated. To improve parameter estimation accuracy, in this work, the recursive least-squares algorithm (see Section 3.2) and its modification will be utilized instead of using conventional projection algorithm [HJ13]. In the current section, a general compact-form of N_y-step-ahead predictive equation is established based on the CFDL concept. This linearized dynamical formula contains a set of the unknown parameter matrices which need to be estimated and predicted repeatedly. The updated PJM will be implemented to define the required control inputs, and therefore to fulfill the initial control requirements.

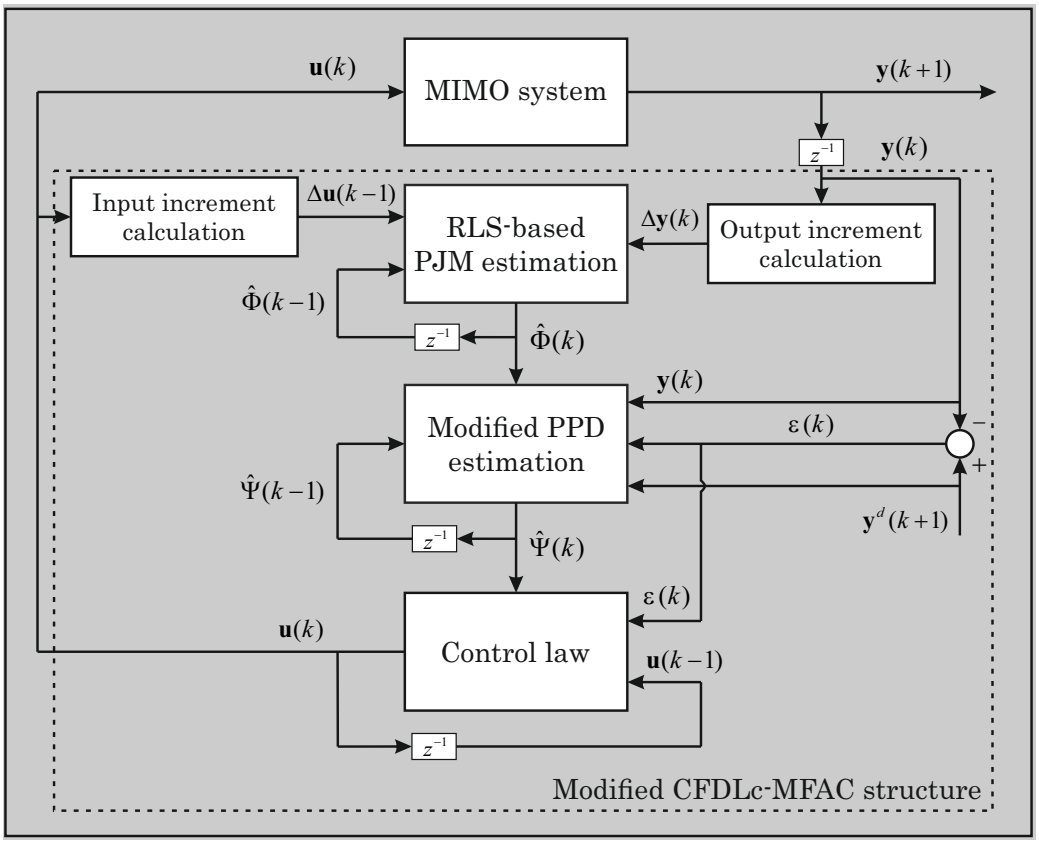

Figure 4.1: Modified CFDLc-based model-free control scheme for unknown MIMO systems [PS20c]

4.3.1 General compact-form predictive equation

As discussed in Section 4.1, for a class of unknown MIMO nonlinear systems a general I/O description can be illustrated in (4.1). Based on the two reasonable assumptions as mentioned in Section 3.1, the original system (4.1) can be linearized locally at each sampling time as a CFDL data model

$$\Delta \mathbf{y}(k+1) = \Phi(k)\Delta \mathbf{u}(k), \tag{4.41}$$

where $\Phi(k)$ is the unknown system parameter matrix described in (4.3). The CFDL model (4.41) also describes one-step-ahead prediction equation of the system outputs

$$\mathbf{y}(k+1) = \mathbf{y}(k) + \Phi(k)\Delta \mathbf{u}(k). \tag{4.42}$$

According to (4.42), N_y-step-ahead prediction equations of the system dynamics can be virtually established as follows

$$\begin{cases} \mathbf{y}(k+1) = \mathbf{y}(k) + \Phi(k)\Delta\mathbf{u}(k) \\ \mathbf{y}(k+2) = \mathbf{y}(k+1) + \Phi(k+1)\Delta\mathbf{u}(k+1) \\ \mathbf{y}(k+2) = \mathbf{y}(k) + \Phi(k)\Delta\mathbf{u}(k) + \Phi(k+1)\Delta\mathbf{u}(k+1) \\ \vdots \\ \mathbf{y}(k+N_u) = \mathbf{y}(k+N_u-1) + \Phi(k+N_u-1)\Delta\mathbf{u}(k+N_u-1) \\ \vdots \\ \mathbf{y}(k+N_y) = \mathbf{y}(k+N_y-1) + \Phi(k+N_y-1)\Delta\mathbf{u}(k+N_y-1) \\ \mathbf{y}(k+N_y) = \mathbf{y}(k) + \Phi(k)\Delta\mathbf{u}(k) \\ +... + \Phi(k+N_u-1)\Delta\mathbf{u}(k+N_u-1) \\ +... + \Phi(k+N_y-1)\Delta\mathbf{u}(k+N_y-1) \end{cases}, \tag{4.43}$$

where N_y, N_u are denoted as the finite prediction horizons of the system output and control input, respectively, with $1 \leq N_u \leq N_y$.

Let the following notations

$$\mathbf{Y}_{N_y}(k+1) = [\mathbf{y}(k+1), ..., \mathbf{y}(k+N_u), ..., \mathbf{y}(k+N_y)]^T, \tag{4.44}$$

$$\Delta\mathbf{U}_{N_y}(k) = [\Delta\mathbf{u}(k), ..., \Delta\mathbf{u}(k+N_u-1), ..., \Delta\mathbf{u}(k+N_y-1)]^T, \tag{4.45}$$

$$\mathbf{E}(k) = [\mathbf{I}_{r\times m}, \mathbf{I}_{r\times m}, ..., \mathbf{I}_{r\times m}]^T, \tag{4.46}$$

$$\mathbf{D}(k) = \begin{bmatrix} \Phi(k) & \mathbf{0} & \mathbf{0} & \dots & \mathbf{0} & \mathbf{0} \\ \Phi(k) & \Phi(k+1) & \mathbf{0} & \dots & \mathbf{0} & \mathbf{0} \\ \vdots & \vdots & \ddots & \ddots & \ddots & \vdots \\ \Phi(k) & \Phi(k+1) & \vdots & \Phi(k+N_u-1) & \mathbf{0} & \mathbf{0} \\ \vdots & \vdots & \ddots & \vdots & \ddots & \vdots \\ \Phi(k) & \Phi(k+1) & \dots & \Phi(k+N_u-1) & \dots & \Phi(k+N_y-1) \end{bmatrix}_{N_y\times N_y}, \tag{4.47}$$

where $\mathbf{Y}_{N_y}(k+1)$ denotes N_y-step-ahead prediction output vector; whilst $\Delta\mathbf{U}_{N_y}(k)$ represents the predicted control input increment vector along the output prediction horizon $k = 1, 2, \ldots, N_u, \ldots, N_y$. Here $\mathbf{I}_{r\times m}$ and $\mathbf{0}_{r\times m}$ are indicated as the identity and zero matrices, correspondingly, with the number of control inputs m and system outputs r.

Consequently, (4.43) can be rewritten in a general compact-form of N_y-step-ahead prediction equation as

$$\mathbf{Y}_{N_y}(k+1) = \mathbf{E}(k)\mathbf{y}(k) + \mathbf{D}(k)\Delta\mathbf{U}_{N_y}(k). \tag{4.48}$$

It can be assumed that the predicted control inputs will not change at a certain sampling interval, that means if $j > N_u$ leading to $\Delta\mathbf{u}(k+j-1) = [0]$ in (4.45),

with $j = 1, 2, \ldots, N_u, \ldots, N_y$. Therefore, the predictive equation (4.48) becomes

$$\mathbf{Y}_{N_y}(k+1) = \mathbf{E}(k)\mathbf{y}(k) + \mathbf{D}_1(k)\Delta\mathbf{U}_{N_u}(k), \tag{4.49}$$

where the predicted control input increment vector is written as

$$\Delta\mathbf{U}_{N_u}(k) = [\Delta\mathbf{u}(k), \Delta\mathbf{u}(k+1), ..., \Delta\mathbf{u}(k+N_u-1)]^T, \tag{4.50}$$

and a set of the unknown time-varying parameter matrices PJM are denoted as

$$\mathbf{D}_1(k) = \begin{bmatrix} \Phi(k) & \mathbf{0} & \mathbf{0} & \mathbf{0} \\ \Phi(k) & \Phi(k+1) & \mathbf{0} & \mathbf{0} \\ \vdots & \vdots & \ddots & \vdots \\ \Phi(k) & \Phi(k+1) & \ldots & \Phi(k+N_u-1) \\ \vdots & \vdots & \ldots & \vdots \\ \Phi(k) & \Phi(k+1) & \ldots & \Phi(k+N_u-1) \end{bmatrix}_{N_y \times N_u}. \tag{4.51}$$

Based on the output predictive equation (4.49), the future control input increment vector $\Delta\mathbf{U}_{N_u}(k)$ as well as the current control input vector $\mathbf{u}(k)$ will be calculated in the next sections.

4.3.2 Parameter estimation and prediction

The general compact-form N_y-step-ahead predictive model of the system output (4.49) contains a set of the unknown time-varying parameter matrices $\Phi(k), \Phi(k+1), \ldots, \Phi(k+N_u-1)$ as illustrated in (4.51). These matrices can be estimated and predicted continuously based on the available system I/O data to determine the predicted system inputs and outputs. To estimate the PJM at current step $\Phi(k)$, instead of using traditional projection algorithm [HJ13], this study considers the CFDL-RLSA and its modification as discussed in Section 3.2 for estimation accuracy improvement. Furthermore, the other unknown PJM matrices $\Phi(k+1), \Phi(k+2), \ldots, \Phi(k+N_u-1)$ can be predicted according to the existing (available) values $\hat{\Phi}(1), \hat{\Phi}(2), \ldots, \hat{\Phi}(k)$ by applying the multilevel hierarchical forecasting algorithm [HJ13].

The recursive least-squares estimation method as introduced in [GS14, ÅW08] has been applied to the equivalent linearized CFDL data model (4.41) of an unknown MIMO plant. As a result, the unknown parameters $\Phi(k)$ is estimated and updated recursively via the obtained CFDL-RLSA in (4.5), (4.6), and (4.7). To improve the performance of the least-squares algorithm, a modified CFDL-RLSA as presented in [HJ13] is considered in this contribution, and could be applied to the CFDL system

model which results in the following equations

$$\hat{\Phi}(k) = \hat{\Phi}(k-1) + \left[\Delta \mathbf{y}(k) - \hat{\Phi}(k-1)\Delta \mathbf{u}(k-1)\right] \Delta \mathbf{u}^T(k-1)\mathbf{P}(k) \\ - \gamma \mathbf{P}(k)\left[\hat{\Phi}(k-1) - \hat{\Phi}(k-2)\right], \tag{4.52}$$

$$\mathbf{P}(k) = \mathbf{P}(k-1) - \mathbf{P}(k-1)\Delta \mathbf{u}^T(k-1) \\ \left[\mathbf{I} + \Delta \mathbf{u}(k-1)\mathbf{P}(k-1)\Delta \mathbf{u}^T(k-1)\right]^{-1} \Delta \mathbf{u}(k-1)\mathbf{P}(k-1), \tag{4.53}$$

where $\gamma > 0$ is a constant design parameter.

To predict the future PJM $\Phi(k+1), \Phi(k+2), \ldots, \Phi(k+N_u-1)$ in (4.51), the available estimated values $\hat{\Phi}(1), \hat{\Phi}(2), \ldots, \hat{\Phi}(k)$ calculated in (4.52), (4.53) will be used explicitly. Based on the multilevel hierarchical forecasting method [HJ13], an auto-regressive prediction model of the PJM in the next sampling instant $k+1$ is given as

$$\hat{\Phi}(k+1) = \theta_1(k)\hat{\Phi}(k) + \theta_2(k)\hat{\Phi}(k-1) + \ldots + \theta_{n_p}(k)\hat{\Phi}(k-n_p+1), \tag{4.54}$$

where $\theta_i,\ i = 1, 2, \ldots, n_p$ are the model coefficients, and $n_p \in [2, 7]$ as recommended in [GHLJ19] is denoted as the fixed model order. In general, the prediction equation of the PJM can be written as

$$\hat{\Phi}(k+j) = \theta_1(k)\hat{\Phi}(k+j-1) \\ + \theta_2(k)\hat{\Phi}(k+j-2) + \ldots + \theta_{n_p}(k)\hat{\Phi}(k+j-n_p), \tag{4.55}$$

where $j = 1, 2, ..., N_u - 1$. Let the following values

$$\theta(k) = \left[\theta_1(k), \theta_2(k), \ldots, \theta_{n_p}(k)\right]^T, \tag{4.56}$$

$$\hat{\Omega}(k-1) = \left[\hat{\Phi}(k-1), \hat{\Phi}(k-2), \ldots, \hat{\Phi}(k-n_p)\right]^T, \tag{4.57}$$

$$\hat{\Phi}(k) = \hat{\Omega}(k-1)\theta^T(k). \tag{4.58}$$

The unknown parameters $\theta_1(k), \theta_2(k), \ldots, \theta_{n_p}(k)$ in (4.54) and (4.55) can be defined by minimizing the following objective function [GHLJ19]

$$J(\theta(k)) = \left\|\Phi(k) - \Omega(k-1)\theta^T(k)\right\|^2 + \delta\|\theta(k) - \theta(k-1)\|^2. \tag{4.59}$$

Differentiating (4.59) with respect to $\theta(k)$ and letting it zero, hence the optimal parameters

$$\theta(k) = \theta(k-1) + \frac{\left[\hat{\Phi}(k) - \theta^T(k-1)\hat{\Omega}(k-1)\right]\hat{\Omega}^T(k-1)}{\delta + \left\|\hat{\Omega}(k-1)\right\|^2}, \tag{4.60}$$

where $\delta \in (0, 1]$ is a positive constant. Based on the vector of parameters $\theta(k)$ which are recursively calculated in (4.60) and the old PJM values up to current step as $\hat{\Phi}(1), \hat{\Phi}(2), \ldots, \hat{\Phi}(k)$, the upcoming PJM matrices $\hat{\Phi}(k+j)$ at steps $j = 1, 2, \ldots, N_u - 1$ are predicted via (4.55).

4.3.3 Control input calculation

A model-free adaptive predictive controller (MFAPC) based on the CFDL concept will be designed in this subsection. The proposed method can be applied to vibration control of a class of mechanical flexible systems. Based on the estimated and predicted system parameter matrices $\hat{\Phi}(k), \hat{\Phi}(k+1), \ldots, \hat{\Phi}(k+N_u-1)$ as well as the predicted output tracking errors denoted as $\mathbf{e}_{N_y}(k+1)$ within the finite output prediction horizon N_y, the required control input vector $\mathbf{u}(k)$ can be calculated.

The future control input increment vector $\Delta\mathbf{U}_{N_u}(k)$ in (4.49) can be predicted at each step of the control input prediction horizon $k = 1, 2, \ldots, N_u$. The control goal is to minimize the predicted tracking errors between the future references $\mathbf{y}^d(k+i)$ and the predicted system outputs $\mathbf{y}(k+i)$ considering input energy limitation by adding a weighting factor λ into objective function, where $i = 1, 2, ..., N_u, ..., N_y$. Hence, the cost function with respect to the control input increment vector $\Delta\mathbf{u}(k)$ is considered as

$$J\left(\Delta\mathbf{u}(k)\right) = \sum_{i=1}^{N_y} \left\|\mathbf{y}^d(k+i) - \mathbf{y}(k+i)\right\|^2 + \lambda \sum_{j=0}^{N_u-1} \left\|\Delta\mathbf{u}(k+j)\right\|^2, \tag{4.61}$$

where $\lambda > 0$ is a constant design parameter which is used to restrict the change rate of the future control inputs. The desired system outputs $\mathbf{y}^d(k+i)$ in (4.61) along the given output prediction horizon N_y is written as

$$\mathbf{Y}^d_{N_y}(k+1) = \left[\mathbf{y}^d(k+1), \ldots, \mathbf{y}^d(k+N_u), \ldots, \mathbf{y}^d(k+N_y)\right]^T. \tag{4.62}$$

By substituting (4.44), (4.50), and (4.62) into (4.61), the above objective function is rewritten as

$$\begin{aligned} J\left(\Delta\mathbf{U}_{N_u}(k)\right) &= \left[\mathbf{Y}^d_{N_y}(k+1) - \mathbf{Y}_{N_y}(k+1)\right]^T \left[\mathbf{Y}^d_{N_y}(k+1) - \mathbf{Y}_{N_y}(k+1)\right] \\ &\quad + \lambda\Delta\mathbf{U}_{N_u}{}^T(k)\Delta\mathbf{U}_{N_u}(k). \end{aligned} \tag{4.63}$$

The future output vector $\mathbf{Y}_{N_y}(k+1)$ in (4.63) can be approximated by the general compact-form predictive model (4.49). Therefore, substituting (4.49) into (4.63) leads to the following function

$$\begin{aligned} J\left(\Delta\mathbf{U}_{N_u}(k)\right) &= \left[\mathbf{Y}^d_{N_y}(k+1) - \mathbf{E}(k)\mathbf{y}(k) - \mathbf{D}_1(k)\Delta\mathbf{U}_{N_u}(k)\right]^2 \\ &\quad + \lambda\Delta\mathbf{U}^T{}_{N_u}(k)\Delta\mathbf{U}_{N_u}(k). \end{aligned} \tag{4.64}$$

Solving the optimal problem by differentiating (4.64) in term of $\Delta\mathbf{U}_{N_u}(k)$ and letting it zero, yields

$$\begin{aligned} \frac{\partial J}{\partial\Delta\mathbf{U}_{N_u}(k)} &= \left[\mathbf{Y}^d_{N_y}(k+1) - \mathbf{E}(k)\mathbf{y}(k) - \mathbf{D}_1(k)\Delta\mathbf{U}_{N_u}(k)\right]\left(-\mathbf{D}^T{}_1(k)\right) \\ &\quad + \lambda\Delta\mathbf{U}_{N_u}(k) = 0. \end{aligned} \tag{4.65}$$

Finally, the predicted control input increment vector is derived as

$$\Delta \mathbf{U}_{N_u}(k) = \left[\mathbf{D}^T{}_1(k)\mathbf{D}_1(k) + \lambda \mathbf{I}\right]^{-1} \mathbf{D}^T{}_1(k) \left[\mathbf{Y}^d_{N_y}(k+1) - \mathbf{E}(k)\mathbf{y}(k)\right], \quad (4.66)$$

where the unknown time-varying parameter PJM in $\mathbf{D}_1(k)$ are estimated and predicted by using the discussed algorithm (4.52), (4.53), (4.55), and (4.60). The updated control input vector at current step $\mathbf{u}(k)$ is computed by utilizing the receding horizon principle [HJ13] as

$$\mathbf{u}(k) = \mathbf{u}(k-1) + \mathbf{g}^T \Delta \mathbf{U}_{N_u}(k), \quad (4.67)$$

with $\mathbf{g} = \left[\mathbf{I}_{r\times m}, \mathbf{0}_{r\times m}, \ldots, \mathbf{0}_{r\times m}\right]^T$; whereas r, m are indicated as the number of system outputs and inputs, respectively.

4.4 Model-free adaptive predictive control using PFDL technique

In this section, the design of MFAPC based on the partial-form dynamic linearization (PFDL) technique [HJ13] is investigated for a class of unknown MIMO nonlinear systems. The key idea of PFDL is that, the upcoming system outputs are also affected by the previous control inputs within an interval determined by the constant L. Therefore, a linearized data-driven model of the unknown system is established which contains a set of time-varying parameter matrices or PJM. Based on this model, compared to [PS20d] a general partial-form predictive equation of the system outputs is constructed within a finite output prediction horizon. The system predictive model needs to be corrected continuously via estimation and prediction of the unknown parameters PJM. In this contribution, the PFDL-based recursive least-squares algorithm is firstly discussed and applied to the MFAPC design. Then, the control input calculation as well as several steps for this kind of data-driven control implementation are illustrated.

4.4.1 Partial-form output predictive model

According to [HJ13], to establish a linearized model for the given system (4.1), every control input or control input increment vectors within a fixed-moving time window or linearization length constant $L \geq 1$ are taken into account. The control input increment vector is described as

$$\Delta \mathbf{U}(k) = [\Delta \mathbf{u}(k), \Delta \mathbf{u}(k-1), \ldots, \Delta \mathbf{u}(k-L+1)]^T, \quad (4.68)$$

where $\Delta \mathbf{u}(k) = \mathbf{u}(k) - \mathbf{u}(k-1); \Delta \mathbf{u}(k-L+1) = \mathbf{u}(k-L+1) - \mathbf{u}(k-L)$ are denoted as the control input increments at instants k and $k-L+1$, respectively.

As introduced in [HJ11a], the original system (4.1), which satisfies two reasonable assumptions (see Chapter 5), is able to be approximated as the PFDL data model

$$\Delta \mathbf{y}(k+1) = \Phi_{p,L}(k)\Delta \mathbf{U}(k), \tag{4.69}$$

where a set of unknown system parameter matrices or PJM at current step k is indicated as $\Phi_{p,L}(k) = [\Phi_1(k), \Phi_2(k), \ldots, \Phi_p(k), \ldots, \Phi_L(k)]$, with $p = 1, 2, \ldots, L$. According to [PS20e], the structure of each element matrix $\Phi_p(k)$ in MIMO case is written as

$$\Phi_p(k) = \begin{bmatrix} \phi_{11p}(k) & \phi_{12p}(k) & \phi_{13p}(k) & \ldots & \phi_{1mp}(k) \\ \phi_{21p}(k) & \phi_{22p}(k) & \phi_{23p}(k) & \ldots & \phi_{2mp}(k) \\ \vdots & \vdots & \vdots & \ddots & \vdots \\ \phi_{r1p}(k) & \phi_{r2p}(k) & \phi_{r3p}(k) & \ldots & \phi_{rmp}(k) \end{bmatrix}_{r\times m}, \tag{4.70}$$

assuming $\|\Phi_p(k)\| \leq b$ [PS20e]. This means that the component matrix $\Phi_p(k)$ is bounded at every instant k.

The PFDL model (4.69) also describes one-step-ahead predictive equation of the system outputs as

$$\mathbf{y}(k+1) = \mathbf{y}(k) + \Phi_{p,L}(k)\Delta \mathbf{U}(k). \tag{4.71}$$

By denoting the constant matrices

$$\mathbf{V} = \begin{bmatrix} \mathbf{0}_{r\times m} & \mathbf{0}_{r\times m} & \mathbf{0}_{r\times m} & \ldots & \mathbf{0}_{r\times m} & \mathbf{0}_{r\times m} \\ \mathbf{I}_{r\times m} & \mathbf{0}_{r\times m} & \mathbf{0}_{r\times m} & \ldots & \mathbf{0}_{r\times m} & \mathbf{0}_{r\times m} \\ \mathbf{0}_{r\times m} & \mathbf{I}_{r\times m} & \mathbf{0}_{r\times m} & \ldots & \mathbf{0}_{r\times m} & \mathbf{0}_{r\times m} \\ \mathbf{0}_{r\times m} & \mathbf{0}_{r\times m} & \mathbf{I}_{r\times m} & \ldots & \mathbf{0}_{r\times m} & \mathbf{0}_{r\times m} \\ \vdots & \vdots & \vdots & \ddots & \vdots & \vdots \\ \mathbf{0}_{r\times m} & \mathbf{0}_{r\times m} & \mathbf{0}_{r\times m} & \mathbf{0}_{r\times m} & \mathbf{I}_{r\times m} & \mathbf{0}_{r\times m} \end{bmatrix}_{rL\times mL}, \mathbf{W} = \begin{bmatrix} \mathbf{I}_{r\times m} \\ \mathbf{0}_{r\times m} \\ \mathbf{0}_{r\times m} \\ \mathbf{0}_{r\times m} \\ \vdots \\ \mathbf{0}_{r\times m} \end{bmatrix}_{rL\times m}, \tag{4.72}$$

(4.71) can be rewritten as

$$\mathbf{y}(k+1) = \mathbf{y}(k) + \Phi_{p,L}(k)\mathbf{V}\Delta \mathbf{U}(k-1) + \Phi_{p,L}(k)\mathbf{W}\Delta \mathbf{u}(k). \tag{4.73}$$

As discussed in [HJ13] for SISO systems, in this thesis along a limited output predic-

tion horizon N_y, the system output predictive equations are established as follows

$$\begin{cases} \mathbf{y}(k+2) = \mathbf{y}(k+1) + \Phi_{p,L}(k+1)\Delta\mathbf{U}(k+1) \\ \mathbf{y}(k+2) = \mathbf{y}(k) + \Phi_{p,L}(k)\mathbf{V}\Delta\mathbf{U}(k-1) + \Phi_{p,L}(k)\mathbf{W}\Delta\mathbf{u}(k) \\ +\Phi_{p,L}(k+1)\Delta\mathbf{U}(k+1) \\ \mathbf{y}(k+2) = \mathbf{y}(k) + \Phi_{p,L}(k)\mathbf{V}\Delta\mathbf{U}(k-1) + \Phi_{p,L}(k)\mathbf{W}\Delta\mathbf{u}(k) \\ +\Phi_{p,L}(k+1)\mathbf{V}^2\Delta\mathbf{U}(k-1) + \Phi_{p,L}(k+1)\mathbf{V}\mathbf{W}\Delta\mathbf{u}(k) \\ +\Phi_{p,L}(k+1)\mathbf{W}\Delta\mathbf{u}(k+1) \\ \vdots \\ \mathbf{y}(k+N_u) = \mathbf{y}(k) \\ +\sum\limits_{q=0}^{N_u-1}\Phi_{p,L}(k+q)\mathbf{V}^{q+1}\Delta\mathbf{U}(k-1) + \sum\limits_{q=0}^{N_u-1}\Phi_{p,L}(k+q)\mathbf{V}^{q}\mathbf{W}\Delta\mathbf{u}(k) \\ +\sum\limits_{q=1}^{N_u-1}\Phi_{p,L}(k+q)\mathbf{V}^{q-1}\mathbf{W}\Delta\mathbf{u}(k+1) + \sum\limits_{q=2}^{N_u-1}\Phi_{p,L}(k+q)\mathbf{V}^{q-2}\mathbf{W}\Delta\mathbf{u}(k+2) \\ +\ldots+\Phi_{p,L}(k+N_u-1)\mathbf{W}\Delta\mathbf{u}(k+N_u-1) \\ \vdots \\ \mathbf{y}(k+N_y) = \mathbf{y}(k) \\ +\sum\limits_{q=0}^{N_y-1}\Phi_{p,L}(k+q)\mathbf{V}^{q+1}\Delta\mathbf{U}(k-1) + \sum\limits_{q=0}^{N_y-1}\Phi_{p,L}(k+q)\mathbf{V}^{q}\mathbf{W}\Delta\mathbf{u}(k) \\ +\sum\limits_{q=1}^{N_y-1}\Phi_{p,L}(k+q)\mathbf{V}^{q-1}\mathbf{W}\Delta\mathbf{u}(k+1) + \sum\limits_{q=2}^{N_y-1}\Phi_{p,L}(k+q)\mathbf{V}^{q-2}\mathbf{W}\Delta\mathbf{u}(k+2) \\ +\ldots+\sum\limits_{q=N_u-1}^{N_y-1}\Phi_{p,L}(k+q)\mathbf{V}^{q-N_u+1}\mathbf{W}\Delta\mathbf{u}(k+N_u-1) \end{cases} \cdot \tag{4.74}$$

The following values are defined

$$\tilde{\mathbf{Y}}_{N_y}(k+1) = [\mathbf{y}(k+1), \mathbf{y}(k+2), \ldots, \mathbf{y}(k+N_u), \ldots, \mathbf{y}(k+N_y)]^T, \tag{4.75}$$

$$\mathbf{S} = [\mathbf{I}_{r\times m}, \mathbf{I}_{r\times m}, ..., \mathbf{I}_{r\times m}]^T, \tag{4.76}$$

$$\bar{\mathbf{Y}}(k) = \begin{bmatrix} \Phi_{p,L}(k)\mathbf{V} \\ \sum\limits_{q=0}^{1}\Phi_{p,L}(k+q)\mathbf{V}^{q+1} \\ \vdots \\ \sum\limits_{q=0}^{N_u-1}\Phi_{p,L}(k+q)\mathbf{V}^{q+1} \\ \vdots \\ \sum\limits_{q=0}^{N_y-1}\Phi_{p,L}(k+q)\mathbf{V}^{q+1} \end{bmatrix}_{rN_y\times mL}, \tag{4.77}$$

$$\Delta\mathbf{U}(k-1) = [\Delta\mathbf{u}(k-1), \Delta\mathbf{u}(k-2), \ldots, \Delta\mathbf{u}(k-L+1)]^T, \tag{4.78}$$

$$\tilde{\mathbf{Y}}(k) = \begin{bmatrix} \Phi_{p,L}(k)\mathbf{W} & \mathbf{0} & \mathbf{0} \\ \sum_{q=0}^{1} \Phi_{p,L}(k+q)\mathbf{V}^q\mathbf{W} & \mathbf{0} & \mathbf{0} \\ \vdots & \ddots & \vdots \\ \sum_{q=0}^{N_u-1} \Phi_{p,L}(k+q)\mathbf{V}^q\mathbf{W} & \ldots & \Phi_{p,L}(k+N_u-1)\mathbf{W} \\ \vdots & \ddots & \vdots \\ \sum_{q=0}^{N_y-1} \Phi_{p,L}(k+q)\mathbf{V}^q\mathbf{W} & \ldots & \sum_{q=N_u-1}^{N_y-1} \Phi_{p,L}(k+q)\mathbf{V}^{q-N_u+1}\mathbf{W} \end{bmatrix}_{r\times m}, \tag{4.79}$$

$$\Delta\tilde{\mathbf{U}}_{N_u}(k) = [\Delta\mathbf{u}(k), \Delta\mathbf{u}(k+1), \ldots, \Delta\mathbf{u}(k+N_u-1)]^T. \tag{4.80}$$

Therefore, (4.73) and (4.74) can be summarized as

$$\tilde{\mathbf{Y}}_{N_y}(k+1) = \mathbf{S}\mathbf{y}(k) + \bar{\mathbf{Y}}(k)\Delta\mathbf{U}(k-1) + \tilde{\mathbf{Y}}(k)\Delta\tilde{\mathbf{U}}_{N_u}(k). \tag{4.81}$$

Equation (4.81) is called general partial-form predictive equation of the system outputs which contains a set of unknown time-varying parameter matrices (PJM) denoted as $\Phi_{p,L}(k+q)$, with $q = 0, 1, \ldots, N_u-1, \ldots, N_y-1$ as given in (4.77) and (4.79). To determine $\Phi_{p,L}(k+q)$, only the available system I/O data from initial step ($k=1$) up to step ($k-1$) are required.

4.4.2 PFDL-based parameter estimation and prediction

To design the PFDL-based model-free adaptive predictive control, the time-varying parameter matrices $\Phi_{p,L}(k+q)$ in (4.77) and (4.79) have to be identified. In this study, the recursive least-squares algorithm (RLSA) [GS14, ÅW08] is utilized. Theoretically speaking, RLSA shows improved on-line estimation accuracy in comparison with the traditional projection algorithm [GS14]. Similar to estimation of the PJM $\Phi(k)$ in SISO case [PS20d], by applying the RLS estimation method to the PFDL model (4.69), the following recursive algorithm called PFDL-RLSA is derived

$$\hat{\Phi}_{p,L}(k) = \hat{\Phi}_{p,L}(k-1) + \Big[\mathbf{y}(k) - \mathbf{y}(k-1) - \hat{\Phi}_{p,L}(k-1)\Delta\mathbf{U}(k-1)\Big]\mathbf{K}_1(k), \tag{4.82}$$

$$\begin{aligned} \mathbf{K}_1(k) &= \Delta\mathbf{U}^T(k-1)\mathbf{P}_1(k) \\ &= \Delta\mathbf{U}^T(k-1)\mathbf{P}_1(k-1)\big[\mathbf{I} + \Delta\mathbf{U}(k-1)\mathbf{P}_1(k-1)\Delta\mathbf{U}^T(k-1)\big]^{-1}, \end{aligned} \tag{4.83}$$

$$\begin{aligned} \mathbf{P}_1(k) = \mathbf{P}_1(k-1) &- \mathbf{P}_1(k-1)\Delta\mathbf{U}^T(k-1) \\ &\big[\mathbf{I} + \Delta\mathbf{U}(k-1)\mathbf{P}_1(k-1)\Delta\mathbf{U}^T(k-1)\big]^{-1}\Delta\mathbf{U}(k-1)\mathbf{P}_1(k-1), \end{aligned} \tag{4.84}$$

where $\mathbf{P}_1(k), \mathbf{K}_1(k)$ are unknown time-varying parameter matrices, and $\mathbf{P}_1^0 = \mathbf{P}_1(0)$ is a positive definite matrix. The initial parameters PJM is given as $\hat{\Phi}_{p,L}(0)$.

To predict the future PJM $\Phi_{p,L}(k+q)$ within a fixed-length of prediction horizon $q = 1, 2, \ldots, N_u - 1, \ldots, N_y - 1$, the estimated/known parameters from initial step $(k = 1)$ up to current step (k) should be used explicitly. Based on the multilevel hierarchical forecasting method [HJ13], an auto-regressive prediction model of the PJM at step $(k+1)$ is considered as

$$\hat{\Phi}_{p,L}(k+1) = G_1(k)\hat{\Phi}_{p,L}(k) + G_2(k)\hat{\Phi}_{p,L}(k-1) + \ldots + G_{n_p}(k)\hat{\Phi}_{p,L}(k-n_p+1), \tag{4.85}$$

where $G_v(k)$, with $v = 1, 2, \ldots, n_p$ are the unknown time-varying model coefficients, and $n_p \in [2, 7]$ as recommended in [HJ13] is the fixed model order. In general, the prediction equation of the PJM is written as

$$\begin{aligned}\hat{\Phi}_{p,L}(k+q) = G_1(k)\hat{\Phi}_{p,L}(k+q-1) + G_2(k)\hat{\Phi}_{p,L}(k+q-2) \\ + \ldots + G_{n_p}(k)\hat{\Phi}_{p,L}(k+q-n_p),\end{aligned} \tag{4.86}$$

where $q = 1, 2, \ldots, N_u - 1, \ldots, N_y - 1$. Let the following values

$$\Gamma(k) = \left[G_1(k), G_2(k), \ldots, G_{n_p}(k)\right]^T, \tag{4.87}$$

$$\hat{\Upsilon}(k-1) = \left[\hat{\Phi}_{p,L}(k-1), \hat{\Phi}_{p,L}(k-2), \ldots, \hat{\Phi}_{p,L}(k-n_p)\right]^T, \tag{4.88}$$

$$\hat{\Phi}_{p,L}(k) = \hat{\Upsilon}(k-1)\Gamma^T(k). \tag{4.89}$$

Instead of using traditional projection algorithm [GHLJ19], this contribution considers application of the recursive least-squares method [GS14] to estimate the unknown coefficients $G_v(k)$ in (4.85) and (4.86). By applying RLSA to (4.89), after several calculations the following equations are obtained

$$\begin{aligned}\mathbf{P}_2(k) = \mathbf{P}_2(k-1) - \mathbf{P}_2(k-1)\hat{\Upsilon}^T(k-1) \\ \left[\mathbf{I} + \hat{\Upsilon}(k-1)\mathbf{P}_2(k-1)\hat{\Upsilon}^T(k-1)\right]^{-1}\hat{\Upsilon}(k-1)\mathbf{P}_2(k-1),\end{aligned} \tag{4.90}$$

$$\mathbf{K}_2(k) = \hat{\Upsilon}^T(k-1)\mathbf{P}_2(k-1)\left[\mathbf{I} + \hat{\Upsilon}(k-1)\mathbf{P}_2(k-1)\hat{\Upsilon}^T(k-1)\right]^{-1}, \tag{4.91}$$

$$\Gamma(k) = \Gamma(k-1) + \left[\hat{\Phi}_{p,L}(k) - \Gamma^T(k-1)\hat{\Upsilon}(k-1)\right]\mathbf{K}_2(k), \tag{4.92}$$

where $\mathbf{P}_2(k), \mathbf{K}_2(k)$ are the unknown time-varying parameter matrices, and $\mathbf{P}_2^0 = \mathbf{P}_2(0)$ is an initial positive definite matrix. The initial coefficients of the prediction models (4.85) and (4.86) are given as $\Gamma(0) = \Gamma_0$. Based on the calculated parameters $\Gamma(k)$ or $G_v(k)$ in (4.90), (4.91), and (4.92) as well as the available PJM $\hat{\Phi}_{p,L}(1), \hat{\Phi}_{p,L}(2), \ldots, \hat{\Phi}_{p,L}(k)$, the future system parameter matrices $\hat{\Phi}_{p,L}(k+q)$ with $q = 1, 2, \ldots, N_u - 1, \ldots, N_y - 1$ in (4.77) and (4.79) are predicted via (4.86).

4.4.3 Control input calculation

To calculate the required control input vector $\mathbf{u}(k)$, the input objective function, in which the future output tracking errors should be minimized within the length of prediction steps N_y considering input energy limitation, is described as

$$J\left(\Delta\mathbf{u}(k)\right) = \sum_{i=1}^{N_y} \left\|\mathbf{y}^d(k+i) - \mathbf{y}(k+i)\right\|^2 + \lambda \sum_{j=0}^{N_u-1} \left\|\Delta\mathbf{u}(k+j)\right\|^2, \tag{4.93}$$

where $\lambda > 0$ is a constant design parameter. The desired system output vector in future $\mathbf{y}^d(k+i)$, with $i = 1, 2, \ldots, N_u, \ldots, N_y$ is illustrated in (4.62). Meanwhile, the upcoming outputs $\mathbf{y}(k+i)$ in (4.93) can be approximated by the general PFDL-based predictive model (4.81). Substituting (4.80), (4.81), and (4.62) into (4.93), results in

$$\begin{aligned} J\left(\Delta\tilde{\mathbf{U}}_{N_u}(k)\right) = &\left[\mathbf{Y}^d_{N_y}(k+1) - \mathbf{S}\mathbf{y}(k) - \bar{\mathbf{Y}}(k)\Delta\mathbf{U}(k-1) - \tilde{\mathbf{Y}}(k)\Delta\tilde{\mathbf{U}}_{N_u}(k)\right]^2 \\ &+ \lambda\Delta\tilde{\mathbf{U}}^T_{N_u}(k)\Delta\tilde{\mathbf{U}}_{N_u}(k). \end{aligned} \tag{4.94}$$

Minimizing (4.94) with respect to $\Delta\tilde{\mathbf{U}}_{N_u}(k)$ by taking $\frac{\partial J}{\partial\Delta\tilde{\mathbf{U}}_{N_u}(k)} = 0$, leads to the predicted control input increment vector

$$\begin{aligned} \Delta\tilde{\mathbf{U}}_{N_u}(k) = &\left[\tilde{\mathbf{Y}}^T(k)\tilde{\mathbf{Y}}(k) + \lambda\mathbf{I}\right]^{-1}\tilde{\mathbf{Y}}^T(k) \\ &\left[\mathbf{Y}^d_{N_y}(k+1) - \mathbf{S}\mathbf{y}(k) - \bar{\mathbf{Y}}(k)\Delta\mathbf{U}(k-1)\right], \end{aligned} \tag{4.95}$$

where the composed matrices $\tilde{\mathbf{Y}}(k)$ and $\bar{\mathbf{Y}}(k)$ described in (4.79) and (4.77), respectively, contain a set of the estimated parameter matrices $\hat{\Phi}_{p,L}(k+q)$, with $q = 0, 1, 2, \ldots, N_u - 1, \ldots, N_y - 1$.

Finally, by applying the receding horizon principle [HJ13] the update control inputs are computed as

$$\mathbf{u}(k) = \mathbf{u}(k-1) + \mathbf{g}^T\Delta\tilde{\mathbf{U}}_{N_u}(k), \tag{4.96}$$

with $\mathbf{g} = \left[\mathbf{I}_{r\times m}, \mathbf{0}_{r\times m}, \ldots, \mathbf{0}_{r\times m}\right]^T$.

4.4.4 Steps for model-free adaptive predictive control design

The proposed MFAPC methods can be applied to a class of unknown MIMO nonlinear systems. A general CFDL-based MFAPC scheme of a MIMO crane representing a mechanical flexible system is depicted in Figure 4.2. To design control, the following steps have to be implemented:

- *Step 1:* Based on the CFDL or PFDL concepts, different predictive models of the system outputs are constructed which contain unknown time-varying parameter matrices (PJM). At current step k, the PJM matrices $\hat{\Phi}(k)$ or $\hat{\Phi}_{p,L}(k)$ are estimated and updated recursively by using the modified CFDL-RLSA (4.52), (4.53) or PFDL-RLSA (4.82), (4.83), and (4.84). According to [HJ13], to improve the ability in tracking time-varying parameters a reset condition is considered as given in (4.38), and (4.39).

- *Step 2:* The current PJM $\hat{\Phi}(k)$ or $\hat{\Phi}_{p,L}(k)$ as well as the available parameter matrices from previous steps are utilized to predict the future PJM $\hat{\Phi}(k+j)$ in (4.55), with $j = 1, 2, \ldots, N_u - 1$ or a set of future PJM $\hat{\Phi}_{p,L}(k+q)$ in (4.86), with $q = 1, 2, \ldots, N_y - 1$. Therefore, the composed parameter matrices $\mathbf{D}_1(k)$, $\tilde{\mathbf{Y}}(k)$, and $\bar{\mathbf{Y}}(k)$ are completely determined. To improve the tracking ability of the PJM prediction algorithms, another reset condition [HJ13] has to be fulfilled as

$$\begin{aligned} \hat{\phi}_{ii}(k+j) = \hat{\phi}_{ii}(1) \;\; if \;\; & \left|\hat{\phi}_{ii}(k+j)\right| < c_2 \;\; or \;\; \left|\hat{\phi}_{ii}(k+j)\right| > \alpha c_2 \\ or \;\; & \operatorname{sgn}\left(\hat{\phi}_{ii}(k+j)\right) \neq \operatorname{sgn}\left(\hat{\phi}_{ii}(1)\right), \end{aligned} \tag{4.97}$$

$$\begin{aligned} \hat{\phi}_{ij}(k+j) = \hat{\phi}_{ij}(1) \;\; if \;\; & \left|\hat{\phi}_{ij}(k+j)\right| > c_1 \\ or \;\; & \operatorname{sgn}\left(\hat{\phi}_{ij}(k+j)\right) \neq \operatorname{sgn}\left(\hat{\phi}_{ij}(1)\right). \end{aligned} \tag{4.98}$$

- *Step 3:* Based on the estimated/predicted PJM and the future output control errors, the control input increment vectors $\Delta\mathbf{U}_{N_u}(k)$ and $\Delta\tilde{\mathbf{U}}_{N_u}(k)$ are defined. Hence, the updated control input vector $\mathbf{u}(k)$ is computed according to (4.67) and (4.96). Finally, the next system outputs from the controlled system need to be collected, and the given procedure is executed repeatedly.

4.5 Vibration control results and discussion

Based on the CFDL and PFDL concepts, different model-free control strategies including the modified CFDLc-MFAC, RLS-based MFAPC, and PFDL-based MFAPC have been developed in the preceding sections. To verify control effectiveness, the design controllers will be applied to reduce the in-plane vibrations of an elastic ship-mounted crane [AS07]. Introduction to the crane system and related configuration have been reviewed in Section 3.3. The crane is represented as a typical flexible system. In the following subsections, simulation results including system output and control input energy-based evaluation of the proposed approaches will be given.

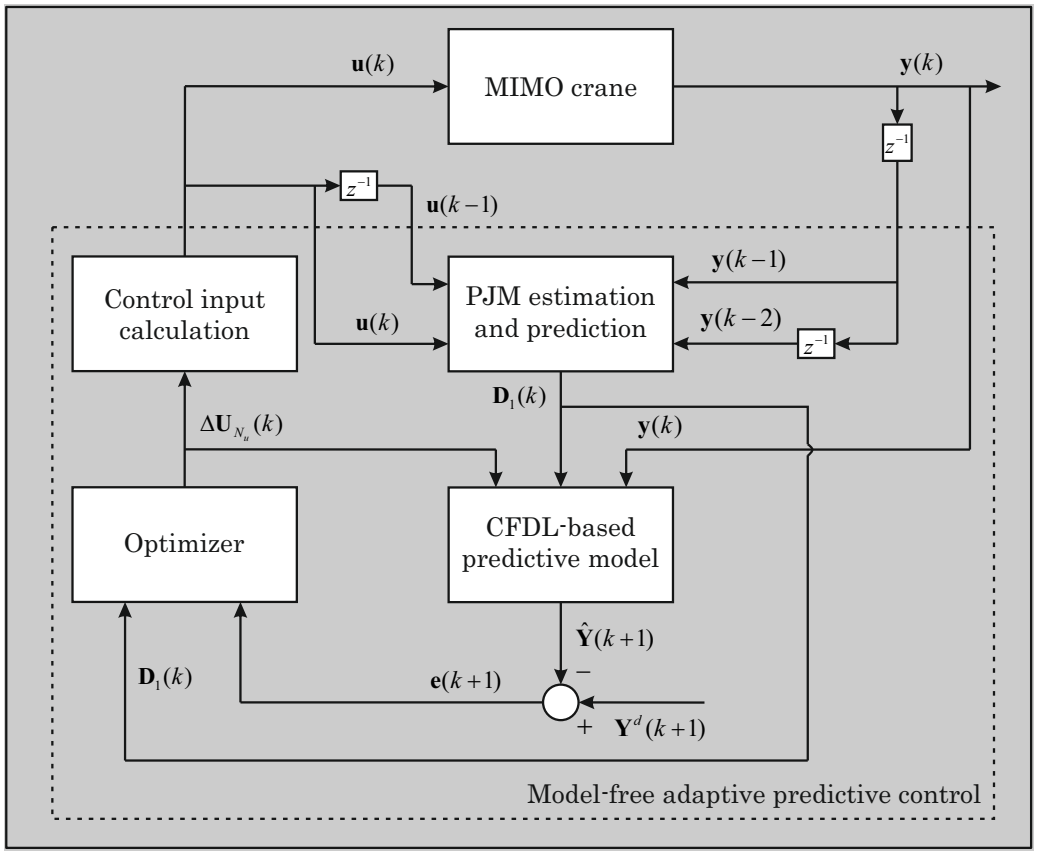

Figure 4.2: General model-free adaptive predictive control scheme of a MIMO crane [PS20d]

4.5.1 Modified CFDLc-MFAC results

The improved CFDLc-MFAC, which uses the modified controller parameter estimation algorithm (4.37) to update the unknown time-varying controller parameters $\Psi(k)$ and the CFDL-RLSA (4.5), (4.6), and (4.7) to estimate the unknown system parameters $\Phi(k)$, is applied to control of the elastic boom crane. Simulation results are obtained in case the effects of the unknown external disturbances such as ship rolling and wind force ($\Delta\delta(k) = p_2(k) = 0$ in (3.103)) are ignored. However, because of the non-zero initial excitation of the payload, large vibrations occur in the system that might lead to dangerous situations in the crane operation. Several initial operating conditions of the crane have been already given in Table 3.1. The design model-free controller so-called modified CFDLc-MFAC is compared with the normal MFAC which utilizes the traditional projection algorithm (4.4) [PS19a] and industrial PI control. In Table 4.1, several design parameters of the model-free controllers are shown.

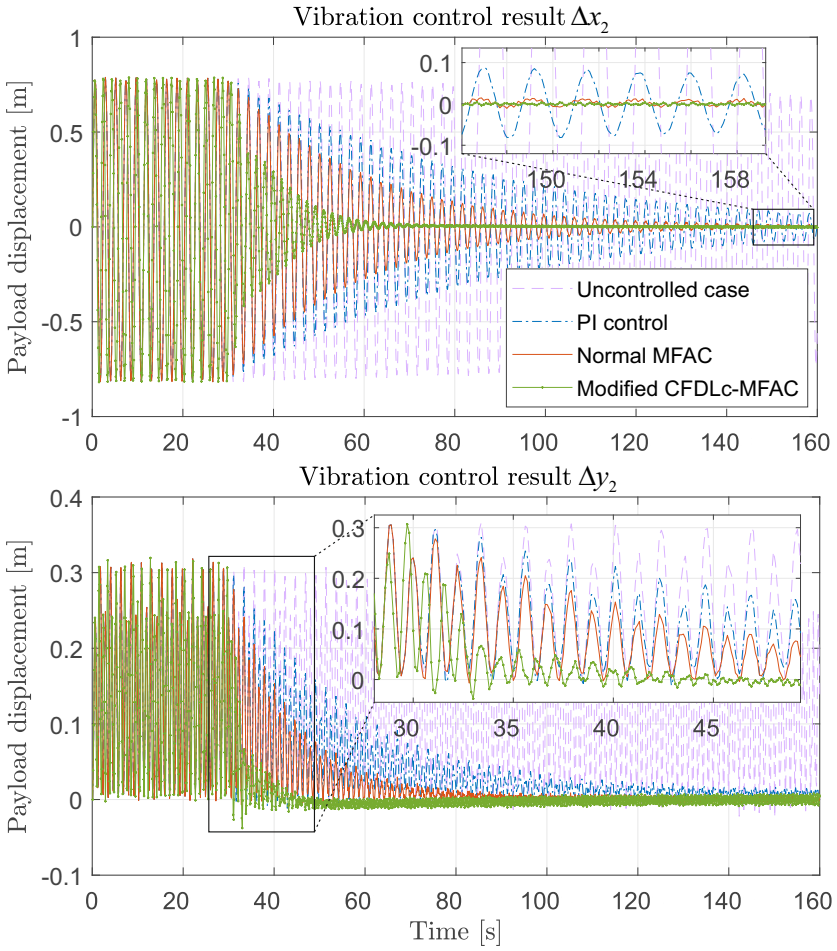

Figure 4.3: Vibration control comparison with respect to the payload position Δx_2 and Δy_2 [PS20c]

The vibration control results of the payload displacement in x_0- and y_0-direction are described in Figure 4.3. Compared to the normal MFAC (red line) and the PI control (blue-dot line), the proposed controller (green line) obtains better control performance with respects to smaller tracking errors and faster control response. The design controllers are activated from $t = 30$ [s] and stopped at $t = 160$ [s]. To simulate the system dynamic behaviors due to the non-zero initial condition of the payload ($\dot{\phi}_2^0 = 5.0$ [rad/s]), the uncontrolled case results (pink-dash line) are also presented. In addition, comparison of vibration control regarding the angular displacements of the upper and payload cables ($\Delta\alpha_2$ and $\Delta\phi_2$) is illustrated in Figure 4.4. It can be seen that these angular oscillations are reduced considerably from around $\Delta\alpha_2 = 30$ [deg] and $\Delta\phi_2 = 50$ [deg] to nearly zero at the end of the simulation by using the modified CFDLc-MFAC. Furthermore, the proposed controller

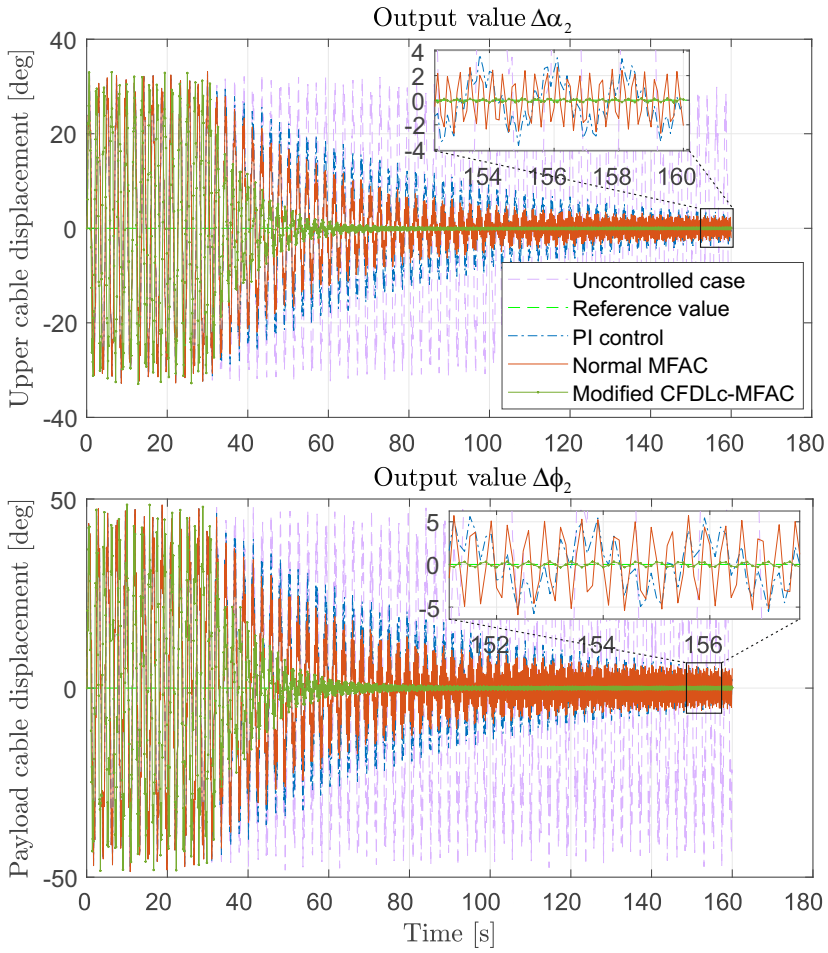

Figure 4.4: Vibration control comparison with respect to the output values $\Delta\alpha_2$ and $\Delta\phi_2$ [PS20c]

gets faster control adaptation in comparison with other conventional approaches. In Figure 4.5, the estimated system parameters PJM $\hat{\Phi}(k)$ and controller parameters PPD $\hat{\Psi}(k)$, when the proposed controller is switched on between $T = [30, 160]$ [s], are shown. From the beginning period of the simulation (up to $t = 30$ [s]), the parameter trajectories depend on their initial values. Because of the recursive estimation algorithms as well as the reset conditions (4.38), (4.39), and (4.40), the estimated parameters need time for adaptation and will converge to their true values when the simulation ends. Additionally, the sign of all elements of the PJM and PPD matrices is unchanged as discussed previously. In Figure 4.6, the calculated control input values of the modified model-free controller are shown.

To evaluate the control performance of the discussed methods when varying controller parameters, the control input energy-based evaluation according to the cri-

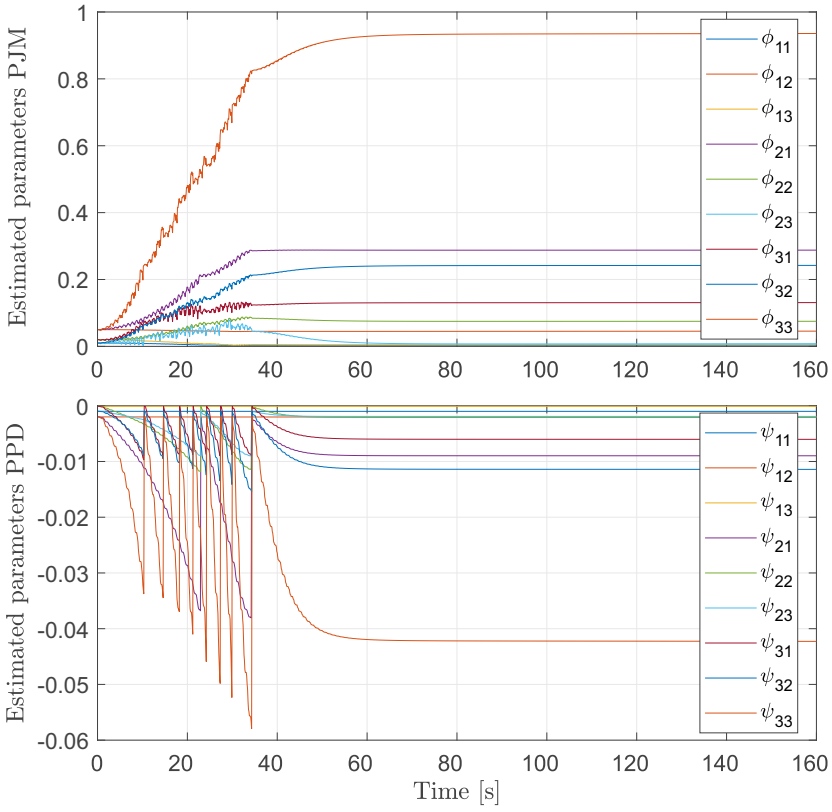

Figure 4.5: Estimated system and controller parameters

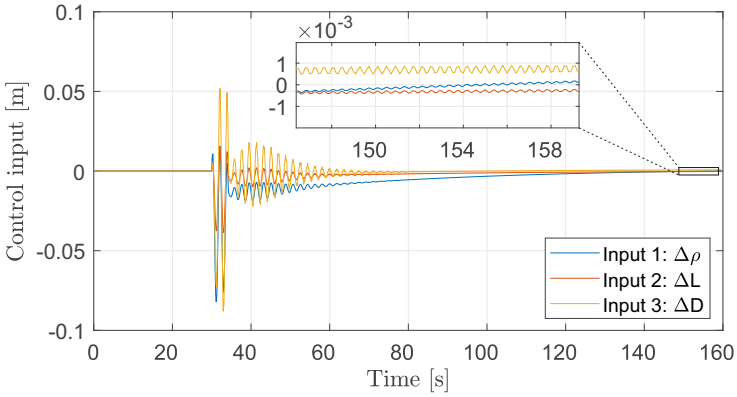

Figure 4.6: Calculated control input values of the modified CFDLc-MFAC

teria (3.104) is considered within a specified length of time $T = [t_1, t_2]$ [s] as

$$P_{K^*} = \left[\int_{t_1}^{t_2} \mathbf{u}^2(t)dt, \int_{t_1}^{t_2} \mathbf{e}^2(t)dt \right]_{K^*}, \tag{4.99}$$

Table 4.1: Several design parameters of the model-free controllers [PS20c]

Parameter	**Meaning**	**Value**
ρ_k	Step-size constant	0.01
λ_k	Weighting factor of the CFDLc-MFAC	4.0
τ	Constant design parameter	0.02
b_1	Small positive constant	0.009
λ	Weighting factor of the normal MFAC	1.25
η	Step-size constant	0.20
μ	Constant weighting factor	15
ρ	Step-size constant	0.15

where a set of controller parameters is denoted as $K^* = \{\lambda_k, \lambda, k_p, k_i\}$, in which the constant weighting factors of the modified CFDLc-MFAC and the normal MFAC are λ_k and λ, respectively, with $\lambda_k, \lambda \in [2.0, 70.0]$. The PI control parameters are chosen as $k_p \in [0.0005, 0.008]$ and $k_i \in [0.0001, 0.25]$. Here, λ_k and λ are the important parameters which can improve the model-free control performance. The model-free and PI control parameters are selected to perform the best control effectiveness via simulation. In Figure 4.7, control performance comparison with respect to the criteria (4.71) within the sampling interval $T_1 = [30, 160]$ [s] (transient phase) is shown. The trajectory P_{K^*} of the modified CFDLc-MFAC (violet dot) is closer to the origin (upper figure) than that of the normal MFAC (blue dot) and the PI control (red dot) when changing the parameters K^*. However, the improved model-free controller still consumes more input energy (lower figure) compared with other controllers. In stationary phase $T_2 = [120, 160]$ [s], the trajectories P_{K^*} of three controllers are depicted in Figure 4.8. Generally speaking, the modified model-free controller always derives small tracking control errors. In addition, the results of total tracking errors and control input energy of the different approaches are numbered in Table 4.2 and Table 4.3 for transient and stationary phase, respectively. In transient phase, the modified MFAC achieves smallest tracking control errors $\int \mathbf{e}^2(t)dt$ (15.2362); whereas the normal data-driven controller requires less control input energy $\int \mathbf{u}^2(t)dt$ (0.0483) in total. In stationary phase, it is clear that the proposed controller has better control performance according to the numbers of MSE ($9.8256e^{-6}$) and E_{input} ($3.2442e^{-7}$).

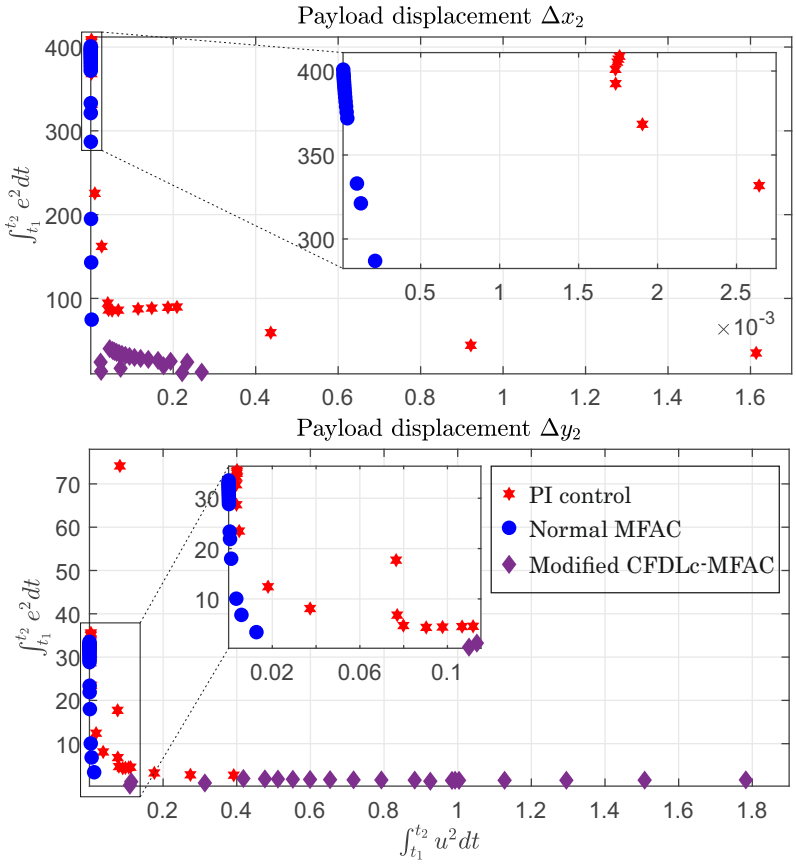

Figure 4.7: Control performance evaluation in transient phase regarding the criteria (4.71) [PS20c]

4.5.2 Modified RLS-based MFAPC results

The discussed modified model-free adaptive predictive control (4.66), (4.67) is applied to reduce the free vibrations of the flexible crane [AS07]. The design controller requires the estimated parameters $\hat{\Phi}(k)$ which are recursively updated from the algorithm (4.52), (4.52), and the predicted PJM values $\hat{\Phi}(k+1), \hat{\Phi}(k+2), \ldots, \hat{\Phi}(k+N_u-1)$ calculated via (4.55), (4.60). In the simulation, the tracking control ability of different approaches will be evaluated in case no external disturbance is considered. In this subsection, the recursive least squares-based model-free adaptive predictive control (RLS-MFAPC) results are illustrated and compared with those of the projection algorithm-based MFAC (PA-MFAC) (3.38) and (4.4) [PS19a], as well as standard PI control. In Figure 4.9, comparison of vibration control results with respect to the payload position is depicted. The control part of the simulation starts from $t = 30$ [s]. It can be observed that, the RLS-MFAPC (green line) has better tracking control performance regarding to smaller error amplitudes in

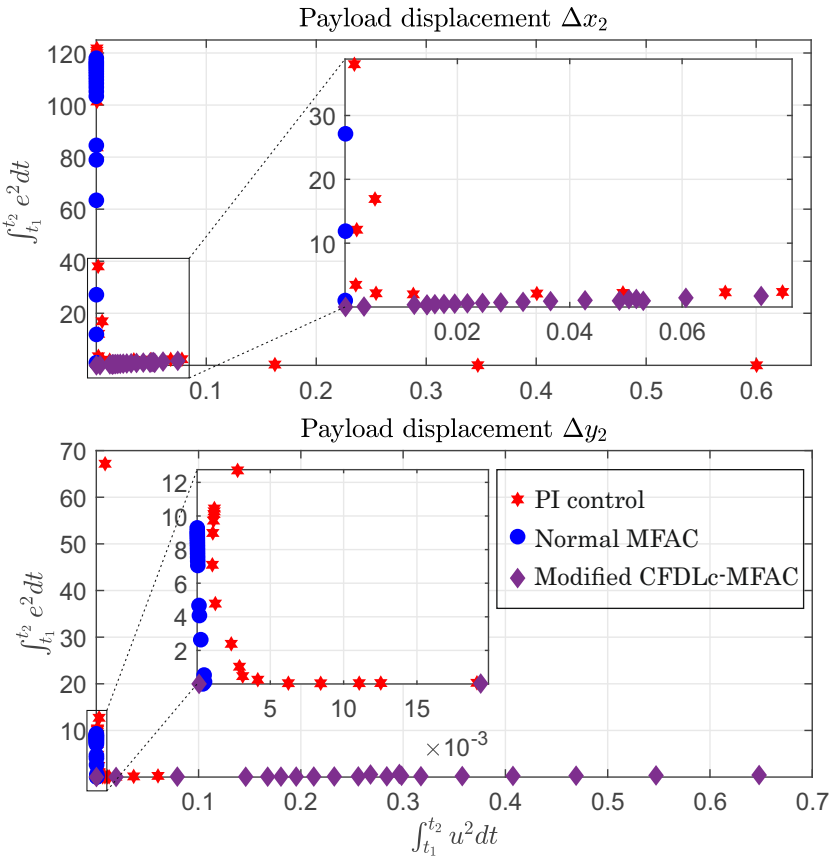

Figure 4.8: Control performance evaluation in stationary phase regarding the criteria (4.71)

comparison with the PA-MFAC (blue line) and PI control (red-dot line). It takes approximately $\Delta t = 15$ [s] to suppress the payload swings in case of utilizing the improved model-free controller. The system dynamic behaviors in uncontrolled case are also simulated (pink-dash line). The design parameters of the RLS-MFAPC and PA-MFAC are chosen in Table 4.4. Furthermore, the vibration control results of the upper cable ($\Delta\alpha_2$) and payload cable ($\Delta\phi_2$) are shown in Figure 4.10. It is obviously seen that, the cable angular displacements are reduced significantly to nearly zero at the end of the simulation by using the modified controller (green line).

In term of control input energy-based evaluation, the criteria (4.99) is applied, in which a set of controller gains $K^* = \{\lambda_1, \lambda_2, \delta, k_p, k_i\}$ should be varied. The design parameters of the RLS-MFAPC indicated as λ_1, δ are chosen as $\lambda_1 \in [73.0, 79.0]$, and $\delta \in [0.005, 0.95]$; whereas the PA-MFAC parameter is designed as $\lambda_2 \in [0.5, 30.0]$. The PI controller parameters include $k_p \in [0.0005, 0.005]$, and $k_i \in [0.0001, 0.25]$. In Figure 4.11, the trajectories P_{K^*} of the design control methods according to the criteria (4.71) are shown in transient phase $T_1 = [30, 160]$

Table 4.2: Comparison of different control methods in transient phase

Control method	$\int \mathbf{e}^2(t)dt$	$\int \mathbf{u}^2(t)dt$	MSE	E_{input}
PI control	98.0669	0.2459	0.0612	$1.5374e^{-4}$
Normal MFAC	60.5173	0.0483	0.0378	$3.0229e^{-5}$
Modified CFDLc-MFAC	15.2362	0.2665	0.0095	$1.6657e^{-4}$

Table 4.3: Comparison of different control methods in stationary phase

Control method	$\int \mathbf{e}^2(t)dt$	$\int \mathbf{u}^2(t)dt$	MSE	E_{input}
PI control	2.8061	0.0580	0.0017	$3.6276e^{-5}$
Normal MFAC	2.5286	0.0021	0.0015	$1.3623e^{-6}$
Modified CFDLc-MFAC	0.0157	$5.1907e^{-4}$	$9.8256e^{-6}$	$3.2442e^{-7}$

[s]. In general, the trajectory P_{K^*} of the RLS-MFAPC (black dot) is closer to the origin $(0, 0)$, that means the proposed controller achieves better control efficiency compared to the conventional PA-MFAC (blue dot) and PI control (red dot). Within the stationary phase $T_2 = [130, 160]$ [s], the results of control input energy-based evaluation are presented in Figure 4.12. Basically, the RLS-MFAPC indicates better control performance regarding to smaller control error amplitudes than the others. The numerical illustrations of the design controller evaluation are also given in Table 4.5, and Table 4.6 for transient and stationary phases, correspondingly. In general, the modified MFAPC derives the smallest control error values $\int \mathbf{e}^2(t)dt$ in both transient phase (12.0811), and stationary phase (0.0038). Meanwhile, the standard MFAC consumes less input energy $\int \mathbf{u}^2(t)dt$ according to transient phase (0.0483) as well as stationary phase (0.0015).

4.5.3 PFDL-based MFAPC results

The introduced PFDL-based MFAPC program is applied to vibration control of a ship-mounted crane [AS07] with the initial crane parameters as given in Table 3.1. To calculate the update control inputs in (4.96), the time-varying parameter matrices $\hat{\Phi}_{p,L}(k+q)$ with $q = 0, 1, 2, \ldots, N_y - 1$ have to be estimated and predicted continuously via (4.86). The obtained results are compared with those from our previous publications including the CFDL-MFAPC [PS20d] (or RLS-MFAPC as mentioned in the previous subsection), conventional PA-MFAC [PS19a], and industrial PI control. In Figure 4.13, comparison of vibration control results with respect to the output values $\Delta\phi_2$ and $\Delta\alpha_2$ is shown. It can be seen that the upper and payload cable displacements are reduced significantly by using the proposed model-free controller (green line). Better control results are observed in comparison with

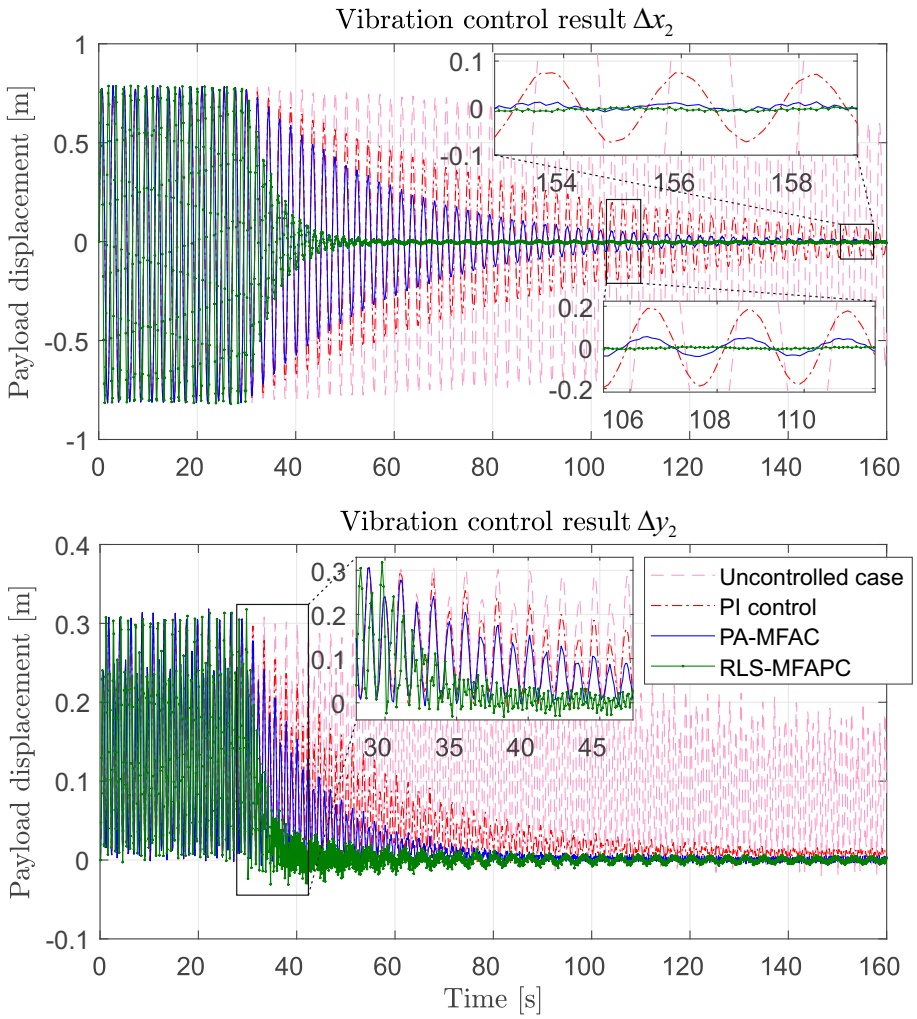

Figure 4.9: Comparison of vibration control with respect to the payload position Δx_2 and Δy_2 [PS20d]

that of the CFDL-MFAPC (yellow line), conventional PA-MFAC (red line), and PI control (blue-dot line). The system dynamic behaviors in uncontrolled case are simulated (pink-dash line) in Figure 4.13 with the non-zero initial excitation of the payload ($\dot{\phi}_2^0 = 5.0$ [rad/s]). Furthermore, the calculated control input signals and estimated parameters PJM are illustrated in Figure 4.14. The system parameters converge to their true values at the end of the simulation. In Table 4.7, several design parameters of the proposed model-free adaptive predictive controller are given.

For control input energy-based evaluation, this work uses the criteria (4.99), in which a set of controller parameters $K^* = \{\lambda_1, \lambda_2, \lambda_3, \delta, k_p, k_i\}$ will be varied. The design parameters of the data-driven controllers are chosen as $\lambda_1 \in [10, 130]$ for the

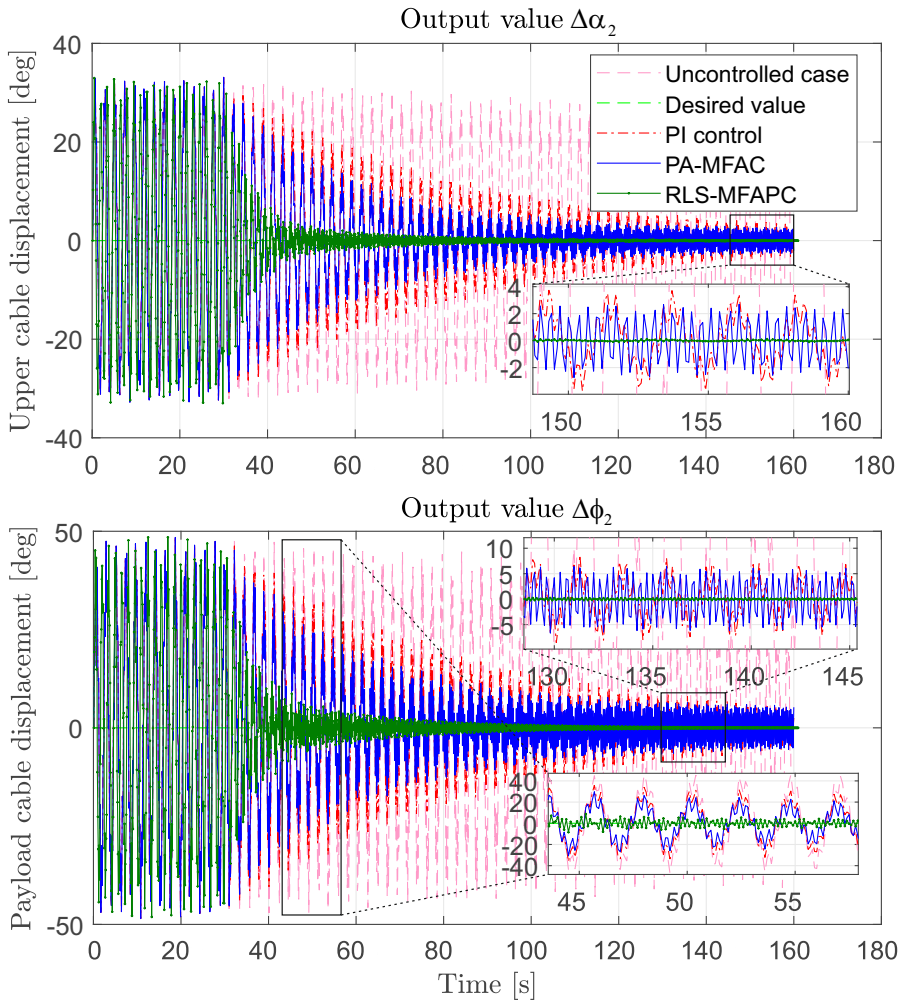

Figure 4.10: Comparison of vibration control with respect to the output values $\Delta\alpha_2$ and $\Delta\phi_2$ [PS20d]

PFDL-MFAPC, $\lambda_2 \in [73.0, 79.0]$ and $\delta \in [0.005, 0.95]$ for the CFDL-MFAPC, and $\lambda_3 \in [0.5, 30.0]$ for the conventional PA-MFAC. The selected PI controller parameters are $k_p \in [0.0005, 0.005]$ and $k_i \in [0.0001, 0.25]$. In Figure 4.15, the trajectories P_{K^*} of different control methods are presented within a pre-defined length of time window $T_1 = [30, 120]$ [s] or transient phase. It can be observed that the PFDL-MFAPC results (green dot) are distributed closer to the origin $(0, 0)$; that means better control performance is achieved in comparison with the CFDL-MFAPC (black dot), traditional MFAC (blue dot), and PI control (red dot). In addition, in stationary phase $T_2 = [90, 120]$ [s] the control performance evaluation is described in Figure 4.16. Generally, the proposed MFAPC (green dot) shows better control results in terms of smaller control errors and less control input energy consumption compared

Table 4.4: Several design parameters of the model-free controllers [PS20d]

Parameter	**Meaning**	**Value**
λ_1	Weighting factor of the RLS-MFAPC	75
δ	Design positive constant	0.75
N_y	Output prediction horizon	6
N_u	Input prediction horizon	2
γ	Constant design parameter	0.75
n_p	Predictive model coefficient	2
λ_2	Weighting factor of the PA-MFAC	1.25

Table 4.5: Control input energy-based comparison in transient phase

Control method	$\int \mathbf{e}^2(t)dt$	$\int \mathbf{u}^2(t)dt$	MSE	E_{input}
PI control	98.0669	0.2459	0.0612	$1.5374e^{-4}$
PA-MFAC	60.5173	0.0483	0.0378	$3.0229e^{-5}$
RLS-MFAPC	12.0811	0.3219	0.0075	$2.0123e^{-4}$

with traditional methods. Moreover, the control input energy-based results are illustrated numerically in Table 4.8 (transient phase) and Table 4.9 (stationary phase). The design PFDL-MFAPC achieves the smallest numbers of the total tracking errors in both transient phase (11.3931) and stationary phase (0.0261).

4.6 Summary

In this chapter, several improved/modified model-free adaptive controllers have been designed for unknown MIMO systems. The first control strategy is based on the CFDL technique which can be applied not only to the unknown plant but also to an assumed nonlinear controller. As a result, a linearized controller structure is established, in which the unknown time-varying parameters namely pseudo-partial derivative of the controller need to be estimated and updated at each system operating point. In addition, an equivalent linearized data-driven model of the original plant is designed. The system model contains unknown parameters which are locally estimated by utilizing the RLS algorithm. To improve tracking control performance, a modified objective function of the controller parameter matrix (or PPD) is proposed by considering minimization of the current control errors and its variations

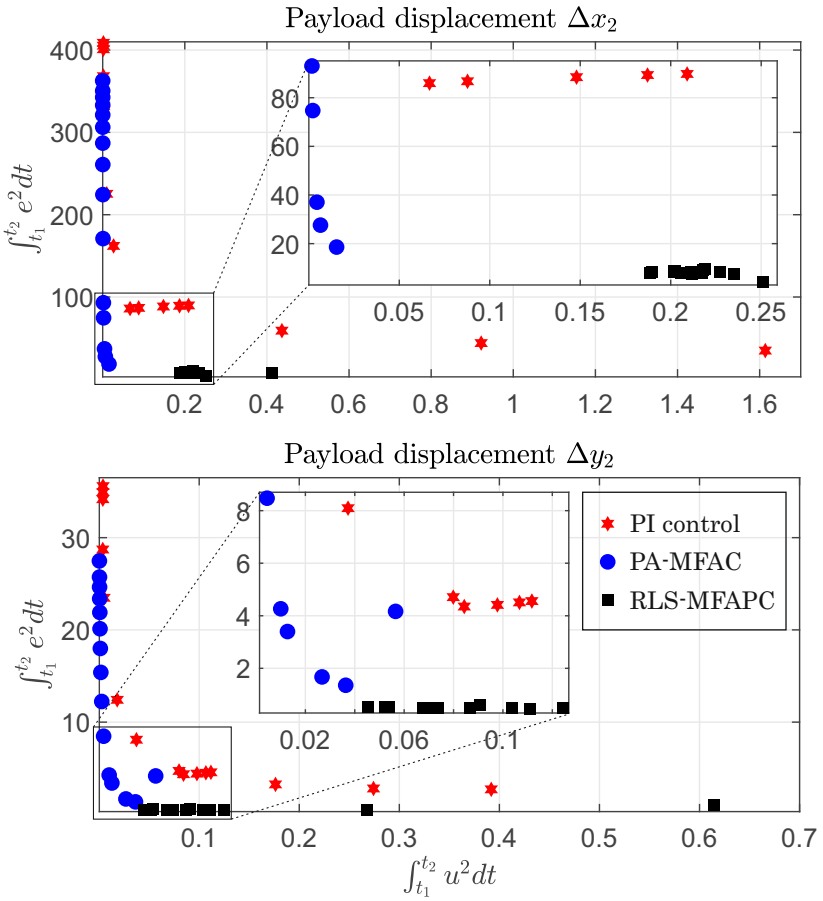

Figure 4.11: Control input energy-based evaluation regarding to the criteria (4.71) within $T_1 = [30, 160]$ [s] [PS20d]

within a pre-defined length of time window. Hence, the estimation algorithm of the controller parameters has been generated with a modified part.

In the second control strategy, based on the main theories of MFAC and MPC, improved model-free adaptive predictive controllers have been proposed. The compact-form and partial-form dynamic linearization techniques are used to construct the system output predictive models. The recursive least-squares method has been applied to estimate and predict the unknown time-varying parameter matrices (or PJM) in the prediction models. The obtained system parameters are necessary for the calculation of the future control input increment vectors and the updated control input signals. To reduce unexpected oscillations in mechanical flexible systems, the discussed control methods have been applied to an elastic ship-mounted crane as an illustrative example. The simulation results indicated that, in case without considering external disturbance effects, the in-plane vibrations of the elastic boom

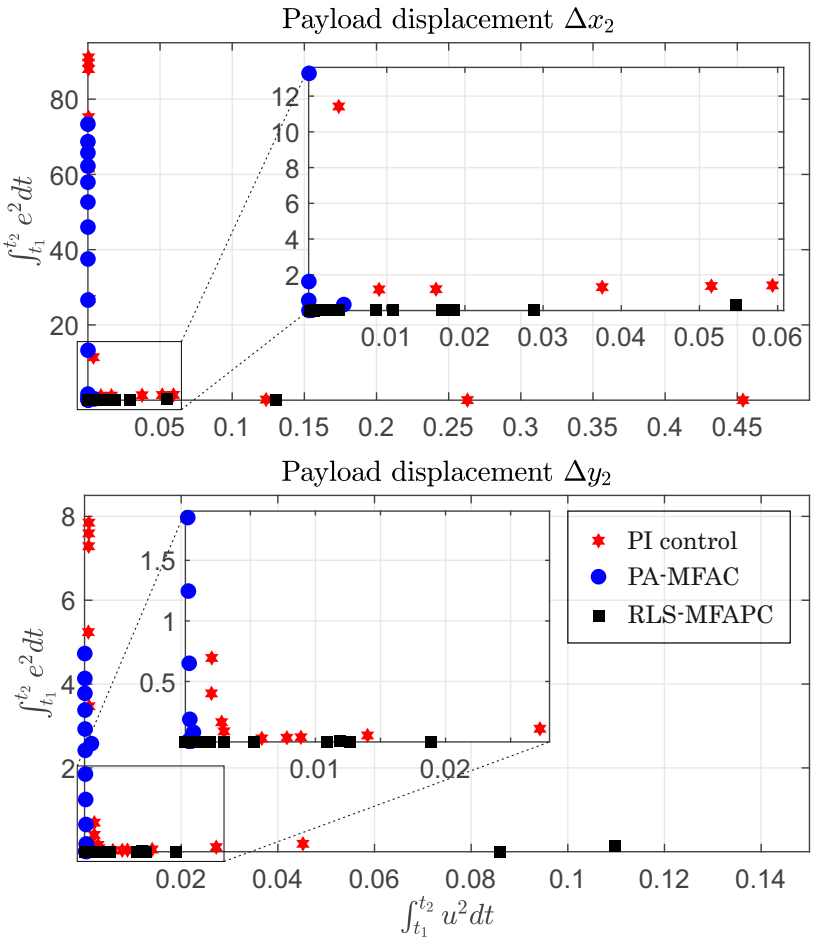

Figure 4.12: Control input energy-based evaluation regarding to the criteria (4.71) within $T_2 = [130, 160]$ [s]

and the payload are reduced considerably, and better control performance could be observed when using the modified/improved model-free controllers in comparison with traditional approaches.

The design model-free adaptive controllers utilize recursive algorithms to estimate and predict the unknown system and controller parameters at current and during a limited future time period, as well as to compute the required control input signals. In addition, the considered crane system showed fast dynamical behavior variations. Therefore, large sampling time has been used in the numerical simulations. For future works, the proposed control programs could be implemented experimentally with a lab-scaled crane test rig to validate the achieved simulation results.

Table 4.6: Control input energy-based comparison in stationary phase

Control method	$\int \mathbf{e}^2(t)dt$	$\int \mathbf{u}^2(t)dt$	MSE	E_{input}
PI control	1.7203	0.0435	0.0010	$2.7216e^{-5}$
PA-MFAC	1.8014	0.0015	0.0011	$9.9542e^{-7}$
RLS-MFAPC	0.0038	0.0071	$2.3794e^{-6}$	$4.4609e^{-6}$

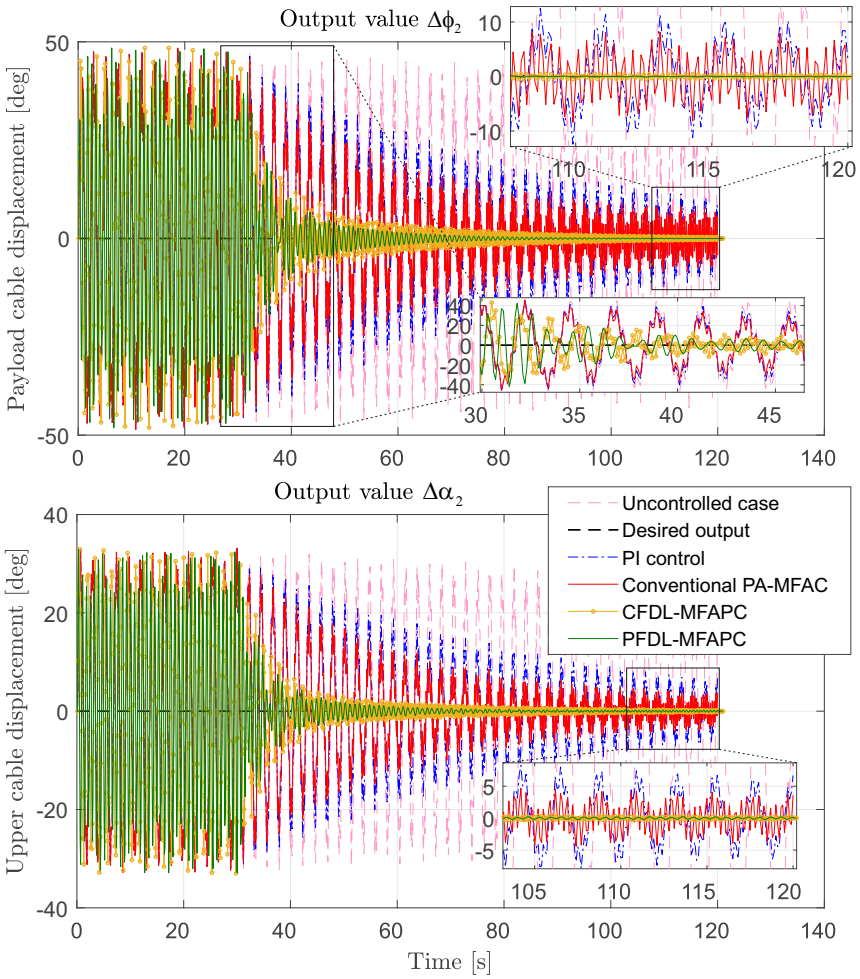

Figure 4.13: Comparison of vibration control with respect to the output values $\Delta\phi_2$ and $\Delta\alpha_2$ [PS20b]

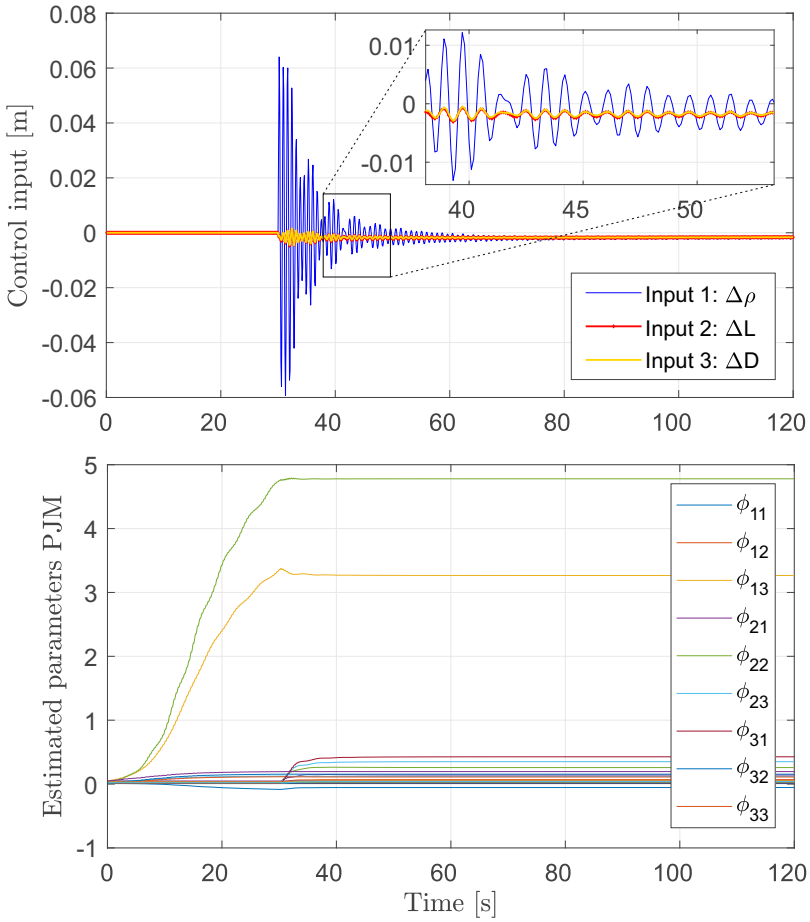

Figure 4.14: Calculated control input signals and estimated parameters PJM [PS20b]

Table 4.7: Several design parameters of the PFDL-MFAPC [PS20b]

Parameter	**Meaning**	**Value**
L	Linearization length constant	3
λ	Constant weighting factor	110
N_y	Output prediction horizon	3
N_u	Input prediction horizon	3
n_p	Predictive model coefficient	3

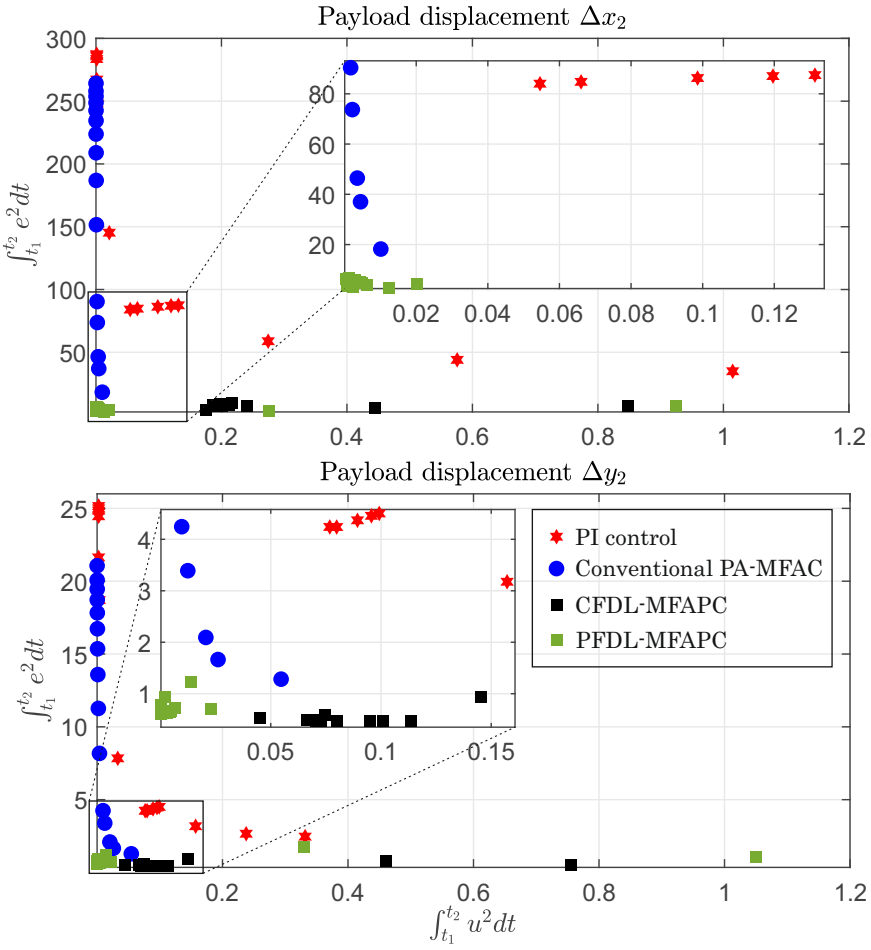

Figure 4.15: Control input energy-based evaluation regarding to the criteria (4.99) within $T_1 = [30, 120]$ [s] [PS20b]

Table 4.8: Control input energy-based evaluation in transient phase [PS20b]

Control method	$\int \mathbf{e}^2(t)dt$	$\int \mathbf{u}^2(t)dt$	MSE	E_{input}
PI control	95.2777	0.1880	0.0793	$1.5671e^{-4}$
Conventional PA-MFAC	57.9982	0.0461	0.0483	$3.8495e^{-5}$
CFDL-MFAPC	12.0748	0.3126	0.0100	$2.6057e^{-4}$
PFDL-MFAPC	11.3931	0.0729	0.0094	$6.0797e^{-5}$

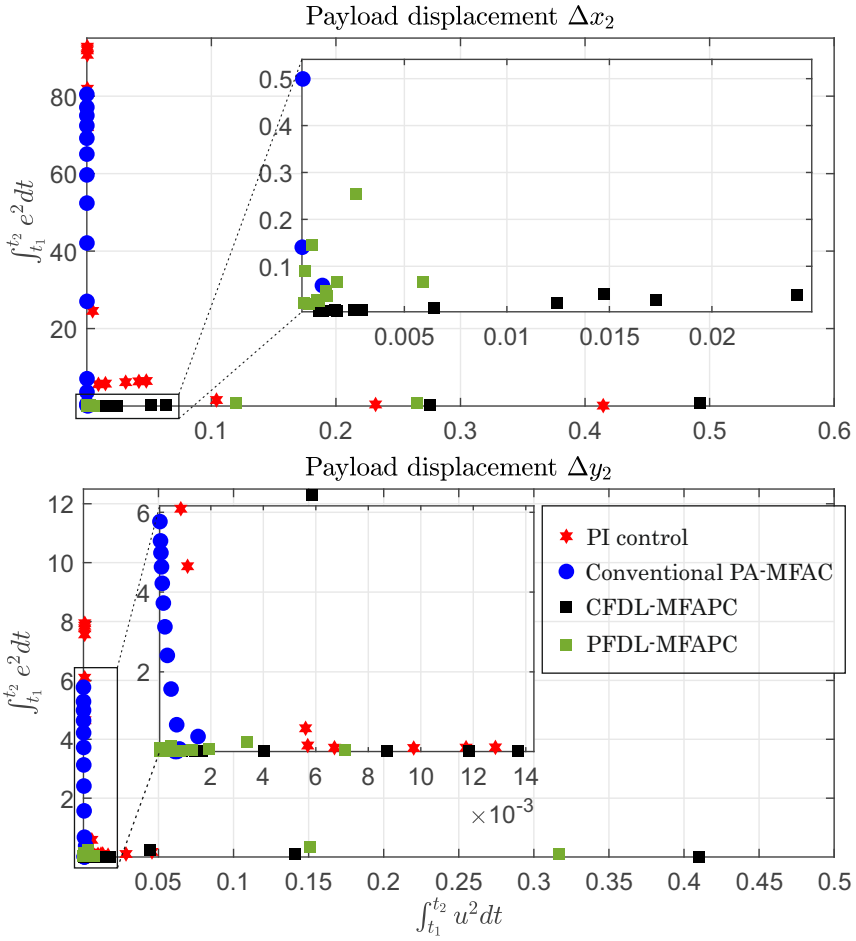

Figure 4.16: Control input energy-based evaluation regarding to the criteria (4.99) within $T_2 = [90, 120]$ [s] [PS20b]

Table 4.9: Control input energy-based evaluation in stationary phase [PS20b]

Control method	$\int \mathbf{e}^2(t)dt$	$\int \mathbf{u}^2(t)dt$	MSE	E_{input}
PI control	7.0399	0.0409	0.0058	$3.4165e^{-5}$
Conventional PA-MFAC	3.0055	0.0020	0.0025	$1.7111e^{-6}$
CFDL-MFAPC	0.0271	0.0061	$2.2614e^{-5}$	$5.0954e^{-6}$
PFDL-MFAPC	0.0261	0.0030	$2.1824e^{-5}$	$2.5167e^{-6}$

5 Improved model-free adaptive control using recursive least-squares algorithm

This chapter discusses the design of an effective MFAC scheme, in which only the measured system I/O signals are required for unknown parameter identification. The novel idea of this contribution is based on the concept of partial-form dynamic linearization (PFDL). An equivalent linearized model structure of the plant is established at every operating point of the system dynamics. The obtained virtual model contains a set of unknown time-varying parameter matrices (or PJM) which could be estimated and updated recursively. To improve on-line parameter estimation accuracy, recursive least-squares algorithm is firstly applied to the partial-form system model instead of using traditional projection algorithm. Furthermore, for control implementation a modified model-free adaptive controller is designed for the purpose of tracking control improvement. Vibration control simulations of an elastic crane are conducted to verify the effectiveness of the design controllers.

This chapter is structured as follows. In Section 5.1, the partial-form dynamic linearization concept will be illustrated. Based on this linearization technique, different on-line parameter estimation approaches, i.e., projection algorithm and recursive least-squares algorithm are discussed. The model-free adaptive control design based on the PFDL concept including the standard and modified control input calculations will be explained in Section 5.2. Simulation results and discussion about oscillation mitigation of an elastic ship-mounted crane are given in Section 5.3. Finally, the chapter summary is mentioned in the last section.

The content, figures, and tables in this chapter have been prepared as a journal article [PS20e]. Some of them are partly modified in this chapter before final submission.

5.1 Partial-form dynamic linearization-based MFAC

As presented in Chapter 3, to design MFAC, the CFDL technique has been applied to a class of unknown MIMO nonlinear systems. An equivalent dynamic data model of the controlled system was established locally. To estimate the unknown time-varying system parameters PJM, two well-known on-line estimation methods including the CFDL-PA (3.32) and CFDL-RLSA (3.75), (3.76), and (3.77) have been discussed in detail. For control design, instead of using the standard control input law (3.38), the modified control input equation (3.85) was proposed to improve tracking control performance. In this section, the main contribution of this chapter will be presented. The concept of partial-form dynamic linearization which considers the effect of the previous control input values within a linearization length constant $L \geq 1$ on the upcoming system outputs $\mathbf{y}(k+1)$ is discussed. Therefore, a linearized partial-form data model of the original system can be generated which contains a

set of unknown parameters PJM denoted as $\Phi_{p,L}(k) = [\Phi_1(k), \Phi_2(k), \ldots, \Phi_L(k)]$. To estimate these time-varying parameter matrices, the given projection algorithm and recursive least-squares algorithm can be applied explicitly. To compute the control signals $\mathbf{u}(k)$, a modified objective function of the control input is proposed by considering minimization of the output tracking errors and its variations within a pre-defined simulation interval $N > 0$. This modified control idea was initially introduced in [MDS18], and applied successfully to a three-tank system as a SISO example. In this study, different adaptive controllers are designed and applied to vibration control of a flexible crane. The results are compared with that of the existing approaches from our previous publications [PS19a, PS19b].

5.1.1 Partial-form dynamic linearization-based projection algorithm

Different from the CFDL concept in Section 3.1, here another dynamic linearization technique namely partial-form dynamic linearization (PFDL) will be investigated. Compared to CFDL, the main difference of this concept is that, to establish a linearized data model of the controlled system, every control input signal or control input increment within a fixed-moving time window (L) is considered explicitly. That means the previous input values also have impact on the future system outputs. The control input increment vector is described as

$$\Delta\mathbf{U}(k) = [\Delta\mathbf{u}(k), \Delta\mathbf{u}(k-1), \ldots, \Delta\mathbf{u}(k-L+1)]^T, \tag{5.1}$$

where $\Delta\mathbf{u}(k) = \mathbf{u}(k) - \mathbf{u}(k-1); \Delta\mathbf{u}(k-L+1) = \mathbf{u}(k-L+1) - \mathbf{u}(k-L)$ is denoted as the control input increment vector at sampling instants k and $k-L+1$, respectively.

Considering a general I/O description for a class of unknown MIMO nonlinear systems as given in (3.15), to establish the equivalent PFDL model, two reasonable assumptions according to [HJ13] need to be fulfilled as

Assumption 5.1: The partial derivatives of $g(\ldots)$ in (3.15) with respect to different control input values $\mathbf{u}(k), \mathbf{u}(k-1), \ldots, \mathbf{u}(k-L)$ exist and are considered as smooth.

Assumption 5.2: The system (3.15) satisfies the following general Lipschitz condition

$$\|\mathbf{y}(k+1) - \mathbf{y}(k)\| \leq b \|\mathbf{U}(k) - \mathbf{U}(k-1)\|, \tag{5.2}$$

at each sampling interval k with $\|\Delta\mathbf{U}(k)\| = \|\mathbf{U}(k) - \mathbf{U}(k-1)\| \neq 0$, and $b > 0$ is a small constant. The system output increment vector is defined as $\mathbf{y}(k+1) - \mathbf{y}(k) = \Delta\mathbf{y}(k+1)$. The original system (3.15) satisfying the above-mentioned assumptions can be formulated in the following PFDL model

$$\Delta\mathbf{y}(k+1) = \Phi_{p,L}(k)\Delta\mathbf{U}(k), \tag{5.3}$$

where the model (5.3) contains a set of unknown time-varying parameter matrices (PJM) denoted as $\Phi_{p,L}(k) = [\Phi_1(k), \Phi_2(k), \ldots, \Phi_p(k), \ldots, \Phi_L(k)]$, with $p \in [1, L]$. The structure of each element matrix $\Phi_p(k)$ in MIMO case is written as

$$\Phi_p(k) = \begin{bmatrix} \phi_{11p}(k) & \phi_{12p}(k) & \phi_{13p}(k) & \ldots & \phi_{1mp}(k) \\ \phi_{21p}(k) & \phi_{22p}(k) & \phi_{23p}(k) & \ldots & \phi_{2mp}(k) \\ \vdots & \vdots & \vdots & \ddots & \vdots \\ \phi_{r1p}(k) & \phi_{r2p}(k) & \phi_{r3p}(k) & \ldots & \phi_{rmp}(k) \end{bmatrix}_{r \times m}, \tag{5.4}$$

assuming $\|\Phi_p(k)\| \leq b$ according to assumption 3.2 (see Section 3.1), and therefore the composed matrix $\Phi_{p,L}(k)$ is bounded at every time instant k. The number of system inputs and outputs are indicated as m and r, correspondingly. In Figure 5.1, a graphical interpretation of the PJM within a length of time window L is depicted for a simple MIMO nonlinear system $\mathbf{y}(k+1) = f_1(\mathbf{U}(k))$, with $\mathbf{U}(k) = [\mathbf{u}(k), \mathbf{u}(k-1), \ldots, \mathbf{u}(k-L)]^T$ [PS20e]. Here, the effect of the previous control inputs from step k to step $k-L$ ($L \geq 1$) on the future outputs is illustrated. At each sampling instant, a linearized data model denoted in green dash lines which include a set of the PJM $\hat{\Phi}_{p,L}(k) = \left[\hat{\Phi}_1(k), \hat{\Phi}_2(k), \ldots, \hat{\Phi}_p(k), \ldots, \hat{\Phi}_L(k)\right]$ is established. Each of the component matrix $\hat{\Phi}_p(k)$ (red dash line) is bounded and can be considered as the derivative value of the function $f_1(.)$. In addition, a graphical explanation of the PFDL concept is shown in Figure 5.2 [PS20e]. The control target is minimization of the control errors between the actual outputs $\mathbf{y}$ and the references $\mathbf{y}^d$ or $\mathbf{e} = \mathbf{y}^d - \mathbf{y}$ during the whole simulation time T.

It can be noted that, in case of $L = 1$, the PFDL data model (5.3) becomes the CFDL data model (3.17), and therefore the system parameters PJM $\Phi_{p,L}(k) = \Phi_1(k)$. Furthermore, for a class of MIMO nonlinear systems with the number of system inputs and outputs are identical ($m = r = n^*$) the following assumption [HJ11a] is essential for system stability analysis.

Assumption 5.3: The first element matrix $\Phi_1(k)$ of $\Phi_{p,L}(k)$ satisfies the diagonally dominant condition with the following boundaries $|\phi_{ij1}(k)| \leq c_1; c_2 \leq |\phi_{ii1}(k)| \leq \alpha c_2$, whereas $i, j = 1, 2, \ldots, n^*$; $i \neq j$; $\alpha \geq 1$, and the sign of all elements in $\Phi_1(k)$ are unchanged. The two positive constants c_1, c_2 should be chosen with the condition $c_2 > c_1(2\alpha + 1)(n^* - 1)$ [HJ11a].

To estimate the unknown system parameters $\Phi_{p,L}(k)$, in this contribution the following cost function is considered

$$\begin{aligned} J(\Phi_{p,L}(k)) &= \|\mathbf{y}(k) - \mathbf{y}(k-1) - \Phi_{p,L}(k)\Delta\mathbf{U}(k-1)\|^2 \\ &\quad + \mu\|\Phi_{p,L}(k) - \Phi_{p,L}(k-1)\|^2, \end{aligned} \tag{5.5}$$

where $\mu > 0$ is a weighting factor utilized to limit the large changes of $\Phi_{p,L}(k)$. The known input increment vector $\Delta\mathbf{U}(k-1)$ in (5.5) is given as

$$\Delta\mathbf{U}(k-1) = [\Delta\mathbf{u}(k-1), \Delta\mathbf{u}(k-2), \ldots, \Delta\mathbf{u}(k-L+1)]^T. \tag{5.6}$$

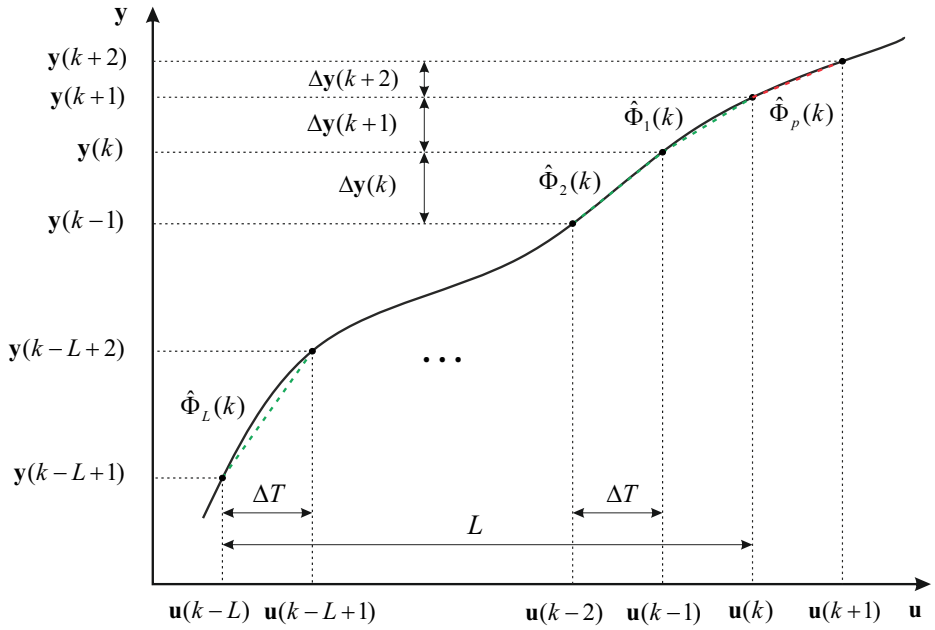

Figure 5.1: Graphical interpretation of the PJM within a linearization length constant L [PS20e]

Minimizing (5.5) with respect to $\Phi_{p,L}(k)$ by taking $\frac{\partial J}{\partial \Phi_{p,L}(k)} = 0$, yields the following equations

$$\begin{aligned}\frac{\partial J}{\partial \Phi_{p,L}(k)} &= \left[\mathbf{y}(k) - \mathbf{y}(k-1) - \Phi_{p,L}(k)\Delta\mathbf{U}(k-1)\right]\left(-\Delta\mathbf{U}^T(k-1)\right) \\ &\quad + \mu\left[\Phi_{p,L}(k) - \Phi_{p,L}(k-1)\right] = 0,\end{aligned} \tag{5.7}$$

$$\begin{aligned}\hat{\Phi}_{p,L}(k) = \hat{\Phi}_{p,L}(k-1) + \left[\Delta\mathbf{y}(k) - \hat{\Phi}_{p,L}(k-1)\Delta\mathbf{U}(k-1)\right]\Delta\mathbf{U}^T(k-1) \\ \left[\mu\mathbf{I} + \Delta\mathbf{U}(k-1)\Delta\mathbf{U}^T(k-1)\right]^{-1},\end{aligned} \tag{5.8}$$

where the output increment vector is denoted as $\Delta\mathbf{y}(k) = \mathbf{y}(k) - \mathbf{y}(k-1)$, and $\mathbf{I}$ is an identity matrix.

To avoid matrix inversion calculation, (5.8) can be rewritten in a simplified formula as

$$\hat{\Phi}_{p,L}(k) = \hat{\Phi}_{p,L}(k-1) + \frac{\eta\left[\Delta\mathbf{y}(k) - \hat{\Phi}_{p,L}(k-1)\Delta\mathbf{U}(k-1)\right]\Delta\mathbf{U}^T(k-1)}{\mu + \|\Delta\mathbf{U}(k-1)\|^2}, \tag{5.9}$$

where $\hat{\Phi}_{p,L}(k)$ indicates the estimated value of $\Phi_{p,L}(k)$, and $\eta \in (0,1]$ is a step-size constant. Equation (5.9) is called partial-form dynamic linearization-based projec-

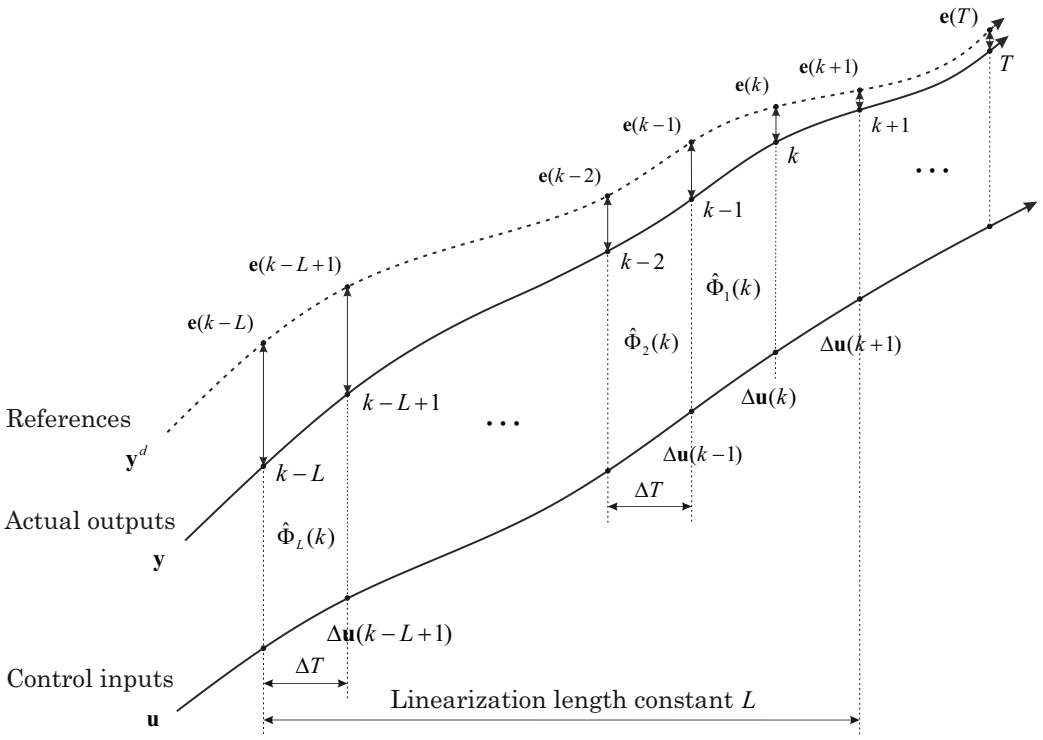

Figure 5.2: Graphical explanation of the PFDL concept [PS20e]

tion algorithm (PFDL-PA) which is implemented to update the system parameters $\Phi_{p,L}(k)$.

5.1.2 Partial-form dynamic linearization-based RLS algorithm

In Section 3.2, the on-line parameter estimation method namely recursive least-squares algorithm (RLSA) has been applied successfully to the CFDL data model of a MIMO system. In this chapter, the discussed RLSA (3.56), (3.58), and (3.59) for SISO nonlinear systems will be implemented to the virtual PFDL data model of an unknown MIMO (nonlinear) system (3.15). The local dynamic model is given as

$$\Delta \mathbf{y}(k) = \Phi_{p,L}(k-1)\Delta \mathbf{U}(k-1), \tag{5.10}$$

where $\Phi_{p,L}(k-1), \Delta \mathbf{U}(k-1)$ are denoted as the available model parameters and control input increment vector from the initial step up to the $(k-1)$-th step, respectively.

By taking the same procedure as presented for the CFDL-RLSA establishment (see Section 3.2) and after several calculations, another RLS algorithm for estimation of

the unknown time-varying parameters $\Phi_{p,L}(k)$ is derived as follows

$$\hat{\Phi}_{p,L}(k) = \hat{\Phi}_{p,L}(k-1) + \Big[\Delta\mathbf{y}(k) - \hat{\Phi}_{p,L}(k-1)\Delta\mathbf{U}(k-1)\Big]\,\mathbf{K}(k), \tag{5.11}$$

$$\begin{aligned}\mathbf{K}(k) &= \Delta\mathbf{U}^T(k-1)\mathbf{P}(k) \\ &= \Delta\mathbf{U}^T(k-1)\mathbf{P}(k-1)\big[\mathbf{I} + \Delta\mathbf{U}(k-1)\mathbf{P}(k-1)\Delta\mathbf{U}^T(k-1)\big]^{-1},\end{aligned} \tag{5.12}$$

$$\begin{aligned}\mathbf{P}(k) = \mathbf{P}(k-1) \; &- \mathbf{P}(k-1)\Delta\mathbf{U}^T(k-1) \\ &\big[\mathbf{I} + \Delta\mathbf{U}(k-1)\mathbf{P}(k-1)\Delta\mathbf{U}^T(k-1)\big]^{-1}\Delta\mathbf{U}(k-1)\mathbf{P}(k-1),\end{aligned} \tag{5.13}$$

where the unknown system parameter matrix is determined as $\mathbf{K}(k) = \Delta\mathbf{U}^T(k-1)\mathbf{P}(k)$, and $\mathbf{P}_0 = \mathbf{P}(0)$ denotes an initial positive definite matrix. The above algorithm (5.11), (5.12), and (5.13) is called PFDL-based recursive least-squares algorithm (PFDL-RLSA).

5.2 MFAC design based on PFDL concept

By applying the discussed parameter estimation algorithms, the estimated PJM $\hat{\Phi}_{p,L}(k)$ can be utilized to compute the required control inputs $\mathbf{u}(k)$. Two control input equations are designed in this section including the standard and modified PFDL-based model-free control laws.

5.2.1 Standard control input calculation

The design of standard control input law based on the PFDL concept is similar to the case of using CFDL as presented in Chapter 3. The control target is to minimize the future tracking errors between the references and actual system outputs. Hence, the control input objective function is considered as

$$J\left(\mathbf{u}(k)\right) = \left\|\mathbf{y}^d(k+1) - \mathbf{y}(k+1)\right\|^2 + \lambda\|\mathbf{u}(k) - \mathbf{u}(k-1)\|^2, \tag{5.14}$$

where $\mathbf{y}^d(k+1), \mathbf{y}(k+1)$ are the desired and actual system output vectors, respectively. To limit the change rate of the required control inputs, a constant weighting parameter $\lambda > 0$ has been added. By using the PFDL concept, the upcoming outputs $\mathbf{y}(k+1)$ in (5.14) are substituted by the equivalent model outputs in (5.3), that means $\mathbf{y}(k+1) = \mathbf{y}(k) + \Phi_{p,L}(k)\Delta\mathbf{U}(k)$. Therefore, the above cost function becomes

$$J\left(\mathbf{u}(k)\right) = \left\|\mathbf{y}^d(k+1) - \mathbf{y}(k) - \Phi_{p,L}(k)\Delta\mathbf{U}(k)\right\|^2 + \lambda\|\Delta\mathbf{u}(k)\|^2, \tag{5.15}$$

where the unknown time-varying parameters $\Phi_{p,L}(k)$, and the control input increment vector $\Delta\mathbf{U}(k)$ are described as

$$\Phi_{p,L}(k) = [\Phi_1(k), \Phi_2(k), \ldots, \Phi_p(k), \ldots, \Phi_L(k)], \tag{5.16}$$

$$\Delta\mathbf{U}(k) = [\Delta\mathbf{u}(k), \Delta\mathbf{u}(k-1), \ldots, \Delta\mathbf{u}(k-L+1)]^T. \tag{5.17}$$

Minimizing (5.15) in term of $\Delta\mathbf{u}(k)$, results in the optimal control input values

$$\begin{aligned}\mathbf{u}(k) = \mathbf{u}(k-1) &+ \frac{\rho_1 \hat{\Phi}_1(k)\left[\mathbf{y}^d(k+1) - \mathbf{y}(k)\right]}{\lambda + \left\|\hat{\Phi}_1(k)\right\|^2} \\ &- \frac{\hat{\Phi}_1(k)\sum_{p=2}^{L}\rho_p\hat{\Phi}_p(k)\Delta\mathbf{u}(k-p+1)}{\lambda + \left\|\hat{\Phi}_1(k)\right\|^2},\end{aligned} \tag{5.18}$$

where $\rho_1, \rho_p \in (0, 1]$ are step-size constants, with $p \in [2, L]$. The time-varying parameter matrices PJM $\hat{\Phi}_1(k), \ldots, \hat{\Phi}_p(k), \ldots, \hat{\Phi}_L(k)$ in (5.18) are estimated continuously by using the PFDL-PA (5.9) or the PFDL-RLSA (5.11), (5.12), and (5.13).

5.2.2 Modified control input calculation

Not only the tracking error amplitudes but also the error variations within a fixed-length of time window $N > 0$ can be minimized to improve the model-free control performance. Therefore, in this work the proposed objective function of $\mathbf{u}(k)$ is written as

$$\begin{aligned}J(\mathbf{u}(k)) = \left\|\mathbf{y}^d(k+1) - \mathbf{y}(k+1)\right\|^2 &+ j\left\|\Delta\mathbf{y}^d(k+1) - \Delta\mathbf{y}(k+1) - \Delta\mathbf{y}(k)\right\|^2 \\ &+ \lambda\|\mathbf{u}(k) - \mathbf{u}(k-1)\|^2,\end{aligned} \tag{5.19}$$

where $j > 0$ is a constant weighting factor. The next system outputs $\mathbf{y}(k+1)$ are assumed to be approximated by the PFDL model outputs (5.3). By substituting (5.3) into (5.19) and taking $\frac{\partial J}{\partial \Delta\mathbf{u}(k)} = 0$, the following equation

$$\begin{aligned}\mathbf{u}(k) = \mathbf{u}(k-1) &+ \frac{\rho_1 \hat{\Phi}_1(k)\left[\mathbf{y}^d(k+1) - \mathbf{y}(k)\right]}{\lambda + (1+j)\left\|\hat{\Phi}_1(k)\right\|^2} \\ &+ \frac{\hat{\Phi}_1(k) j\left[\mathbf{y}^d(k+1) - \mathbf{y}^d(k) - (\mathbf{y}(k) - \mathbf{y}(k-1))\right]}{\lambda + (1+j)\left\|\hat{\Phi}_1(k)\right\|^2} \\ &- \frac{(1+j)\,\hat{\Phi}_1(k)\sum_{p=2}^{L}\rho_p\hat{\Phi}_p(k)\Delta\mathbf{u}(k-p+1)}{\lambda + (1+j)\left\|\hat{\Phi}_1(k)\right\|^2},\end{aligned} \tag{5.20}$$

is derived. To improve control performance, the extended error variations within a fixed-length of time window $N > 0$ represented by $[\varepsilon(k) - \varepsilon(k-N)]$, with $\varepsilon(k) = \mathbf{y}^d(k+1) - \mathbf{y}(k)$; $\varepsilon(k-N) = \mathbf{y}^d(k-N+1) - \mathbf{y}(k-N)$ are also minimized. As a result, the final control input vector is calculated as

$$\begin{aligned}\mathbf{u}(k) = \mathbf{u}(k-1) &+ \frac{\rho_1 \hat{\Phi}_1(k)\left[\mathbf{y}^d(k+1) - \mathbf{y}(k)\right]}{\lambda + (1+j)\left\|\hat{\Phi}_1(k)\right\|^2} \\ &+ \frac{\hat{\Phi}_1(k) j\left[\varepsilon(k) - \varepsilon(k-N)\right]}{\lambda + (1+j)\left\|\hat{\Phi}_1(k)\right\|^2} \\ &- \frac{(1+j)\,\hat{\Phi}_1(k)\sum_{p=2}^{L}\rho_p \hat{\Phi}_p(k)\Delta\mathbf{u}(k-p+1)}{\lambda + (1+j)\left\|\hat{\Phi}_1(k)\right\|^2}.\end{aligned} \tag{5.21}$$

A block diagram of the modified PFDL-RLSA-based model-free adaptive controller for unknown MIMO systems is shown in Figure 5.3.

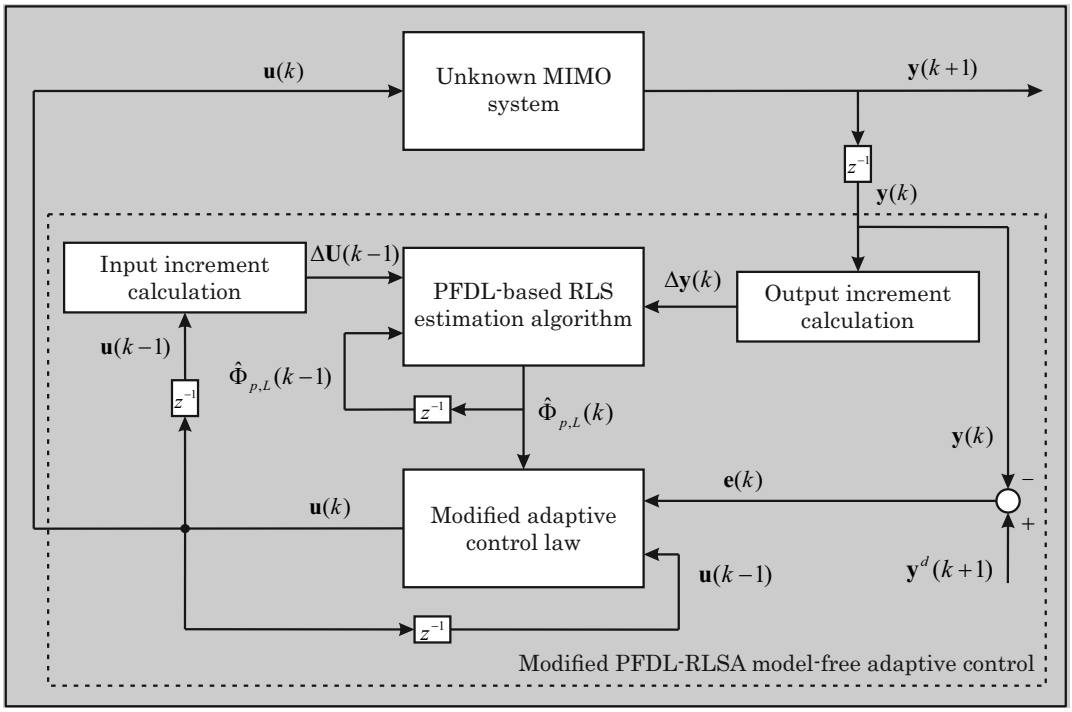

Figure 5.3: Modified PFDL-RLSA-based MFAC structure for unknown MIMO systems [PS20e]

5.3 Simulation results and discussion

In this section, the effectiveness of the proposed PFDL-MFAC is verified numerically. As an illustrative example, vibration control of an elastic ship-mounted crane [AS07] representing a typical flexible system is studied. Introduction to the crane system and its configuration have been briefly reviewed in Section 3.3. The design model-free adaptive controller, which utilizes the PFDL technique, requires the estimated system parameters $\hat{\Phi}_{p,L}(k)$. First, different on-line estimation algorithms such as the PFDL-PA (5.9) or the PFDL-RLSA (5.11), (5.12), and (5.13) can be applied to update the PJM $\hat{\Phi}_{p,L}(k)$ recursively. Then, the required control input values $\mathbf{u}(k)$ are computed by using the standard control input (5.18) or the modified control input (5.21) equations. In the following parts, output tracking control and control input energy-based evaluation regarding to different control approaches will be presented.

5.3.1 Tracking control evaluation

The proposed MFAC which applies the PFDL-RLSA and improved control input law namely modified RLS-MFAC is implemented to the crane. The control method is compared with the modified PA-MFAC [PS19b], standard PA-MFAC [PS19a], and industrial PI control.
In this study, the simulations are conducted in case no external disturbance is considered. However, due to the non-zero initial excitation of the payload ($\dot{\phi}_2^0 = 5.0$ [rad/s] in Table 3.1), significant undesirable oscillations in the crane are observed. In Figure 5.4, vibration control comparison of the payload position in x_0- and y_0-direction is presented. When the controllers start from $t = 30$ [s], it can be seen that the modified RLS-MFAC (green line) indicates better tracking control results according to smaller displacement amplitudes as well as faster control response compared to the modified PA-MFAC (violet line), standard PA-MFAC (red line), and PI control (blue-dot line). By using the improved model-free controller (green line), it takes approximately $\Delta t = 15$ [s] to reduce the payload displacement from $\Delta x_2 = 0.6$ [m] and $\Delta y_2 = 0.3$ [m] to nearly zero (see Figure 5.4). In addition, the system dynamic behaviors due to the initial payload excitation is simulated in uncontrolled case (pink-dash line) within the whole simulation time $T = 140$ [s]. Several design parameters of the modified RLS-MFAC are shown in Table 5.1 [PS20e].
The output results including vibration control of the upper cable $\Delta\alpha_2$ and payload cable $\Delta\phi_2$ are illustrated in Figure 5.5. The angular displacements in the crane are reduced significantly from $\Delta\alpha_2 = 30$ [deg] and $\Delta\phi_2 = 50$ [deg] to nearly zero after around $\Delta t = 20$ [s] by applying the modified RLS-MFAC (green line). The modified RLS-based controller results are improved in terms of control response and error amplitude in comparison with that of the conventional approaches.

In Figure 5.6, the calculated control input values $\mathbf{u}(k)$ and estimated system parameters $\hat{\Phi}_{p,L}(k)$ of the modified RLS-MFAC are presented. Since the controller activated (from $\Delta t = 30$ [s]), the sign of all elements in the PJM parameters $\hat{\Phi}_{p,L}(k)$ are unchanged, and the updated PJM converge to their true values at the end of the simulation.

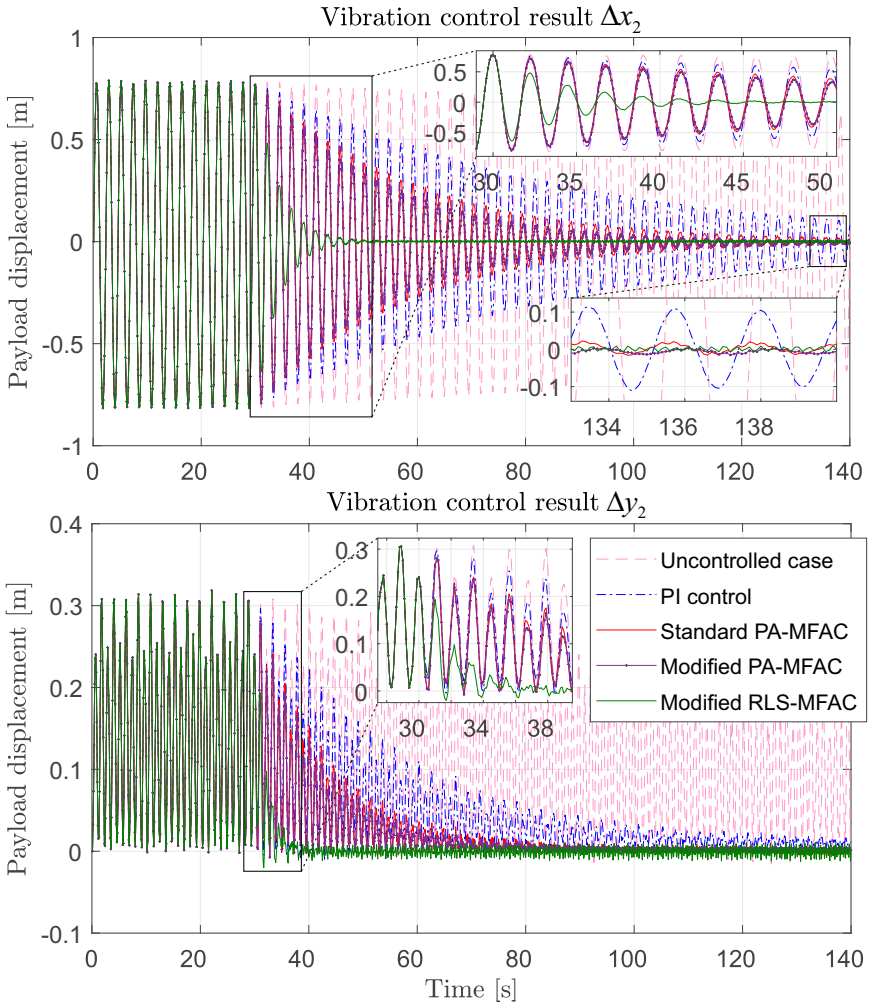

Figure 5.4: Vibration control comparison with respect to the payload position Δx_2 and Δy_2 [PS20e]

5.3.2 Control input energy-based evaluation

To evaluate control performance when varying design controller parameters, the control input energy-based criteria (4.71) is implemented within a specified length

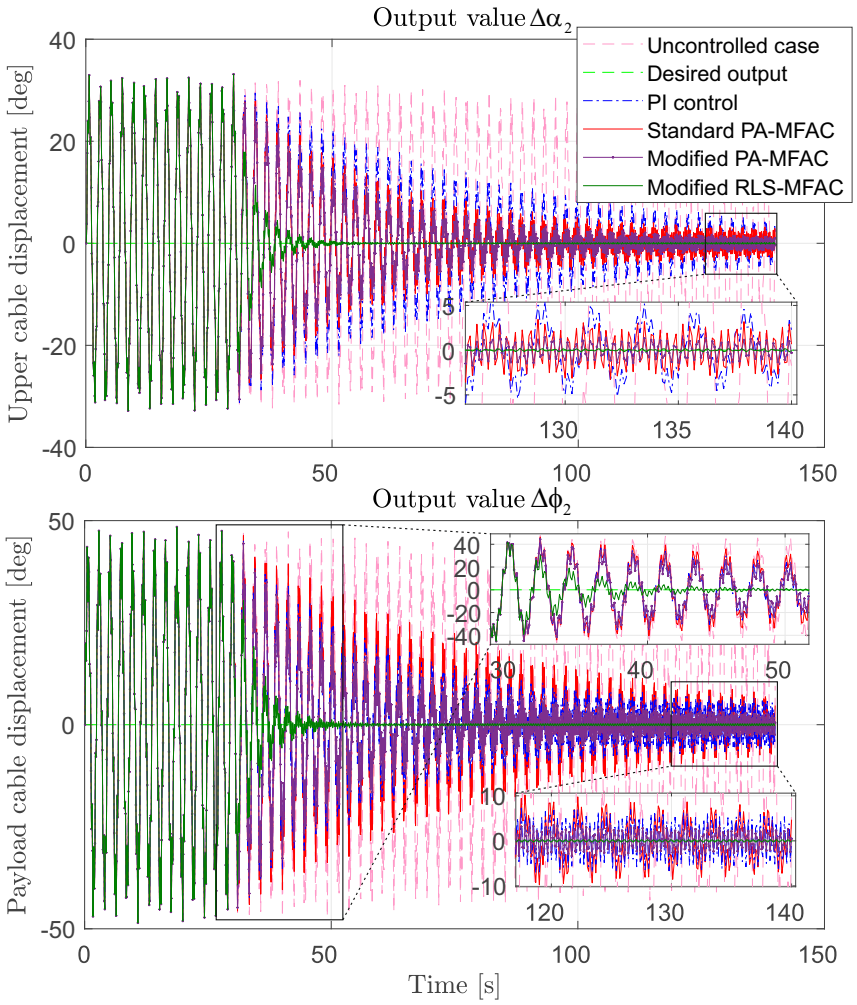

Figure 5.5: Vibration control comparison with respect to the system outputs $\Delta\alpha_2$ and $\Delta\phi_2$ [PS20e]

of simulation time $T = [t_1, t_2]$ [s] as

$$P_{K^*} = \left[\int_{t_1}^{t_2} \mathbf{u}^2(t)dt, \int_{t_1}^{t_2} \mathbf{e}^2(t)dt\right]_{K^*}, \tag{5.22}$$

where $K^* = \{\lambda_p, \lambda_{c1}, \lambda_{c2}, k_p, k_i\}$ is a set of tuning parameters of the different model-free and PI controllers. Here, $\lambda_p, \lambda_{c1}, \lambda_{c2} \in [0.5, 40.0]$ are chosen as the important weighting factors of the modified RLS-MFAC (λ_p in (5.21)), modified PA-MFAC (λ_{c1} in (3.85)), and standard PA-MFAC (λ_{c2} in (3.38)). Suitable choices of them can improve the model-free control efficiency. The variation of PI control parameters are given as $k_p \in [0.0005, 0.008]$ and $k_i \in [0.0001, 0.25]$. In Figure 5.7, the trajectories P_{K^*} of the discussed control approaches are illustrated when altering

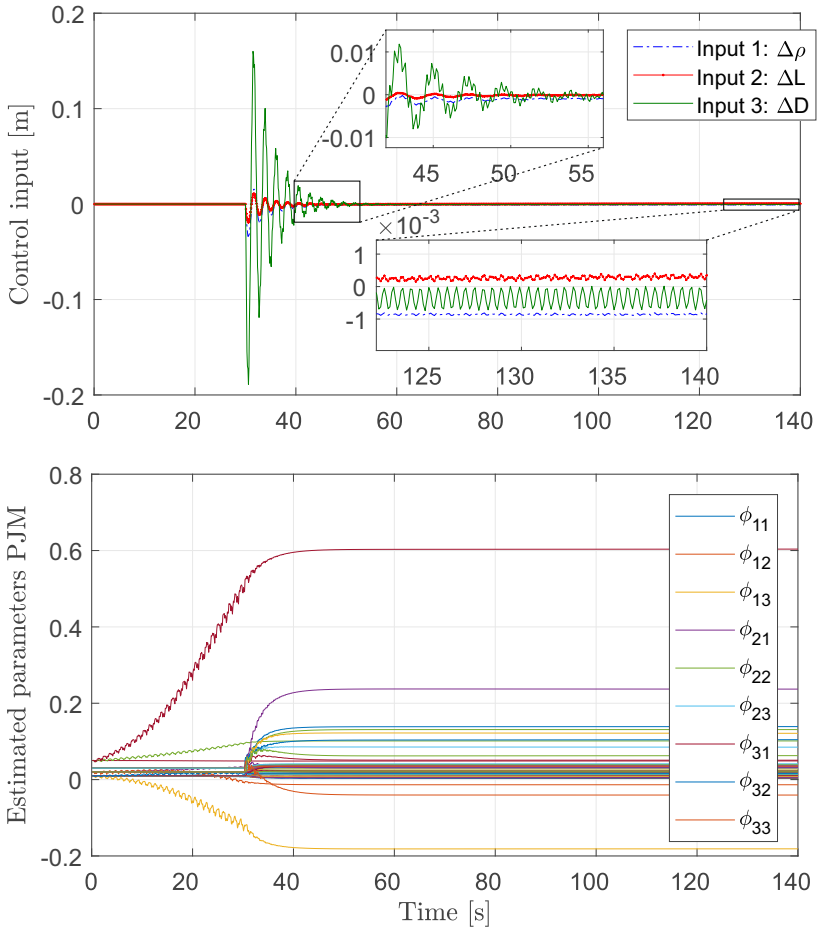

Figure 5.6: Calculated control inputs $\mathbf{u}(k)$ and system parameters $\hat{\Phi}_{p,L}(k)$ [PS20e]

the parameter set K^* in transient phase $T_1 = [30, 140]$ [s]. It can be observed that, the modified RLS-MFAC results (green dot) are distributed closer to the origin $(0, 0)$, and smaller control errors are derived in comparison with the modified PA-MFAC (violet dot), standard PA-MFAC (blue dot), and PI control (red dot) results. Furthermore, the control input-tracking error relation in stationary phase $T_2 = [110, 140]$ [s] is presented in Figure 5.8. Generally, the improved PFDL-based model-free controller (green dot) seems to show improved results in term of obtained smaller payload displacements in both x_0- and y_0-direction than other methods. Finally, the control results calculated in (3.105), and (3.106) are described numerically in Table 5.2 and Table 5.3 for transient and stationary phase, subsequently. In transient phase T_1 (see Table 5.2), the modified RLS-MFAC derives the smallest control errors according to $\int \mathbf{e}^2(t)dt$ (8.1852) and MSE (0.0058), but still requires more

Table 5.1: Design parameters of the modified RLS-MFAC [PS20e]

Parameter	**Meaning**	**Value**
L	Linearization length constant	6
ρ_1	Step-size constant	0.25
ρ_p	Step-size constant	0.25
λ	Constant weighting factor	1.20
j	Design weighting parameter	0.03
$\mathbf{P}_0$	Positive definite parameter	1.90

Table 5.2: Control performance evaluation in transient phase [PS20e]

Control method	$\int \mathbf{e}^2(t)dt$	$\int \mathbf{u}^2(t)dt$	MSE	E_{input}
PI control	97.1267	0.2163	0.0693	$1.5457e^{-4}$
Standard PA-MFAC	59.3759	0.0473	0.0424	$3.3792e^{-5}$
Modified PA-MFAC	44.9898	0.0843	0.0321	$6.0265e^{-5}$
Modified RLS-MFAC	8.1852	0.5116	0.0058	$3.6546e^{-4}$

input energy with $\int \mathbf{u}^2(t)dt$ (0.5116). On the other hand, in stationary phase T_2 (see Table 5.3), the novel control method achieves less control error amplitudes $\int \mathbf{e}^2(t)dt$ (0.0144) as well as the total control input energy $\int \mathbf{u}^2(t)dt$ ($2.9983e^{-4}$).

5.4 Summary

In this chapter, an improved MFAC scheme for a class of unknown MIMO systems, in which only the available system I/O measurements are necessary for feedback, is discussed. To linearize the unknown system dynamics, beside CFDL this chapter considers the PFDL concept. A local linearized data model has been constructed which contains a set of unknown time-varying parameter matrices (PJM). To improve the PJM estimation accuracy, the recursive least-squares method is applied firstly to the virtual PFDL model instead of using traditional projection algorithm. For control realization, standard and modified PFDL-based model-free control input algorithms are designed for tracking control improvement. The proposed data-driven control schemes have been implemented to an elastic boom crane for vibration reduction purpose. The simulation results indicate that the modified RLS-MFAC which

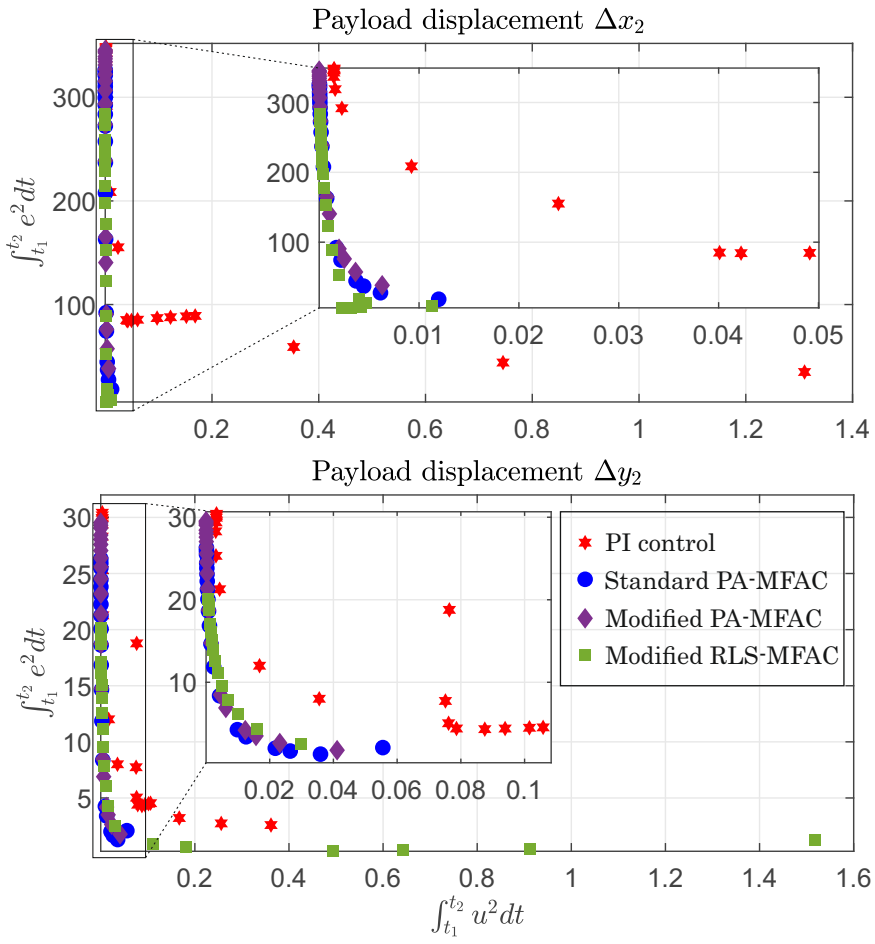

Figure 5.7: Control performance evaluation in transient phase regarding the criteria (5.22) [PS20e]

is based on the PFDL concept generates improved results for both tracking control and control input energy-based evaluation in comparison with traditional methods.

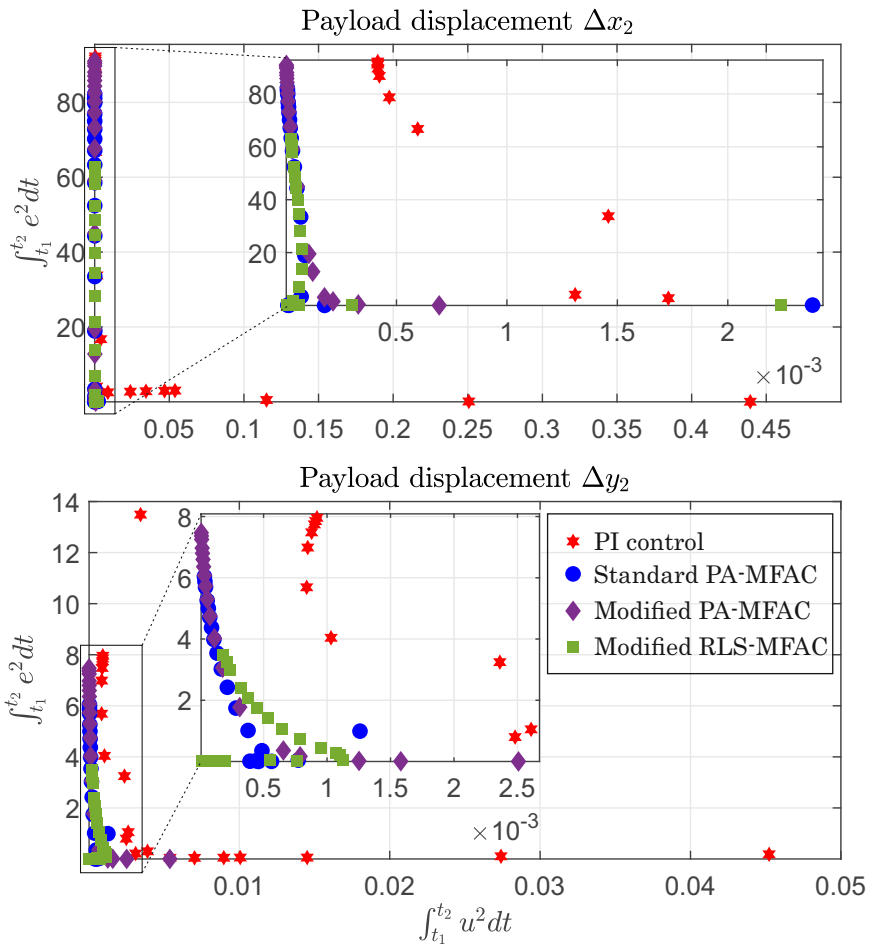

Figure 5.8: Control performance evaluation in stationary phase regarding the criteria (5.22) [PS20e]

Table 5.3: Control performance evaluation in stationary phase [PS20e]

Control method	$\int \mathbf{e}^2(t)dt$	$\int \mathbf{u}^2(t)dt$	MSE	E_{input}
PI control	3.4127	0.0414	0.0024	$2.9631e^{-5}$
Normal CFDL-MFAC	2.2092	0.0016	0.0015	$1.2084e^{-6}$
Modified CFDL-MFAC	0.5653	0.0107	$4.0381e^{-4}$	$7.6549e^{-6}$
Modified CFDL-MFAC	0.0144	$2.9983e^{-4}$	$1.0313e^{-5}$	$2.1416e^{-7}$

6 Summary, conclusion, and future work

6.1 Summary and conclusion

In this research, the main theory of MFAC has been investigated in detail. Several modified/improved control ideas were proposed focusing on the improvements of on-line parameter estimation accuracy and tracking control performance. To give an overview of model-free or data-driven control, the selected methods were classified into four categories including: on-line, off-line, hybrid data usage, and MBC in combination with MFC. In each category, some of the existing data-driven control approaches which are primarily concerned in literature have been discussed in terms of fundamental theory, important characteristics, and impressive applications. The last MFC group presented two innovative methods by combining MFAC with the other robust MBC theories namely model predictive control and sliding mode control. This work concentrates on vibration reduction of a class of complex and flexible mechanical systems represented by an elastic offshore boom crane. Therefore, vibration control problems and a variety of existing solutions to deal with oscillation mitigation in vibrating structures were discussed carefully. In particular, a review of vibration and tracking control for different types of crane, e.g., boom crane, tower crane, overhead crane, or container crane has been illustrated in the theoretical chapter. From literature analysis, it can be seen that, many effective control strategies have been successfully developed for cranes ranging from open-loop control to closed-loop control systems. Recently, intelligent control and data-driven control have become more attractive, and these modern/advanced control techniques can be considered as the innovative solutions to design active controllers for complicated industrial machines, especially for cranes. From the discussion about the given model-free control as well as the crane control methodologies, MFAC has been selected for further development because the approach shown the ability in control design modifications, and potential applications in vibration control of complicated and flexible systems. Furthermore, MFAC can also be easily combined with other traditional MBC methods to improve the overall control system performance. The novel MFAC strategies are also expected to deal with unknown external disturbances as most of actual processes have to encounter in reality.

Conventional CFDL-based MFAC normally utilizes projection algorithm for estimation of the unknown time-varying system parameters (or PJM). In this contribution, the recursive least-squares method is firstly applied, in which the estimated parameters shown faster in estimation convergence to their correct values. The discussed RLS method was initially implemented to a general SISO system. Then, the obtained results can be extended to a class of MIMO nonlinear systems, in which the unknown system parameters could be identified continuously by using only the available system I/O data. Moreover, regarding to control realization, the modified

control input calculation was proposed for the tracking control improvement. The idea of modification has been utilized previously to control simple SISO and MIMO systems. In this research, novel control input laws have been proposed, and the design control schemes were applied to reduce the in-plane vibrations of a multi-variable elastic ship-mounted crane represented as a typical complex and flexible machine. The design controllers have been verified via simulations. Due to the non-zero initial excitation of the payload, large oscillations might occur in the crane if no controller is used. It can be concluded from the simulation results that, the improved CFDL-based MFAC approaches which relied on the RLS algorithm and/or modified control input law, obtained better control performance with respects to smaller output control errors and required less control input energy (particularly in stationary phase) compared to the other traditional methods.

As a simplified dynamic linearization technique, CFDL has been widely applied in MFAC design because of the obtained simple linearized system model. In this contribution, by using the CFDL concept not only for linearization of the original unknown plant but also for the assumed nonlinear controller, a simplified controller structure for a MIMO (nonlinear) system was established. Afterwards, a modified estimation algorithm of the unknown controller parameter matrices (or PPD) was proposed by considering minimization of the output tracking error variations into its objective function. Furthermore, different modified/improved model-free adaptive predictive control schemes have been presented and applied to reduce the unexpected vibrations of the elastic crane. Based on the CFDL and PFDL concepts, general system output predictive equations, which are linearized and contain the future unknown time-varying parameter matrices (or PJM) within a finite prediction horizon, were generated. To estimate and predict the PJM, the standard and modified recursive least-squares algorithms were firstly implemented. The design model-free control programs have been verified numerically, in which the introduced ship-mounted crane was considered. The simulation results indicated that, in case of without considering external disturbances, e.g., wave motion or wind force, the proposed controllers derived better control performance in comparison with the normal CFDL-PA-based MFAC and industrial PI control. The control effectiveness might be enhanced by choosing appropriate controller parameters. Hence, the trajectory P_{K^*} of the relationship between the total output control errors and the consumed input energy was considered. From the simulation results, the modified model-free controllers performed better control efficiency regarding smaller numbers of the total control error amplitudes.

When constructing a linearized system dynamic model, the effects of previous control input signals to the upcoming system output values can be integrated explicitly. This is the key idea of the PFDL concept. In this work, an improved model-free adaptive controller structure based on the PFDL data model of the original system and RLS algorithm for on-line parameter estimation has been introduced. The obtained linearized system model contains a set of unknown parameter matrices

(PJM) which can be updated/corrected recursively by using directly the measured or calculated system I/O signals. Based on the estimated system parameters and the current control errors, the required control input vector was determined by implementing a novel control input equation. The design RLSA-MFAC based on PFDL has been applied to the elastic crane for vibration reduction purpose. For control performance evaluation, the proposed approach was compared with three other types of traditional model-free control methods including the standard CFDL-PA-MFAC, modified CFDL-PA-MFAC, and industrial PI control. The simulation results shown that, the vibrations of the elatic boom and the payload in the crane were reduced considerably at the end of the simulation by using the modified controllers. In addition, when varying the design control parameters, the improved data-driven controllers obtained smaller tracking errors, and the trajectories P_{K^*} were distributed closer to the origin compared to the conventional approaches. However, in most of the proposed MFAC methods, more input energy has been consumed to drive the output signals converge to their desired values, particularly in transient phase.

From the above analysis, the main contributions and new results in this thesis can be pointed out as follows:

- Improved MFAC schemes by applying firstly the recursive least-squares estimation method to the linearized CFDL system model are designed. In addition, a modified CFDL-based control input law is proposed to control a class of unknown MIMO systems.

- Based on the CFDL concept, a modified CFDLc-MFAC program is proposed by considering minimization of the tracking error differences into its objective function.

- Model-free adaptive control has been combined with model predictive control to design improved data-driven control systems. Recursive least-squares method has been applied to the compact-form and partial-form output predictive models which shows improved results in parameter estimation.

- Not only using CFDL, the concept of PFDL is investigated for control of MIMO (nonlinear) systems. An improved model-free controller which applies the RLS-based estimation algorithm and modified control input equation has been proposed.

- As a case study of vibration control of complex and flexible systems, simulation results of an elastic ship-mounted crane are shown. In case of using the proposed controllers, better control performance can be observed in comparison with other conventional methods.

6.2 Future work

For further research in the future, the following ideas can be considered to develop robust/advanced model-free adaptive controllers:

- Robust/advanced MFAC should be designed to get faster control response. Improved MFAC programs to deal with control of practical systems, in which the dynamics change quickly, could be motivated. Furthermore, in actual control problems of complex and flexible mechanical systems, unknown external perturbations are inevitable which might deteriorate the model-free control performance. Therefore, the development of advanced MFAC strategies to derive disturbance rejection could be interested for further studies.
- Beside using the CFDL and PFDL concept for system linearization, the full-form dynamic linearization technique may be utilized explicitly to fully describe the system dynamic behaviors, particularly in complicated industrial machines/processes.
- Model-free adaptive control can be combined with other well-developed MBC methods such as sliding mode control, observer-based control for vibration control purpose. Additionally, the combined model-free control schemes may be applied to other classes of nonlinear system.
- The simulation control results in this thesis verified the effectiveness of the proposed data-driven control algorithms. For future works, experimental implementation of the design control programs can be executed. The real-time control problems of the elastic lab-scaled crane can be further investigated and compared with the derived simulation results.

Bibliography

[ACL05] Ang, K. H. ; Chong, G. ; Li, Y.: PID control system analysis, design, and technology. In: *IEEE Transactions on Control Systems Technology* 13 (2005), No. 4, pp. 559–576

[ACM07] Ahn, H. ; Chen, Y. ; Moore, K. L.: Iterative Learning Control: Brief Survey and Categorization. In: *IEEE Transactions on Systems, Man, and Cybernetics, Part C (Applications and Reviews)* 37 (2007), No. 6, pp. 1099–1121

[ÅH95] Åström, K. J. ; Hägglund, T.: *PID Controllers: Theory, Design, and Tuning*. ISA - The Instrumentation, Systems and Automation Society, (1995)

[ÅH01] Åström, K. J. ; Hägglund, T.: The future of PID control. In: *Control Engineering Practice* 9 (2001), No. 11, pp. 1163–1175

[Aha97] Aha, D. W.: *Lazy Learning*. Springer Netherlands, (1997) (Artificial intelligence review)

[ÅHHH93] Åström, K. J. ; Hägglund, T. ; Hang, C. C. ; Ho, W. K.: Automatic tuning and adaptation for PID controllers - a survey. In: *Control Engineering Practice* 1 (1993), No. 4, pp. 699–714

[Al-06] Al-Sweiti, Y. M.: *Modeling and Control of an Elastic Ship-Mounted Crane Using Variable-Gain Model-Based Controller*, University of Duisburg-Essen, Dissertation, (2006)

[AMS97] Atkeson, C. ; Moore, A. ; Schaal, S.: Locally Weighted Learning for Control. In: *Artificial Intelligence Review* 11 (1997), pp. 75–113

[AS07] Al-Sweiti, Y. M. ; Söffker, D.: Planar Cargo Control of Elastic Ship Cranes with the "Maryland Rigging" System. In: *Journal of Vibration and Control* 13 (2007), No. 3, pp. 241–267

[ÅW08] Åström, K. J. ; Wittenmark, B.: *Adaptive Control*. Dover Publications, (2008) (Dover Books on Electrical Engineering)

[AX11] Abidi, K. ; Xu, J.: Iterative Learning Control for Sampled-Data Systems: From Theory to Practice. In: *IEEE Transactions on Industrial Electronics* 58 (2011), No. 7, pp. 3002–3015

[BB04] Bontempi, G. ; Birattari, M.: From Linearization to Lazy Learning: A Survey of Divide-and-Conquer Techniques for Nonlinear Control (Invited Paper). In: *International Journal of Computational Cognition* 3 (2004), No. 1, pp. 56–73

[BFS98] Brugarolas, P. B. ; Fromion, V. ; Safonov, M. G.: Robust switching missile autopilot. In: *Proceedings of the 1998 American Control Conference. ACC (IEEE Cat. No.98CH36207)* Vol. 6, (1998), pp. 3665–3669

[BHZ18] Bu, X. ; Hou, Z. ; Zhang, H.: Data-Driven Multiagent Systems Consensus Tracking Using Model Free Adaptive Control. In: *IEEE Transactions on Neural Networks and Learning Systems* 29 (2018), No. 5, pp. 1514–1524

[BKdS05] Bukkems, B. ; Kostic, D. ; de Jager, B. ; Steinbuch, M.: Learning-based identification and iterative learning control of direct-drive robots. In: *IEEE Transactions on Control Systems Technology* 13 (2005), No. 4, pp. 537–549

[BMST10] Battistelli, G. ; Mosca, E. ; Safonov, M. G. ; Tesi, P.: Stability of Unfalsified Adaptive Switching Control in Noisy Environments. In: *IEEE Transactions on Automatic Control* 55 (2010), No. 10, pp. 2424–2429

[BPU02] Bartolini, G. ; Pisano, A. ; Usai, E.: Second-order sliding-mode control of container cranes. In: *Automatica* 38 (2002), No. 10, pp. 1783–1790

[BTA06] Bristow, D. A. ; Tharayil, M. ; Alleyne, A. G.: A survey of iterative learning control. In: *IEEE Control Systems Magazine* 26 (2006), No. 3, pp. 96–114

[BWHQ18] Bu, X. ; Wang, Q. ; Hou, Z. ; Qian, W.: Data driven control for a class of nonlinear systems with output saturation. In: *ISA Transactions* 81 (2018), pp. 1–7

[CBA04] Camacho, E. F. ; Bordons, C. ; Alba, C. B.: *Model Predictive Control*. Springer London, (2004) (Advanced Textbooks in Control and Signal Processing)

[CC09] Coelho, L. ; Coelho, A.: Model-free adaptive control optimization using a chaotic particle swarm approach. In: *Chaos, Solitons & Fractals* 41 (2009), pp. 2001–2009

[CFS19] Chen, H. ; Fang, Y. ; Sun, N.: An adaptive tracking control method with swing suppression for 4-DOF tower crane systems. In: *Mechanical Systems and Signal Processing* 123 (2019), pp. 426–442

[CHJH18] Chi, R. ; Hou, Z. ; Jin, S. ; Huang, B.: Computationally Efficient Data-Driven Higher Order Optimal Iterative Learning Control.

In: *IEEE Transactions on Neural Networks and Learning Systems* 29 (2018), No. 12, pp. 5971–5980

[CPSC10] Coelho, L. ; Pessôa, M. W. ; Sumar, R. R. ; Coelho, A.: Model-free adaptive control design using evolutionary-neural compensator. In: *Expert Syst. Appl.* 37 (2010), pp. 499–508

[CS04] Cabral, F. B. ; Safonov, M. G.: Unfalsified model reference adaptive control using the ellipsoid algorithm. In: *International Journal of Adaptive Control and Signal Processing* 18 (2004), No. 8, pp. 683–696

[CS06] Campi, M. C. ; Savaresi, S. M.: Direct nonlinear control design: the virtual reference feedback tuning (VRFT) approach. In: *IEEE Transactions on Automatic Control* 51 (2006), No. 1, pp. 14–27

[DUKY12] Duong, S. C. ; Uezato, E. ; Kinjo, H. ; Yamamoto, T.: A hybrid evolutionary algorithm for recurrent neural network control of a three-dimensional tower crane. In: *Automation in Construction* 23 (2012), pp. 55–63

[ES98] Edwards, C. ; Spurgeon, S.: *Sliding Mode Control: Theory And Applications*. Taylor & Francis, (1998) (Series in Systems and Control)

[FJ08] Fliess, M. ; Join, C.: Intelligent PID controllers. In: *Mediterranean Conference on Control and Automation - Conference Proceedings, MED'08*, (2008), pp. 326–331

[FJ09] Fliess, M. ; Join, C.: Model-free control and intelligent PID controllers: towards a possible trivialization of nonlinear control? In: *IFAC Proceedings Volumes* 42 (2009), No. 10, pp. 1531–1550

[FJ13] Fliess, M. ; Join, C.: Model-free control. In: *International Journal of Control* 86 (2013), pp. 2228–2252

[FWSZ14] Fang, Y. ; Wang, P. ; Sun, N. ; Zhang, Y.: Dynamics Analysis and Nonlinear Control of an Offshore Boom Crane. In: *IEEE Transactions on Industrial Electronics* 61 (2014), No. 1, pp. 414–427

[GA07] Glossiotis, G. ; Antoniadis, I.: Digital Filter Based Motion Command Preconditioning of Time Varying Suspended Loads in Boom Cranes for Sway Suppression. In: *Journal of Vibration and Control* 13 (2007), No. 5, pp. 617–656

[GA15] Granichin, O. ; Amelina, N.: Simultaneous Perturbation Stochastic Approximation for Tracking Under Unknown but Bounded Disturbances. In: *IEEE Transactions on Automatic Control* 60 (2015), No. 6, pp. 1653–1658

[GC20] Guo, B. ; Chen, Y.: Fuzzy robust fault-tolerant control for offshore ship-mounted crane system. In: *Information Sciences* 526 (2020), pp. 119–132

[GHLJ19] Guo, Y. ; Hou, Z. ; Liu, S. ; Jin, S.: Data-Driven Model-Free Adaptive Predictive Control for a Class of MIMO Nonlinear Discrete-Time Systems With Stability Analysis. In: *IEEE Access* 7 (2019), pp. 102852–102866

[Gor97] Gorez, R.: A survey of PID auto-tuning methods : Feature issue controller tuning. In: *Mathematics*, (1997)

[GP11] Grüne, L. ; Pannek, J.: *Nonlinear Model Predictive Control: Theory and Algorithms*. Springer London, (2011) (Communications and Control Engineering)

[GP19] Golovin, I. ; Palis, S.: Robust control for active damping of elastic gantry crane vibrations. In: *Mechanical Systems and Signal Processing* 121 (2019), pp. 264–278

[GS00] Guardabassi, G. O. ; Savaresi, S. M.: Virtual reference direct design method: an off-line approach to data-based control system design. In: *IEEE Transactions on Automatic Control* 45 (2000), No. 5, pp. 954–959

[GS14] Goodwin, G. C. ; Sin, K. S.: *Adaptive Filtering Prediction and Control*. Dover Publications, (2014) (Dover Books on Electrical Engineering)

[HB11] Hou, Z. ; Bu, X.: Model free adaptive control with data dropouts. In: *Expert Systems with Applications* 38 (2011), No. 8, pp. 10709–10717

[HCG17] Hou, Z. ; Chi, R. ; Gao, H.: An Overview of Dynamic-Linearization-Based Data-Driven Control and Applications. In: *IEEE Transactions on Industrial Electronics* 64 (2017), No. 5, pp. 4076–4090

[HGG94] Hjalmarsson, H. ; Gunnarsson, S. ; Gevers, M.: A convergent iterative restricted complexity control design scheme. In: *Proceedings of 33rd IEEE Conference on Decision and Control* Vol. 2, (1994), pp. 1735–1740

[HGGL98] Hjalmarsson, H. ; Gevers, M. ; Gunnarsson, S. ; Lequin, O.: Iterative feedback tuning: theory and applications. In: *IEEE Control Systems Magazine* 18 (1998), No. 4, pp. 26–41

[HH97] Hou, Z. ; Huang, W.: The model-free learning adaptive control of a class of SISO nonlinear systems. In: *Proceedings of the 1997 American Control Conference (Cat. No.97CH36041)* Vol. 1, (1997), pp. 343–344

[HJ08] Hou, Z. ; Jin, S.: Model-Free Adaptive Control for a Class of Nonlinear Discrete-Time Systems Based on the Partial Form Linearization. In: *IFAC Proceedings Volumes* 41 (2008), No. 2, pp. 3509–3514

[HJ11a] Hou, Z. ; Jin, S.: Data-Driven Model-Free Adaptive Control for a Class of MIMO Nonlinear Discrete-Time Systems. In: *IEEE Transactions on Neural Networks* 22 (2011), No. 12, pp. 2173–2188

[HJ11b] Hou, Z. ; Jin, S.: A Novel Data-Driven Control Approach for a Class of Discrete-Time Nonlinear Systems. In: *IEEE Transactions on Control Systems Technology* 19 (2011), No. 6, pp. 1549–1558

[HJ13] Hou, Z. ; Jin, S.: *Model Free Adaptive Control: Theory and Applications*. Taylor & Francis, (2013)

[Hja98] Hjalmarsson, H.: Control of nonlinear systems using iterative feedback tuning. In: *Proceedings of the 1998 American Control Conference. ACC (IEEE Cat. No.98CH36207)* Vol. 4, (1998), pp. 2083–2087

[Hja02] Hjalmarsson, H.: Iterative feedback tuning - an overview. In: *International Journal of Adaptive Control and Signal Processing* 16 (2002), No. 5, pp. 373–395

[HLT17] Hou, Z. ; Liu, S. ; Tian, T.: Lazy-Learning-Based Data-Driven Model-Free Adaptive Predictive Control for a Class of Discrete-Time Nonlinear Systems. In: *IEEE Transactions on Neural Networks and Learning Systems* 28 (2017), No. 8, pp. 1914–1928

[HPJ09] Huusom, J. K. ; Poulsen, N. K. ; Jørgensen, S. B.: Improving convergence of Iterative Feedback Tuning. In: *Journal of Process Control* 19 (2009), No. 4, pp. 570–578

[HPO18] Hassani, V. ; Pascoal, A. M. ; Onstein, T. F.: Data-driven control in marine systems. In: *Annual Reviews in Control* 46 (2018), pp. 343–349

[HVO16] Heertjes, M. F. ; Van der Velden, B. ; Oomen, T.: Constrained Iterative Feedback Tuning for Robust Control of a Wafer Stage System. In: *IEEE Transactions on Control Systems Technology* 24 (2016), No. 1, pp. 56–66

[HW13] Hou, Z. ; Wang, Z.: From model-based control to data-driven control: Survey, classification and perspective. In: *Information Sciences* 235 (2013), pp. 3–35

[HX19] Hou, Z. ; Xiong, S.: On Model-Free Adaptive Control and Its Stability Analysis. In: *IEEE Transactions on Automatic Control* 64 (2019), No. 11, pp. 4555–4569

[HYY18] Hou, Z. ; Yu, X. ; Yin, C.: A Data-Driven Iterative Learning Control Framework Based on Controller Dynamic Linearization. In: *2018 Annual American Control Conference (ACC)*, (2018), pp. 5588–5593

[HZ13] Hou, Z. ; Zhu, Y.: Controller-Dynamic-Linearization-Based Model Free Adaptive Control for Discrete-Time Nonlinear Systems. In: *IEEE Transactions on Industrial Informatics* 9 (2013), No. 4, pp. 2301–2309

[IFH01] Ikeda, M. ; Fujisaki, Y. ; Hayashi, N.: A model-less algorithm for tracking control based on input-output data. In: *Nonlinear Analysis: Theory, Methods & Applications* 47 (2001), No. 3, pp. 1953–1960

[IS12] Ioannou, P. A. ; Sun, J.: *Robust Adaptive Control*. Dover Publications, Incorporated, (2012) (Dover Books on Electrical Engineering Series)

[JLT17] Jin, M. ; Lee, J. ; Tsagarakis, N. G.: Model-Free Robust Adaptive Control of Humanoid Robots With Flexible Joints. In: *IEEE Transactions on Industrial Electronics* 64 (2017), No. 2, pp. 1706–1715

[JPS13] Janssens, P. ; Pipeleers, G. ; Swevers, J.: A Data-Driven Constrained Norm-Optimal Iterative Learning Control Framework for LTI Systems. In: *IEEE Transactions on Control Systems Technology* 21 (2013), No. 2, pp. 546–551

[KCT+16] Kandasamy, R. ; Cui, F. ; Townsend, N. ; Foo, C. C. ; Guo, J. ; Shenoi, A. ; Xiong, Y.: A review of vibration control methods for marine offshore structures. In: *Ocean Engineering* 127 (2016), pp. 279–297

[Kha02] Khalil, H. K.: *Nonlinear Systems*. Prentice Hall, (2002) (Pearson Education)

[Kir04] Kirk, D. E.: *Optimal Control Theory: An Introduction*. Dover Publications, (2004) (Dover Books on Electrical Engineering Series)

[LCS02] Lecchini, A. ; Campi, M. C. ; Savaresi, S. M.: Virtual reference feedback tuning for two degree of freedom controllers. In: *International Journal of Adaptive Control and Signal Processing* 16 (2002), No. 5, pp. 355–371

[LD01] Liu, G. P. ; Daley, S.: Optimal-tuning PID control for industrial systems. In: *Control Engineering Practice* 9 (2001), No. 11, pp. 1185–1194

[LDJ19] Liao, Y. ; Du, T. ; Jiang, Q.: Model-free adaptive control method with variable forgetting factor for unmanned surface vehicle control. In: *Applied Ocean Research* 93 (2019), pp. 101945

[LFS19] Lu, B. ; Fang, Y. ; Sun, N.: Enhanced-coupling adaptive control for double-pendulum overhead cranes with payload hoisting and lowering. In: *Automatica* 101 (2019), pp. 241–251

[LFSW18] Lu, B. ; Fang, Y. ; Sun, N. ; Wang, X.: Antiswing Control of Offshore Boom Cranes With Ship Roll Disturbances. In: *IEEE Transactions on Control Systems Technology* 26 (2018), No. 2, pp. 740–747

[LHP+18] Le, A. T. ; Hoang, M. C. ; Pham, V. T. ; Luong, C. N. ; Vu, D. T. ; Le, V. A.: Adaptive neural network sliding mode control of shipboard container cranes considering actuator backlash. In: *Mechanical Systems and Signal Processing* 112 (2018), pp. 233–250

[LHT+19] Liu, S. ; Hou, Z. ; Tian, T. ; Deng, Z. ; Li, Z.: A Novel Dual Successive Projection-Based Model-Free Adaptive Control Method and Application to an Autonomous Car. In: *IEEE Transactions on Neural Networks and Learning Systems* 30 (2019), No. 11, pp. 3444–3457

[Lju99] Ljung, L.: *System Identification: Theory for the User*. Prentice Hall PTR, (1999) (Prentice Hall information and system sciences series)

[LL13] Le, A. T. ; Lee, S. G.: Sliding Mode Controls of Double-Pendulum Crane Systems. In: *Journal of Mechanical Science and Technology* 27 (2013), pp. 1863–1873

[Luu15] Luu, Q. K.: *Stability-Oriented Dynamics and Control of Complex Rigid-Flexible Mechanical Systems Using the Example of a Bucket-Wheel Excavator*, University of Duisburg-Essen, Dissertation, (2015)

[LY17] Liu, D. ; Yang, G.: Event-based model-free adaptive control for discrete-time non-linear processes. In: *IET Control Theory Applications* 11 (2017), No. 15, pp. 2531–2538

[LY18] Liu, D. ; Yang, G. H.: Performance-based data-driven model-free adaptive sliding mode control for a class of discrete-time nonlinear processes. In: *Journal of Process Control* 68 (2018), pp. 186–194

[LY19a] Liu, D. ; Yang, G.: Data-Driven Adaptive Sliding Mode Control of Nonlinear Discrete-Time Systems With Prescribed Performance. In: *IEEE Transactions on Systems, Man, and Cybernetics: Systems* 49 (2019), No. 12, pp. 2598–2604

[LY19b] Liu, D. ; Yang, G.: Prescribed Performance Model-Free Adaptive Integral Sliding Mode Control for Discrete-Time Nonlinear Systems. In: *IEEE Transactions on Neural Networks and Learning Systems* 30 (2019), No. 7, pp. 2222–2230

[LYZW05] Liu, D. ; Yi, J. ; Zhao, D. ; Wang, W.: Adaptive sliding mode fuzzy control for a two-dimensional overhead crane. In: *Mechatronics* 15 (2005), No. 5, pp. 505–522

[LZYQ18] Liu, Y. ; Zhang, H. ; Yu, R. ; Qu, Q.: Data-driven optimal tracking control for discrete-time systems with delays using adaptive dynamic programming. In: *Journal of the Franklin Institute* 355 (2018), No. 13, pp. 5649–5666

[MA14] Masoud, Z. ; Alhazza, K.: Frequency-modulation input shaping control of double-pendulum overhead cranes. In: *Journal of Dynamic Systems, Measurement and Control, Transactions of the ASME* 136 (2014), No. 2, pp. 021005

[Mad19] Madadi, E.: *Model-Free Control Design for Nonlinear Mechanical Systems*, University of Duisburg-Essen, Dissertation, (2019)

[MC08] Maryak, J. L. ; Chin, D. C.: Global Random Optimization by Simultaneous Perturbation Stochastic Approximation. In: *IEEE Transactions on Automatic Control* 53 (2008), No. 3, pp. 780–783

[MDS18] Madadi, E. ; Dong, Y. ; Söffker, D.: Comparison of Different Model-Free Control Methods Concerning Real-Time Benchmark. In: *Journal of Dynamic Systems Measurement and Control* 140 (2018), No. 12, pp. 121014

[MN03] Masoud, Z. ; Nayfeh, A.: Sway Reduction on Container Cranes Using Delayed Feedback Controller. In: *Nonlinear Dynamics* 34 (2003), pp. 347–358

[MS18] Madadi, E. ; Söffker, D.: Model-Free Control of Unknown Nonlinear Systems using an Iterative Learning Concept: Theoretical Development and Experimental Validation. In: *Nonlinear Dynamics* 94 (2018), pp. 1151–1163

[NH12] Ngo, Q. H. ; Hong, K.: Sliding-Mode Antisway Control of an Offshore Container Crane. In: *IEEE/ASME Transactions on Mechatronics* 17 (2012), No. 2, pp. 201–209

[Oga10] Ogata, K.: *Modern Control Engineering*. Prentice Hall, (2010) (Instrumentation and controls series)

[PS03] Paul, A. ; Safonov, M. G.: Model reference adaptive control using multiple controllers and switching. In: *42nd IEEE International Conference on Decision and Control (IEEE Cat. No.03CH37475)* Vol. 4, (2003), pp. 3256–3261

[PS19a] Pham, H. A. ; Söffker, D.: Model-Free Adaptive Control Method Applied to Vibration Reduction of a Flexible Crane as MIMO System. In: *Proceedings in Applied Mathematics and Mechanics* 19 (2019), No. 1, pp. e201900145

[PS19b] Pham, H. A. ; Söffker, D.: Modified Model-Free Adaptive Control Method Applied to Vibration Control of an Elastic Crane. In: *International Design Engineering Technical Conferences and Computers and Information in Engineering Conference* Vol. 6, (2019), pp. V006T09A042

[PS20a] Pham, H. A. ; Söffker, D.: Improved model-free adaptive control method using recursive least-squares estimation algorithm. In: *2020 European Control Conference (ECC)*, (2020), pp. 47–52

[PS20b] Pham, H. A. ; Söffker, D.: Improved Model-Free Adaptive Predictive Control based on Recursive Least-Squares Estimation Algorithm. In: *Asian Journal of Control* (2020), pp. submitted

[PS20c] Pham, H. A. ; Söffker, D.: Modified Model-Free Adaptive Control using Compact-Form Dynamic Linearization Technique. In: *21st IFAC World Congress (IFAC 2020)*, (2020), pp. accepted

[PS20d] Pham, H. A. ; Söffker, D.: Modified Model-Free Adaptive Predictive Control Applied to Vibration Reduction of Mechanical Flexible Systems. In: *International Design Engineering Technical Conferences and Computers and Information in Engineering Conference* Vol. 2, (2020), pp. V002T02A025

[PS20e] Pham, H. A. ; Söffker, D.: Vibration Control of Flexible Structures using Model-Free Adaptive Control Algorithms. In: *Journal of Dynamic Systems Measurement and Control* (2020), pp. submitted

[PSSH04] Previdi, F. ; Schauer, T. ; Savaresi, S. M. ; Hunt, K. J.: Data-driven control design for neuroprotheses: a virtual reference feedback tuning (VRFT) approach. In: *IEEE Transactions on Control Systems Technology* 12 (2004), No. 1, pp. 176–182

[QFL17] Qian, Y. ; Fang, Y. ; Lu, B.: Adaptive repetitive learning control for an offshore boom crane. In: *Automatica* 82 (2017), pp. 21–28

[QFL19] Qian, Y. ; Fang, Y. ; Lu, B.: Adaptive robust tracking control for an offshore ship-mounted crane subject to unmatched sea wave disturbances. In: *Mechanical Systems and Signal Processing* 114 (2019), pp. 556–570

[RI87] Radke, F. ; Isermann, R.: A parameter-adaptive PID-controller with stepwise parameter optimization. In: *Automatica* 23 (1987), No. 4, pp. 449–457

[RMA+17] Ramli, L. ; Mohamed, Z. ; Abdullahi, A. M. ; Jaafar, H. I. ; Lazim, I. M.: Control strategies for crane systems: A comprehensive review. In: *Mechanical Systems and Signal Processing* 95 (2017), pp. 1–23

[ROC+15] Rahman, M. ; Ong, Z. C. ; Chong, W. T. ; Julai, S. ; Khoo, S. Y.: Performance enhancement of wind turbine systems with vibration control: A review. In: *Renewable and Sustainable Energy Reviews* 51 (2015), pp. 43–54

[RPP+11] Rădac, M. B. ; Precup, R. E. ; Petriu, E. M. ; Preitl, S. ; Dragoş, C. A.: Convergent Iterative Feedback Tuning of State Feedback-Controlled Servo Systems. In: *Informatics in Control Automation and Robotics*, Springer Berlin Heidelberg, (2011), pp. 99–111

[RPP+19] Roman, R. ; Precup, R. ; Petriu, E. M. ; Hedrea, E. ; Bojan-Dragos, C. ; Radac, M.: Model -Free Adaptive Control With Fuzzy Component for Tower Crane Systems. In: *2019 IEEE International Conference on Systems, Man and Cybernetics (SMC)*, (2019), pp. 1384–1389

[RRP16] Roman, R. ; Radac, M. ; Precup, R.: Multi-input–multi-output system experimental validation of model-free control and virtual reference feedback tuning techniques. In: *IET Control Theory Applications* 10 (2016), No. 12, pp. 1395–1403

[RRPP17] Roman, R. C. ; Radac, M. B. ; Precup, R. E. ; Petriu, E.: Virtual Reference Feedback Tuning of Model-Free Control Algorithms for Servo Systems. In: *Machines* 5 (2017), No. 4, pp. 25

[SA94] Schaal, S. ; Atkeson, C. G.: Robot juggling: implementation of memory-based learning. In: *IEEE Control Systems Magazine* 14 (1994), No. 1, pp. 57–71

[Saa05] Saab, S. S.: Optimal selection of the forgetting matrix into an iterative learning control algorithm. In: *IEEE Transactions on Automatic Control* 50 (2005), No. 12, pp. 2039–2043

[Saf03] Safonov, M. G.: Data-Driven Robust Control Design: Unfalsified Control. In: *Engineering*, (2003)

[SC93] Spall, J. C. ; Cristion, J. A.: Model-free control of general discrete-time systems. In: *Proceedings of 32nd IEEE Conference on Decision and Control* Vol. 3, (1993), pp. 2792–2797

[SC98] Spall, J. C. ; Cristion, J. A.: Model-free control of nonlinear stochastic systems with discrete-time measurements. In: *IEEE Transactions on Automatic Control* 43 (1998), No. 9, pp. 1198–1210

[SDPB05] Skoczowski, S. ; Domek, S. ; Pietrusewicz, K. ; Broel-Plater, B.: A method for improving the robustness of PID control. In: *IEEE Transactions on Industrial Electronics* 52 (2005), No. 6, pp. 1669–1676

[Sin09] Singhose, W. E.: Command shaping for flexible systems: A review of the first 50 years. In: *International Journal of Precision Engineering and Manufacturing* 10 (2009), pp. 153–168

[SL91] Slotine, J. J. E. ; Li, W.: *Applied Nonlinear Control*. Prentice Hall, (1991)

[Smo14] Smoczek, J.: Fuzzy crane control with sensorless payload deflection feedback for vibration reduction. In: *Mechanical Systems and Signal Processing* 46 (2014), No. 1, pp. 70–81

[SOYU11] Sano, S. ; Ouyang, H. ; Yamashita, H. ; Uchiyama, N.: LMI Approach to Robust Control of Rotary Cranes under Load Sway Frequency Variance. In: *Journal of System Design and Dynamics* 5 (2011), No. 7, pp. 1402–1417

[Spa92] Spall, J. C.: Multivariate stochastic approximation using a simultaneous perturbation gradient approximation. In: *IEEE Transactions on Automatic Control* 37 (1992), No. 3, pp. 332–341

[SS98] Sadegh, P. ; Spall, J. C.: Optimal random perturbations for stochastic approximation using a simultaneous perturbation gradient approximation. In: *IEEE Transactions on Automatic Control* 43 (1998), No. 10, pp. 1480–1484

[SSSN08] Song, Q. ; Spall, J. C. ; Soh, Y. C. ; Ni, J.: Robust Neural Network Tracking Controller Using Simultaneous Perturbation Stochastic Approximation. In: *IEEE Transactions on Neural Networks* 19 (2008), No. 5, pp. 817–835

[ST95] Safonov, M. G. ; Tsao, T. C.: The unfalsified control concept: A direct path from experiment to controller. In: *Feedback Control, Nonlinear Systems, and Complexity*, Springer Berlin Heidelberg, (1995), pp. 196–214

[ST97] Safonov, M. G. ; Tsao, T. C.: The unfalsified control concept and learning. In: *IEEE Transactions on Automatic Control* 42 (1997), No. 6, pp. 843–847

[Ste99] Stenman, A.: Model-free predictive control. In: *Proceedings of the 38th IEEE Conference on Decision and Control (Cat. No.99CH36304)* Vol. 4, (1999), pp. 3712–3717

[SWFC18] Sun, N. ; Wu, Y. ; Fang, Y. ; Chen, H.: Nonlinear Antiswing Control for Crane Systems With Double-Pendulum Swing Effects and Uncertain Parameters: Design and Experiments. In: *IEEE Transactions on Automation Science and Engineering* 15 (2018), No. 3, pp. 1413–1422

[TBT18] Tutsoy, O. ; Barkana, D. E. ; Tugal, H.: Design of a completely model free adaptive control in the presence of parametric, non-parametric uncertainties and random control signal delay. In: *ISA Transactions* 76 (2018), pp. 67–77

[THLL99] Tan, K. K. ; Huang, S. N. ; Lee, T. H. ; Leu, F. M.: Adaptive-predictive PI control of a class of SISO systems. In: *Proceedings of the 1999 American Control Conference (Cat. No. 99CH36251)* Vol. 6, (1999), pp. 3848–3852

[TS99] Tsao, T. C. ; Safonov, M. G.: Unfalsified direct adaptive control of a two-link robot arm. In: *Proceedings of the 1999 IEEE International Conference on Control Applications (Cat. No.99CH36328)* Vol. 1, (1999), pp. 680–686

[Utk77] Utkin, V.: Variable structure systems with sliding modes. In: *IEEE Transactions on Automatic Control* 22 (1977), No. 2, pp. 212–222

[VKS10] Vaughan, J. ; Kim, D. ; Singhose, W.: Control of Tower Cranes With Double-Pendulum Payload Dynamics. In: *IEEE Transactions on Control Systems Technology* 18 (2010), No. 6, pp. 1345–1358

[VV07] Verhaegen, M. ; Verdult, V.: *Filtering and System Identification: A Least Squares Approach*. Cambridge University Press, (2007)

[WGD09] Wang, Y. ; Gao, F. ; Doyle, F. J.: Survey on iterative learning control, repetitive control, and run-to-run control. In: *Journal of Process Control* 19 (2009), No. 10, pp. 1589–1600

[WH19] Wang, Y. ; Hou, M.: Model-free adaptive integral terminal sliding mode predictive control for a class of discrete-time nonlinear systems. In: *ISA Transactions* 93 (2019), pp. 209–217

[WLW+16] Wang, X. ; Li, X. ; Wang, J. ; Fang, X. ; Zhu, X.: Data-driven model-free adaptive sliding mode control for the multi degree-of-freedom robotic exoskeleton. In: *Information Sciences* 327 (2016), pp. 246–257

[WN15] Wagg, D. ; Neild, S.: *Nonlinear Vibration with Control*. Springer International Publishing, (2015)

[WXZ15] Wu, Z. ; Xia, X. H. ; Zhu, B.: Model predictive control for improving operational efficiency of overhead cranes. In: *Nonlinear Dynamics* 79 (2015), pp. 2639–2657

[WZWC18] Wen, L. ; Zhou, P. ; Wang, H. ; Chai, T.: Model Free Adaptive Predictive Control of Multivariate Molten Iron Quality in Blast Furnace Ironmaking. In: *2018 IEEE Conference on Decision and Control (CDC)*, (2018), pp. 2617–2622

[XA20] Xie, F. ; Aly, A. M.: Structural control and vibration issues in wind turbines: A review. In: *Engineering Structures* 210 (2020), pp. 110087

[XHL13] Xie, X. ; Huang, J. ; Liang, Z.: Vibration reduction for flexible systems by command smoothing. In: *Mechanical Systems and Signal Processing* 39 (2013), No. 1, pp. 461–470

[XJL16] Xu, D. ; Jiang, B. ; Liu, F.: Improved data driven model free adaptive constrained control for a solid oxide fuel cell. In: *IET Control Theory Applications* 10 (2016), No. 12, pp. 1412–1419

[XJS14] Xu, D. ; Jiang, B. ; Shi, P.: A Novel Model-Free Adaptive Control Design for Multivariable Industrial Processes. In: *IEEE Transactions on Industrial Electronics* 61 (2014), No. 11, pp. 6391–6398

[XSBS18] Xie, Y. ; Shi, H. ; Bi, F. ; Shi, J.: A MIMO data driven control to suppress structural vibrations. In: *Aerospace Science and Technology* 77 (2018), pp. 429–438

[XSJ18] Xu, D. ; Shi, Y. ; Ji, Z.: Model-Free Adaptive Discrete-Time Integral Sliding-Mode-Constrained-Control for Autonomous 4WMV Parking Systems. In: *IEEE Transactions on Industrial Electronics* 65 (2018), No. 1, pp. 834–843

[Xu11] Xu, J. X.: A survey on iterative learning control for nonlinear systems. In: *International Journal of Control* 84 (2011), No. 7, pp. 1275–1294

[XWSS18] Xie, Y. ; Wang, C. ; Shi, H. ; Shi, J.: A data driven control method for structure vibration suppression. In: *Acta Astronautica* 143 (2018), pp. 302–309

[XXL05] Xu, J. X. ; Xu, J. ; Lee, T. H.: Iterative learning control for systems with input deadzone. In: *IEEE Transactions on Automatic Control* 50 (2005), No. 9, pp. 1455–1459

[YDXL14] Yin, S. ; Ding, S. X. ; Xie, X. ; Luo, H.: A Review on Basic Data-Driven Approaches for Industrial Process Monitoring. In: *IEEE Transactions on Industrial Electronics* 61 (2014), No. 11, pp. 6418–6428

[YHZ18] Yu, X. ; Hou, Z. ; Zhang, X.: Model-free Adaptive Control for a Vapour-Compression Refrigeration Benchmark Process. In: *IFAC-PapersOnLine* 51 (2018), No. 4, pp. 527–532

[You78] Young, K. D.: Controller Design for a Manipulator Using Theory of Variable Structure Systems. In: *IEEE Transactions on Systems, Man, and Cybernetics* 8 (1978), No. 2, pp. 101–109

[YTY09] Yamamoto, T. ; Takao, K. ; Yamada, T.: Design of a Data-Driven PID Controller. In: *IEEE Transactions on Control Systems Technology* 17 (2009), No. 1, pp. 29–39

[YXH10] Yin, C. ; Xu, J. ; Hou, Z.: A High-Order Internal Model Based Iterative Learning Control Scheme for Nonlinear Systems With Time-Iteration-Varying Parameters. In: *IEEE Transactions on Automatic Control* 55 (2010), No. 11, pp. 2665–2670

[YY07] Yang, J. H. ; Yang, K. S.: Adaptive coupling control for overhead crane systems. In: *Mechatronics* 17 (2007), No. 2, pp. 143–152

[ZBH20] Zuo, H. ; Bi, K. ; Hao, H.: A state-of-the-art review on the vibration mitigation of wind turbines. In: *Renewable and Sustainable Energy Reviews* 121 (2020), pp. 109710

[ZH12] Zhu, Y. ; Hou, Z.: Controller compact form dynamic linearization based model free adaptive control. In: *2012 IEEE 51st IEEE Conference on Decision and Control (CDC)*, (2012), pp. 4817–4822

[ZH14] Zhu, Y. ; Hou, Z.: Data-Driven MFAC for a Class of Discrete-Time Nonlinear Systems With RBFNN. In: *IEEE Transactions on Neural Networks and Learning Systems* 25 (2014), No. 5, pp. 1013–1020

[ZH15] Zhu, Y. ; Hou, Z.: Controller dynamic linearisation-based model-free adaptive control framework for a class of non-linear system. In: *IET Control Theory Applications* 9 (2015), No. 7, pp. 1162–1172

[ZLL18] Zhang, Y. ; Li, S. ; Liu, X.: Neural Network-Based Model-Free Adaptive Near-Optimal Tracking Control for a Class of Nonlinear Systems. In: *IEEE Transactions on Neural Networks and Learning Systems* 29 (2018), No. 12, pp. 6227–6241

[ZMR+16] Zhang, M. ; Ma, X. ; Rong, X. ; Tian, X. ; Li, Y.: Adaptive tracking control for double-pendulum overhead cranes subject to tracking error limitation, parametric uncertainties and external disturbances. In: *Mechanical Systems and Signal Processing* 76-77 (2016), pp. 15–32

[ZXW15] Zhao, D. ; Xia, Z. ; Wang, D.: Model-Free Optimal Control for Affine Nonlinear Systems With Convergence Analysis. In: *IEEE Transactions on Automation Science and Engineering* 12 (2015), No. 4, pp. 1461–1468

This thesis is based on the results and development steps presented/published in the previous publications or prepared for submission to the following journals:

Journal articles

[PS20b] PHAM, H. A. ; SÖFFKER, D.: Improved Model-Free Adaptive Predictive Control based on Recursive Least-Squares Estimation Algorithm. In: *Asian Journal of Control* (2020), submitted.

[PS20e] PHAM, H. A. ; SÖFFKER, D.: Vibration Control of Flexible Structures using Model-Free Adaptive Control Algorithms. In: *ASME Journal of Dynamic Systems, Measurement, and Control* (2020), submitted.

Conference papers

[PS19a] PHAM, H. A. ; SÖFFKER, D.: Model-Free Adaptive Control Method Applied to Vibration Reduction of a Flexible Crane as MIMO System. In: *PAMM - Proceedings in Applied Mathematics and Mechanics*, 19(1) (2019), pp. e201900145.

[PS19b] PHAM, H. A. ; SÖFFKER, D.: Modified Model-Free Adaptive Control Method Applied to Vibration Control of an Elastic Crane. In: *ASME 2019 International Design Engineering Technical Conferences and Computers and Information in Engineering Conference (IDETC/CIE 2019)*, Anaheim, California, USA, Vol. 6, (2019), pp. V006T09A042.

[PS20a] PHAM, H. A. ; SÖFFKER, D.: Improved Model-Free Adaptive Control Method Using Recursive Least-Squares Estimation Algorithm. In: *European Control Conference (ECC)*, Saint Petersburg, Russia, May 12-15 (2020), pp. 47-52.

[PS20c] PHAM, H. A. ; SÖFFKER, D.: Modified Model-Free Adaptive Control using Compact-Form Dynamic Linearization Technique. In: *21st IFAC World Congress (IFAC 2020)*, Berlin, Germany, July 12-17 (2020), accepted.

[PS20d] PHAM, H. A. ; SÖFFKER, D.: Modified Model-Free Adaptive Predictive Control Applied to Vibration Reduction of Mechanical Flexible Systems. In: *ASME 2020 International Design Engineering Technical Conferences and Computers and Information in Engineering Conference (IDETC/CIE 2020)*, St. Louis, Missouri, USA, Vol. 2, (2020), pp. V002T02A025.

DOI: 10.17185/duepublico/73748
URN: urn:nbn:de:hbz:464-20210120-091651-1